



Durham E-Theses

Redox active cyclophanes and donor-acceptor systems from new

Christensen, Christian Ausig

How to cite:

Christensen, Christian Ausig (2002) *Redox active cyclophanes and donor-acceptor systems from new*, Durham theses, Durham University. Available at Durham E-Theses Online: <http://etheses.dur.ac.uk/3880/>

Use policy

The full-text may be used and/or reproduced, and given to third parties in any format or medium, without prior permission or charge, for personal research or study, educational, or not-for-profit purposes provided that:

- a full bibliographic reference is made to the original source
- a [link](#) is made to the metadata record in Durham E-Theses
- the full-text is not changed in any way

The full-text must not be sold in any format or medium without the formal permission of the copyright holders.

Please consult the [full Durham E-Theses policy](#) for further details.

**REDOX ACTIVE CYCLOPHANES AND DONOR-ACCEPTOR SYSTEMS
FROM NEW TTFAQ BUILDING BLOCKS**

The copyright of this thesis rests with the author.
No quotation from it should be published without
his prior written consent and information derived
from it should be acknowledged.

CHRISTIAN AUSIG CHRISTENSEN, M.Sc.

GRADUATE SOCIETY

DEPARTMENT OF CHEMISTRY

UNIVERSITY OF DURHAM



A Thesis submitted for the degree of Doctor of Philosophy
at the University of Durham

24 MAR 2003
August 2002

STATEMENT OF COPYRIGHT

The copyright of this thesis rests with the author. No quotation from it should be published without his prior written consent and information derived from it should be acknowledged.

DECLARATION

The work described in this thesis was carried out in the Department of Chemistry at the University of Durham, and at the Department of Chemistry, Odense University, Denmark, between October 1998 and September 2001. All the work was carried out by the author unless otherwise stated, and has not previously been submitted for a degree at this or any other university.

TABLE OF CONTENTS

Abstract	vii
Acknowledgements	viii
Abbreviations	x
1 Introduction.....	1
1.1 Cyclophanes.....	1
1.1.1 Reasons for the synthesis of cyclophanes.....	1
1.1.2 Cyclophanes - their historic origin	2
1.2 TTF Cyclophanes.....	3
1.2.1 Properties of TTF.....	4
1.2.2 TTF in a historical perspective	5
1.2.3 TTF cyclophanes - an introduction.....	5
1.2.4 Monomeric TTF cyclophanes.....	7
1.2.5 Double-bridged dimeric TTF cyclophanes.....	10
1.2.6 Quadruple-bridged dimeric TTF cyclophanes.....	13
1.2.7 Oligomeric TTF cyclophanes	17
1.2.8 TTF-acceptor cyclophanes.....	18
1.3 Conclusions.....	20
2 An Introduction to TTFAQ	21
2.1 Extended Tetrathiafulvalenes – The Genesis of TTFAQ	21
2.1.1 Vinylogous tetrathiafulvalenes	21
2.2 TTFAQ and its Properties.....	22
2.2.1 The solid state conformation of TTFAQ and the TTFAQ dication.....	22
2.2.2 The conformation of TTFAQ in solution	24
2.2.3 Solution redox properties of TTFAQ	25
2.2.4 An electrocrystallised dication salt of TTFAQ derivative 54.....	26
2.2.5 Optical properties of TTFAQ derivative 54 and its oxidised species.....	29
2.3 Synthesis of TTFAQ.....	30
2.4 Conclusions.....	33
3 New Conjugated Donor-Acceptor and Donor-Donor Dyads Containing TTFAQ...34	
3.1 Covalently Linked TTF- and TTFAQ-Acceptor Systems.....	34

3.1.1	TTFAQ-Acceptor Systems	35
3.1.2	TTF-quinone systems	36
3.2	TTF in Diels-Alder Reactions	38
3.3	Designing the Synthesis.....	39
3.4	Synthesis of the Donor-Acceptor Dyad.....	41
3.4.1	Synthesis of protected bis(hydroxymethyl) derivative 101	41
3.4.2	Formation of the ketone 104 by an addition-elimination reaction	42
3.4.3	Synthesis of bis(hydroxymethyl) derivative 106.....	43
3.4.4	Bromination of 106 – the formation of a rearrangement product.....	44
3.4.5	Optimised synthesis and X-ray analysis of aldehyde 108	46
3.4.6	Synthesis and reaction of a new diene precursor.....	48
3.4.7	Chlorination of bis(hydroxymethyl) derivative 106.....	51
3.4.8	Synthesis of donor-acceptor dyad 130.....	52
3.5	A Conjugated Donor-Donor Dyad.....	55
3.5.1	Donor-donor dyads containing TTFAQ	56
3.5.2	Synthesis of a conjugated TTFAQ dimer	57
3.5.3	Proton NMR analysis of the TTFAQ dimer and its tetracation.....	58
3.6	Electrochemical and Optical Properties.....	61
3.6.1	Optical properties.....	61
3.6.2	Solution electrochemical properties	62
3.6.3	Spectroelectrochemical studies.....	64
3.7	Conclusions.....	66
4	Pyrrolo-Annelated TTFAQ Derivatives	67
4.1	Introduction.....	67
4.1.1	Examples of assemblies containing pyrrolo-TTF	67
4.1.2	Synthesis of the pyrrolo building block.....	69
4.2	Strategy	70
4.3	Synthesis of Pyrrolo-Annelated TTFAQ Derivatives.....	70
4.3.1	Synthesis of phosphonate esters containing the pyrrole moiety	71
4.3.2	Synthesis of monopyrrolo-annelated TTFAQ derivatives.....	73
4.4	Monopyrrolo-Annelated TTFAQ Derivatives in Synthesis	75
4.4.1	Functionalisation by <i>N</i> -alkylation of monopyrrolo-TTFAQ	75
4.4.2	New donor-acceptor dyads from formylated pyrrolo-TTFAQ derivatives	76

4.4.3	Attempted synthesis of a TTFAQ-annelated porphyrin	77
4.5	X-Ray Crystallographic Analysis	78
4.6	Optical and Electrochemical Properties.....	81
4.6.1	Solution electrochemical properties	82
4.6.2	UV-vis absorption spectra of dyads 179 and 180	83
4.7	Conclusions.....	84
5	Cyclophanes from 2,6-Bisfunctionalised TTFAQ Building Blocks.....	85
5.1	Background and Strategy.....	85
5.2	Novel Cyclophanes from 2,6-Bisfunctionalised TTFAQ Building Blocks.....	87
5.2.1	A new set of 2,6-bisfunctionalised TTFAQ building blocks.....	88
5.2.2	X-ray crystallographic analysis of TTFAQ building block 203	89
5.2.3	Synthesis of TTFAQ cyclophanes	92
5.2.4	X-ray crystallographic analysis of the cyclophanes and a dication salt	94
5.2.5	Solution electrochemical properties	100
5.3	Donor-Acceptor Triads from 2,6-Bisfunctionalised TTFAQ	101
5.3.1	A novel TTFAQ fluorene charge-transfer salt.....	101
5.3.2	Donor-acceptor triads	104
5.3.3	Solution electrochemistry	105
5.4	Future Projects: Phenanthroline Cyclophanes and Catenates.....	107
5.4.1	Background.....	107
5.4.2	Synthesis of TTFAQ phenanthroline cyclophanes	108
5.4.3	X-ray crystallographic analysis	111
5.4.4	Future projects	112
5.5	Conclusions.....	113
6	A Novel Route to Highly Functionalised TTFAQ Derivatives	114
6.1	Background.....	114
6.1.1	TTFAQ derivatives by lithiation of the 1,3-dithiole rings.....	114
6.1.2	Cyanoethyl protected TTF thiolates	115
6.2	The Phosphite Coupling – A New Route to TTFAQ Derivatives	117
6.3	Synthesis of New TTFAQ Building Blocks	122
6.3.1	Synthesis of symmetrical TTFAQ derivatives	123
6.3.2	A two-step synthesis of unsymmetrical TTFAQ derivatives	123
6.3.3	Monodeprotection of a bisprotected TTFAQ thiolate derivative	124

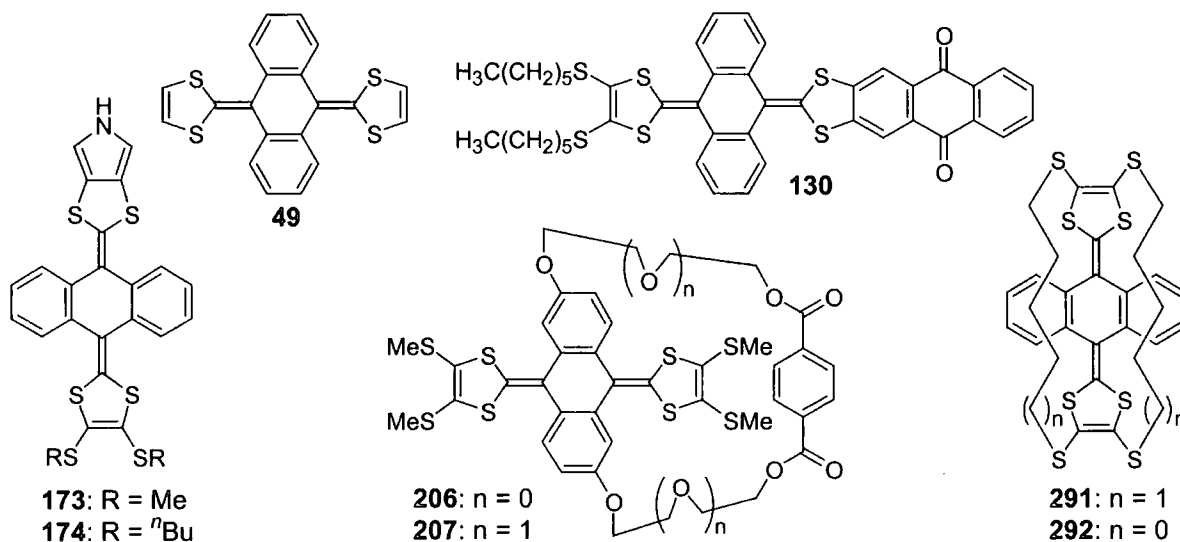
6.4	Novel TTFAQ Building Blocks in Synthesis	125
6.4.1	A new TTFAQ derivative for solid state hydrogen bonding.....	125
6.4.2	A high-yielding synthesis of a single-bridged TTFAQ cyclophane.....	129
6.4.3	A one-pot synthesis of a novel dimeric TTFAQ cyclophane	132
6.4.4	Synthesis of a TTFAQ trimer - towards novel TTFAQ dendrimers	135
6.5	Solution Electrochemical Properties.....	136
6.6	Future Projects	138
6.7	Conclusions.....	140
7	Multiple-Bridged TTFAQ Cyclophanes	141
7.1	Double-Bridged TTFAQ Cyclophanes.....	141
7.1.1	Background for bridging the 1,3-dithiole rings of TTFAQ.....	141
7.1.2	Designing the synthesis	142
7.1.3	Synthesis of double-bridged TTFAQ cyclophanes.....	143
7.1.4	X-ray crystallographic analysis of cyclophanes 291 and 292	147
7.2	Triple-Bridged TTFAQ Cyclophanes.....	149
7.2.1	Synthesis of a triple-bridged TTFAQ cyclophane.....	150
7.2.2	X-ray crystallographic analysis of triple-bridged cyclophane 297.....	153
7.3	Optical and Electrochemical Properties.....	155
7.3.1	UV-vis absorption spectra	155
7.3.2	Solution electrochemical properties	156
7.3.3	Spectroelectrochemical studies – the hunt for the cation radical.....	159
7.4	Conclusions.....	162
8	Experimental Procedures.....	163
8.1	General Methods.....	163
8.2	Experimental Procedures to Chapter 3	165
8.3	Experimental Procedures to Chapter 4	173
8.4	Experimental Procedures to Chapter 5	180
8.5	Experimental Procedures to Chapter 6	194
8.6	Experimental Procedures to Chapter 7	203
	References	213
	Appendix One: Synthesis of Phosphonate Esters	226
	Appendix Two: Supplementary Spectroelectrochemical Data	237

ABSTRACT

Redox Active Cyclophanes and Donor-Acceptor Systems From New TTFAQ Building Blocks

Christian Ausig Christensen, University of Durham, 2002

The saddle-shaped electron donor 9,10-bis(1,3-dithiol-2-ylidene)-9,10-dihydroanthracene (TTFAQ) **49**, which oxidises in a single, quasi-reversible, two-electron wave, accompanied by a dramatic conformational change, has been incorporated into donor-acceptor system **130**. However, no significant charge-transfer interaction was observed. Pyrrolo-annulated TTFAQ derivatives **173** and **174** were synthesised, and donor-acceptor dyads, which showed intramolecular charge-transfer interactions, derived. TTFAQ cyclophanes **206** and **207** were synthesised in good yields, paving the way for the incorporation of more elaborate functionalities into TTFAQ cyclophanes, as exemplified by the synthesis of a TTFAQ-phenanthroline cyclophane with potential use as an electroactive sensor. A new methodology for the synthesis of TTFAQ derivatives has been developed, allowing the synthesis of cyanoethyl protected TTFAQ thiolate derivatives. These derivatives afforded several TTFAQ cyclophanes, of which the most interesting were the double-bridged cyclophanes **291** and **292**. Due to the rigidity imposed by the two bridges, little conformational change is possible upon oxidation, which for the first time allowed us to study the elusive TTFAQ cation radical using cyclic voltammetry and spectroelectrochemistry, since **291** and **292** are oxidised in two, reversible, one-electron waves. The X-ray crystal structures of numerous new TTFAQ derivatives are also presented.



ACKNOWLEDGEMENTS

I would like to express my gratitude to the following people who have been involved, offering technical help, friendship and support, in the creation of this work.

My supervisor Prof. Martin R. Bryce for offering me a Ph.D. grant and for giving me free hands to conduct my own research, but at the same time supporting me with his insight, wisdom and ever motivating optimism.

Prof. Jan Becher, Odense University, for introducing me to the world of TTF chemistry and for allowing me to return for a 6 months stay in his research group in Odense in 2000.

Dr. Dmitri “Dima” Perepichka for passing on part of his vast technical and theoretical knowledge, but not least for his friendship and good company during late hours in the lab.

The rest of the Bryce group over the years. The old gang from my visit in 1997 (Adrian, Alex, Brian and Derek – and Chez who tragically passed away in 2001) and everybody I worked with during my Ph.D. Especially Dr. Wang for many interesting discussions, Dr. Farren for a good trip to Japan, Paul for giving me numerous lifts to the airport and Greg for his friendship and for introducing me to “real Geordie” culture.

Past and present members of the Becher group. Particular Thomas and Kent who were great company during my visit in Odense, Jan O. for useful discussions and Mogens for running mass spectra, giving good advice and not least for proof reading this thesis.

The academic, administrative and technical staff at University of Durham for keeping everything running smoothly and for providing me with analysis. Especially Dr. Andrei Batsanov for spending many nights and weekends solving crystal structures, Dr. Alan Kenwright for useful NMR discussions, Dr. Paul Low for allowing me unlimited use of his spectroelectrochemistry facilities and Dr. Andrew Beeby for some good days at RAL.

Graeme for his friendship, my family for their support and last but not least Pernille for her love and incredible patience, both while I was away and when I was home writing up.

For Pernille

ABBREVIATIONS

BEDT-TTF	-	Bis(ethylenedithio)tetrathiafulvalene
CI	-	Chemical ionisation
CT	-	Charge-transfer
CV	-	Cyclic voltammetry
DCM	-	Dichloromethane
DDQ	-	2,3-Dichloro-5,6-dicyano-1,4-benzoquinone
DEAD	-	Diethyl azodicarboxylate
DMAD	-	Dimethyl acetylenedicarboxylate
DMF	-	<i>N,N</i> -Dimethylformamide
DMSO	-	Dimethylsulfoxide
EI	-	Electron impact
EPR	-	Electron paramagnetic resonance
eq.	-	Equivalent(s)
ES	-	Electrospray
ICT	-	Intramolecular charge-transfer
IR	-	Infrared
LB	-	Langmuir-Blodgett
LDA	-	Lithium diisopropylamide
MALDI	-	Matrix assisted laser desorption/ionisation
mp	-	Melting point
MS	-	Mass spectrometry
NLO	-	Non-linear optic
NMR	-	Nuclear magnetic resonance
PD	-	Plasma desorption
rt	-	Room temperature
TCNQ	-	7,7,8,8-Tetracyano- <i>p</i> -quinodimethane
THF	-	Tetrahydrofuran
TLC	-	Thin layer chromatography
TMTSF	-	Tetramethyltetraselenafulvalene
Ts	-	<i>p</i> -Toluenesulfonyl (tosyl)
TTF	-	Tetrathiafulvalene
TTFQAQ	-	9,10-Bis(1,3-dithiol-2-ylidene)-9,10-dihydroanthracene
UV	-	Ultraviolet
vis	-	Visible

1 INTRODUCTION

Since the dawn of civilisation, man has been fascinated by rings, as proven by discoveries of ancient jewellery, and rings have been considered symbols of eternity, magic and power. Thus, it is not strange that chemists have always found great interest in molecular rings, and one class of such structures are the cyclophanes.¹

1.1 CYCLOPHANES

The name *cyclophane* was given by Cram to structures consisting of methylene bridged benzene rings. Vögtle and Neumann expanded the class to denote all compounds consisting of bridged aromatic ring systems (including both heteroaromatic ring systems and heteroaliphatic bridges, see Figure 1 for examples 1 and 2), but changed the generic heading to *phane*.¹ Hence, cyclophanes became merely the subclass of phanes consisting of bridged benzene rings. Similar bridged naphthalene and pyridine would belong to the subclasses naphthalenophanes and pyridinophanes, respectively. However, a literature search reveals the inconsistent use of this nomenclature, which also becomes complicated for more exotic bridged structures, thus the term cyclophane generally designates bridged aromatic ring systems, and this definition will also be used in this thesis.

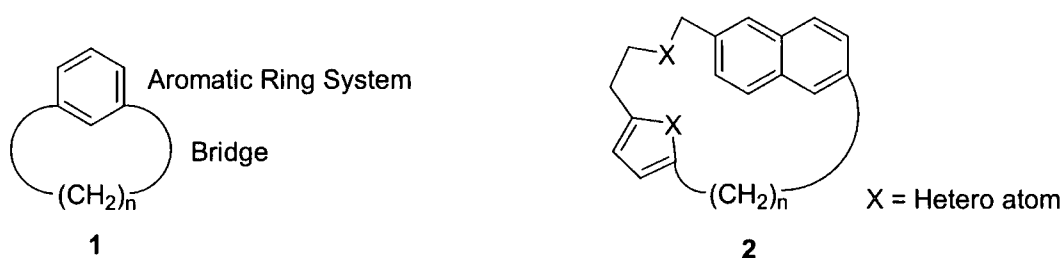


Figure 1: Examples of *phanes* or *cyclophanes*, consisting of aliphatically or heteroaliphatically bridged aromatic or heteroaromatic ring systems.

1.1.1 Reasons for the synthesis of cyclophanes

Apart from their often beautiful and fascinating architecture, cyclophanes are interesting for several reasons. They offer a unique possibility for placing aromatic rings relative to one



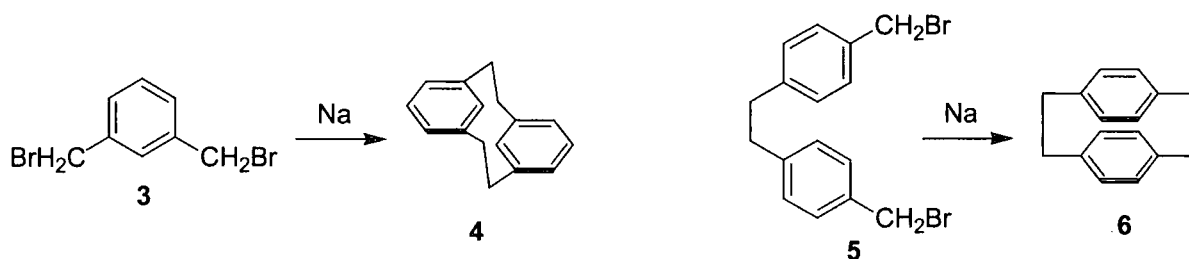
another in a tailor-made fashion and for altering the properties of aromatic systems by the infliction of strain imposed by the bridges. Thus, cyclophanes are important:

- For the study of electronic interactions between aromatic rings placed face-to-face.
- For the study of strained aromatic ring systems.
- For the formation of intramolecular charge-transfer complexes.
- In supramolecular chemistry, as host molecules for guest molecules.
- In supramolecular chemistry, as cyclic components for molecular interlocked rings (catenanes) and molecular shuttles (rotaxanes).

This chapter will give a brief historical introduction to cyclophanes and a review of redox active cyclophanes containing the good electron donor tetrathiafulvalene, since they are the compounds which most resemble those presented in this thesis.

1.1.2 Cyclophanes - their historic origin

The first cyclophane **4**, at the time designated di-*m*-xylylene, was synthesised by Pellegrin in 1899 by a Wurtz coupling of 1,3-bis(bromomethyl)benzene **3** (Scheme 1).² However, the chemistry of cyclophanes was not initiated until Cram *et al*, more than five decades later, reported the first directed synthesis of paracyclophane **6**, also by a Wurtz coupling (Scheme 1).³ Cyclophane **6** was the first example in which the two benzene rings are fixed in a face-to-face manner, whereas **4** adopts a step like conformation with, in comparison, negligible transannular interactions.¹



Scheme 1: Synthesis of early cyclophanes **4**² and **6**³ by a Wurtz coupling.

In 1954 Cram *et al*. showed the dependence between the electronic absorption spectra and the length of the bridges for a series of double-bridged cyclophanes **7**, which were compared with

the open model system **8** (Figure 2). The explanations of the long-wavelength bands for cyclophanes **7** with m and $n < 4$ were ring strain and transannular electronic interactions due to the rigidly enforced proximity of the benzene rings.⁴ Thus, these were some of the first examples of electronically interacting chromophores as a result of molecular defined orientation and proximity.

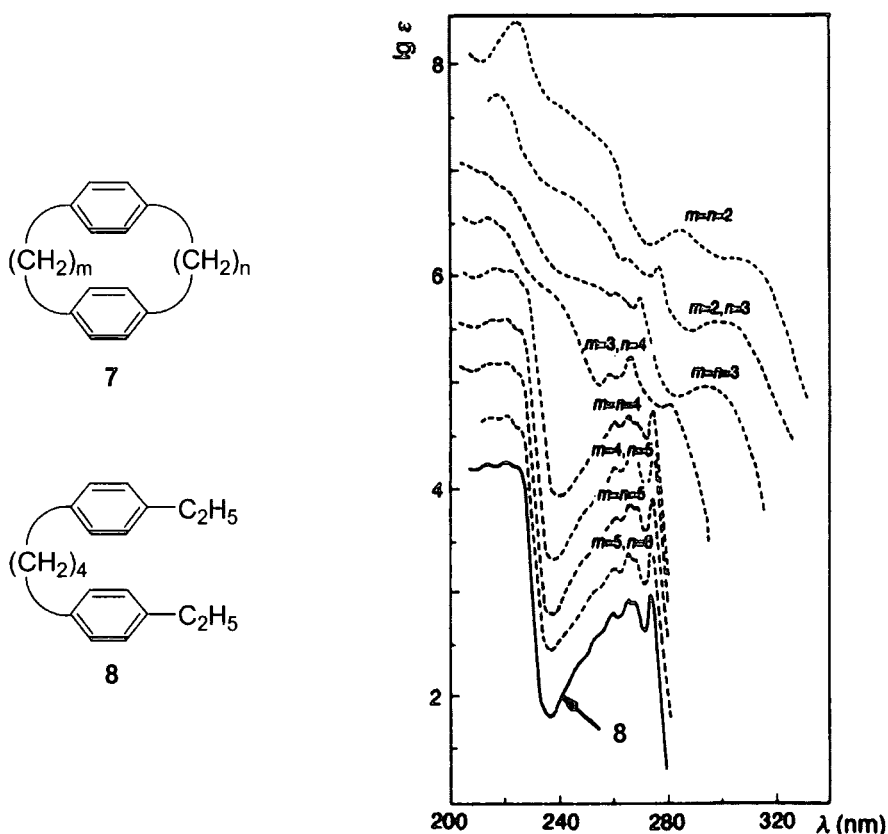


Figure 2: Comparison of the electronic spectra of double-bridged cyclophanes **7** with reference compound **8** (indicated by an arrow) in 95% ethanol. All spectra are moved up one ordinate unit relative to the spectrum immediately below.⁵

1.2 TTF CYCLOPHANES

During the last 3 decades tetrathiafulvalene (TTF) **9** especially, but also its higher chalcogen analogues (Figure 3), have attracted great attention.⁶ This is mainly due to their ability to form organic metals and in some cases even superconducting compounds (see section 1.2.2). However, the emphasis has changed, and the last ten years has seen a growing interest in incorporating TTF into supramolecular assemblies. In this context TTF cyclophanes have been important milestones for the design and construction of more complex TTF assemblies.

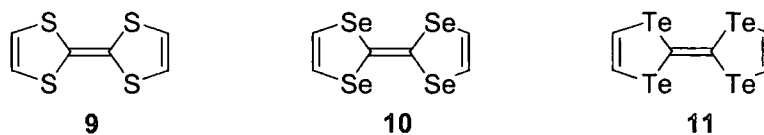
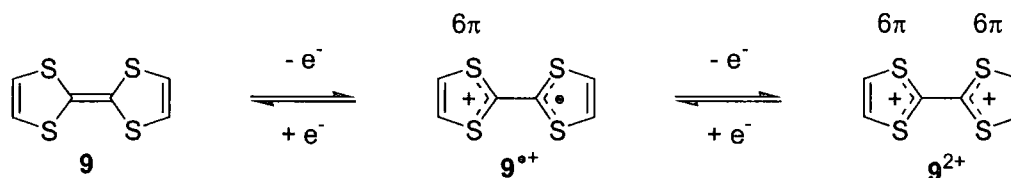


Figure 3: Tetrathiafulvalene 9 and the higher chalcogen analogues 10 and 11.

1.2.1 Properties of TTF

Tetrathiafulvalene possesses a range of interesting properties:

- Oxidation of TTF to the cation radical $9^{\bullet+}$ and dication species 9^{2+} occurs sequentially and reversibly (Scheme 2).
- The oxidation potentials are easily available in a range of organic solvents (for TTF $E_1^{1/2} = +0.34$ V and $E_2^{1/2} = +0.78$ V vs. Ag/AgCl in acetonitrile).
- The oxidation potentials can be finely tuned by substituents on the TTF ring system.
- TTF cation radicals are kinetically very stable and easily form dimers or stacks with a high degree of order, stabilised by intermolecular π - π interactions.
- TTF is stable towards a wide range of reaction conditions, although oxidising agents and strongly acidic conditions have to be avoided.



Scheme 2: Oxidation of TTF 9 to the cation radical $9^{\bullet+}$ and dication species 9^{2+} .

The cation radical $9^{\bullet+}$ and the dication 9^{2+} are stable due to the aromatisation of the 1,3-dithiole units when oxidised, because even though TTF is a planar molecule with a 14π -electron system, it is not aromatic according to the Hückel definition, since the π -electrons are not in cyclic conjugation. Apart from being stabilised by the 6π -electron 1,3-dithiolium rings, the cation radical $9^{\bullet+}$ and the dication 9^{2+} are also stabilised by the polarisable sulfur atoms. Altogether this makes TTF a good electron donor with low oxidation potentials. Electron donating substituents provide a better donor with lower oxidation potentials, whereas the opposite is true for electron withdrawing groups.⁶

1.2.2 TTF in a historical perspective

TTF was first reported by Wudl *et al.* in 1970,⁷ even though the dibenzo derivative **12** has been known since 1926.⁸ Wudl also described how the cation radical $9^{\bullet+}$ and the dication 9^{2+} could be made by treatment of TTF with chlorine gas.

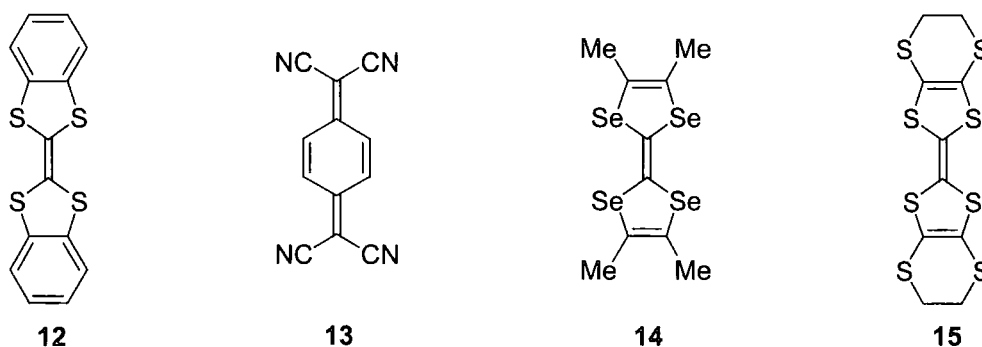


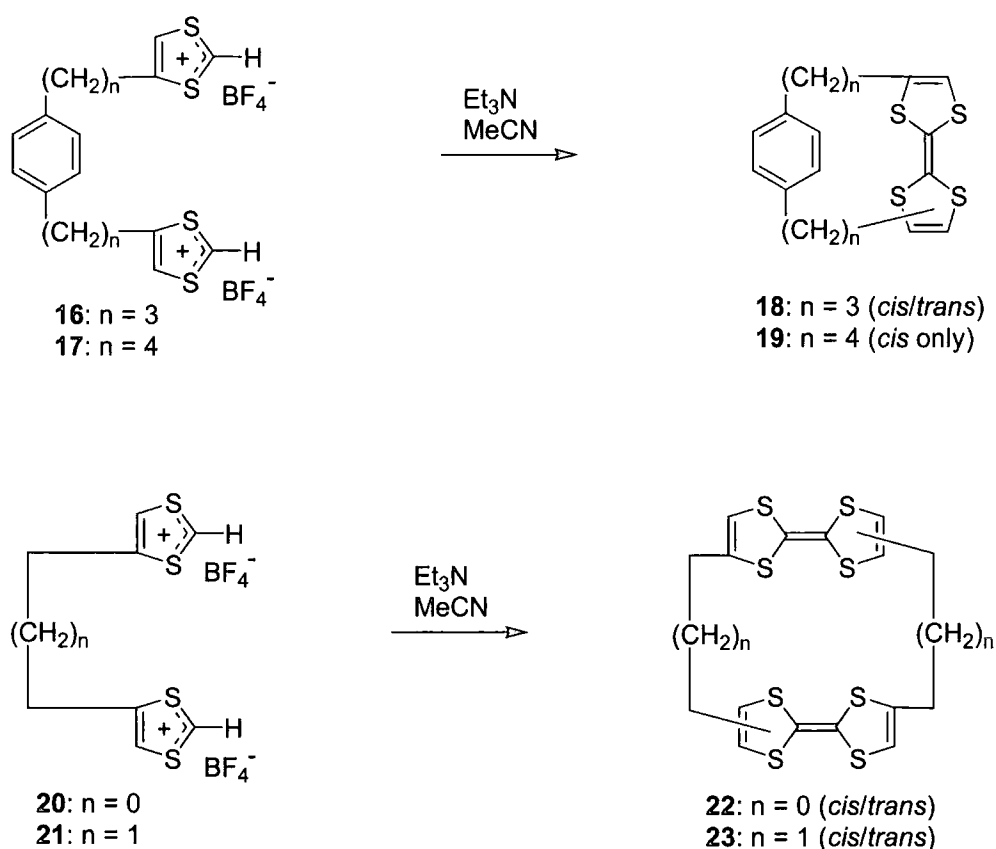
Figure 4: Structures of dibenzo-TTF **12**, TCNQ **13**, TMTSF **14** and BEDT-TTF **15**.

However, it was not until the first organic metal, a charge-transfer (CT) salt between TTF and the good π -electron acceptor TCNQ⁹ (7,7,8,8-tetracyano-*p*-quinodimethane) **13**, was reported in 1973¹⁰ that TTF attracted considerable attention. Interest increased further when the first organic superconductor, the hexafluorophosphate salt of tetramethyltetraselenafulvalene (TMTSF) **14**, was synthesised by Bechgaard *et al.* in 1980. Later, a series of organic superconductors made from BEDT-TTF **15** was reported, and to this date **15** has given the most organic superconductors.¹¹

1.2.3 TTF cyclophanes - an introduction

The first TTF cyclophanes¹² were reported by Staab *et al.* in 1980 (Scheme 3). The rationale was to manipulate the crystal structure of derived donor-acceptor salts, in order to obtain better conductors. In a cyclophane structure either a TTF moiety and an acceptor unit, or two TTF moieties could be forced together in a face-to-face manner, which should change the arrays of donors and acceptors otherwise observed in the crystals of donor-acceptor complexes. The first TTF cyclophanes **18** and **19**,¹³ incorporating a benzene ring, were models for future TTF-acceptor cyclophanes, with the benzene ring symbolising a good acceptor as TCNQ **13**. The strategy involved formation of the central fulvene bond in the final step, by intramolecular macrocyclisation of the bis(1,3-dithiolium tetrafluoroborate) salts **16** and **17** in a base mediated coupling. The short-bridged cyclophane **18** was obtained as a

cis/trans mixture, and the *cis* isomer could be obtained pure by fractional crystallisation, as evidenced by X-ray crystallography. Surprisingly, the long-bridged cyclophane **19** was obtained as the *cis* isomer only. The dimeric TTF cyclophanes **22** and **23** were synthesised in a similar manner, using the bis(1,3-dithiolium tetrafluoroborate) salts **20** and **21** possessing very short linkers, which only afforded intermolecular macrocyclisation.¹⁴ Both cyclophanes **22** and **23** were obtained as mixtures of isomers, but the (*cis,cis*)¹⁵ isomer of **22** was isolated by fractional crystallisation (X-ray crystallographic evidence).



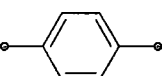
Scheme 3: The synthesis of the first TTF cyclophanes by Staab *et al.* Short bridges as in **20 and **21** only allow intermolecular coupling.^{13,14}**

Staab and co-workers did not report any electrochemical properties of the cyclophanes mentioned above (Scheme 3). However, TTF cyclophanes often possess interesting solution electrochemical properties, which can be very different from the properties of non-bridged TTF derivatives. This can be due to both ring strain and intramolecular electronic interaction between TTF moieties.

1.2.4 Monomeric TTF cyclophanes

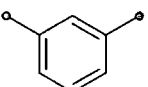
After the work of Staab *et al.*, Robert and co-workers were the next to report the synthesis of single-bridged monomeric TTF cyclophanes **24** (Figure 5). Cyclophanes **24a** and **24b** were made in a macrocyclisation reaction forming the fulvene bond.¹⁶ Only the *cis* isomers were obtained, both possessing strongly bent TTF moieties, as evidenced by X-ray crystallographic analysis. Contrary to non-bridged TTF derivatives, both **24a** and **24b** showed a single irreversible oxidation wave in the cyclic voltammogram (CV), instead of two reversible oxidation waves, and the oxidation potentials were significantly anodically shifted (harder to oxidise). Three years later Robert *et al.* reported the non-strained TTF cyclophanes **24c** and **24d**, in which the bridges were long enough to yield the *trans* isomers.¹⁷ Thus, **24c** and **24d** displayed normal redox behaviour, showing two reversible oxidation waves. However, isomerisation from *trans* to *cis* occurred upon oxidation to the cation radical species, which was observed in both X-ray crystal structures and in the cyclic voltammograms. The redox behaviour of the strained TTF moieties can be explained by the inefficient delocalisation of the 6π -system of the bent 1,3-dithiolium rings, resulting in a diminished stabilisation of the oxidised species, which makes bent TTF moieties harder to oxidise.

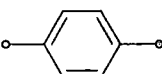
a: X = (CH₂)₆, R = *p*-CH₃Ph

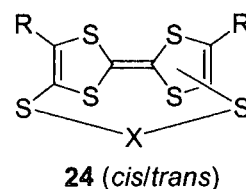
b: X = , R = *p*-CH₃Ph

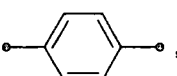
c: X = (CH₂)₁₀, R = CH₃

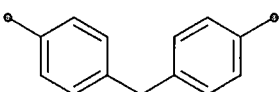
d: X = (CH₂)₁₂, R = CH₃

e: X = , R = CO₂Me

f: X = , R = CO₂Me



g: X = , R = H

h: X = , R = SMe

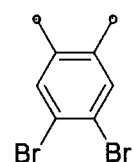
i: X = , R = SMe

Figure 5: Examples of single-bridged monomeric TTF cyclophanes.

Becher *et al.* reported the synthesis of cyclophanes **24e-h**.¹⁸ The short-bridged cyclophanes **24e-g** were obtained only as the *cis* isomers, whereas both the *cis* and *trans* isomers were

isolated for **24h**. This was also reflected in the solution electrochemical behaviour, since cyclophanes **24e-g** all showed positively shifted irreversible redox waves, whereas both *cis* and *trans* **24h** oxidised in two reversible oxidation waves. It should also be noted that **24e** possessing a short *meta*-bridge had $\lambda_{\max} = 414$ nm, whereas **24f** possessing the longer *para*-bridge had $\lambda_{\max} = 424$ nm in the electronic absorption spectrum, showing that the more distorted TTF moiety in **24e** allows for less π -delocalisation. The last example of a single-bridged cyclophane possessing a severely bent TTF moiety was reported by Bryce *et al.*¹⁹ Indeed, the six-membered bridge in **24i** is the shortest bridge ever reported to connect the two dithiole rings of a TTF moiety. Only the *cis* isomer was formed in the phosphite mediated coupling reaction leading to **24i** and the X-ray crystal structure (Figure 6) revealed the TTF moiety to be the most bent TTF derivative published. Not surprisingly, the oxidation potential of **24i** was significantly higher than for non-bridged TTF derivatives and only a single irreversible oxidation wave was observed in the CV.

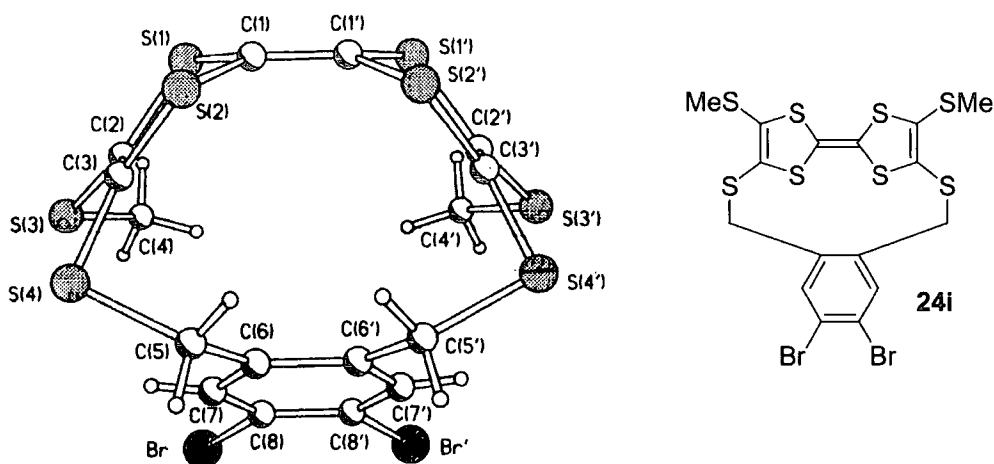
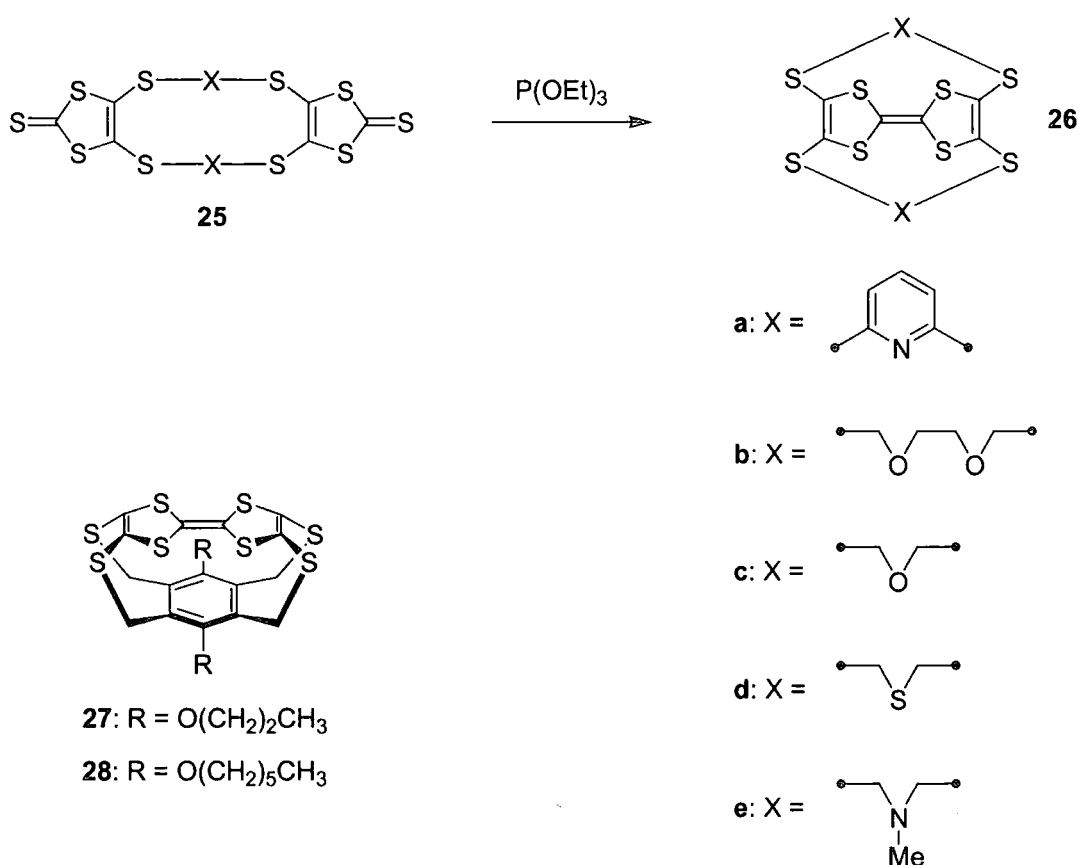


Figure 6: X-ray crystal structure of **24i** possessing a severely bent TTF moiety.²⁰

The first double-bridged monomeric TTF cyclophanes **27** and **28** were reported by Müllen *et al.* in 1988 (Scheme 4), and they were also the first examples of strongly bent TTF units.²¹ The redox behaviour of **27** and **28** was peculiar (see section 1.2.6), but the first scan of the CV was similar to the bent TTF derivatives mentioned above, *i.e.* a single irreversible oxidation wave significantly anodically shifted. The work of Müllen *et al.* inspired Becher and co-workers to synthesise the series **26a-e**²² possessing 2,6-pyridino **26a**,²³ crown **26b** and **26c**,²⁴ thiocrown **26d**²⁵ or azacrown **26e**²⁶ bridges. All the cyclophanes **26a-e** were synthesised by a phosphite mediated coupling reaction of precursors **25**, which almost exclusively afforded the intramolecular coupled monomers. A first sign of a bent

conformation of the TTF moieties was that compounds **26a-e** were almost colourless, due to the lesser degree of π -delocalisation of the bent structures, whereas TTF derivatives are typically an orange colour. X-ray crystallographic analysis later confirmed the bent conformation of the TTF moieties in cyclophanes **26a-e**. The solution electrochemistry of **26a** was somewhat surprising. Cyclophanes **26c** and **26e** showed the expected positively shifted irreversible oxidation wave and **26d** was too insoluble for solution electrochemical analysis. The long-bridged cyclophane **26b** showed two reversible oxidation potentials, which was reasonable for a less strained TTF moiety, but this behaviour was also observed for the severely strained **26a**, which was even oxidised at very low potentials. This was explained by a through-space stabilisation of the oxidised species by the lone-pairs of the pyridine nitrogens. None of the crowned cyclophanes **26b-e** showed significant ligand properties towards metal cations, which was originally anticipated.²²



Scheme 4: Examples of strained double-bridged monomeric TTF cyclophanes synthesised in an intramolecular phosphite mediated coupling reaction.

The long-bridged cyclophanes **29** and **30** synthesised by Becher *et al.* are also double-bridged monomeric TTF cyclophanes, but they have electrochemical properties typical for TTF

derivatives, since they are not strained. Instead, the purpose of synthesising **29** and **30** was to obtain supramolecular building blocks, which were used in the formation of redox-active catenanes. Cyclophanes **29** and **30** were not synthesised deploying a phosphite mediated coupling reaction as the last macrocyclisation step, but rather from a premade TTF building block possessing protected thiolate functionalities (see section 6.1.2).²⁷

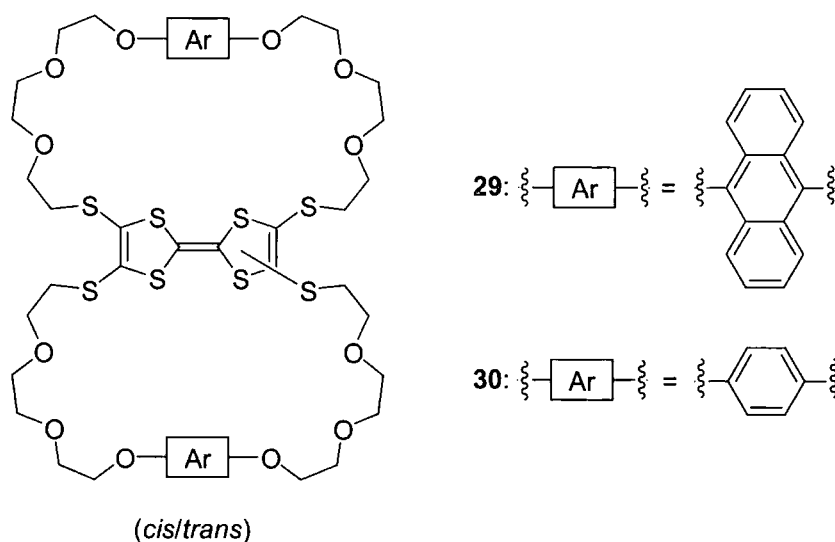


Figure 7: The non-strained double-bridged monomeric TTF cyclophanes **29** and **30** were used for catenane synthesis.

1.2.5 Double-bridged dimeric TTF cyclophanes

Dimeric TTF cyclophanes²⁸ are interesting for studies of intramolecular electronic interactions between the two TTF moieties, and as host molecules for electron accepting guest molecules which could be sandwiched between the TTF units. A famous example of the latter is the molecular tweezers **31** reported by Sugawara *et al.* (Figure 8). This double-bridged dimeric TTF cyclophane belongs to the class **32** (Figure 9). Dimeric TTF **31**, which is based upon the BEDT-TTF derivative **15** (Figure 4), formed inclusion complexes with acceptors as different as C₆₀²⁹ and DDQ,³⁰ as seen from the X-ray crystal structures presented in Figure 8. In both cases the π -electron acceptor is clamped between the two TTF moieties, which deviates from planarity. A significant charge-transfer interaction was indicated by the intermolecular distances, and the UV-vis spectra of the complexes in solid KBr pellets showed distinctive CT bands.

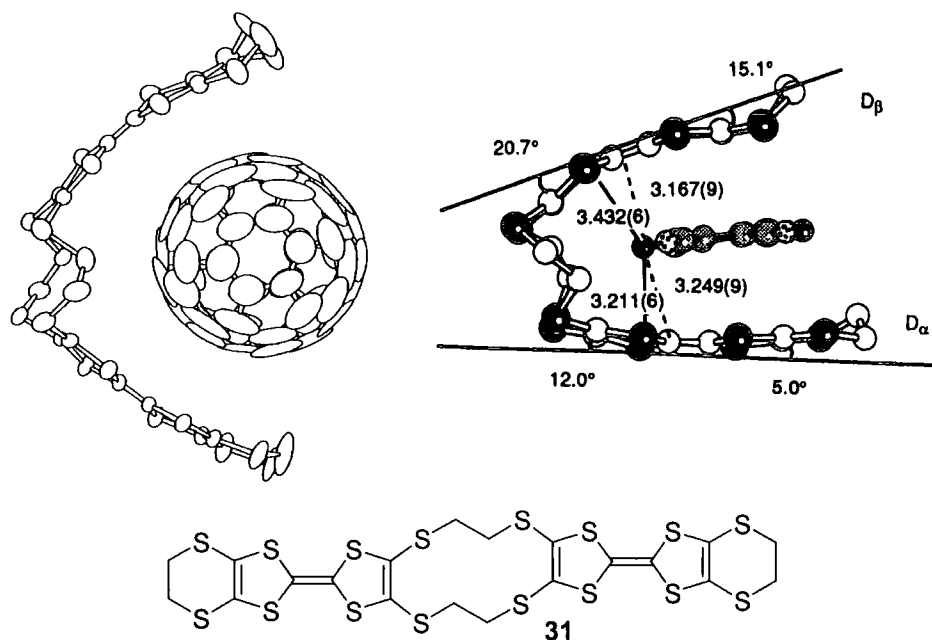


Figure 8: X-ray crystal structures of molecular tweezers 31 complexating the acceptors C₆₀ (left) and DDQ (right).³¹

Deploying premade TTF building blocks,³² Becher and co-workers reported the double-bridged dimeric TTF cyclophanes **32a-j** (Figure 9). Cyclophanes **32a-c**, possessing rigid linkers, showed two oxidation waves at potentials typical for tetrakis(alkylthio)TTF, indicating no intramolecular electronic interaction.³³

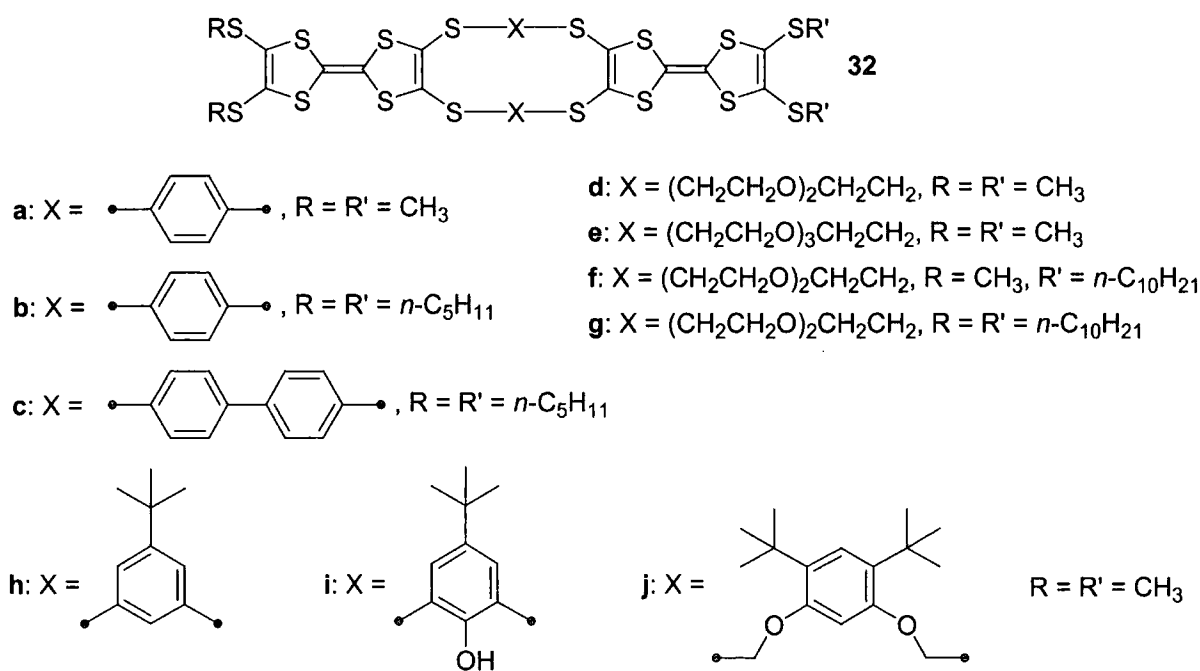


Figure 9: Double-bridged dimeric TTF cyclophanes.

Compounds **32d-e** in turn possess flexible glycol bridges, and were synthesised in order to derive CT salts in which the crowns could form ion channels. In collaboration with the group of Nakamura, several CT complexes were obtained, as evidenced by both X-ray and electronic spectroscopic analysis.³⁴ However, none of them were inclusion complexes similar to those Sugawara *et al.* had reported (Figure 8), possibly due to the flexible linkers, and also no ions were situated in the crowns. Recently the related cyclophanes **32f-g**, which are functionalised with decylthio groups for the formation of LB-films, have been shown to form nanowires with orientations corresponding to the directions of the potassium ion array on a mica surface, thus showing cation recognition.³⁵ Cyclophanes **32d-g** showed no electronic interactions in their cyclic voltammograms. Electronic interactions were observed in the series **32h-j**, especially for **32h** possessing a very rigid linker allowing intramolecular interactions.³⁶ This was seen as a clear split of the first oxidation wave in the CV, affording two, reversible, one-electron waves followed by a single, reversible, two-electron oxidation wave to give the fully oxidised species. Further evidence of interacting TTF moieties was a mixed valence band in the electronic absorption spectrum of the cation radical species **32h⁺** (see discussion section 7.3.3).

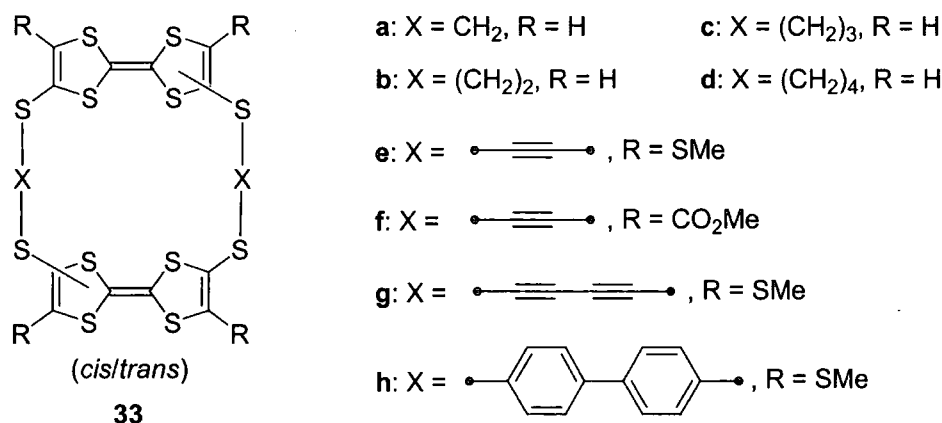


Figure 10: Double-bridged dimeric TTF cyclophanes.

Another class of double-bridged dimeric TTF cyclophanes is **33** (Figure 10), to which the first dimeric TTF cyclophanes by Staab *et al.* belong (Scheme 3).¹⁴ The most impressive work, however, is the series **33a-d** synthesised by Otsubo *et al.*³⁷ All compounds were obtained as a mixture of three stereo isomers (*cis,cis*), (*cis,trans*) and (*trans,trans*),¹⁵ but they were separated by elaborate fractional crystallisation, as evidenced by both X-ray and ¹H NMR analysis. Several CT salts were derived from **33a-d**, and all except one adopted a (*trans,trans*) conformation and were semiconducting. Only a triiodide salt of **33b**, which crystallised in a

(*cis,cis*) conformation, showed metallic behaviour ($\sigma_{\pi} = 28 \text{ S cm}^{-1}$). In **33d** the two TTF moieties are too far apart to interact, but for **33a-c** interaction is observed for the first oxidation wave in the CV, which is split. Two opposing effects are involved: charge delocalisation and Coulombic repulsion. The former lowers the first one-electron oxidation and raises the second one-electron oxidation to form the cation radical state for both TTF moieties in the cyclophane. Oxidation to the fully oxidised species occurs in a single two-electron oxidation wave, which is reversible for **33b-c**, but irreversible for the short-bridged **33a**. Thus, double-bridged dimeric TTF cyclophanes **33a-d** can serve as models of interacting dimeric TTF units, but not necessarily afford CT salts of high conductivity. Work of Becher *et al.* also needs to be mentioned. The series **33e-h** was made using only rigid bridges, which in spite of their length should be able to impose electronic interactions between the TTF moieties, by fixating them in a favourable position. Indeed, a splitting of the first oxidation wave was seen for the cyclophanes **33e-f**, whereas the longer bridges of **33g-h** were too long for any interaction.³³

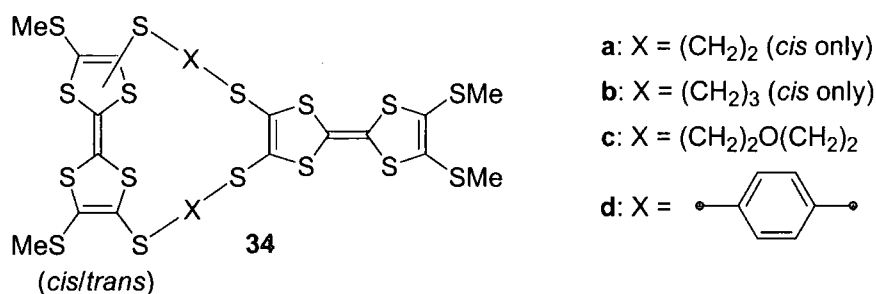


Figure 11: Orthogonal dimeric double-bridged TTF cyclophanes synthesised by Bryce *et al.*³⁸

The last class of double-bridged dimeric TTF cyclophanes are those in which the TTF moieties are orthogonal: the series **34a-d** of Bryce *et al.* are the best example.³⁸ Especially the short-bridged derivatives **34a-b** are interesting, since these bridges cause a bend in one of the TTF moieties, which offers different oxidation potentials for the two TTF units, making mixed valence CT-salts more likely. Thus the semiconducting ($\sigma_{\pi} = 10^{-2} \text{ S cm}^{-1}$) salt (**34a₂**)⁺ClO₄⁻ was obtained by electrocrystallisation.

1.2.6 Quadruple-bridged dimeric TTF cyclophanes

One class of quadruple-bridged dimeric TTF cyclophanes are the criss-cross overlapped systems **35**, studied independently and simultaneously by two Japanese groups. Sugawara

et al. reported the cyclophanes **35a** and **35b**,³⁹ whereas the group of Otsubo synthesised the entire series **35a-d** (Figure 12).⁴⁰

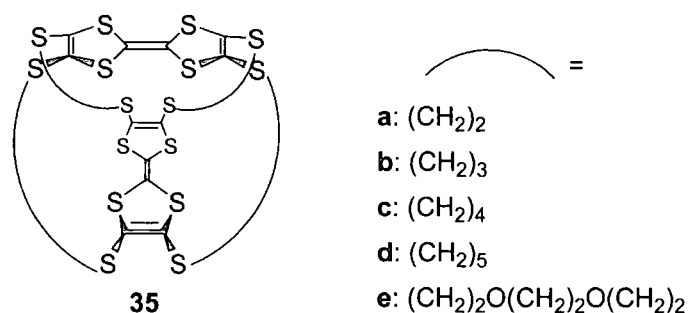


Figure 12: Criss-cross overlapped quadruple-bridged dimeric TTF cyclophanes.

The structures of **35a,c,d** were elucidated by X-ray crystallography. The short ethylenedithio bridges in **35a** force the TTF moieties into a bent boat-shape, whereas the TTF moieties in long-bridged **35d** are free from strain and the structure even allows for a molecule of chloroform to co-crystallise in the cavity (Figure 13).

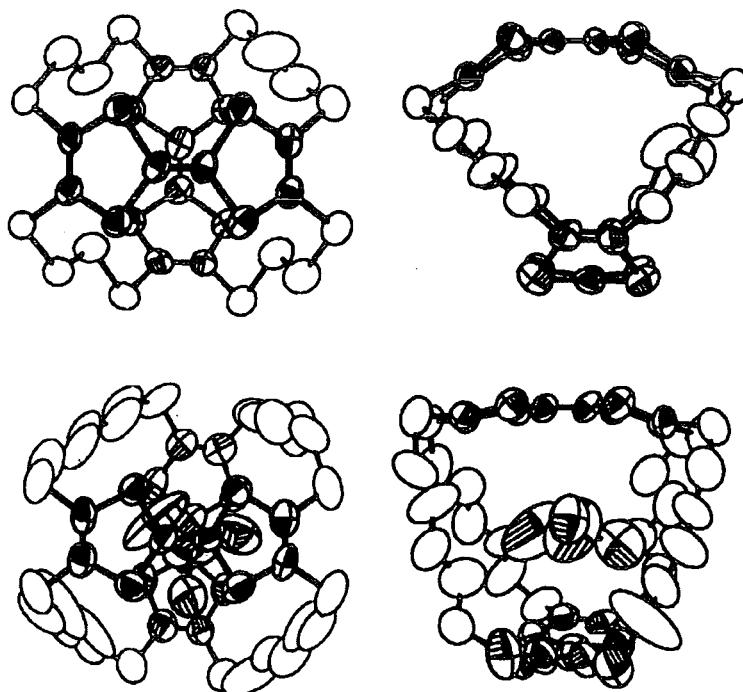
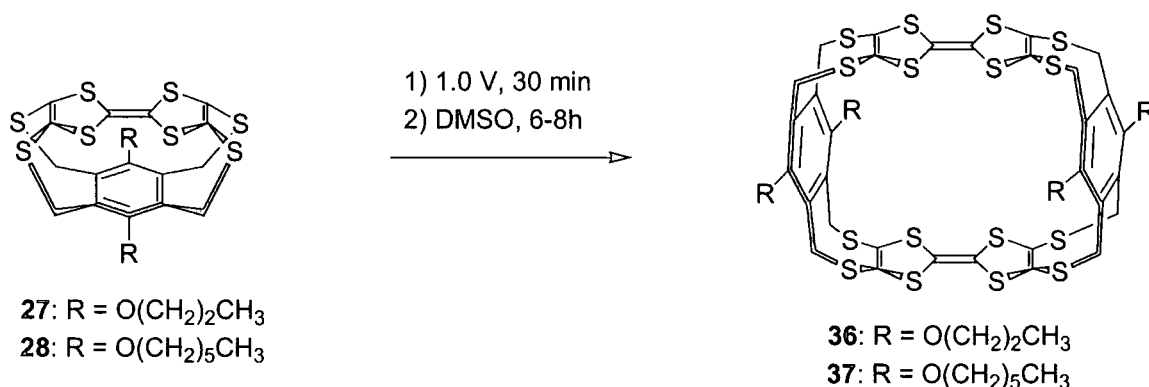


Figure 13: Top and side view of X-ray crystal structures of criss-cross overlapped dimeric TTF cyclophanes **35a (top) and **35d**·CHCl₃ (bottom).**⁴¹

The redox properties of **35a-d** are interesting. An irreversible oxidation wave at extraordinarily high potential was observed for the most strained **35a**, similar to what was

observed for the bent TTF cyclophanes mentioned above (section 1.2.4). Compound **35b** showed four, reversible, one-electron oxidation waves, indicating that each electron is removed from the system at different potentials, due to strong transannular Coulombic repulsion. For **35c** the transannular interaction is absent, and therefore the two TTF units within the same molecule act as electrochemically independent species, giving rise to two, reversible, two-electron oxidation waves. However, compound **35d** shows some unusual behaviour. The first wave is not split, but the potential is cathodically shifted in comparison to **35a,b,c** and the second wave is split into two. Thus electronic interaction is possible in pentamethylenedithio bridged **35d**. Even for the long-bridged cyclophane **35e** reported subsequently by Becher *et al*, an interaction is established between the two TTF moieties. For **35e** both oxidation waves were split into two.⁴²



Scheme 5: The first belt type TTF cyclophanes **36** and **37** were prepared by anodic oxidation of the strongly bent double-bridged monomeric TTF cyclophanes **27** and **28**, respectively.⁴³

The other class of quadruple-bridged dimeric TTF cyclophanes are the belt type systems **38** (Figure 14), in which the planes of the TTF moieties are overlapping parallel to each other. The first cyclophanes **36** and **37** of this type were prepared by anodic oxidation of the strongly bent double-bridged monomeric TTF cyclophanes **27** and **28**,²¹ respectively, followed by treatment of the isolated green-black microcrystalline solid with dimethylsulfoxide (Scheme 5).⁴³ Over the course of 6-8 h the green-black colour disappeared and a yellow solid of **36** and **37**, respectively, precipitated. X-ray analysis proved the structures of the products of this electrochemical reaction, which is believed to proceed through a metathesis-like dimerisation, although the mechanism has not been established. This explains why the CV of monomeric TTF cyclophanes **27** and **28** showed a single, irreversible, oxidation wave on the first scan, but common TTF redox behaviour on the following scans.

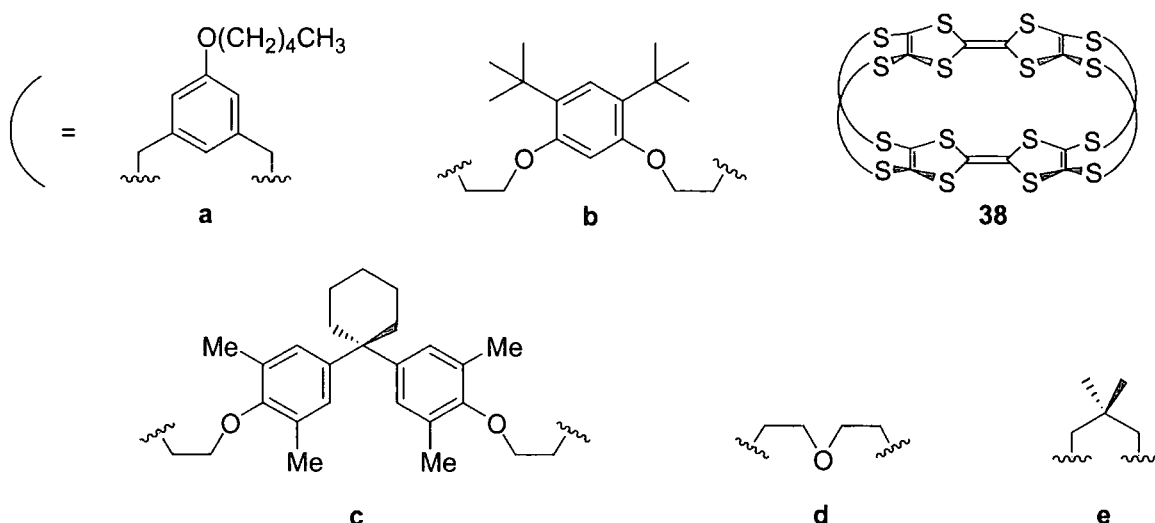


Figure 14: Examples of quadruple-bridged belt type TTF cyclophanes.

The first organic synthesis of a belt type TTF cyclophane **38e** (Figure 14) was reported by Otsubo *et al*, from a phosphite mediated coupling reaction of a precursor **25**, as depicted in Scheme 4, however, using the short 2,2-dimethylpropylene linker prevented intramolecular coupling to give **26** and also enhanced the solubility of the product **38e**.⁴⁴ The X-ray crystal structure of **38e** (Figure 15) shows that the TTF moieties are stacking in a face-to-face manner, with a slight bend into a boat shape. Surprisingly the CV of **38e** showed two, reversible, two-electron oxidation waves which were slightly anodically shifted, indicating only a weak intramolecular electronic interaction.

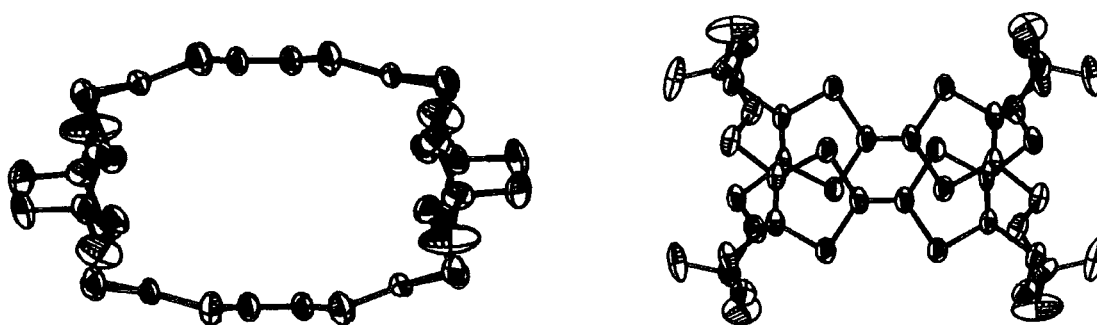


Figure 15: X-ray crystal structure of the belt type dimeric TTF cyclophane **38e** viewed from the side (left) and from the top (right).⁴⁵

The big push in the synthesis of TTF belts came from the group of Becher, who readily synthesised the series **38a-c** from premade TTF building blocks.³² The goal was to obtain TTF belts possessing large cavities, so they could act as potential host molecules for the inclusion of suitable π -electron acceptor guests. Hence long bridges were deployed. The

bridges used were also chosen for their rigidity and for possessing solubilising groups, since insolubility easily becomes a problem for TTF cyclophanes. The X-ray crystal structure of **38c** was reported, but results from complexation experiments or CV analysis were not given.⁴⁶ Subsequently Becher *et al.* published a different route to **38b**, and also the short-bridged belt **38d** was reported. The CV of both **38b** and **38d** showed two, reversible, two-electron oxidation waves, but only the potentials of **38b** were significantly anodically shifted.³⁶

1.2.7 Oligomeric TTF cyclophanes

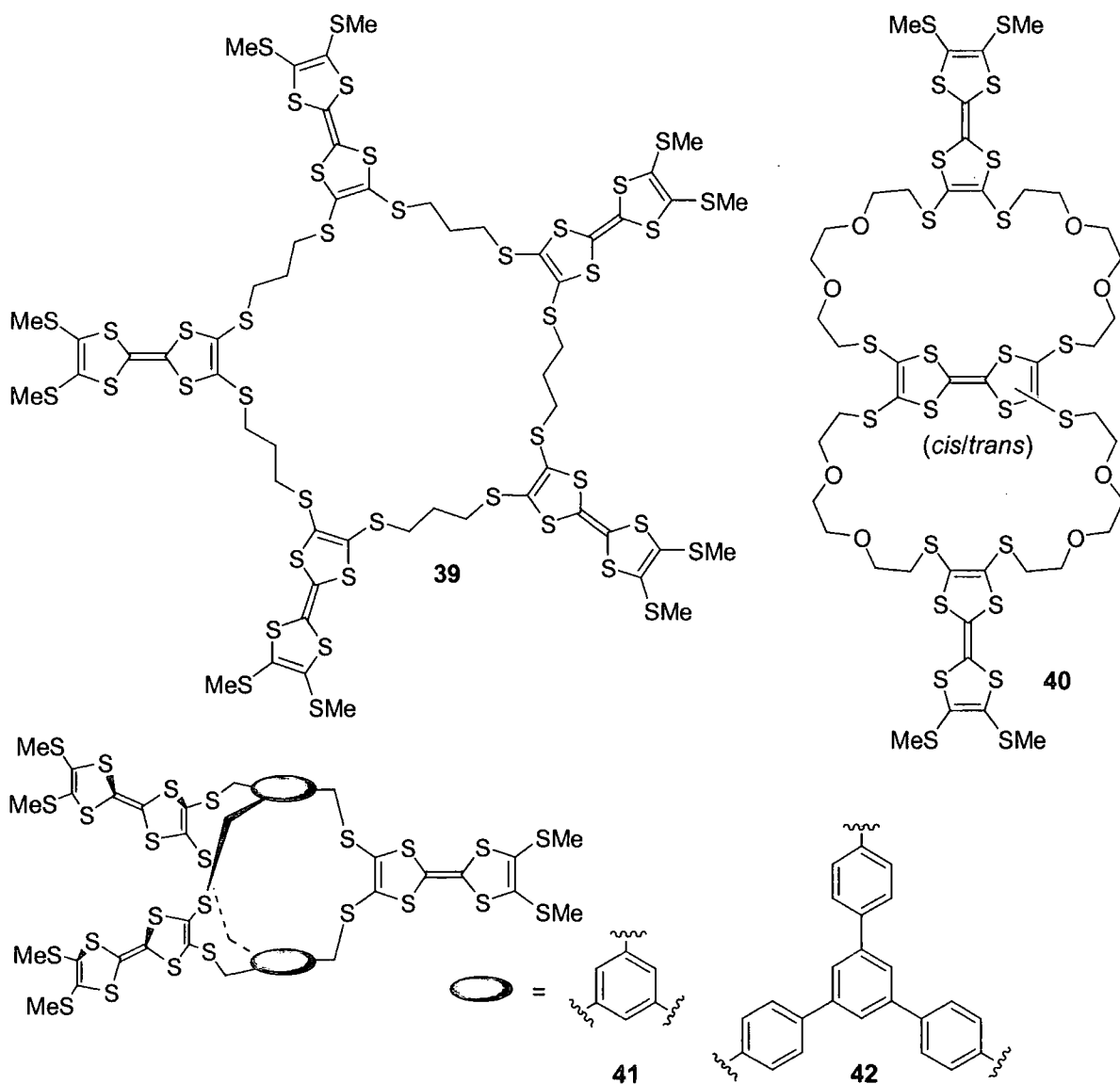


Figure 16: Oligomeric TTF cyclophanes synthesised from premade TTF building blocks.

Becher and co-workers have reported several complex oligomeric cyclophanes synthesised from premade TTF building blocks,³² but only four examples will be mentioned here (Figure 16). A series of cyclophanes, of which **39** was the highest oligomer, were synthesised to provide new donor assemblies which could potentially increase the dimensionality in derived conducting CT complexes.⁴⁷ The trimeric TTF cyclophane **40** was obtained as an inseparable *cis/trans* mixture, however, only the *cis* isomer was able to participate in subsequent catenane synthesis.⁴⁸ The cage molecules **41** and **42** are examples of the first three-directional macrobicyclic TTF cyclophanes, reported in 1996.⁴⁹ Large TTF cages like **42** should potentially be able to work as host molecules for acceptors in host-guest complexes, but no such complexes were reported for **42** or the related cyclophanes. Instead, an intramolecular electronic interaction was observed in the CV of **41**, in which the TTF moieties are positioned in close proximity, resulting in a broadening/splitting of the first oxidation wave.

1.2.8 TTF-acceptor cyclophanes

TTF readily forms intermolecular charge-transfer complexes with π -electron acceptors (section 1.2.2). Thus, incorporating both a TTF and an acceptor moiety in a cyclophane structure, in which the two redox active moieties could be locked in a face-to-face manner, should afford systems ideal for the study of through-space intramolecular charge-transfer (ICT) interactions, as originally proposed by Staab *et al.* (section 1.2.3).¹³ However, due to synthetic difficulties, only recently a few of such TTF-acceptor cyclophanes have been reported. An example of a TTF-benzoquinone cyclophane⁵⁰ will be discussed in section 3.1, and compared with other donor-acceptor systems which are not cyclophanes. The remaining examples will be reviewed in this section.

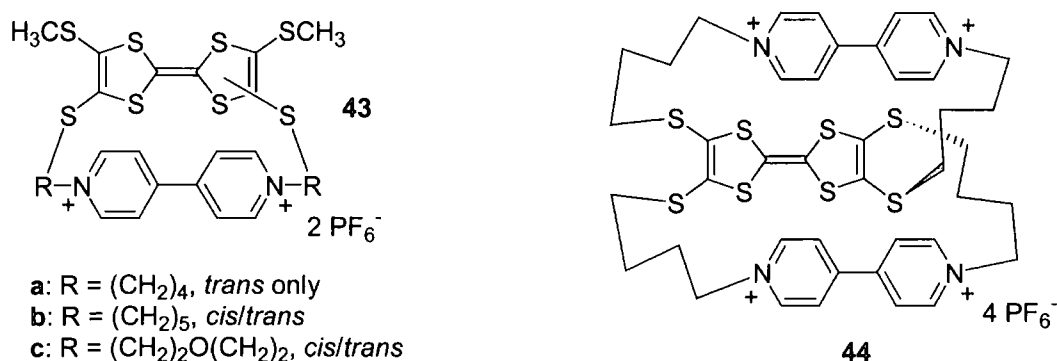


Figure 17: TTF-bipyridinium cyclophanes synthesised by Becher *et al.*^{51,52}

A series of TTF-bipyridinium cyclophanes **43** were reported by Becher and co-workers in 1997 as the first TTF-acceptor cyclophanes (Figure 17).⁵¹ For short-bridged **43a** only the *trans* isomer was formed, resulting in a rather rigid molecule as evidenced by an X-ray crystal structure, whereas a mixture of isomers was obtained for **43b** and **43c**. All cyclophanes **43a-c** showed ICT bands in their UV-vis absorption spectra, at $\lambda_{\max} = 650\text{-}673$ nm in acetonitrile. However, the absorption of the ICT band from short-bridged **43a** was *ca.* 4 times stronger than for **43b-c** possessing longer bridges, indicating a stronger electronic interaction when the redox active moieties are forced into close proximity. The following year the impressive acceptor-donor-acceptor cyclophane **44** was reported, showing properties similar to **43a**.⁵²

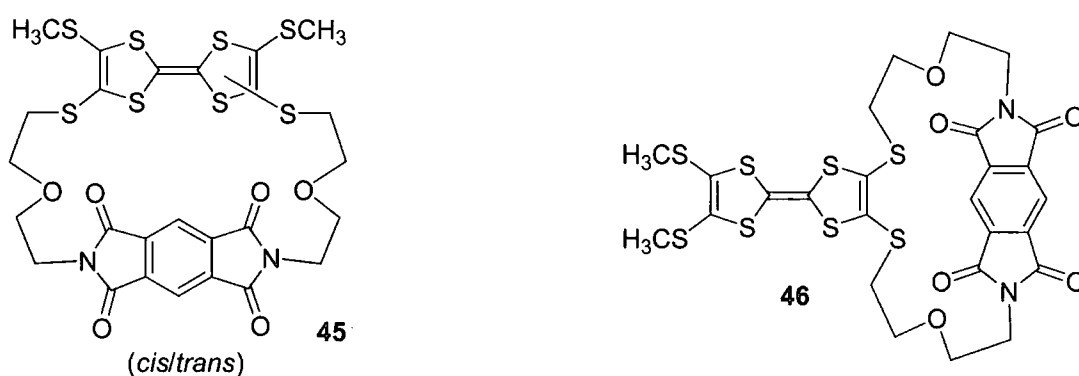


Figure 18: Pyromellitic diimide-TTF cyclophanes synthesised by Becher *et al.*⁵³

The final examples **45** and **46** incorporate the acceptor pyromellitic diimide into TTF cyclophanes.⁵³ Cyclophane **45** was obtained as a *cis/trans* mixture which crystallised as orange and green crystals, respectively, hence the crystals of the two isomers could be separated mechanically. The explanation for the difference in colour of **45-cis** and **45-trans** can be found in their X-ray crystal structures (Figure 19). For both **45-cis** and **45-trans** the TTF and the pyromellitic diimide moieties are nearly parallel. However, in **45-cis** the interplanar distance is 6.9 Å and the two redox active units are separated by a solvated toluene molecule, allowing no intramolecular charge-transfer interaction, whereas in **45-trans** the interplanar distance is only 3.45 Å, indicating an ICT interaction. Likewise, the solution UV-vis absorption spectra of **45-cis**, **45-trans** and **46** only showed a significant CT band for **45-trans** ($\lambda_{\max} = 590$ nm in dichloromethane), indicating that the *trans* configuration allows for efficient intramolecular electronic interaction.

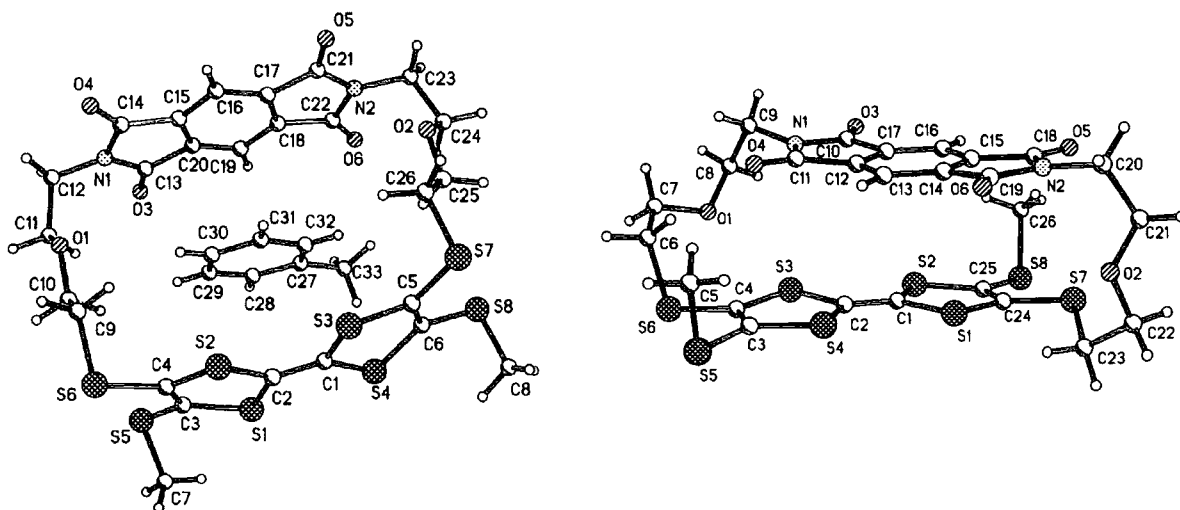


Figure 19: X-ray crystal structures of pyromellitic diimide-TTF cyclophanes **45-cis** (left) and **45-trans** (right). The structure of **45-cis** contains one molecule of toluene.⁵⁴

1.3 CONCLUSIONS

Cyclophanes are not just molecules with beautiful architecture, but offer a unique possibility for placing aromatic rings relative to one another in a tailor-made fashion, thereby inflicting ring strain and/or intramolecular electronic interaction between the aromatic moieties. Incorporation of the good π -electron donor TTF into cyclophane structures has afforded compounds with interesting redox properties unlike any other TTF derivatives, which has awarded the TTF chemist with invaluable knowledge. Furthermore, the chemistry of TTF is no longer restricted to the synthesis of new CT salts, since TTF cyclophanes have found applications in supramolecular chemistry.

In this chapter we have seen many examples of TTF cyclophanes with properties modified by altering the positions, number and nature of the bridges. Alternatively, new interesting redox active cyclophanes could be synthesised by incorporation of analogues, but structurally modified, TTF derivatives. In our group, we have intensively studied a derivative suitable for this purpose, namely the TTF analogue TTFAQ.

2 AN INTRODUCTION TO TTFAQ

The redox active species which is fundamental to the work presented in this thesis is 9,10-bis(1,3-dithiol-2-ylidene)-9,10-dihydroanthracene **49** (section 2.2), which in the remainder of this text will be abbreviated to TTFAQ. This chapter will give an introduction to TTFAQ, with emphasis on its chemical and physical properties, by reviewing the most important results from the literature available at the outset of this project. One new result (section 2.2.4), obtained by the author during the course of this work, will also be included. The most recent TTFAQ literature containing results of more special interest, will be compared to the results of this thesis and will be discussed in the appropriate chapter.

2.1 EXTENDED TETRATHIAFULVALENES – THE GENESIS OF TTFAQ

The story of TTFAQ starts with tetrathiafulvalene (TTF) **9** (see section 1.2.2). Much synthetic effort has been devoted to systematically varying the structure of TTF, thereby changing the oxidation potentials, symmetry and size of the donor. One area has been derivatives of TTF in which a conjugated π -framework separates the 1,3-dithiole rings, *i.e.* “extended tetrathiafulvalenes”. Extending conjugation in this manner increases the stability of the cation radical and dication because of greater π -delocalisation. More importantly, the dication state is stabilised considerably, relative to the TTF dication, due to the reduced intramolecular Coulombic repulsion energy.

2.1.1 Vinylogous tetrathiafulvalenes

One class of extended tetrathiafulvalenes is the vinylogous tetrathiafulvalenes. The first two examples **47**⁵⁵ and **48**⁵⁶ were reported by Yoshida *et al.* in 1983.



Figure 20: Vinylogous tetrathiafulvalenes synthesised by Yoshida *et al.*^{55,56}

A lowering of the oxidation potentials relative to TTF **9** was observed in the cyclic voltammograms (see oxidation potentials in Table 1). Compound **47** showed two, reversible, one-electron oxidation waves like TTF, but not only were the potentials lower, but also $E_2^{1/2} - E_1^{1/2}$ was smaller, which indicates that Coulombic repulsion in the dication 47^{2+} has decreased compared to the TTF dication. For compound **48** oxidation is seen as a single, reversible, two-electron oxidation wave, indicating that the two 1,3-dithiole units behave independently.^{55,56}

Compound	$E_1^{1/2}/V$	$E_2^{1/2}/V$	$(E_2^{1/2} - E_1^{1/2})/V$
9	0.34 (1)	0.71 (1)	0.37
47	0.20 (1)	0.36 (1)	0.16
48	0.22 (2)	-	-

Table 1: CV data for TTF **9**, compound **47** and **48**. The number in parenthesis indicates the number of electrons involved in the oxidation wave. The CV experiments were carried out in a 0.1 M acetonitrile solution of tetraethylammonium perchlorate using Ag/AgCl as reference.⁵⁷

2.2 TTFAQ AND ITS PROPERTIES

TTFAQ **49** can be considered as another class of extended tetrathiafulvalenes having the 1,3-dithiole units separated by an anthraquinonoid spacer, hence the abbreviation TTFAQ.

2.2.1 The solid state conformation of TTFAQ and the TTFAQ dication

The first TTFAQ derivative **50** was reported by Akiba *et al.* in 1978,⁵⁸ although it was not made with any reference to extended TTF derivatives. Pioneering work on TTFAQ derivatives was carried out by Bryce *et al.* in the late 1980's.⁵⁹ The synthesis of tetramethyl derivative **52** was reported in 1988,⁶⁰ and the TTFAQ analogue of BEDT-TTF, compound **51**,⁶¹ was another early example. The first report of the parent system, TTFAQ **49**, was by Yamashita *et al.* in 1989.⁶²

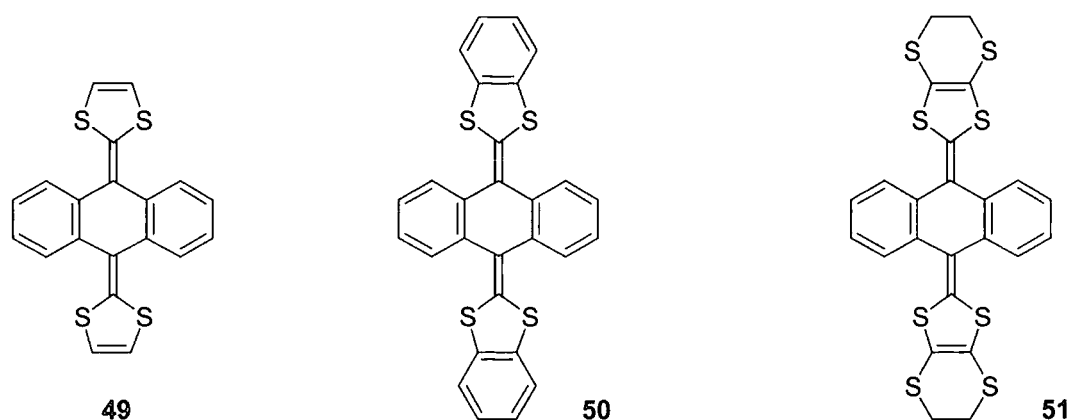


Figure 21: Examples of early TTFAQ derivatives.

The X-ray crystal structure of TTFAQ derivative **52** (Figure 22), revealed that the molecule is not flat like TTF, but saddle-shaped with the central quinonoid ring distorted into a boat form. The reason is steric repulsion between the 1,3-dithiole ring sulfur atoms and the *peri*-hydrogen atoms.⁶³ The structure of **52** has later been supported by theoretical calculations, and the calculated structure of **52** was very similar to the calculated structure of TTFAQ **49** itself. For TTFAQ the short contacts between the sulfur atoms and the hydrogen atoms in *peri* positions were calculated to be 1.78 Å, *i.e.* half of the van der Waals distance of 3.60 Å. To avoid these contacts, the molecule has to fold into the saddle-shape.⁶⁴

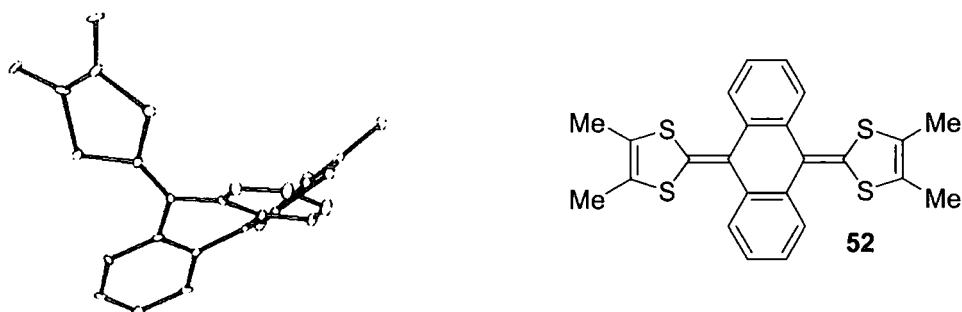


Figure 22: The X-ray crystal structure of compound **52** shows the characteristic saddle-shape.⁶⁵

The charge-transfer salt between **52** and TCNQ **13** showed good conductivity, and crystals suitable for X-ray crystallography provided the first opportunity to compare the structure of a TTFAQ derivative in its oxidised state with that of the neutral derivative. The crystal structure of oxidised **52** (Figure 23) revealed that the TTFAQ unit, now in its dication state **52**²⁺, adopted a dramatically different conformation from that of the neutral species. The central anthraquinonoid system had become aromatic anthracene and the two oxidised aromatic

1,3-dithiolium moieties formed dihedral angles of 86.0° with the planar anthracene unit.⁶³ This solid state structural behaviour upon oxidation should also be reflected in the solution redox properties of TTFAQ (section 2.2.3).

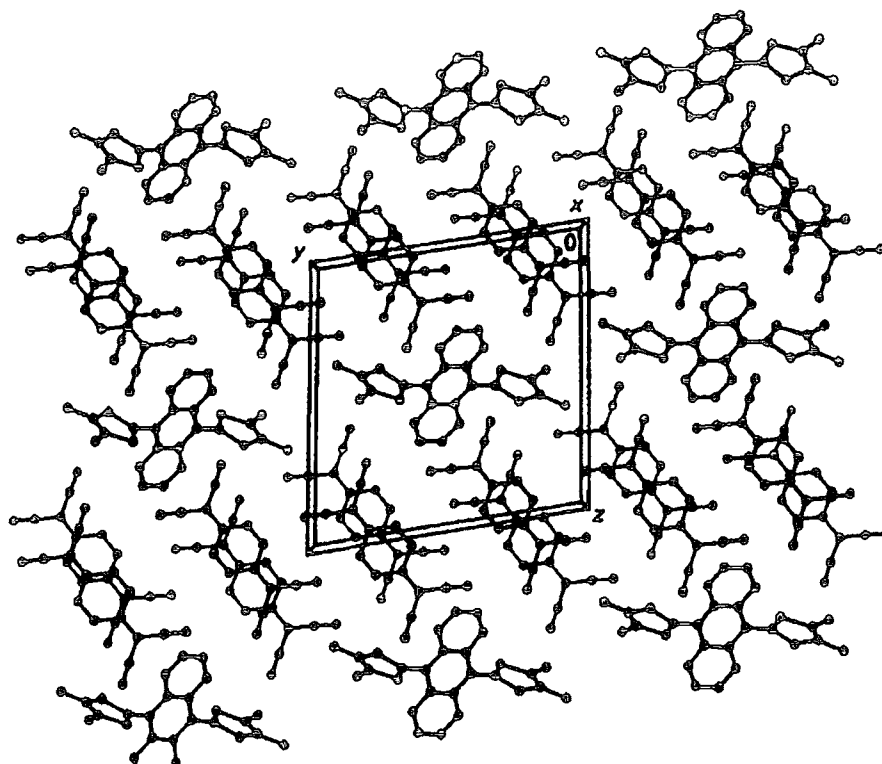


Figure 23: The packing diagram of the 1:4 CT complex of **52** with TCNQ **13**.⁶⁵

2.2.2 The conformation of TTFAQ in solution

Inspection of the ^1H NMR spectra of some TTFAQ derivatives indicated that TTFAQ was also non-planar in solution. Godbert in our group studied derivative **53** (Figure 24).⁶⁶ At room temperature the two methylene protons H_A and H_B have different chemical shifts, proving that they are diastereotopic and hence that **53** is not planar in solution. The difference in chemical shift for H_A and H_B at 20°C suggested that the molecule exists as two conformers (Figure 24) which interconvert slowly (by a boat-boat flipping of the central ring) on the NMR timescale at this temperature, giving a four-line AB system ($J_{\text{AB}} \approx 13$ Hz). However, at 100°C these four lines have coalesced, *i.e.* interconversion is fast, with H_A and H_B no longer differentiated.

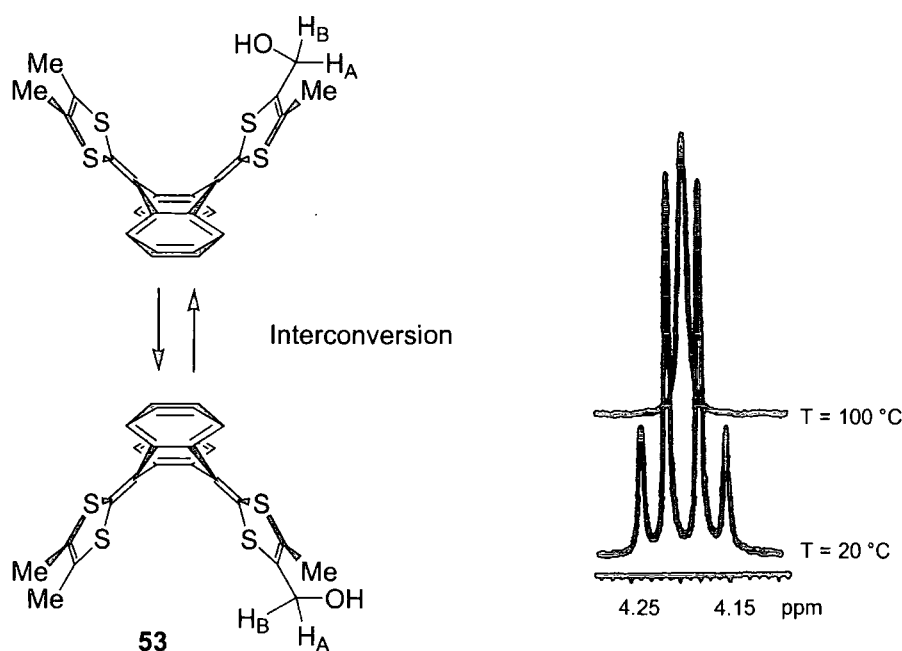
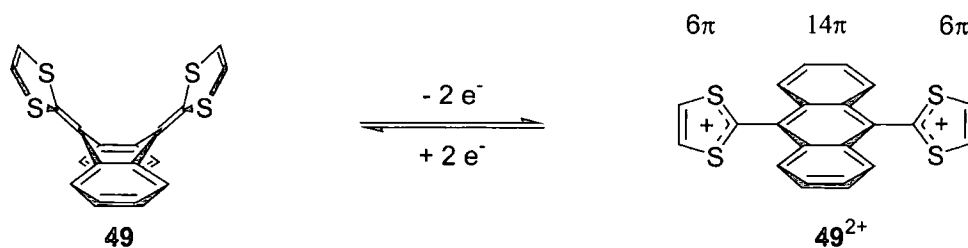


Figure 24: In solution TTFAQ and its derivatives, like **53**, are flipping between two conformers (left). The two diastereotopic protons H_A and H_B of **53** form an AB system and become indistinguishable in the ^1H NMR spectrum at 100 °C in $\text{DMSO-}d_6$ (right).⁶⁷

2.2.3 Solution redox properties of TTFAQ

The introduction of the anthraquinonoid spacer unit has effects on the solution redox properties similar to those seen for the vinylogous extended TTF derivatives (section 2.1.1). However, not only is the dication of TTFAQ **49**²⁺ stabilised compared to the TTF dication **9**²⁺, due to a reduction of the Coulombic repulsion between the two 1,3-dithiolium rings, but also because the anthraquinonoid spacer becomes a flat 14π aromatic system (Scheme 6). Contrary to this, the TTFAQ cation radical **49**^{•+} (Figure 29), which has never been isolated (see section 2.2.5), retains most of its saddle-shaped conformation, according to theoretical calculations.⁶⁴ Hence the cation radical gains only little aromaticity, which makes it unstable with respect to the TTFAQ dication. Therefore, the potential of the first oxidation to form the TTFAQ cation radical **49**^{•+} is anodically shifted to coalesce with the second oxidation potential,⁶⁴ and as a consequence the CV of TTFAQ **49** shows a single, two-electron, redox couple (oxidation peak potential E_{pa} at 0.37 V vs. Ag/AgCl in a 0.1 M acetonitrile solution of tetrabutylammonium hexafluorophosphate, scan rate 100 mV s⁻¹).⁶⁸ However, contrary to both TTF and the extended TTF derivatives **47** and **48**, the oxidation is not electrochemically reversible, instead it is quasi-reversible.⁶⁹ This can be explained by the dramatic conformational change upon oxidation, as observed in the crystal structures of **52** and **52**²⁺

(section 2.2.1). Upon oxidation of the saddle-shaped TTFAQ **49**, the anthraquinonoid system becomes aromatic and planar anthracene, and the 1,3-dithiolium rings are free to rotate until they are nearly perpendicular to the anthracene plane (Scheme 6). To overcome the energy barrier of making the aromatised and thermodynamically very stable TTFAQ dication $\mathbf{49}^{2+}$ revert into the saddle-shape, an overpotential is needed, hence the quasi-reversibility of the system. This explanation is supported by the fact that upon cooling the oxidation peak is unchanged, whereas the peak for reduction of the dication is shifted progressively to more negative potentials with decreasing temperature.⁷⁰ Furthermore, similar redox behaviour was observed for a dibenzoannelated terphenoquinone derivative, the two-electron reduction wave of which was also quasi-reversible, due to restricted conformational change.⁷¹



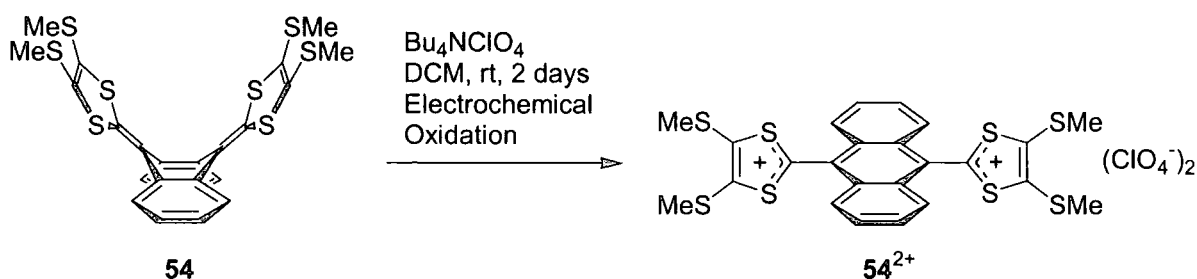
Scheme 6: Oxidation of TTFAQ **49** to the dication species $\mathbf{49}^{2+}$ is only quasi-reversible, due to the conformational change upon oxidation.

Similar to derivatives of TTF, electron withdrawing substituents shift the oxidation potential of TTFAQ to more positive values, whereas the opposite is true for electron donating substituents.⁶⁴

2.2.4 An electrocrystallised dication salt of TTFAQ derivative **54**

Prior to the work presented in this thesis, only 3 crystal structures of dication salts of TTFAQ derivatives were known, all of them from donor-acceptor complexes with TCNQ **13**.^{63,72,73} Electrocrystallisation is a well known and powerful tool to assemble molecular ions into high quality single crystals,⁷⁴ and a crystal with relatively small closed shell anions, instead of bigger acceptor molecules, could shed more light on the structure of the TTFAQ dication. The very crystalline TTFAQ derivative **54**, which was first reported briefly by Saito *et al.* in 1994,⁷⁵ and which has also been known in the Bryce group for several years,⁷⁶ was chosen as the candidate for electrocrystallisation.⁷⁷ The dication salt was obtained using tetrabutylammonium perchlorate as the electrolyte in dichloromethane (Scheme 7). After only

two days thin red needle-shaped crystals, up to 5 mm in length, were harvested from the anode and submitted for an X-ray crystallographic analysis.⁷⁸



Scheme 7: Electrocrystallisation of TTFAQ derivative 54.

For comparison, the X-ray crystal structure of neutral **54** is shown in Figure 25.⁷⁶ The molecule adopts the characteristic saddle-shape, as a consequence of the steric repulsion between the sulfur atoms and the *peri*-hydrogen atoms.

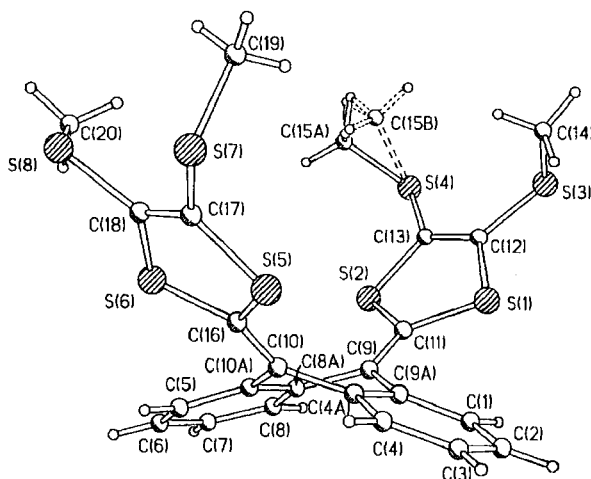


Figure 25: X-ray crystal structure of neutral 54 possessing the characteristic saddle-shape. One of the methyl groups is disordered over two positions.⁷⁹

In the crystal structure of $\mathbf{54}^{2+}(\text{ClO}_4^-)_2$, the anion occupies a general position, while the dication $\mathbf{54}^{2+}$ has crystallographic C_i symmetry (Figure 26).⁷⁷ The conformation of the dication is very different from the saddle-shape of neutral **54**. The anthracene moiety is planar and has essentially the geometry of the anthracene molecule,⁸⁰ that is, it is fully aromatic. The planar 1,3-dithiolium rings and the anthracene system form a dihedral angle of 77.2° and are linked through an essentially single bond: C(7)-C(8) 1.490(3) Å. The 1,3-dithiolium rings in $\mathbf{54}^{2+}$ display stronger π -conjugation than in the neutral molecule **54**. The C-S bonds in the

dication [“inner” S(1)-C(8) 1.695(2) Å and S(2)-C(8) 1.672(2) Å; “outer” S(1)-C(9) 1.734(2) and S(2)-C(10) 1.708(2) Å] are contracted compared with neutral **54** with averages 1.767(4) Å and 1.759(5) Å for the “inner” and “outer” C-S bonds, respectively,⁷⁶ while the C(9)-C(10) bond is lengthened from 1.334(7) Å in **54** to 1.375(3) Å in **54**²⁺(ClO₄)₂.⁸¹

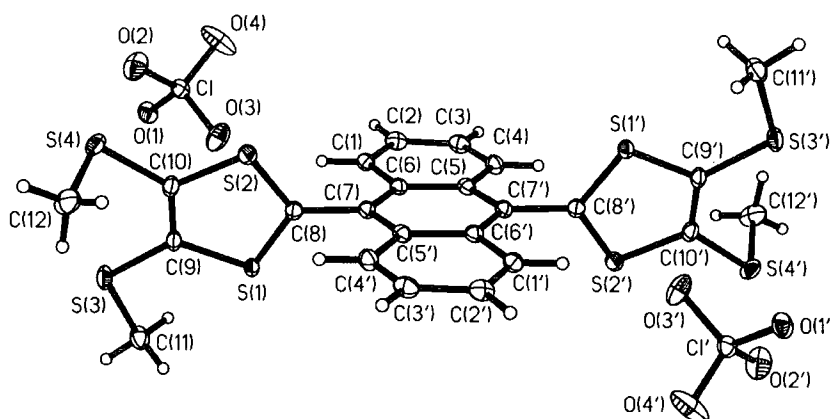


Figure 26: X-ray crystal structure of **54**²⁺(ClO₄)₂ showing 50% thermal ellipsoids. Primed atoms are generated by the inversion centre. The saddle-shape of neutral **54** is not retained upon oxidation to the dication.⁷⁸

The crystal packing of **54**²⁺(ClO₄)₂ is shown in Figure 27. Interactions of the S(1) atom with two perchlorate anions can explain the weakening of the S(1)-C bonds in the dithiolium ring compared with the S(2)-C bonds. There are no S...S contacts significantly shorter than twice the van der Waals radius of S (3.68 Å).⁸²

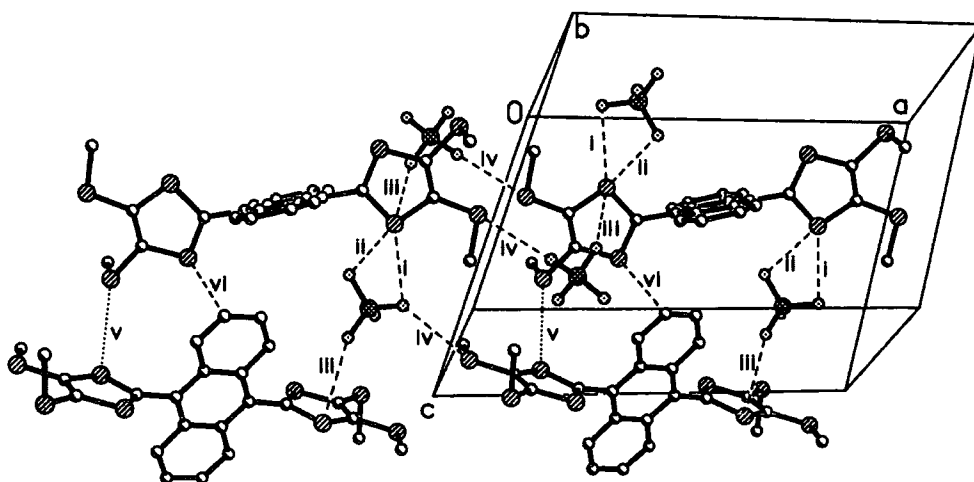


Figure 27: Crystal packing of **54**²⁺(ClO₄)₂. Shortest intermolecular contacts (in Å): S...O i = 3.335(2), ii = 3.205(2), iii = 3.277(2), iv = 3.157(2); S...S v = 3.655(1); S...C vi = 3.450(2).⁷⁸

2.2.5 Optical properties of TTFAQ derivative 54 and its oxidised species

We have also obtained the electronic absorption spectra of TTFAQ derivative **54**, which is representative for the TTFAQ derivatives presented in this thesis, and of the oxidised species of **54**, by performing spectroelectrochemistry.⁸³ The UV-vis absorption spectrum of neutral **54** has two strong bands at $\lambda_{\text{max}} = 366$ and 435 nm, typical for alkylthio substituted TTFAQ derivatives. Upon oxidation these bands collapse giving way to bands ascribed to the dication **54**²⁺ (see Scheme 7) at $\lambda_{\text{max}} = 377$, 392 and 419 nm, and a broad band which tails into the visible part of the spectrum with $\lambda_{\text{max}} = 479$ nm (Figure 28).⁷⁸

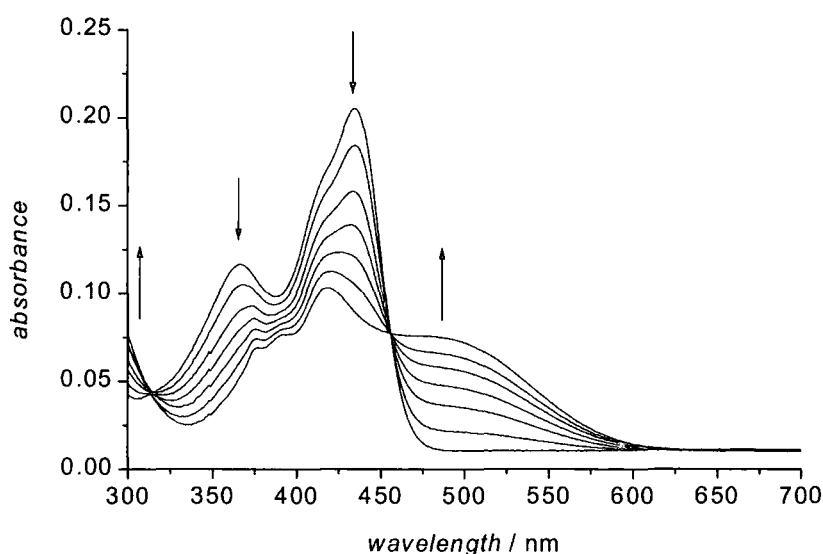


Figure 28: Spectroelectrochemistry of TTFAQ derivative **54** in dichloromethane.⁷⁸

Although no cation radical salt of any TTFAQ derivative has ever been isolated, or even observed in the cyclic voltammogram (see section 2.2.3), the cation radical of **54** has been generated as a transient species, both by our group⁷⁷ and by Martín *et al.*⁸⁴

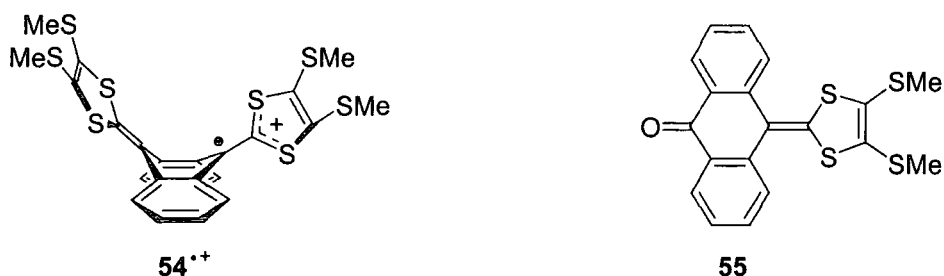


Figure 29: The unstable cation radical **54**^{•+} and the degradation product **55**.

Flash photolysis of **54** in degassed chloroform afforded $54^{*\cdot+}$ (Figure 29) as a transient species, which decayed to half its initial intensity over a period of 80 μs , by disproportionation to **54** and the dication 54^{2+} . When photolysis was carried out in aerated chloroform, the degradation product instead was ketone **55** (Figure 29), but the mechanism of the formation of **55** was never established.⁷⁷ The cation radical $54^{*\cdot+}$ has a characteristic absorption band at $\lambda_{\text{max}} = 650 \text{ nm}$ (Figure 30).⁷⁸ Consistent with this, Martín *et al.* reported an absorption band of the cation radical species, generated by pulse radiolysis of **54** in oxygenated dichloromethane, at $\lambda_{\text{max}} = 675 \text{ nm}$.⁸⁴ Martín and co-workers also obtained transient charge-separated species, generated by photoinduced charge-transfer in TTFAQ- C_{60} dyads, containing a TTFAQ cation radical moiety (see section 3.1.1).⁸⁵

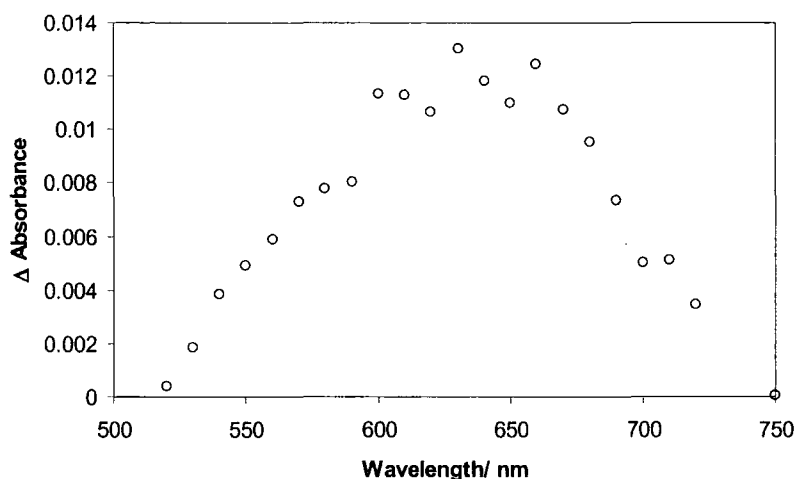


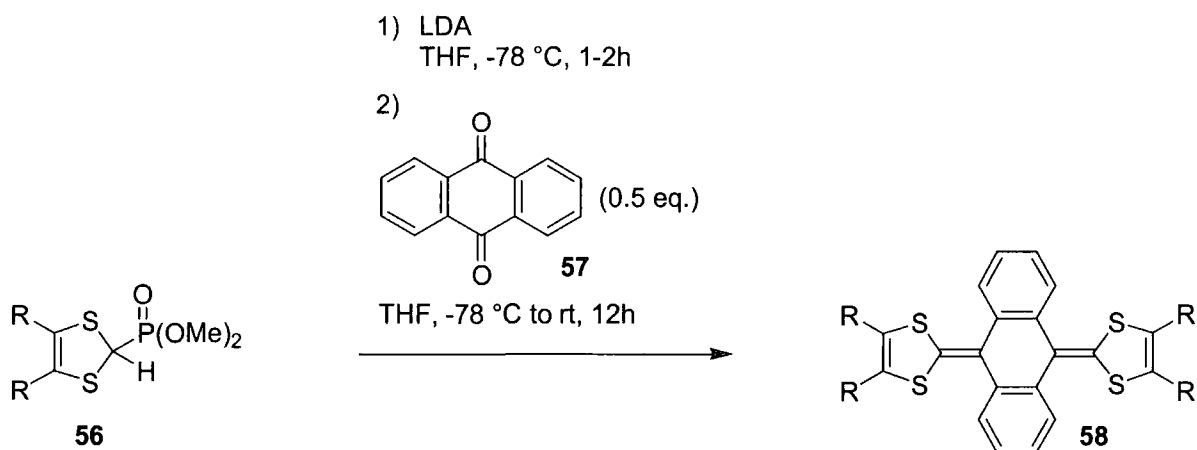
Figure 30: Absorption spectrum of the transient cation radical $54^{*\cdot+}$ obtained upon 266 nm irradiation of **54 in degassed chloroform.**⁷⁸

The Raman spectrum of $54^{*\cdot+}$ was also recorded,⁷⁸ which supported the theoretical calculations by Martín *et al.*,⁶⁴ stating that the cation radical species retains a folded quinonoid conformation similar to the neutral species **54**, which makes it unstable with respect to the aromatised dication.

2.3 SYNTHESIS OF TTFAQ

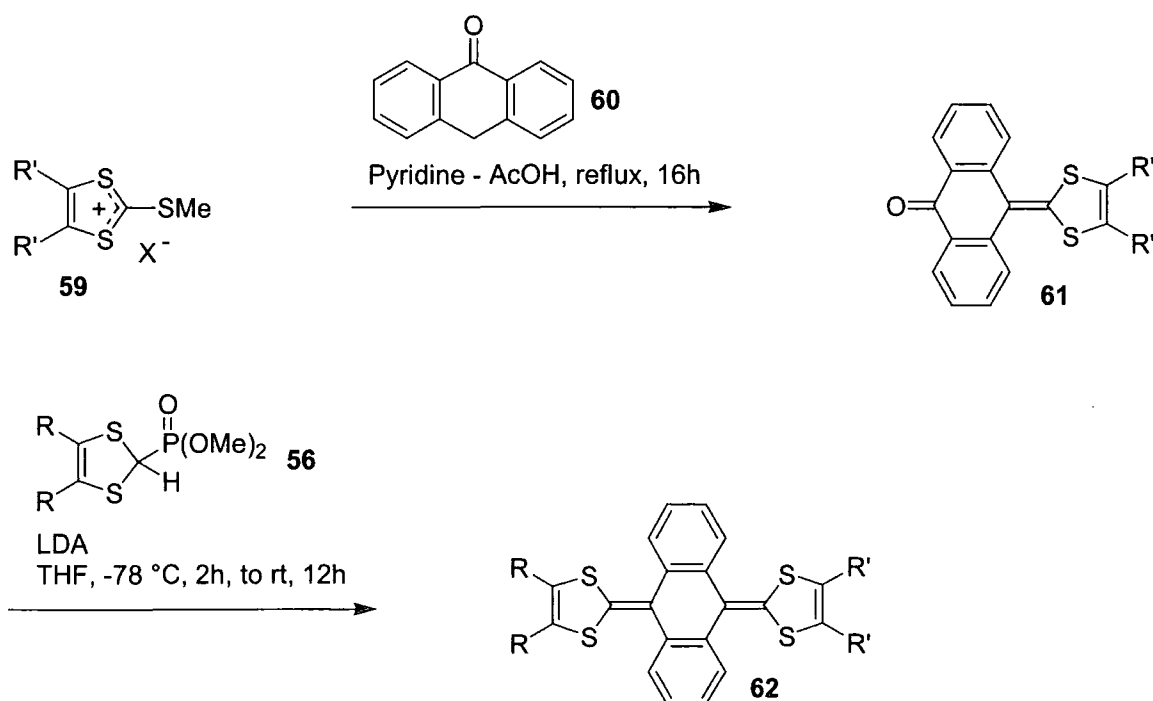
The general methodology for synthesising TTFAQ derivatives was first described in detail by Moore and Bryce in 1991.⁸⁶ For simple symmetric⁸⁷ TTFAQ derivatives **58** two-fold Horner-Wadsworth-Emmons olefination between anthraquinone **57** and the carbanion from the

corresponding 1,3-dithiole phosphonate ester **56**, generated by deprotonation using butyl lithium or lithium diisopropylamide (LDA), leads to the desired TTFAQ derivative (Scheme 8). Phosphoranes have also been reacted with anthraquinone in Wittig reactions to give TTFAQ derivatives, but the Horner-Wadsworth-Emmons reaction was found to be superior.^{58,86,88}



Scheme 8: Synthesis of symmetric TTFAQ derivatives.⁸⁷

Unsymmetrical TTFAQ derivatives **62**, that is derivatives comprising two different 1,3-dithiole units, are synthesised in two steps (Scheme 9).



Scheme 9: Synthesis of unsymmetrical TTFAQ derivatives.⁸⁷

First a 1,3-dithiolium salt **59** is reacted with anthrone **60** in refluxing pyridine-acetic acid 3:1 (v/v) affording the ketone **61** in an addition-elimination reaction. The source of the other 1,3-dithiole unit is a phosphonate ester **56** which undergoes Horner-Wadsworth-Emmons olefination with the ketone **61** under conditions similar to those used for the synthesis of symmetrical TTFAQ derivatives **58**. Since both steps give good yields, this two-step synthesis is to be preferred over any cross-coupling method which always gives rise to complex product mixtures.^{86,89}

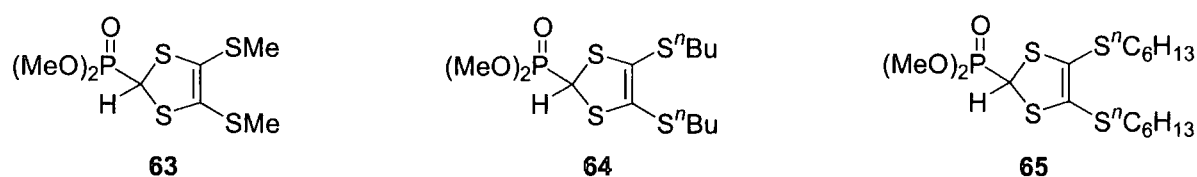


Figure 31: Phosphonate esters used in this thesis.

A wide range of phosphonate ester derivatives **56** are readily available, but throughout the work presented in this thesis, 4,5-bis(alkylthio)-1,3-dithiole phosphonate esters **63-65** (Figure 31) have been used exclusively. Phosphonate ester **63** was first reported by Bryce *et al.*,⁹⁰ and soon after used by Fourmigué and co-workers.⁹¹ The phosphonate esters **64** and **65** bearing butylthio and hexylthio groups, respectively, were reported by Yamashita *et al.*, who synthesised several phosphonate esters.⁹² Appendix One will give a detailed account of the synthesis of the phosphonate esters **63-65**, even though they are all known from the literature. The reason is the often limited information concerning their synthesis available in the literature, combined with the unpublished modifications which have been developed over the years.

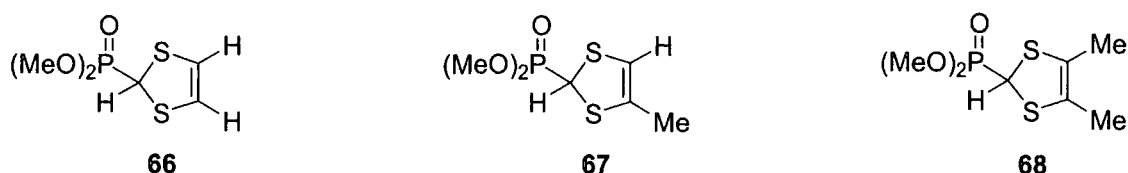


Figure 32: Three of the most commonly used phosphonate esters.

The synthesis of three other phosphonate esters, the very common **66**,⁹³ **67**⁹⁴ and **68**⁹⁵ reported by Bryce and co-workers, will also be reviewed in Appendix One. Especially **66** and **67** are important, since they are needed for unsubstituted TTFAQ derivatives, which again are precursors for TTFAQ derivatives functionalised by lithiation (see also section 6.1.1).⁹⁶

2.4 CONCLUSIONS

During the last decade, the chemistry of TTFAQ has been investigated and developed, because of its interesting electrochemical and conformational properties. TTFAQ is a saddle-shaped electron donor which is readily oxidised to its dication in a single, quasi-reversible, two-electron oxidation wave. Upon oxidation the TTFAQ molecule dramatically changes conformation. The central anthraquinonoid moiety becomes aromatic planar anthracene, and the formed 1,3-dithiolium rings rotate until they are nearby perpendicular to the anthracene plane. These features make TTFAQ remarkably different from other electron donors, including TTF, and thus an obvious candidate as the active unit in new redox active cyclophanes.

The TTFAQ cation radical has never been isolated, or even seen in a cyclic voltammogram, but it has been generated as a transient species by flash photolysis. Theoretical calculations show that the reason for the instability of the TTFAQ cation radical is its saddle-shaped conformation, which makes it unstable towards the aromatised TTFAQ dication. However, incorporating TTFAQ into more complex molecular assemblies, whether cyclophanes or donor-acceptor systems, could manipulate the properties of TTFAQ to stabilise its cation radical state. Especially interesting would be the behaviour of the TTFAQ moiety upon oxidation, when conformationally locked in a cyclophane structure. Hence, the task was to synthesise new TTFAQ building blocks which would be ideal for the incorporation of the TTFAQ unit into cyclophanes and other challenging structures.

3 NEW CONJUGATED DONOR-ACCEPTOR AND DONOR-DONOR DYADS CONTAINING TTFAQ

This chapter describes the synthesis and characterisation of a new conjugated donor-acceptor and a new conjugated donor-donor dyad containing TTFAQ. Originally the emphasis of this project was to develop a TTFAQ building block, which could be utilised in the synthesis of new donor-acceptor systems linked through conjugation. Thus, this chapter will begin with a short introduction to some covalently linked TTF- and TTFAQ-acceptor systems.

3.1 COVALENTLY LINKED TTF- AND TTFAQ-ACCEPTOR SYSTEMS

Although substantial research on intermolecular charge-transfer materials containing TTF **9** has been done in the last 3 decades (see section 1.2.2), TTF has only recently been utilised as a donor in intramolecular systems, mainly due to synthetic obstacles. Nonetheless, systems containing TTF covalently linked to different acceptors such as TCNQ-derivatives, quinones, pyridinium units, pyromellitic diimide and fullerenes have been reported.^{51,53,97}

When TTF is covalently linked to an electron acceptor, it sometimes gives rise to intramolecular charge-transfer (ICT), which is most frequently manifested in the optical and electrochemical properties. Hence these and other covalently linked donor-acceptor molecules have potential use as molecular electronic devices, as chromophores for dyes, as artificial photosynthetic models, in non-linear optics (NLO) and for studying excited-state energy transfer processes.⁹⁷ Incorporating TTFAQ into donor-acceptor derivatives should yield very interesting structures, because of the very stable aromatised TTFAQ dication and its only quasi-reversible reduction to give the neutral species (section 2.2.3), which should help to stabilise a potential charge-separated state. The correct donor-acceptor system would maybe even give us the chance to study the structure and optical properties of the first stable TTFAQ radical cation species.

3.1.1 TTFAQ-Acceptor Systems

At the planning stages of this project, only 2 publications in which TTFAQ had been covalently linked to an acceptor were known. Martín *et al.* reported the first TTFAQ-C₆₀ dyad, showing clean amphoteric redox active behaviour, having 4 one-electron, quasi-reversible, reduction waves from the C₆₀ moiety and a single, quasi-reversible, two-electron oxidation wave from the TTFAQ unit. However, no charge-transfer, neither intra- nor intermolecularly, was observed. Calculations suggested an unfavourable geometry for ICT to be the reason.⁹⁸ Instead, Martín and co-workers the following year reported TTFAQ-dicyanovinyl derivatives **69-74** (Figure 33), having the donor and acceptor moieties separated by a conjugated system. Compounds **69-74** showed an ICT band with $\lambda_{\text{max}} = 549\text{-}571$ nm in the absorption spectrum, and were found to behave as efficient NLO chromophores.⁹⁹

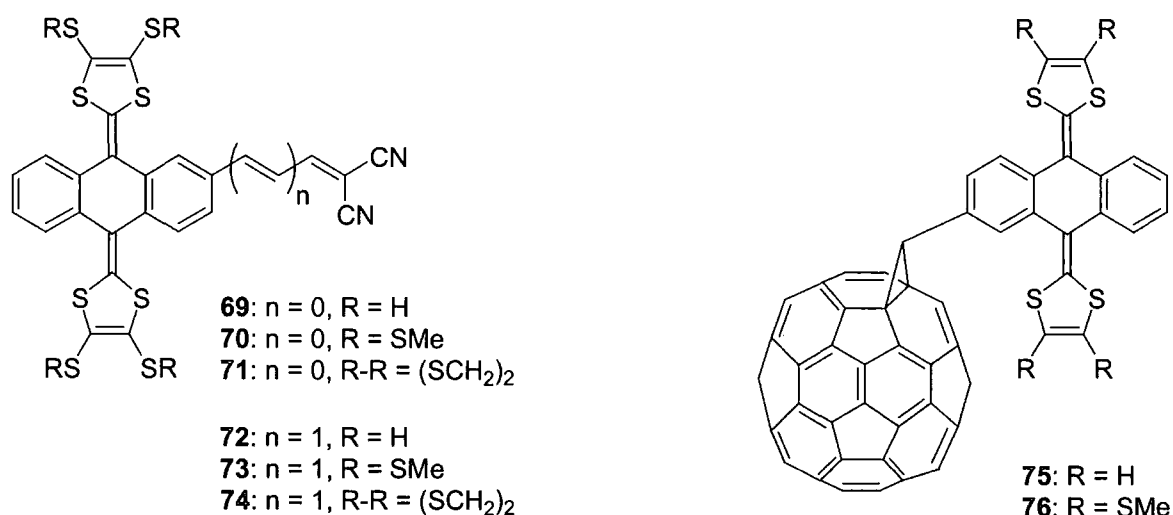


Figure 33: TTFAQ based donor-acceptor compounds synthesised by Martín *et al.*^{85,99}

Since the completion of our work, Martín *et al.* has reported other TTFAQ-acceptor compounds. These include further elaboration on the system **69-74**,¹⁰⁰ but predominantly it has been new results with TTFAQ-C₆₀ dyads,¹⁰¹ and also some triads containing TTF as the third redox active species have been reported.¹⁰² None of the TTFAQ-C₆₀ dyads or triads showed any charge-transfer in the ground state, but ICT could be photoinduced.^{85,102} Hence, photoexcitation of **75-76** afforded the fullerene singlet excited state, which is a stronger acceptor, and thus the dyad rapidly underwent intramolecular electron transfer to give the charge-separated radical pair TTFAQ^{•+}-C₆₀^{•-} as a transient species. The lifetimes of these charge-separated states were in the range of several hundred nanoseconds in deoxygenated

benzonitrile, *ca.* one hundred times longer than for similar TTF-C₆₀ dyads, which was assigned to an increased stabilisation of the oxidised moiety.⁸⁵

We became interested in linking a TTFAQ unit to anthraquinone, with the aim of obtaining ICT and maybe even the first example of a stable TTFAQ cation radical species. Thus we looked for examples where TTF had been covalently linked to quinones, since they could inspire us to the best synthetic strategy.

3.1.2 TTF-quinone systems

Cava, Metzger and co-workers synthesised compound **77**¹⁰³ which consists of a TTF unit linked through a σ -spacer to a quinone, substituted with a bulky triptycene unit to prevent intermolecular CT. The CV data for **77** are consistent with non-interacting TTF and quinone moieties and also no CT band was seen in the UV-vis spectra. The reason is probably the long flexible linker which cannot position the donor and acceptor units in a favourable geometry for ICT through space, and which is too long to allow any charge-transfer through the σ -bonds.

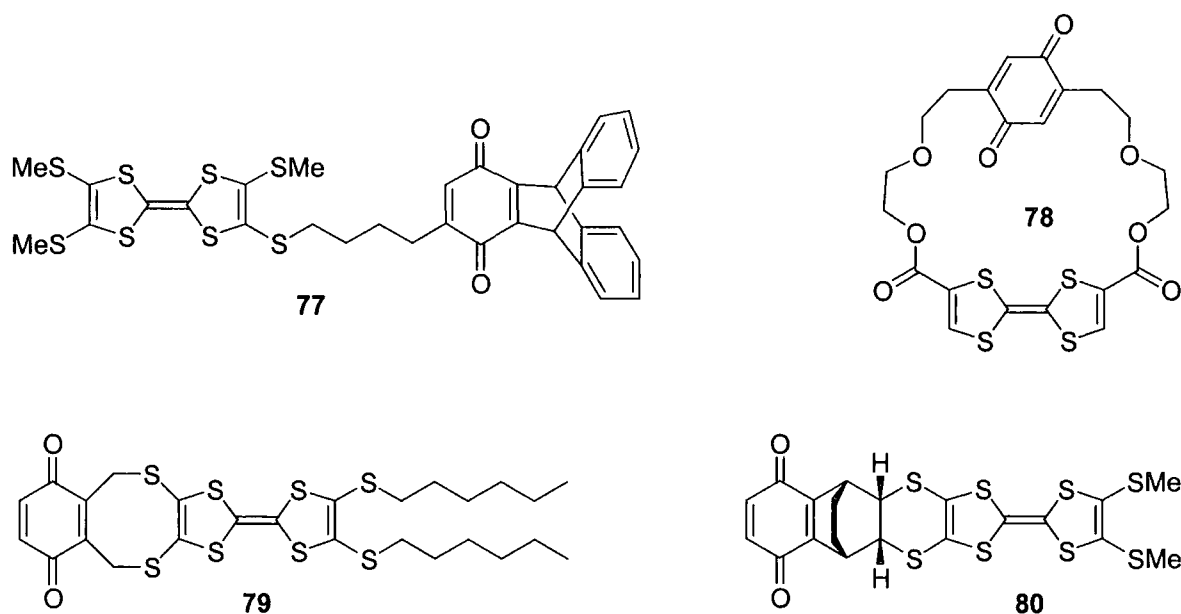


Figure 34: Examples of TTF-quinone systems.^{50,103,104,105}

The cyclophane **78** contains both TTF and benzoquinone linked through glycol chains. Although **78** is a black crystalline solid, the UV-vis spectrum of a solution of **78** in chloroform did not show any charge-transfer, probably since the bridges are too long for ICT.

The X-ray crystal structure of **78** revealed no intramolecular overlap between the TTF and the quinone planes, whereas partial intermolecular overlap was seen, thus the charge-transfer must be assigned as being intermolecular.⁵⁰ The TTF-benzoquinone system **79**, linked by two rigid methylenethio bridges, was synthesised by Martín *et al.*¹⁰⁴ The UV-vis spectrum and the CV data for **79** were consistent with independent and non-interacting TTF and quinone units. Again this is probably due to the saturated linkers. The bridges, although short, are still isolating the donor from the acceptor and their rigidity also does not allow any through-space ICT interaction. Another example of TTF linked covalently by σ bridges to benzoquinone was reported by Becker *et al.*¹⁰⁵ By utilising two cycloadditions, they created **80**, having a rigid and bent bicyclic linker between the TTF and the quinone, fixing the donor and acceptor moieties in parallel overlapping planes. The X-ray crystal structure (Figure 35) reveals the distance between the donor and the acceptor plane to be only 3.29 Å, which is comparable to distances in some mixed-stack charge-transfer complexes. In solution the UV-vis spectrum of **80** showed a broad band centred at 685 nm, indicating charge-transfer interaction. Since the absorption of this band varied with concentration in accordance with Beer-Lambert's law, the CT was assigned as intramolecular. The CV data seemed unaffected by any CT, the TTF and benzoquinone behaving as non-interacting and independent moieties.¹⁰⁵

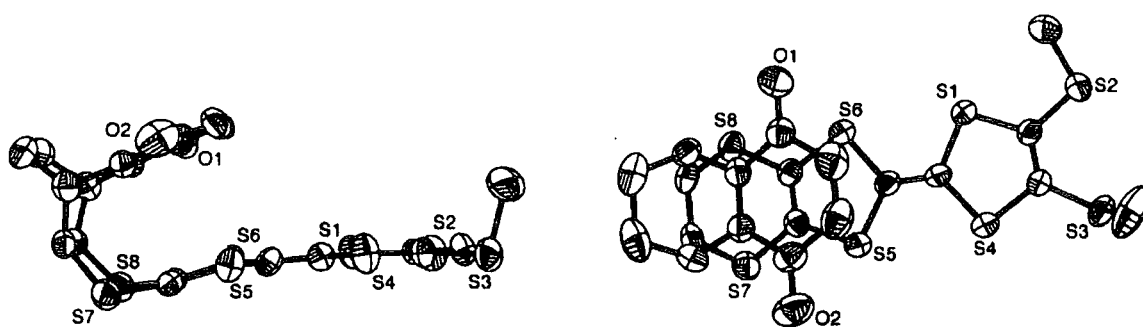


Figure 35: In these two views of the X-ray crystal structure of **80** the bent of the molecule is easily seen.¹⁰⁶

Further examples are triads where the tetrathiafulvalenes and the quinones form one large conjugated system. Watson and co-workers synthesised compound **81**, but insolubility prevented detailed characterisation. Irreversible redox behaviour was reported, with no evidence for ICT.¹⁰⁷ In contrast to **81**, compound **82** reported by Müllen *et al.* was soluble and could be more thoroughly characterised.¹⁰⁸ A CT absorption band was observed both in solution and in the solid state. The CT band in toluene ($\lambda_{\max} = 819$ nm) was independent of concentration, and therefore was assigned as an intramolecular CT interaction. CV data for **82**

showed a one-electron reduction of the quinone and two two-electron oxidation waves for the TTF units, suggesting that the TTF units act independently of each other. The influence from the electron-withdrawing quinone unit was seen in the raised oxidation potentials for the TTF units.¹⁰⁸

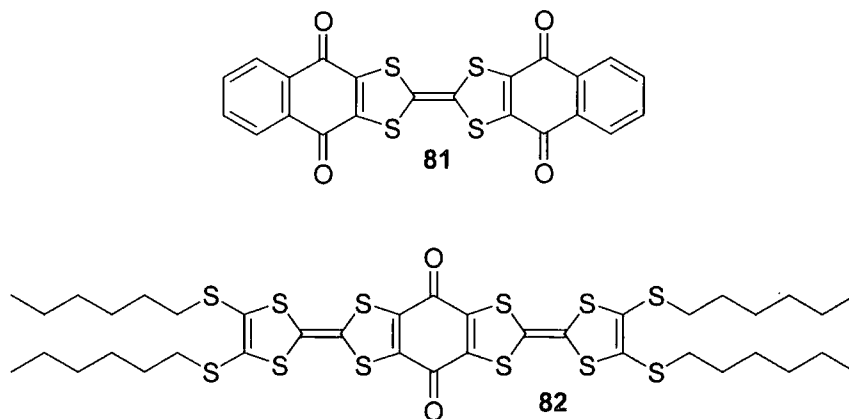
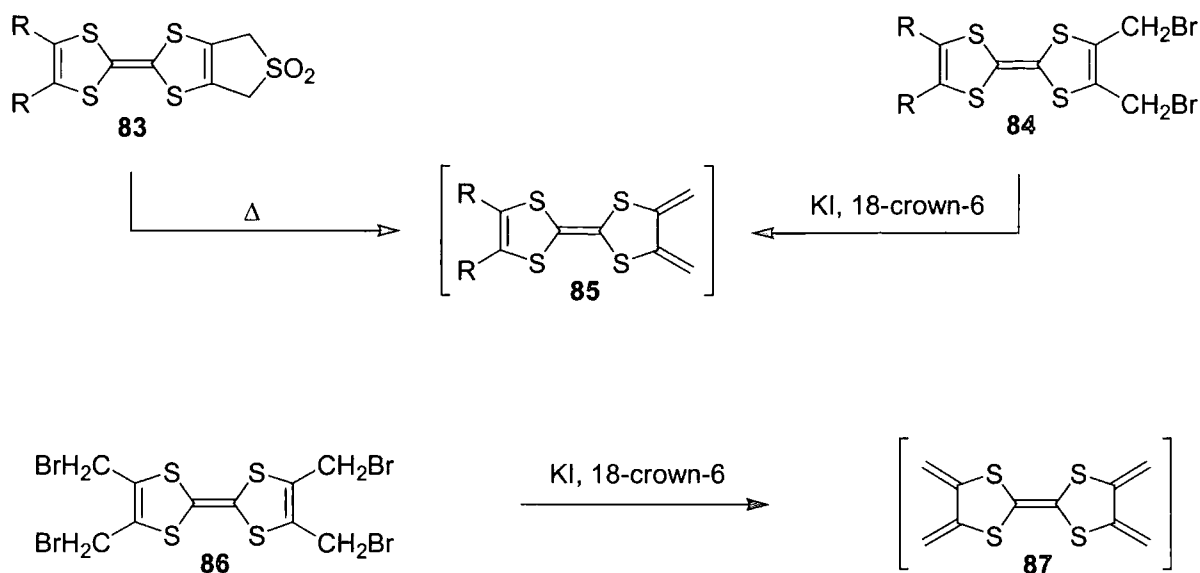


Figure 36: Conjugated donor-acceptor systems containing TTF and quinones.^{107,108}

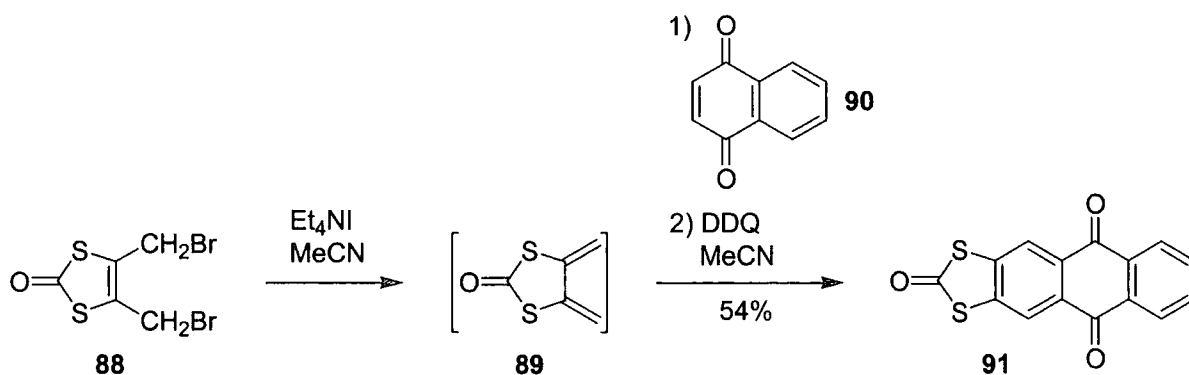
To attain ICT it seemed important either to have the donor and acceptor fixed in positions where through-space interaction is possible, *e.g.* by incorporation of the donor and acceptor unit into a cyclophane structure (see section 1.2.8) or a rigid system like **80**, or to have a conjugated or otherwise non-insulating linker. We decided to explore the Diels-Alder reaction as a means to link TTFAQ with anthraquinone. This could lead to a conjugated donor-acceptor system, making intramolecular charge-transfer more likely. Thus, we next looked for examples in the literature where TTF had taken part in Diels-Alder reactions, since no TTFAQ derivative had ever been used for this purpose before.

3.2 TTF IN DIELS-ALDER REACTIONS

Only a few examples of Diels-Alder reactions involving TTF derivatives were known. Among the most successful examples were the adducts between C₆₀ and TTF made by Rovira *et al.*,¹⁰⁹ who chose as the diene precursor TTF derivative **83** containing the 3-sulfolene moiety, which upon heating releases SO₂ and yields a diene derivative **85** *in situ* (Scheme 10).¹¹⁰ Gorgues *et al.* had published the synthesis of TTF derivatives containing two vicinal bromomethyl groups **84**, and also tetrakis(bromomethyl)tetrathiafulvalene **86** had been reported.¹¹¹ When treated with iodide, these compounds undergo reductive elimination to form the corresponding dienes **85** and bisdiene **87**, respectively, *in situ* (Scheme 10).^{111,112}

Scheme 10: Preparation of transient TTF dienes **85** and a bisdiene **87**.^{110,111}

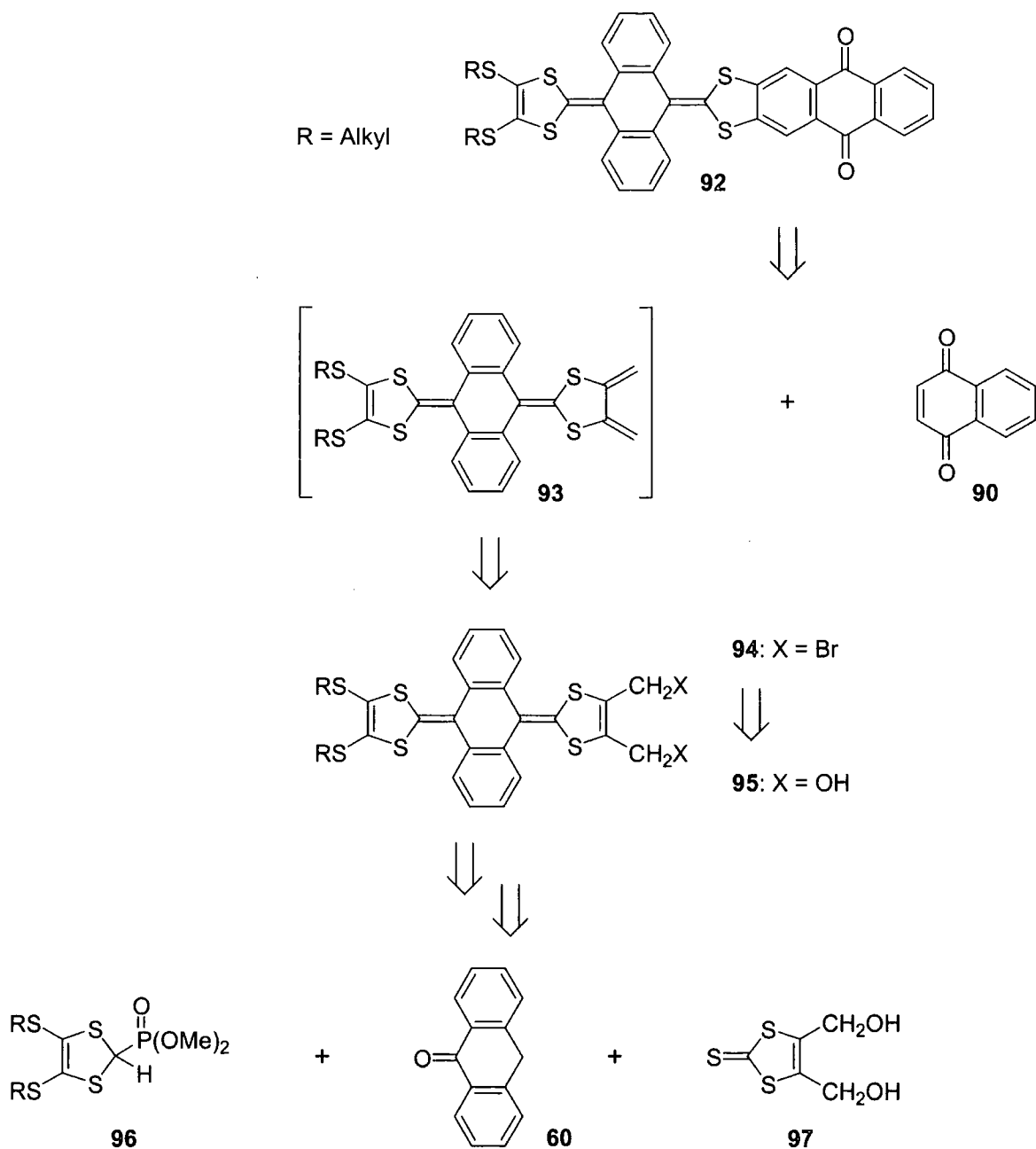
At the planning stages of our project, the results of the Diels-Alder reactions from these precursors were only briefly described,¹¹³ but Gorgues *et al.* had previously used the equivalent precursor 1,3-dithiole **88** for Diels-Alder reactions with success (Scheme 11). Both adducts with C_{60} ¹¹⁴ and with 1,4-naphthoquinone¹¹⁵ **90** had been reported. Further results from Gorgues *et al.* have been published after the completion of our work. Especially the reactions of C_{60} with TTF diene derivatives **85**¹¹⁶ and with bisdiene **87**¹¹⁷ afforded interesting structures, but also reactions of **85** with quinones were reported,¹¹⁸ which will be discussed later in this chapter (section 3.4.8).

Scheme 11: The vicinal bromomethyl groups serves as a diene precursor.¹¹⁵

3.3 DESIGNING THE SYNTHESIS

As our target molecule the conjugated donor-acceptor dyad **92** was chosen (Scheme 12). The alkyl groups should ensure good solubility,¹⁰⁸ since insolubility was known to have been a

problem for similar compounds (see section 3.1.2).¹⁰⁷ Compound **92** is an aromatised Diels-Alder adduct from the reaction of the transient diene **93** with 1,4-naphthoquinone **90**.



Scheme 12: The conjugated donor-acceptor system **92** could be formed after a Diels-Alder reaction and subsequent aromatisation, and the diene precursor **94** could be obtained from anthrone **60** and compounds **96** and **97** which were well-known from the literature.

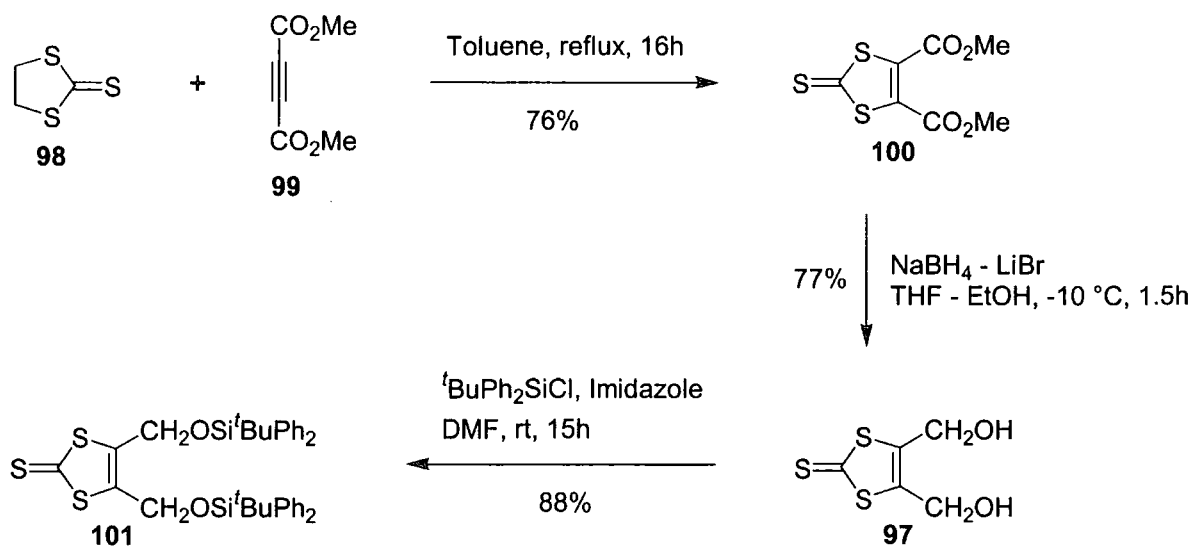
As a precursor for **93**, the dibromide **94** was chosen, and not a derivative containing the 3-sulfolene moiety, since synthesising the dibromide from the analogous bis(hydroxymethyl) derivative **95** seemed much more straightforward. Compound **95** is an unsymmetrical TTFAQ

derivative,⁸⁷ which could be made using the two-step methodology described in Scheme 9. Phosphonate esters with alkylthio substituents in the 4- and 5-position **96** were already known (see Appendix One), as was **97**, which, when converted into its 2-methylthio-1,3-dithiolium salt, could react with anthrone **60** via the addition-elimination reaction mentioned earlier.

3.4 SYNTHESIS OF THE DONOR-ACCEPTOR DYAD

3.4.1 Synthesis of protected bis(hydroxymethyl) derivative **101**

It had been shown by Fox and co-workers that the desired 1,3-dithiole **97** could be obtained by reduction of 4,5-bis(methoxycarbonyl)-1,3-dithiole-2-thione **100**.¹¹⁹ Compound **100** is available from a cycloaddition of ethylene trithiocarbonate **98** and dimethyl acetylenedicarboxylate **99**, as first reported by Easton and Leaver,¹²⁰ and can easily be made in large quantities.¹²¹ Hence, **98** and **99** were refluxed in toluene overnight to give the diester **100** as yellow crystals in 76% yield (Scheme 13).



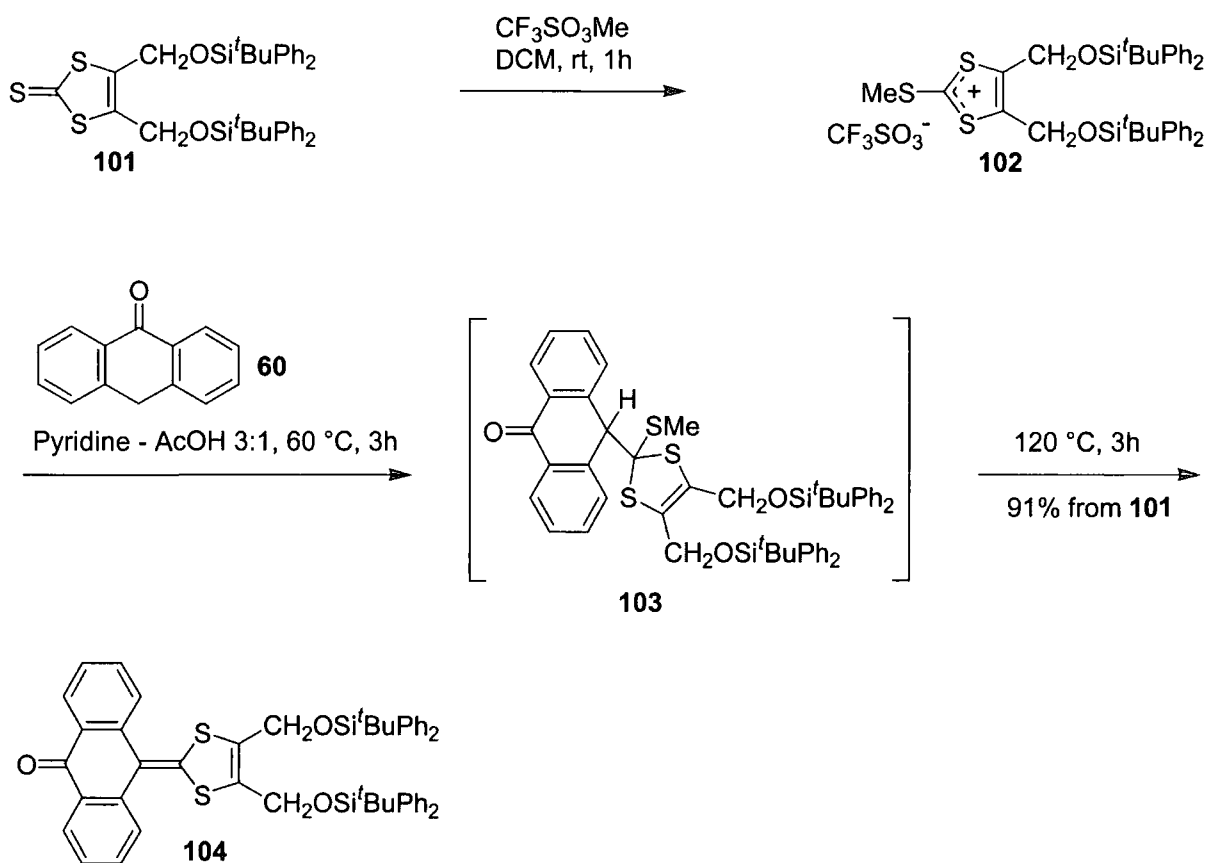
Scheme 13: Formation of the 1,3-dithiole **101** possessing two protected hydroxymethyl groups, using literature procedures.^{121,122}

A procedure for large scale reduction of **100**, based on the early work of Fox *et al.*,¹¹⁹ was developed by Becher and co-workers.¹²² The reduction, using sodium borohydride in the presence of lithium bromide, afforded 4,5-bis(hydroxymethyl)-1,3-dithiole-2-thione **97** as yellow crystals in 77% yield. Since the alcohols of **97** would not survive the subsequent

Horner-Wadsworth-Emmons olefination, they were protected, which had the added benefit of increasing the solubility. Following the literature procedure of Becher *et al.*,¹²² reaction of **97** with *tert*-butyldiphenylchlorosilane in *N,N*-dimethylformamide, using imidazole as base, afforded the corresponding bis(*tert*-butyldiphenylsilyl ether) **101** in 88% yield.

3.4.2 Formation of the ketone **104** by an addition-elimination reaction

The ketone **104** was made following the methodology shown in Scheme 9. Methylation of thione **101** to give the 2-methylthio-1,3-dithiolium salt **102** was carried out in dichloromethane using 1 equivalent of methyl triflate.



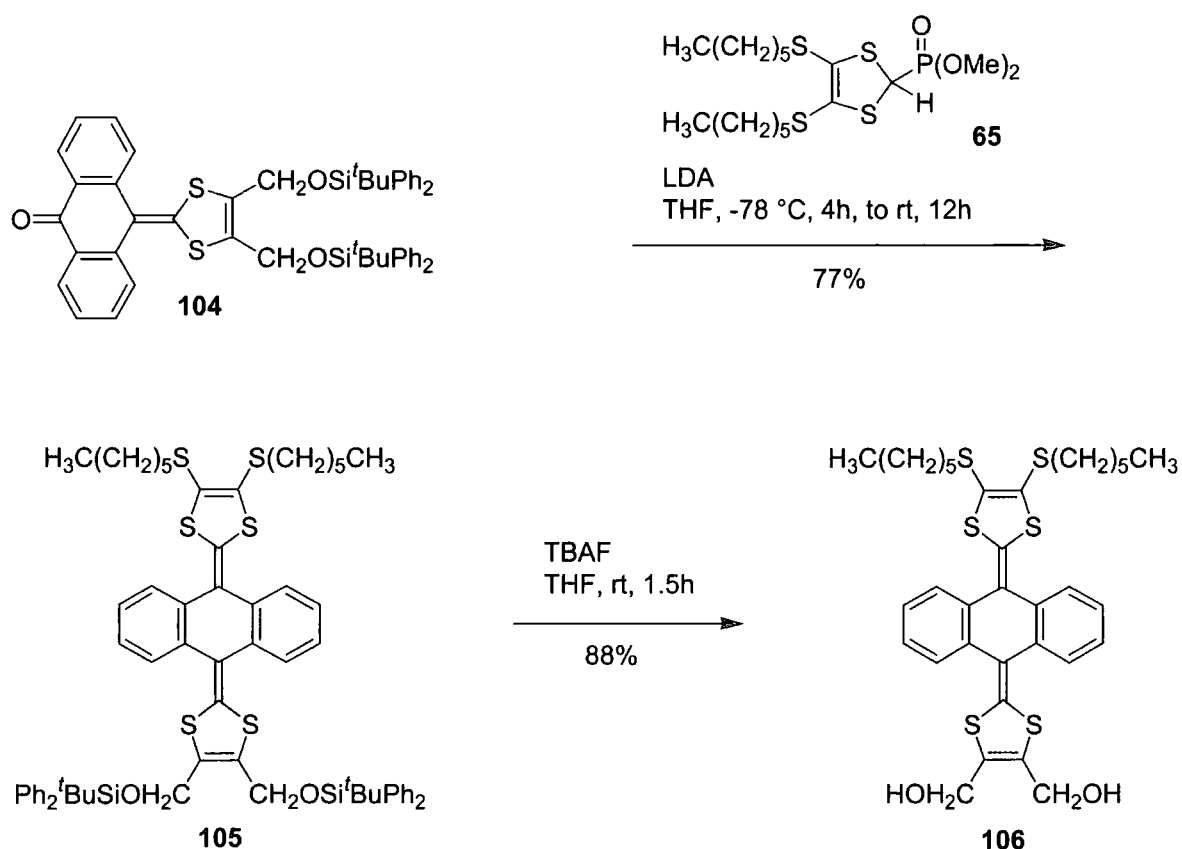
Scheme 14: Formation of the ketone **104** via an addition elimination synthesis.

The crude triflate salt **102** was sufficiently pure (^1H NMR evidence) for further reaction and, due to its instability, **102** was reacted immediately with anthrone **60** in a 3:1 (v/v) mixture of pyridine and acetic acid, initially only at 60 °C to avoid any decomposition of **102**. The reaction was worked up after 5 h, but the major product seemed to be intermediate **103** (^1H NMR inspection of the crude product) and only a little **104** was observed. Purification of

the products **103** and **104** on a silica column was complicated due to spontaneous elimination of methanethiol from **103** to form **104** on the column. Indeed, upon standing in a dichloromethane solution for 7 days, almost all of **103** was converted into **104**. In a second attempt, the reaction was heated at 60 °C for 3 h, and then for an extra 3 h at 120 °C to furnish exclusively **104**, which after column chromatography was isolated as an orange powder in 91% yield from the thione **101**.

3.4.3 Synthesis of bis(hydroxymethyl) derivative **106**

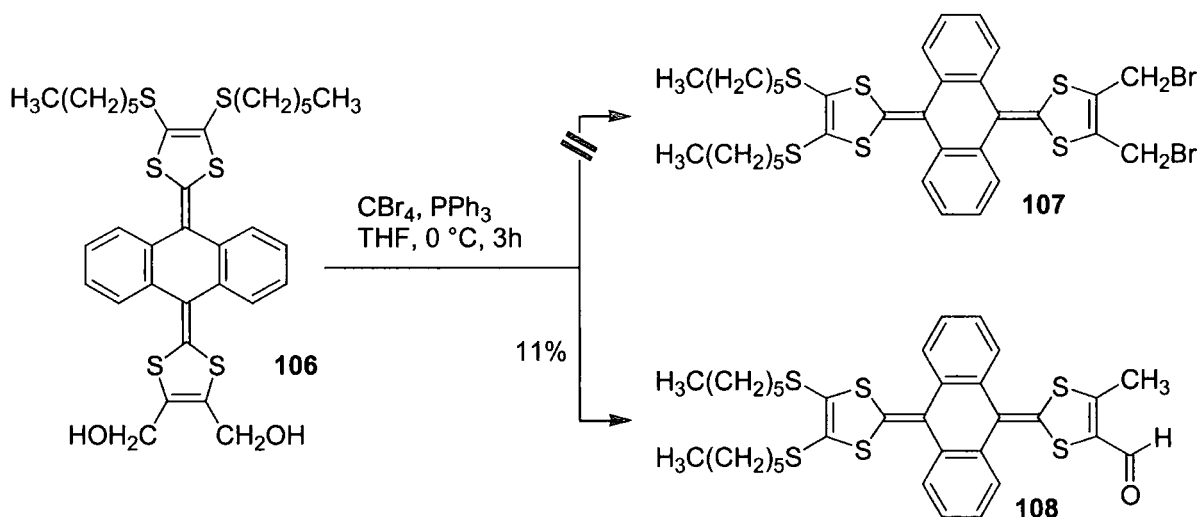
The TTFAQ derivative **105** was made in a Horner-Wadsworth-Emmons olefination using the phosphonate ester **65** (see Appendix One), since its hexylthio groups would increase the solubility of the final donor-acceptor compound. Reagent **65** was deprotonated in tetrahydrofuran at -78 °C, using lithium diisopropylamide (LDA). To the resulting lithium salt was added the ketone **104** to form **105** in good yield. The final step was deprotection, using tetrabutylammonium fluoride in tetrahydrofuran, affording **106** in 88% yield as a yellow solid.



Scheme 15: The Horner-Wadsworth-Emmons olefination followed by deprotection, led to the formation of the bis(hydroxymethyl) derivative **106**.

3.4.4 Bromination of 106 – the formation of a rearrangement product

The last step to give the diene precursor **107** was the conversion of the alcohols of **106** to bromides. The procedure was adopted from Becher *et al.*,¹²² who also synthesised TTF derivatives **84** (Scheme 10), but in higher yields than reported by Gorgues and co-workers.¹¹¹ This was probably due to the use of milder bromination conditions. Gorgues *et al.* used phosphorus tribromide, whereas the mixture of carbon tetrabromide and triphenylphosphine achieved the bromination in the work of Becher *et al.* Hence, the bis(hydroxymethyl) derivative **106** in dry tetrahydrofuran at 0 °C was reacted with carbon tetrabromide and triphenylphosphine. A lot of yellow baseline material and one minor product were obtained; the latter was isolated as a red-brown solid. The ¹H NMR spectrum revealed all the expected peaks of the desired dibromide **107**, except the important singlet from -CH₂Br was missing. Instead, most diagnostic, was a singlet at 9.70 ppm which integrated to 1 proton. Also a singlet at 2.43 ppm which integrated to 3 protons was seen. The structure of the aldehyde **108** was supported by a mass spectrum and confirmed by an X-ray crystal structure (section 3.4.5).

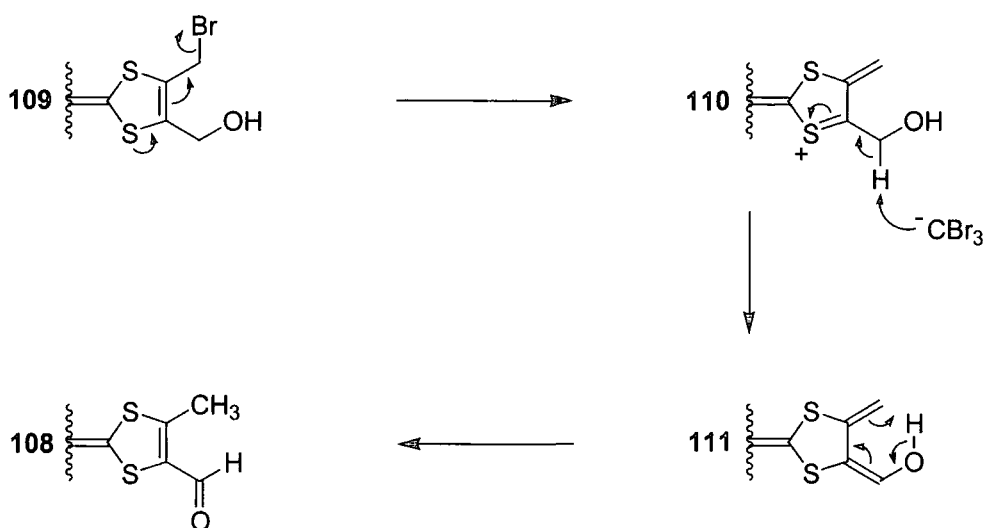


Scheme 16: Bromination of 106 failed. Instead the aldehyde 108, a rearrangement product, was formed.

That bromination of **106** would not be straightforward, became clear after we had a closer look at the recent literature. The group of Gorgues stressed the importance of the experimental conditions when synthesising TTF derivatives **84** containing two vicinal bromomethyl groups (Scheme 10) using phosphorus tribromide. The binary solvent system tetrahydrofuran-carbon tetrachloride and constant bubbling of nitrogen gas seemed crucial. Also the dibromides **84**

were not stable in dichloromethane and chloroform, rapid degradation was observed upon heating *in vacuo* and the dibromides had to be stored at $-10\text{ }^{\circ}\text{C}$ under argon.¹¹¹

Becher *et al.* also observed formation of aldehydes during the synthesis of **84** using carbon tetrabromide and triphenylphosphine,¹²² and proposed the following mechanism (Scheme 17), which we published jointly.¹²³ Loss of bromide from monobrominated intermediate **109** would give **110**, which is deprotonated to form the intermediate **111** which then could undergo rearrangement to give the isolated aldehyde **108**.



Scheme 17: A proposed mechanism for the rearrangement to give the aldehyde **108**.

In more attempts to synthesise the dibromide **107** using carbon tetrabromide and triphenylphosphine by varying the ratios of reagents, the concentration and temperature, TLC in some cases revealed formation of a new product in a very low yield, but it seemed to decompose in the subsequent workup. Perhaps the methodology of Gorgues *et al.*¹¹¹ should have been tried, but if TTFAQ dibromide **107** was rather unstable, it seemed more fruitful to find another solution (see section 3.4.7). Shortly after our publication describing this reaction,¹²³ Martín *et al.* reported the synthesis of bis(hydroxymethyl)TTFAQ derivatives **112-114**, compounds similar to **106**, as new building blocks for Diels-Alder reactions and also one adduct with C_{60} was presented.¹²⁴ The synthesis of **112-114** was very similar to the synthesis of **106** (Scheme 14 and Scheme 15), but all the reported yields were lower than we had obtained. Martín and co-workers in turn managed to convert the bis(hydroxymethyl) derivative **113** to the corresponding dibromide **115**, using phosphorus tribromide in a mixture of tetrahydrofuran and carbon tetrachloride, the conditions first reported by Gorgues *et al.*¹¹¹

The dibromide **115** was reported to be stable for a few days in the refrigerator, but unlike the bis(hydroxymethyl) derivatives **112-114** and the Diels-Alder adduct, no spectroscopic data of **115** was published. It is likely that TTFAQ dibromide **107** with *n*-hexyl groups would be even less stable, since it would not be as crystalline as the dibromo derivative **115** chosen by Martín *et al.* No formation of TTFAQ aldehydes during the synthesis of **115** was reported.¹²⁴

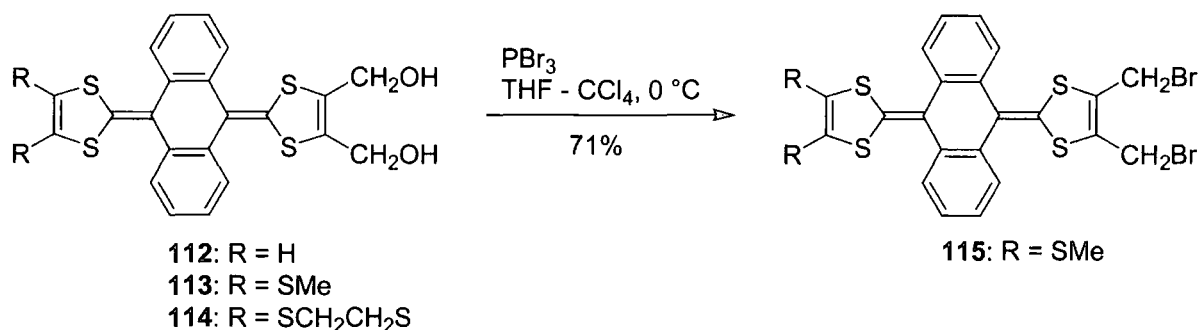
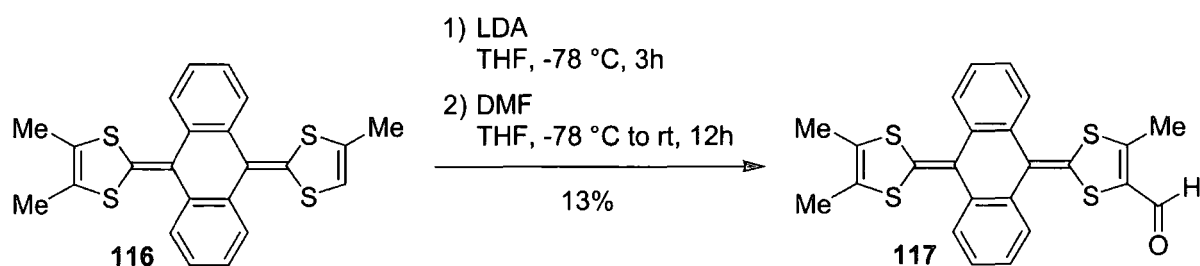


Figure 37: Martín *et al.* synthesised dibromide **115** using Gorgues' conditions.¹²⁴

3.4.5 Optimised synthesis and X-ray analysis of aldehyde **108**

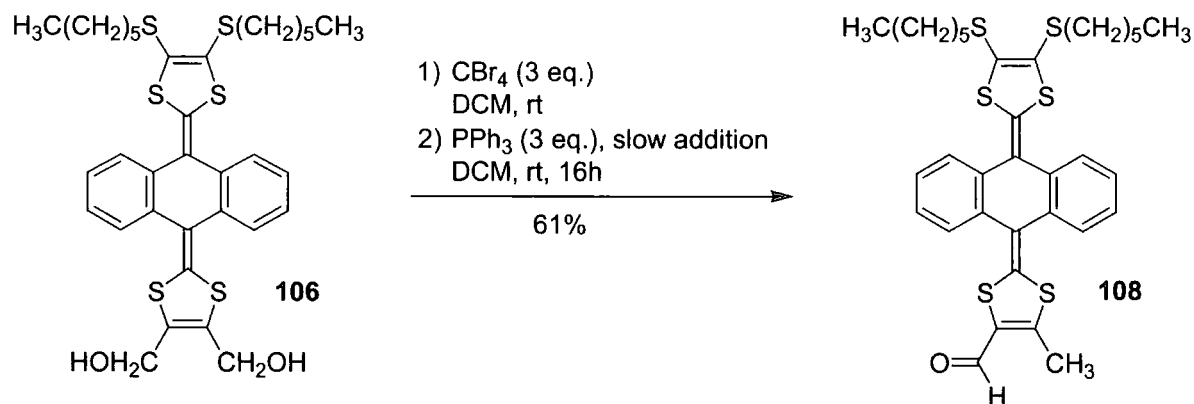
Although the failed synthesis of TTFAQ dibromide **107** put a temporary obstacle to our main objective, the formation of the by-product aldehyde **108** could be of great synthetic benefit. Thus far, the only TTFAQ derivative with one of the 1,3-dithiole rings formylated **117**, was synthesised by lithiation of **116** followed by electrophilic substitution (Scheme 18). The formylation of the equivalent TTF derivative works well (88%),⁹⁵ but for TTFAQ the optimised yield was only 13%.^{94,125} Since TTFAQ aldehyde **108** was already formed in 11% unintentionally (Scheme 16), we decided to optimise the synthesis of **108**.



Scheme 18: The previous synthesis of TTFAQ aldehyde **117** proceeded in only 13% yield.^{94,125}

The reaction was carried out under dilute conditions at room temperature, since according to the proposed mechanism (Scheme 17), this would allow intermediate **109** to exist for longer,

instead of being dibrominated, and hence increase the possibility of rearrangement to the aldehyde. To make the concentration of the active bromination species even lower, triphenylphosphine was added over 2 h. The reaction was stirred overnight, and the aldehyde **108** was isolated in 61% yield. This is a considerably higher yield than reported for **117** using the lithiation methodology, so the rearrangement is of synthetic use.



Scheme 19: Optimised synthesis of aldehyde **108**.

Brown prisms of **108** were grown and the X-ray crystal structure determined. The asymmetric unit of **108** comprises two molecules of similar but non-identical conformations (see Figure 38 for the structure of one of the conformers). In both conformers the formyl and methyl substituents are equally distributed between two positions at the dithiolenyl ring, and both conformers adopt the saddle-shape typical for TTFAQ derivatives. The central anthraquinonoid system is folded along the C(9)–C(10) vector by *ca.* 41° and both dithiolenyl rings are folded inward along the S–S vectors. Thus, the TTFAQ system has an acute angle between the S(1)C(16)C(17)S(2) and S(3)C(19)C(20)S(4) planes of 80° or 84° for the two conformers. The formyl groups in both conformers are nearly co-planar with the dithiolenyl ring, on which they are substituted, and the oxygen atoms are in *syn*-orientations towards the adjacent sulfur atoms of the ring. The *n*-hexyl chains adopt essentially planar all-*trans* conformations and their mean planes are parallel to the S(3)C(19)C(20)S(4) plane of the opposite dithiolenyl ring within 7–11°. As can be seen in Figure 39, the packing diagram consists of pseudo-dimers of mutually engulfing molecules, symmetrically related *via* an inversion centre, forming a four-layered sandwich with the hexyl chains outside and the dithiolenyl rings inside.

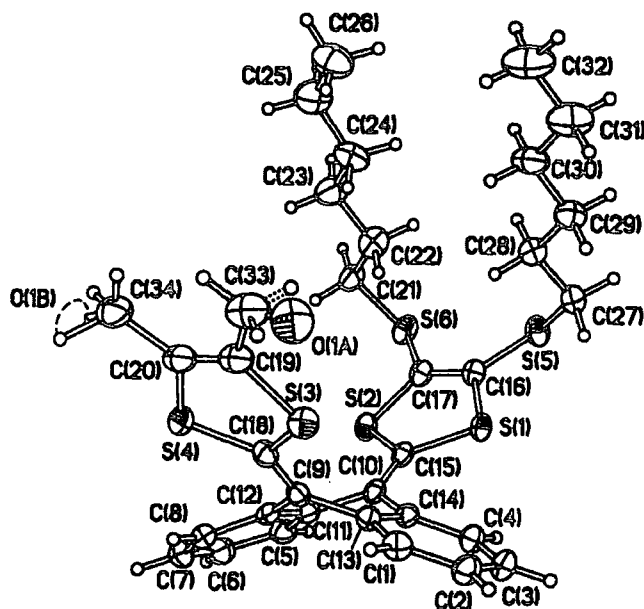


Figure 38: The X-ray crystal structure of the aldehyde 108 showing one of the two conformers. The formyl and methyl substituents are equally distributed between two positions A and B.

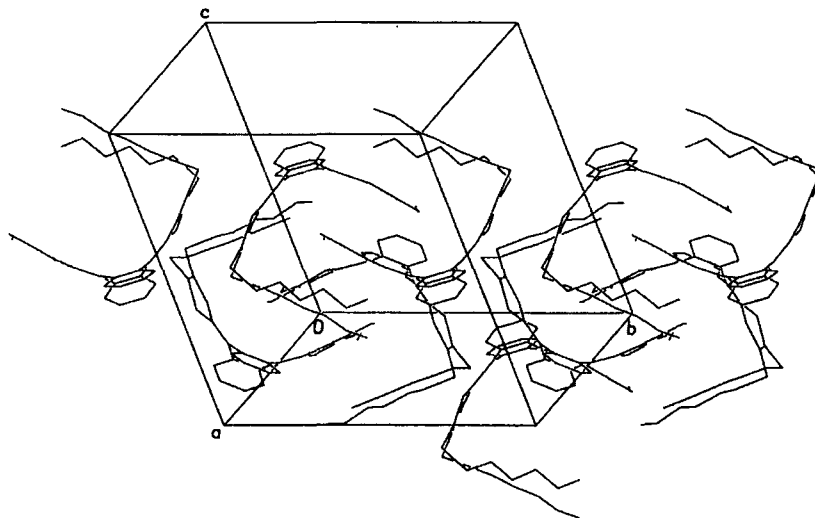
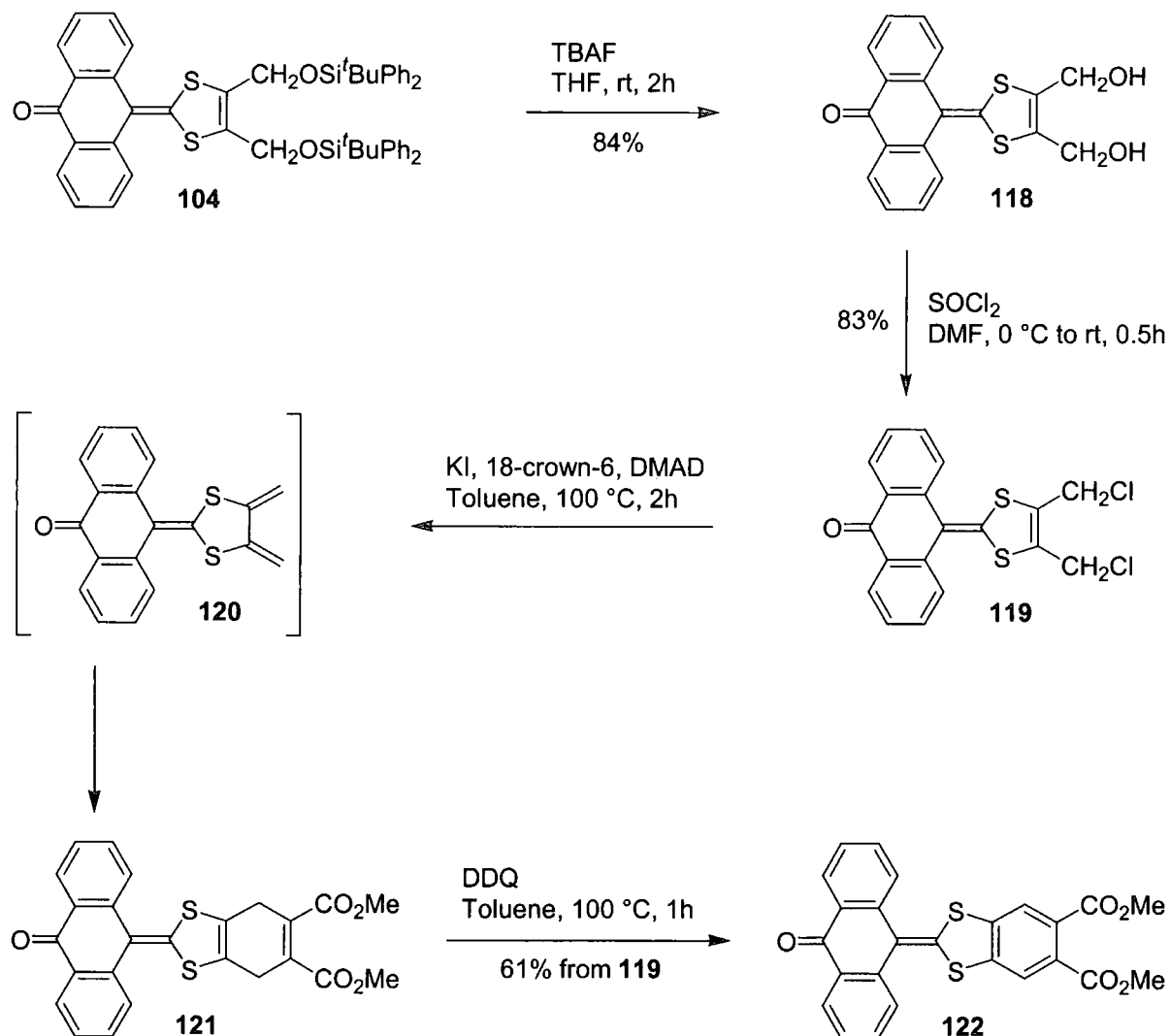


Figure 39: The packing diagram of aldehyde 108 showing pseudo-dimers of mutually engulfing molecules.

3.4.6 Synthesis and reaction of a new diene precursor

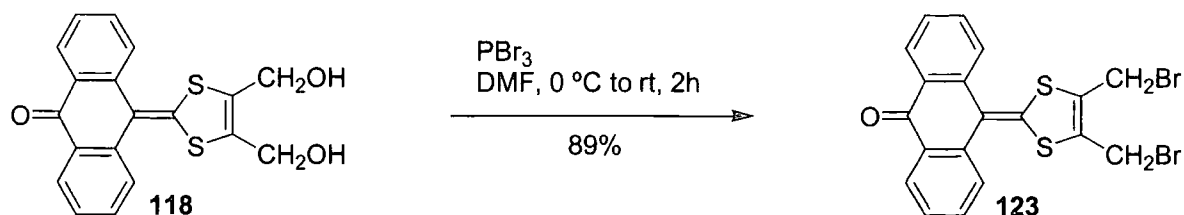
The bromination of **106** having proved unsuccessful, we decided to investigate the equivalent bis(chloromethyl) derivative. We first tested a more simple bis(chloromethyl) derivative **119**, to see if the diene **120** could be formed and take part in a Diels-Alder reaction. Silyl derivative **104** was deprotected using tetrabutylammonium fluoride in tetrahydrofuran to give

118 in 84% yield. Chlorination was carried out using thionyl chloride in *N,N*-dimethylformamide, one of the few solvents that could give a concentrated solution of **118**, so as to suppress any potential rearrangement to the corresponding aldehyde (*cf.* Scheme 17). The reaction took place almost instantly, and **119** was obtained as yellow microcrystals in 83% yield.



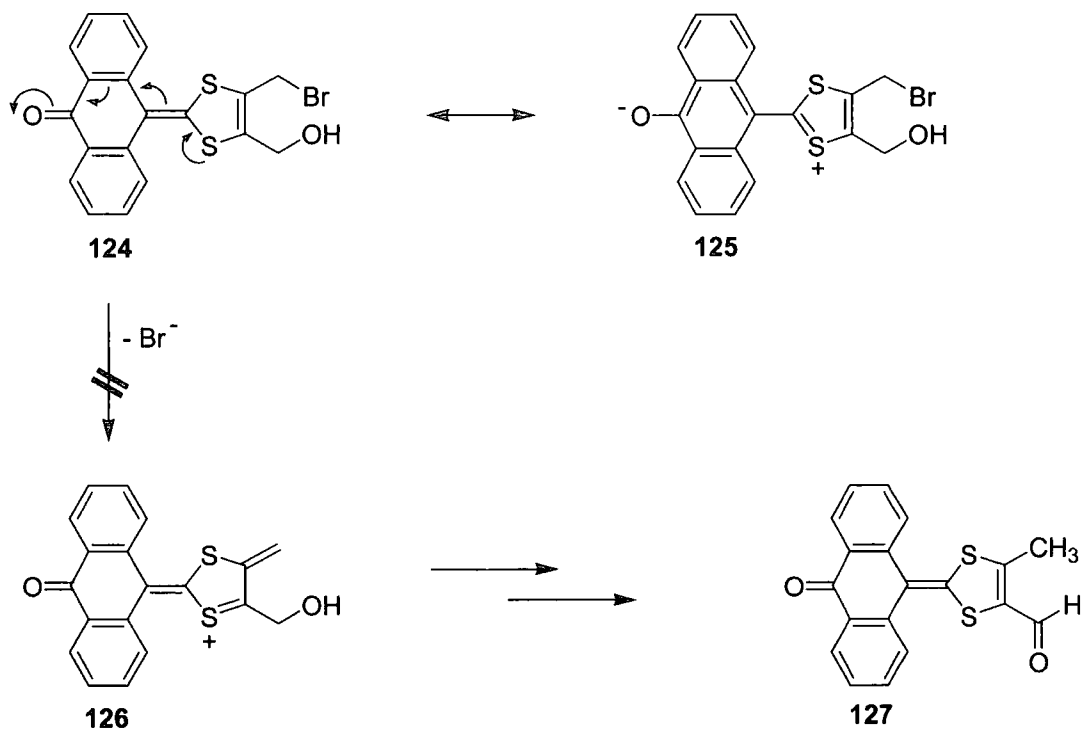
Scheme 20: Chlorination of 118 was done in high yield and subsequent Diels-Alder reaction worked well.

Since chlorination of **118** was very high yielding and the dichloride **119** seemed to be very stable, we explored the bromination of **118**. This time a *N,N*-dimethylformamide solution of bis(hydroxymethyl) derivative **118** was treated with phosphorus tribromide to afford **123** as a yellow powder in 89% yield. Furthermore, the dibromide was shelf stable for more than 2 years.



Scheme 21: Bromination of bis(hydroxymethyl) derivative **118** proceeded in almost quantitative yield.

The ease of both the chlorination and the bromination of **118** was in great contrast to the difficulties encountered in attempted bromination of **106**. A possible explanation could be the stabilisation of the intermediate **124** by the contribution from resonance form **125** (Scheme 22) which would not be possible for the equivalent TTFAQ intermediate **109**. Thus loss of bromide to form **126** followed by rearrangement to give aldehyde **127**, similar to that proposed for the TTFAQ series (Scheme 17) is not likely.



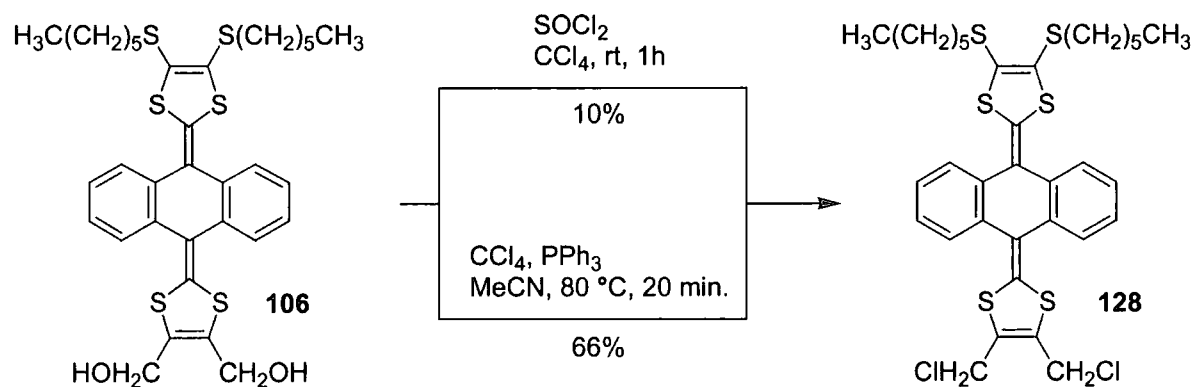
Scheme 22: Probably due to the contribution from resonance form **125**, intermediate **124** does not undergo rearrangement to the aldehyde **127**.

Dibromide **123** was not used for Diels-Alder reactions, but played a crucial role as a synthon in the work presented in Chapter 4. Instead, dichloro derivative **119** was tested as a diene precursor in a Diels-Alder reaction using the conditions of Müllen¹¹² and Gorgues *et al.*,^{113,114} with dimethyl acetylenedicarboxylate (DMAD) as the dienophile. The synthesis of **122** was

carried out in dry toluene at 100 °C in one pot. A mixture of dichloro compound **119**, potassium iodide, 18-crown-6 and dimethyl acetylenedicarboxylate was heated for 2 h, after which time no more starting material could be observed using TLC. Instead, two new compounds had formed, presumably the direct adduct **121** and the fully aromatised product **122**. To facilitate aromatisation, 2,3-dichloro-5,6-dicyano-*p*-benzoquinone (DDQ) was added to the reaction mixture, which was stirred for another 1 h at 100 °C. In the workup the presence of iodine was observed, which was removed by washing with diluted solutions of sodium thiosulphate. The aromatised Diels-Alder adduct **122** was isolated as small golden needles in 61%, proving that bis(chloromethyl) derivative **119** was indeed a suitable diene precursor.

3.4.7 Chlorination of bis(hydroxymethyl) derivative **106**

Having proved the diene precursor properties of **119**, we returned to the bis(hydroxymethyl) derivative **106**. First chlorination using thionyl chloride was attempted. Compound **106** was dissolved in dry carbon tetrachloride and thionyl chloride was added dropwise, which made the reaction mixture turn black immediately. Workup gave crude **128** (¹H NMR evidence), but a lot of very polar black decomposition products were filtered off. The yield was only 10%, but it was clear that compound **128** could be formed. Further attempts using thionyl chloride were tried applying different reaction conditions, but the yield never improved significantly.



Scheme 23: Chlorination of **106** was carried out in two different ways.

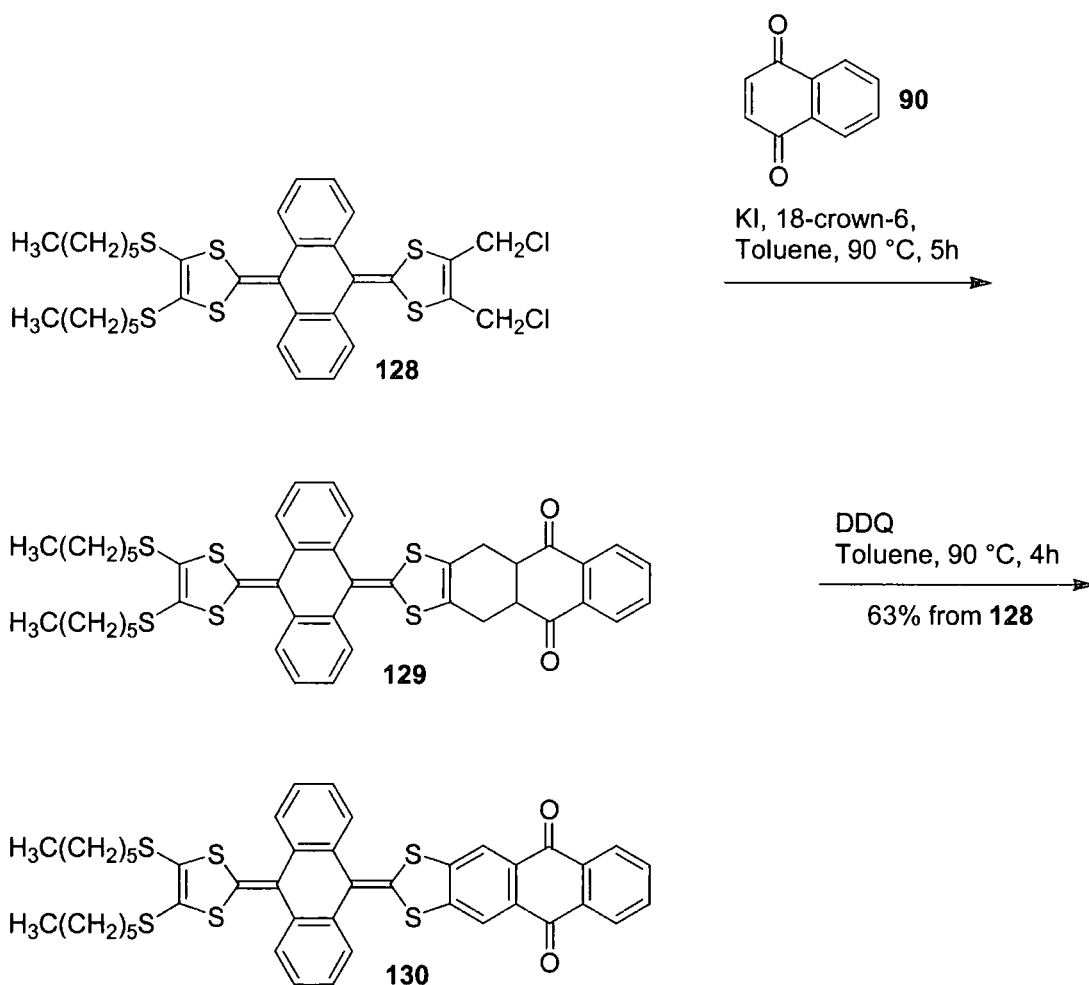
It is known that carbon tetrachloride can be a source of chloride similar to carbon tetrabromide in a halogenation reaction with an equimolar amount of triphenylphosphine.¹²⁶

Hence, chlorination was attempted using carbon tetrachloride/triphenylphosphine in different solvents and at different temperatures. Neat carbon tetrachloride was not polar enough for reaction to take place, even at reflux, but when mixed with the more polar solvents tetrahydrofuran and acetonitrile reaction was seen, which was in accordance with the literature.¹²⁶ In most cases the aldehyde **108** was isolated in the same yield as the dichloride **128**, and a lot of black decomposition products were also always formed. However, as was the experience when the synthesis of **108** was optimised (section 3.4.5), it was found that aldehyde formation was suppressed when as high a concentration as possible was used. Reaction time and temperature were also important. Too low a temperature gave a slow reaction and as a consequence pronounced formation of aldehyde **108** (*cf.* section 3.4.5). Too high a reaction temperature in turn afforded more decomposition products, and the reaction should not be heated longer than absolutely necessary. Thus, a concentrated solution of bis(hydroxymethyl) derivative **106** and triphenylphosphine in a *ca.* 1:3 (v/v) mixture of carbon tetrachloride and acetonitrile was stirred at 80 °C for 20 min, which afforded dichloride **128** as the only product (TLC evidence). Rapid workup avoiding columns on silica gave **128** in 66% yield. Dichloride **128** was found to be shelf-stable for several months, but in solution in dichloromethane or chloroform **128** decomposes overnight, which was also the case for the bis(bromomethyl)TTF derivatives **84** (Scheme 10),¹¹¹ as mentioned above (section 3.4.4).

3.4.8 Synthesis of donor-acceptor dyad **130**

The synthesis of donor-acceptor dyad **130**, which was also the first Diels-Alder reaction involving a TTFAQ derivative, was carried out similar to the synthesis of **122**. Dichloro derivative **128**, potassium iodide, 18-crown-6 and 1,4-naphthoquinone **90** were heated for 5 h, after which time two new compounds had been formed, and in one case the reaction was worked up at this stage to identify (using ¹H NMR) the compounds as the direct adduct **129** (the major product) and the fully aromatised adduct **130** (the minor product). Since we had no interest in **129**, the reaction was, in all other cases, completed by adding DDQ to the mixture and heating for another 4 h. Shiny black microcrystals of **130** were thereby obtained in 63% yield. The solubility of donor-acceptor system **130** was considerably lower than for *e.g.* bis(hydroxymethyl) derivative **106**, but still good enough (in solvents like dichloromethane,

chloroform, toluene, ethyl acetate and acetonitrile) for full spectroscopic characterisation. Our choice to functionalise **130** with hexyl groups proved to be very beneficial.



Scheme 24: The Diels-Alder reaction followed by aromatisation, afforded the desired donor-acceptor dyad **130**.

To further investigate the structural properties of **130**, the X-ray crystal structure was obtained. Although the crystals were dark coloured, inspection of the bond lengths suggested no charge-transfer in the crystal structure. The asymmetric unit contains only one independent molecule (Figure 40), possessing the saddle-shape characteristic for TTFAQ derivatives. The central anthracenediylidene system is folded along the C(9)···C(10) vector by *ca.* 39° and the dithiophene rings are folded inwards along the S···S vectors to further reduce the acute angle between the S(1)C(16)C(17)S(2) and S(3)C(19)C(20)S(4) planes to 83°, similar to that observed for the two conformers of aldehyde **108**. The anthraquinone system fused to one of the dithiophene rings is almost planar, with only a slight folding of 4° along the C(35)···C(42) axis.

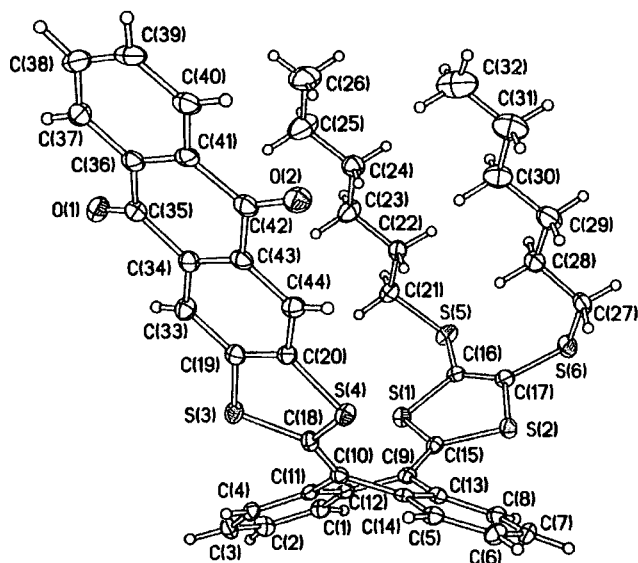


Figure 40: The X-ray crystal structure of donor-acceptor dyad 130.

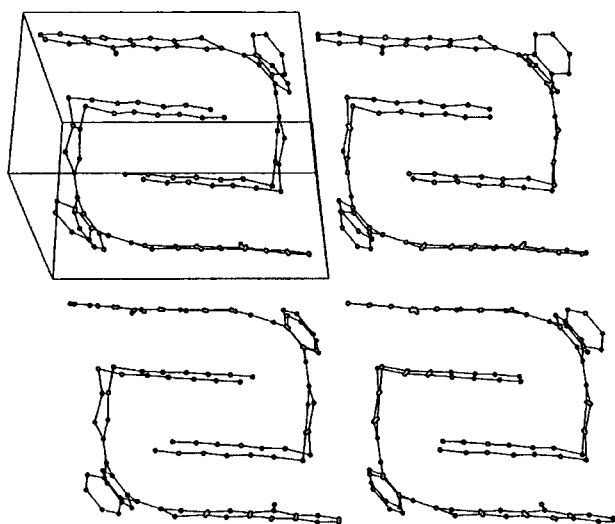


Figure 41: The highly ordered packing of 130 showing stacks of pseudo-dimers of mutually engulfing molecules.

As for the TTFAQ aldehyde **108**, the *n*-hexyl chains adopt essentially planar all-*trans* conformations and their mean planes are parallel to the opposite anthraquinone moiety to within 2° . The anthraquinone moiety is similar in length to the hexyl chains, and together they make up the walls of a very deep cavity. This is perhaps the reason for the highly ordered packing (Figure 41), which could be assisted by the similar lengths of the cavity walls. As was seen in the packing of **108** (Figure 39) the molecules are mutually engulfing, forming

pseudo-dimers where the molecules are symmetrically related *via* an inversion centre. Contrary to the packing of **108**, the dimers of compound **130** form four-layered sandwiches with the hexyl chains *inside* and the aromatic system *outside*, again probably a consequence of the ratio between the length of the hexyl chains and the opposite π -conjugated system. Adjacent dimers extend the sandwiches into infinite stacks, but there is no sign of any network of close S...S contacts.

Simultaneously with our publication of this work, the group of Gorgues published the synthesis of dyads **131** and **132**.¹¹⁸ The TTF-anthraquinone adduct **131** was synthesised from bis(bromomethyl)TTF **84** (Scheme 10) in analogy with our synthesis of **130**, in 20% yield. The only difference was that the reductive elimination to generate the transient diene **85** was carried out using a mixture of magnesium and magnesium bromide in tetrahydrofuran. An X-ray crystal structure of **131** was obtained, showing the conjugated donor-acceptor system to be essentially planar, but the electrochemical and optical properties of **131** were not reported. The TTF-TTFAQ donor-donor system **132** was synthesised by two-fold Horner-Wadsworth-Emmons olefination of **131**, in a reaction similar to our work described below (section 3.5.2). Also no electrochemical or optical properties were reported for **132**.¹¹⁸

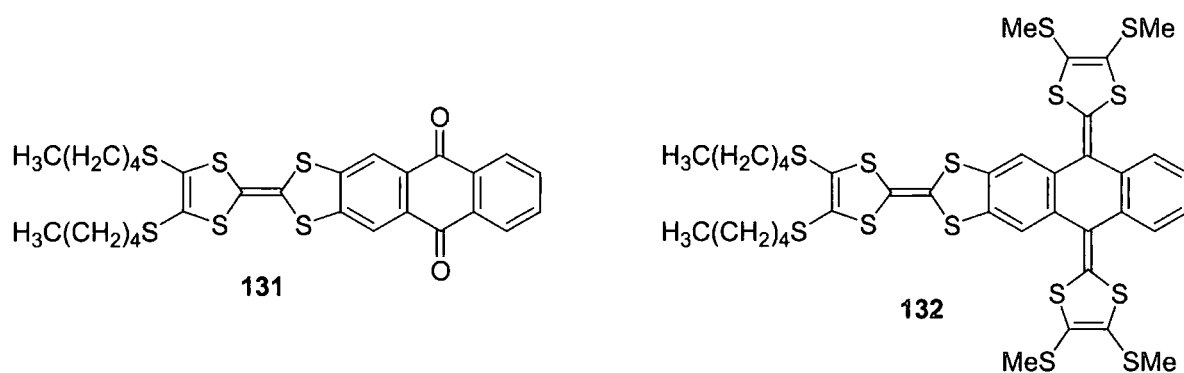


Figure 42: Dyads synthesised by Gorgues *et al.*¹¹⁸

3.5 A CONJUGATED DONOR-DONOR DYAD

During the course of this work, our attention was drawn towards donor-donor systems for which intramolecular electronic interaction could be studied. By converting the anthraquinone moiety of **130** to a TTFAQ unit, a conjugated TTFAQ dimer could be obtained. This was timely in the light of recent publications of Martín *et al.*,¹²⁷ the on-going work in our group⁶⁶ and the simultaneous work of Gorgues *et al.*¹¹⁸ (Figure 42).

3.5.1 Donor-donor dyads containing TTFAQ

Martín and co-workers reported the first series of TTFAQ dimers **133-135** (Figure 43). Their cyclic voltammograms showed only one oxidation wave involving four electrons, to form the corresponding tetracation, indicating that both TTFAQ units behave independently. The lack of intramolecular electronic interaction was explained by the distance between the active donor centres in **133-135**, in spite of the very short oxygen linker. However, according to Martín *et al*, modifying the connectivity between the TTFAQ units should yield interacting redox systems.¹²⁷

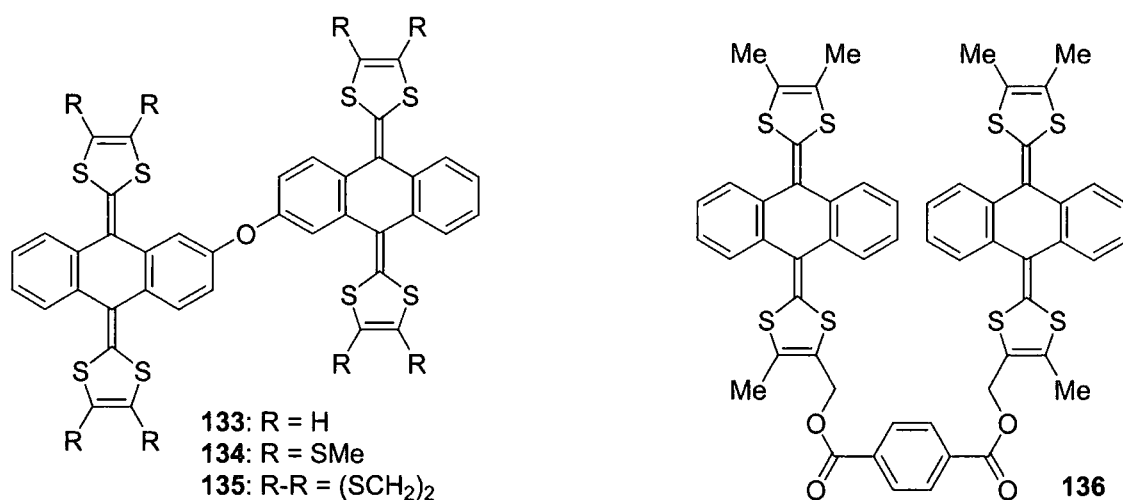


Figure 43: For dimers **133-135**¹²⁷ and **136**,⁶⁶ the TTFAQ moieties behaved independently, yielding only a single oxidation wave in the CV.

Godbert from our group synthesised TTFAQ dimer **136**.⁶⁶ Not surprisingly, taking this relatively long linker into account, dimer **136** also showed a single oxidation wave in the CV. In contrast, a conjugatively linked TTFAQ dimer should offer a much bigger chance of electronic interaction between the TTFAQ units upon oxidation. Indeed, electronic interaction was observed between the TTFAQ unit and the TTF or the ferrocene moiety in **137-139**¹²⁸ and **140-142**,⁶⁸ respectively (Figure 44). These donor-donor dyads, which were reported after the completion of this work, are linked in conjugation *via* a vinyl spacer. The effect of the conjugation is most easily seen for the final oxidation wave of the dyads *i.e.* TTFAQ²⁺-TTF⁺ → TTFAQ²⁺-TTF²⁺ for **137-139** and TTFAQ²⁺-Fc → TTFAQ²⁺-Fc⁺ for **140-142**, respectively. For **137-139** the oxidation potentials for this final oxidation is positively shifted by 30-55 mV compared to unsubstituted TTF, and for **140-142** the oxidation potential for the ferrocene moiety is positively shifted by 56-83 mV compared to unsubstituted ferrocene. This

electronic interaction can be explained by the electron withdrawing effect of the TTFAQ dication through the vinyl spacer.^{68,128}

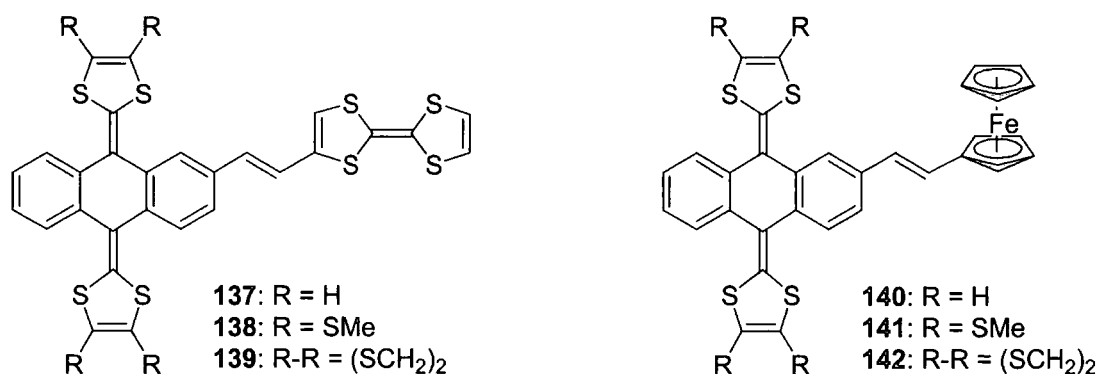
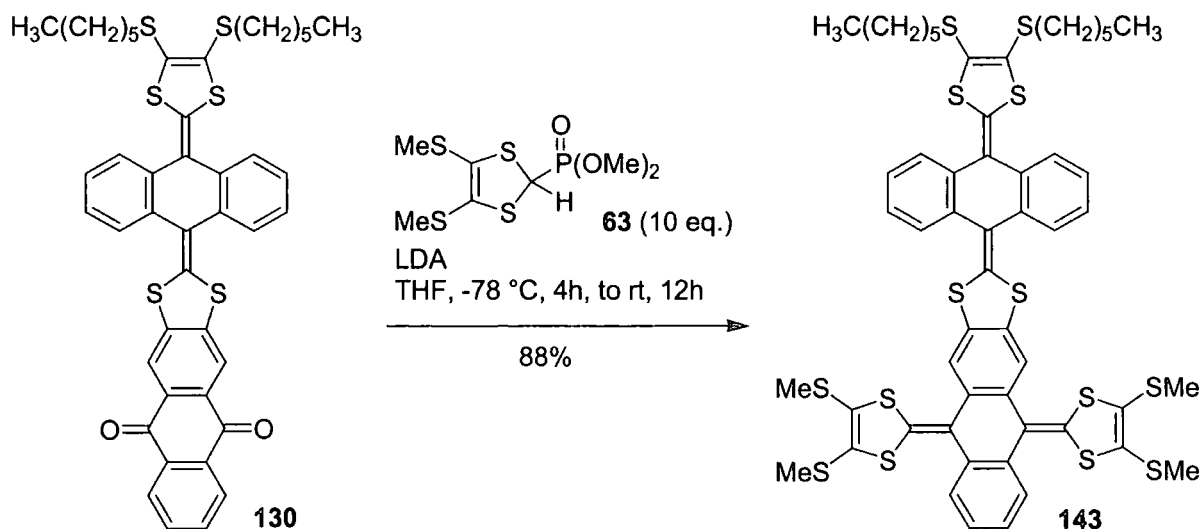


Figure 44: Donor-donor dyads linked through conjugation showing electronic interaction.^{68,128}

3.5.2 Synthesis of a conjugated TTFAQ dimer

Donor-acceptor dyad **130** was reacted with the anion generated by reaction of the Horner-Wadsworth-Emmons reagent **63** with lithium diisopropylamide. We estimated that no further solubilising groups were needed, but **63** was also chosen since it was our experience that TTF derivatives possessing methylthio groups showed a high propensity to grow crystals.



Scheme 25: Synthesis of a conjugated TTFAQ dimer **143**.

To ensure conversion of both carbonyl groups of **130**, 10 equivalents of **63** were used, which is also what Gorgues *et al.* found necessary for similar reactions.^{115,118} This furnished complete conversion of **130** to the TTFAQ dimer **143** (as inspected by TLC, no starting

material or mono-olefinated products were seen), but the excess phosphonate ester, which had decomposed after reaction with lithium diisopropylamide, caused some problems. Two columns were needed to purify the product **143**, which was isolated as a yellow powder in 88% yield. We were unable to grow crystals of TTFAQ dimer **143**, but the solubility of **143** was significantly better than for the precursor **130**.

3.5.3 Proton NMR analysis of the TTFAQ dimer and its tetracation

At first glance the ^1H NMR spectrum of **143** (Figure 45) did not match the expected spectrum. Instead of two singlets from the two non-equivalent SMe groups, two pairs were seen, of which one pair initially was assigned as impurities. However, the larger pair integrated approximately to 4 protons for each singlet, whereas the smaller pair integrated to 2 protons for each singlet. In total this fitted the 12 protons from the 4 SMe groups. A closer look also revealed that the aromatic multiplets at 7.80 and 7.72 ppm integrated to *ca.* 0.6 and 1.4 protons, respectively, and finally two triplets were seen for the terminal methyl groups of the hexylthio chains, which also roughly integrated in a 1:2 ratio. This can be explained by the flipping of the TTFAQ moiety in solution, which was described previously (section 2.2.2). In the case of **143** the spectrum is further complicated, since **143** consists of two TTFAQ units which are joined in a rigid and locked fashion. They have no possibility to rotate relative to each other as for the dimers **133-136** (Figure 43). Hence **143** will be able to adopt two different conformations, one where each TTFAQ moiety is flipped up ([up, up] = [down, down]) and another conformer where one TTFAQ moiety is flipped up and the other flipped down ([up, down] = [down, up]). This explains the two pairs of singlets for the SMe groups and the integrals in 1:2 ratio suggests that the molecule is approximately twice as long in one conformation than in the other.

A simple test to support this explanation and the structure of the product was to oxidise **143** to its tetracation **143**⁴⁺. According to the X-ray structure of the TTFAQ dication, *e.g.* **54**²⁺ (Figure 26), this would afford a structure consisting solely of flat moieties able to rotate freely, which, due to symmetry, should afford a much simpler ^1H NMR spectrum. Thus, part of the NMR sample which afforded the ^1H NMR spectrum of **143** in Figure 45 was oxidised by a solution of iodine in deuteriated chloroform, which caused formation of a red precipitate, expected to be the tetracation salt. The precipitate was redissolved in deuteriated dimethylsulfoxide, whereupon the ^1H NMR spectrum of **143**⁴⁺ was recorded (Figure 46).

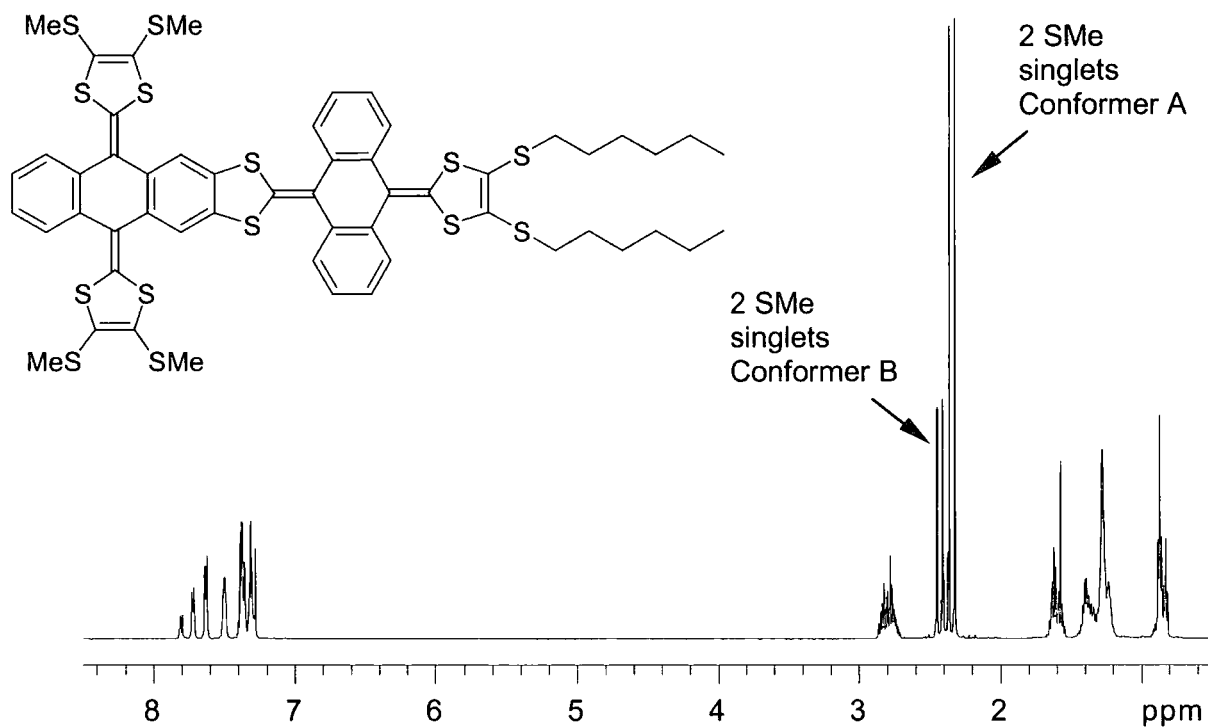


Figure 45: The ^1H NMR spectrum (at 400 MHz) of neutral 143 in CDCl_3 . The presence of the 2 conformers A and B is clearly seen from the 2 pairs of singlets arising from the 2 non-equivalent SMe groups.

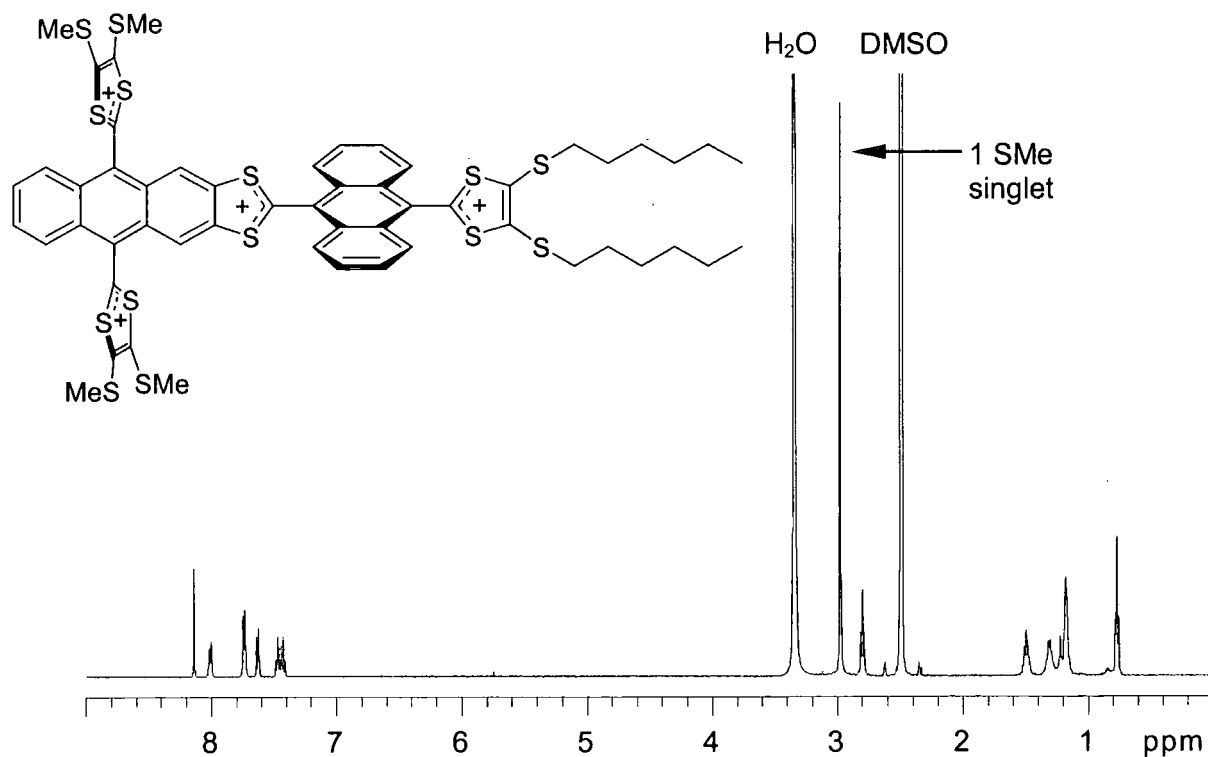


Figure 46: The ^1H NMR spectrum (at 400 MHz) showing 143^{4+} in $\text{DMSO-}d_6$. The more simple spectrum of the tetracation has only 1 singlet arising from the 4 equivalent SMe groups.

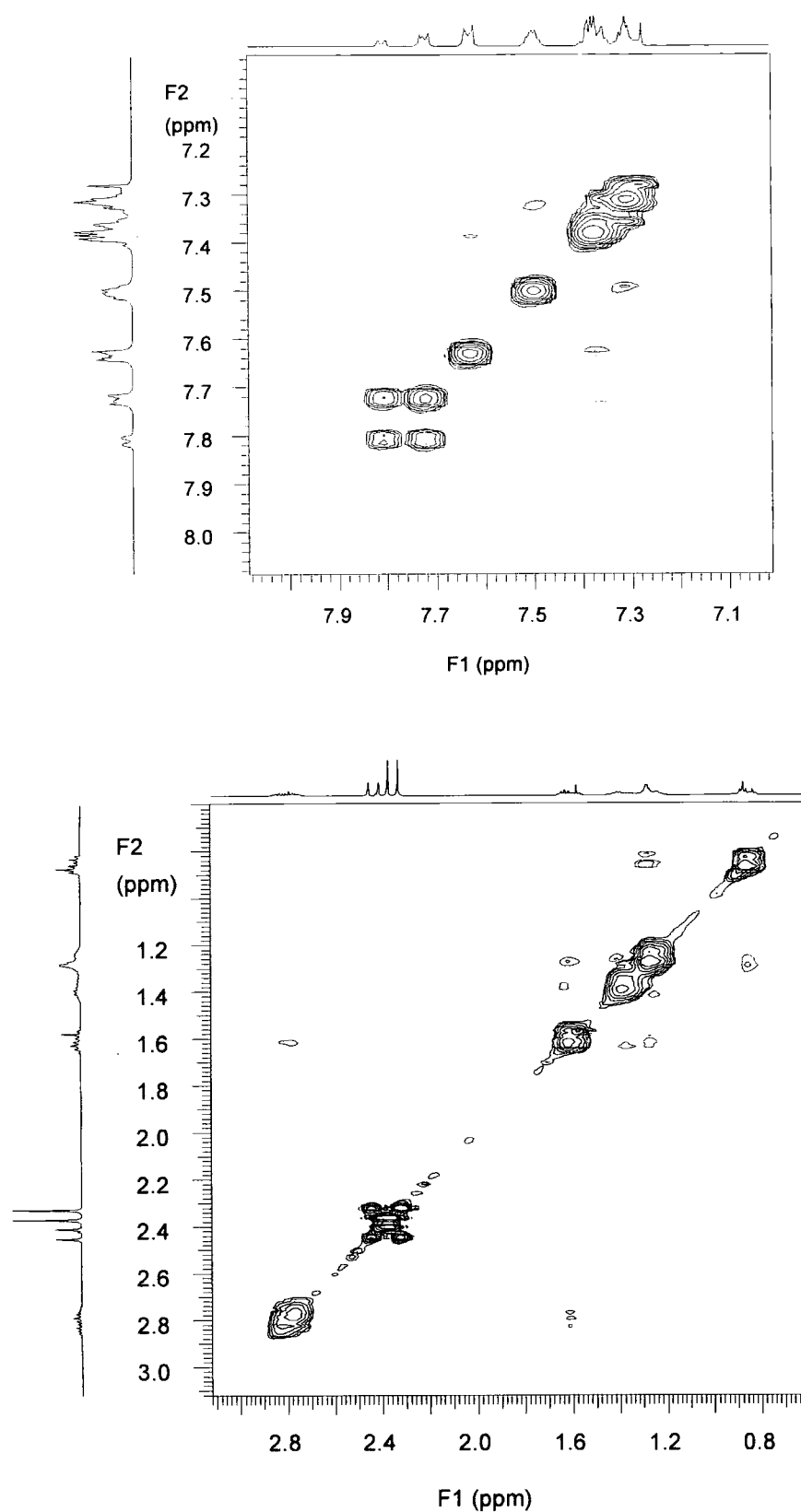


Figure 47: The aromatic (top) and aliphatic (bottom) part of the NOE experiment carried out on 143 (at 400 MHz). Red peaks mark the NOE effect and the black peaks show the exchange between the two conformers, which is especially clear for the multiplets at 7.80 and 7.72 ppm, respectively (top) and the SMe singlets at 2.43-2.31 ppm (bottom).

Oxidation changed the ^1H NMR spectrum of **143** dramatically, and also it is worth noting the sharp lines in the spectrum of 143^{4+} , eliminating all speculations of the presence of cation radical species. The ^1H NMR spectrum of 143^{4+} is, as predicted, a lot simpler than the spectrum of the neutral species. Only one singlet, integrating to 12 protons, is seen for the 4 SMe groups, which have become equivalent due to symmetry of the tetracation (see structure in Figure 46). Also the multiplets and the singlet in the aromatic region of the spectrum now all have integrals divisible by 2, and the two triplets arising from the terminal methyl groups of the hexylthio groups have collapsed into one triplet integrating to 6 protons. This simple experiment strongly supports the theory of **143** being in two different conformations in solution. To further prove the existence of the two conformers of **143**, a NOE experiment was carried out (Figure 47). The red peaks mark the NOE effect (*i.e.* exchange of magnetisation between neighbouring groups), whereas the black peaks show exchange between the two conformers. This exchange is most clearly seen for the multiplets at 7.80 and 7.72 ppm, respectively, which have large off-diagonal peaks. It was those two multiplets which integrated to 0.6 and 1.4 protons, respectively. Pronounced off-diagonal peaks are also seen for the singlets arising from the SMe groups. It can be seen that the two *outer* singlets (at 2.43 and 2.31 ppm, respectively) exchange, and that the same is the case for the two *inner* singlets (at 2.39 and 2.35 ppm, respectively). Again it fits the integrals, since both exchanging couples in total integrate to 6 protons each, corresponding to only two non-equivalent SMe groups, which would have been the case if **143** had been flat. Thus, these experiments confirm that the saddle-shaped TTFAQ units flip in solution, which in the case of the conjugated TTFAQ dimer **143** afforded a rather complicated ^1H NMR spectrum.

3.6 ELECTROCHEMICAL AND OPTICAL PROPERTIES

3.6.1 Optical properties

The UV-vis spectrum of **130** (see Figure 48) shows two bands characteristic of TTFAQ derivatives at 350 and 427 nm, although the intensity of the former band was stronger. No bands were observed in the region 600-900 nm, but a very weak shoulder in the region 475-625 nm is present. The TTFAQ derivatives of Martín *et al.* showing good NLO properties (Figure 33),⁹⁹ had charge-transfer bands in this region, but the shoulder in the spectrum of **130** is indeed very weak. Hence, we were reluctant to assign any significant charge-transfer to the

donor-acceptor system **130** from its UV-vis spectrum. Probably the acceptor moiety of **130** is not strong enough for ICT through the conjugated system. The other TTFAQ derivatives presented in this chapter, including the TTFAQ dimer **143**, had UV-vis spectra typical for TTFAQ derivatives (see Figure 28).

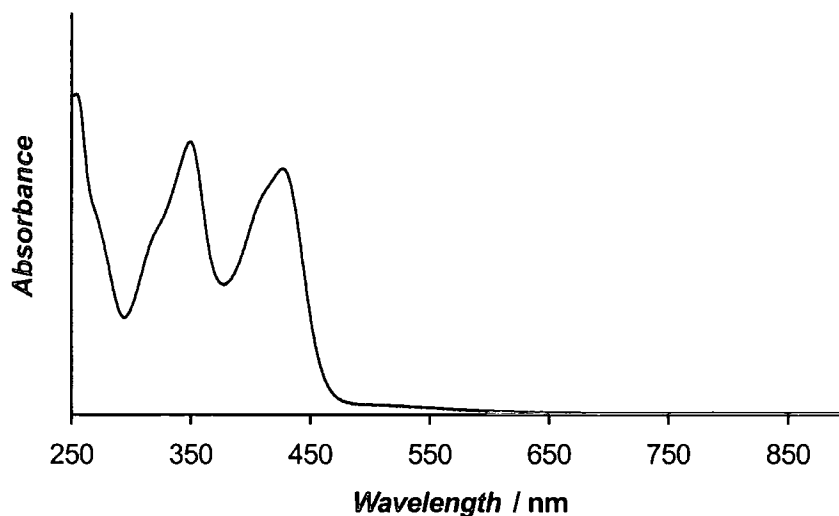


Figure 48: The UV-vis spectrum of **130** recorded in dichloromethane. Two bands [λ_{\max} ($\lg \epsilon$): 350 (4.55), 427 (4.50) nm] characteristic for TTFAQ were observed, together with a very weak shoulder in the region 475-625 nm.

3.6.2 Solution electrochemical properties

Cyclic voltammograms were recorded for the TTFAQ derivatives, and the oxidation potentials are collated in Table 2, together with the reduction potential of **130**. The simple TTFAQ derivatives **105**, **106**, **108** and **128** showed a single, quasi-reversible,⁶⁹ two-electron oxidation wave. The bis(hydroxymethyl) derivative **106** has an oxidation potential $E_{\text{pa}}^{\text{ox}} = 0.45$ V, which is higher than for unsubstituted TTFAQ, but this can be accounted for by the hexylthio groups, since alkylthio substituents are known to raise the oxidation potential.⁶⁴ The oxidation potentials are further raised for **108** and **128** substituted with electron withdrawing formyl and chloromethyl groups, respectively. Only the potential for **105** is hard to explain. It is raised by 90 mV compared to **106**, and also it is the most quasi-reversible of all the compounds ($E_{\text{pa}}^{\text{ox}} - E_{\text{pc}}^{\text{ox}} = 310$ mV). This could possibly be due to a steric effect from the bulky protecting groups.

Compound	$E^{\text{ox}}_{\text{pa}}/\text{V}$	$E^{\text{ox}}_{\text{pc}}/\text{V}$	$E^{\text{red}}_{\text{pc}}/\text{V}$	$E^{\text{red}}_{\text{pa}}/\text{V}$
105	0.54	0.23	-	-
106	0.45	0.32	-	-
108	0.62	0.50	-	-
128	0.58	0.48	-	-
130	0.71	0.61	-0.85	-0.79
143, E^1	0.54	0.45	-	-
143, E^2	0.67	0.62	-	-

Table 2: Redox potentials from cyclic voltammetric measurements vs. Ag/AgCl. Compound ca. 1×10^{-3} M and electrolyte 0.1 M Bu_4NPF_6 in dichloromethane, 20 °C, scan rate 100 mV s^{-1} .^{129, 130}

Donor-acceptor dyad **130** has the highest oxidation potential, since the electron withdrawing anthraquinone moiety will destabilise the TTFAQ dication and raise the oxidation potential of the TTFAQ moiety, as was seen for the TTF-quinone triad **82** of Müllen *et al.*¹⁰⁸ (Figure 36) and also for TTFAQ- C_{60} dyads of Martín and co-workers.¹²⁴ However, it is difficult to estimate more precisely the intramolecular electronic interaction, since no suitable reference compound has been synthesised (*e.g.* TTFAQ derivative **144**). Donor-acceptor dyad **130** also showed a single, reversible,⁶⁹ one-electron reduction wave from the anthraquinone moiety, but the second reduction wave could not be measured, which was also the case for triad **82**.¹⁰⁸

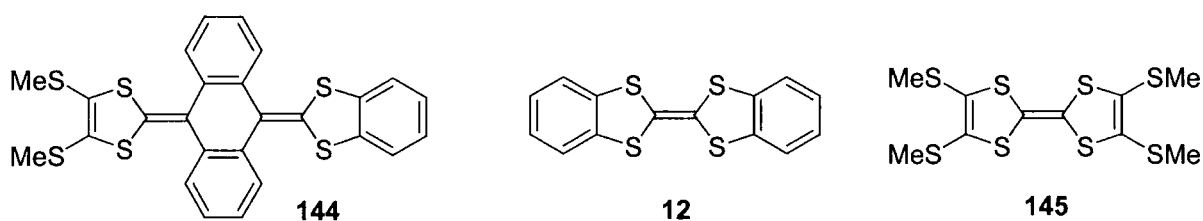


Figure 49: Suitable reference compounds for the interpretation of the oxidation potentials.

The CV of the conjugated TTFAQ dimer **143** showed to our surprise two finely resolved, quasi-reversible, two-electron oxidation waves ($\Delta E^{\text{ox}}_{\text{pa}} = 130$ mV, see Figure 50). For TTF derivatives **12** and **145** the difference in oxidation potentials are within 100 mV, with the dibenzoannelated derivative **12** having the lowest oxidation potential.^{6c} Thus, the difference in oxidation potentials for the two TTFAQ moieties making up **143** [they can be considered to be **144** and tetrakis(methylthio)TTFAQ **54**] cannot alone be explained by the difference in

substituents, but must also be due to a significant intramolecular electronic interaction, as was seen for the TTFAQ-donor dyads **137-139**¹²⁸ and **140-142**⁶⁸ linked through conjugation (Figure 44). Whichever TTFAQ moiety oxidises first becomes a good electron acceptor, and thus the dication **143**²⁺ can be considered as a conjugated donor-acceptor dyad. We wanted to investigate whether a charge-transfer band was present in the absorption spectrum of **143**²⁺, which could be done by spectroelectrochemistry, since this would confirm an electronic interaction between the two TTFAQ moieties of **143**.

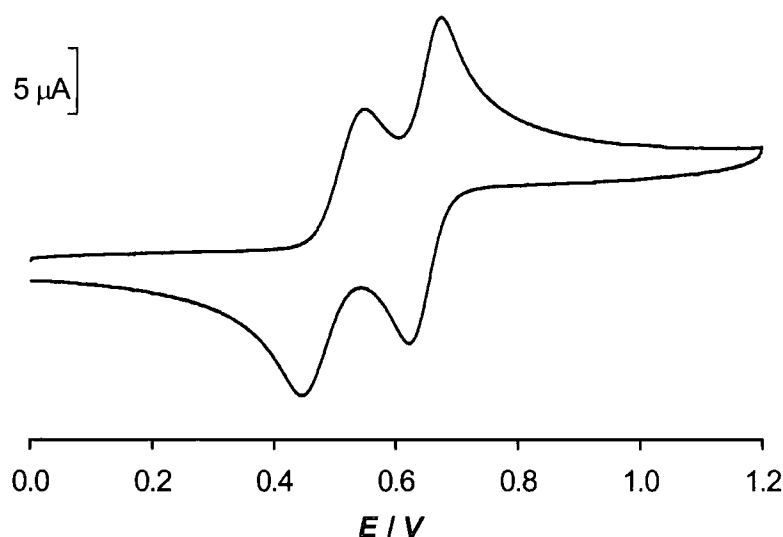


Figure 50: Cyclic voltammogram of conjugated TTFAQ dimer **143** showing two redox waves. Experimental conditions as in Table 2.

3.6.3 Spectroelectrochemical studies

Upon oxidation of **143** to the dication **143**²⁺ (Figure 51, Top) a UV-vis absorption spectrum resembling the sum of the spectra for neutral **54** and its dication (Figure 28) is formed. However, the broad band with $\lambda_{\text{max}} = 500$ nm extends to 850 nm, whereas the equivalent band for **54**²⁺ ended more sharply at 600 nm. This could indicate the presence of a charge-transfer band at $\lambda_{\text{max}} = 650$ nm overlaid with the broad band characteristic for the TTFAQ dication ($\lambda_{\text{max}} = 500$ nm). The CT band for the donor-acceptor system **143**²⁺ at $\lambda_{\text{max}} = 650$ nm is clearly seen upon further oxidation (Figure 51, Bottom). As the tetracation species **143**⁴⁺ is being formed, the donor moiety of the donor-acceptor system is being destroyed and the CT band collapses. The resulting absorption spectrum of **143**⁴⁺ resembles the sum of two typical spectra of the TTFAQ dication with one spectrum shifted *ca.* 50 nm compared to the other.

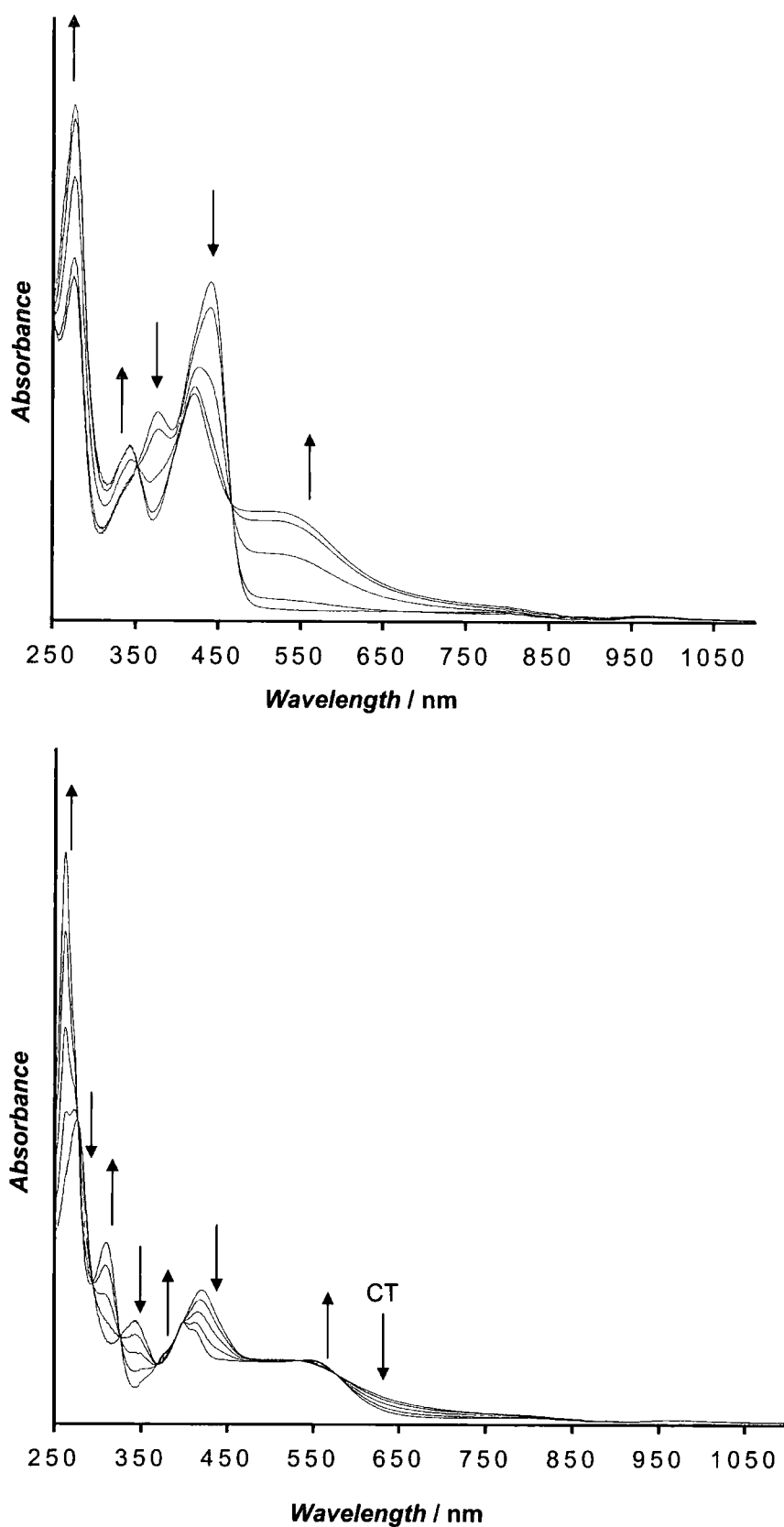


Figure 51: Spectroelectrochemistry of TTFAQ dimer 143 in dichloromethane. Top: Oxidation to form the dication species, *i.e.* donor-acceptor system 143²⁺. Bottom: formation of the tetracation 143⁴⁺ showing the collapse of the CT band at $\lambda_{\text{max}} = 650$ nm.

Since no intermolecular CT band was seen upon oxidation of TTFAQ derivative **54** to its dication species (Figure 28), we assign the CT band found for **143**²⁺ as being intramolecular, showing the interaction through conjugation of the two redox active moieties. For both the oxidation of **143** and **143**²⁺ isosbestic points indicate a clean formation of the dication and tetracation species, respectively. Also, both the spectrum of **143**²⁺ and neutral **143** could be fully recovered upon reduction of **143**⁴⁺, proving that no decomposition products could have afforded the assigned CT band at $\lambda_{\text{max}} = 650$ nm. Thus, this work did indeed lead to a donor-acceptor system **143**²⁺ showing ICT.

3.7 CONCLUSIONS

The synthesis of a TTFAQ diene precursor, building block **128** bearing two vicinal chloromethyl substituents, was successfully developed. Subsequent Diels-Alder reaction followed by aromatisation afforded conjugated donor-acceptor dyad **130**, consisting of a TTFAQ and an anthraquinone moiety, in good yield. However, **130** showed little or no charge-transfer. During the synthetic work, a rearrangement product identified as TTFAQ aldehyde **108** was discovered. Optimisation afforded a new and much more efficient synthesis of TTFAQ aldehydes. The crystal structures of both aldehyde **108** and donor-acceptor dyad **130** were obtained. The high crystallinity and dense packing of **130** seemed to be assisted by the right choice of alkylthio substituents. Conversion of **130** to the donor-donor dyad **143** afforded an interesting compound. In solution **143** is flipping between 2 conformers, which was proven by NOE experiments. The cyclic voltammogram of **143** showed two well-resolved two-electron oxidation waves, indicating intramolecular electronic interaction. This was further proved by the existence of an ICT band in the UV-vis spectrum of the dication species, which consists of a TTFAQ and a TTFAQ dication moiety, thus making up a conjugated donor-acceptor system. This work opens up the possibility for the incorporation of the TTFAQ unit into larger assemblies using the Diels-Alder reaction, and paves the way for further investigations into TTFAQ-acceptor systems.

4 PYRROLO-ANNELATED TTFAQ DERIVATIVES

In this chapter the work that was carried out during my stay in the group of Prof. Jan Becher, Odense University, will be described.

4.1 INTRODUCTION

Prior to my visit, the group of Prof. Becher had developed the synthesis of new mono- and bispyrrolo-annelated TTF derivatives **146** and **147**.¹³¹ TTF derivatives possessing fused heterocycles are well-known to be able to increase the dimensionality in the crystals of conducting charge-transfer salts.¹¹ For this reason alone, **146** and **147** should be very interesting, however, since pyrrole derivatives can be easily *N*-alkylated, this series of TTF derivatives were considered important new building blocks for the incorporation of TTF into macrocyclic and supramolecular assemblies.

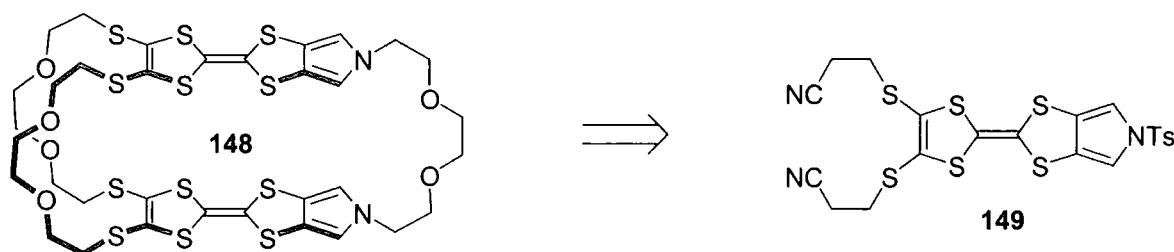


Figure 52: Mono- and bispyrrolo-annelated TTF derivatives synthesised by Becher and co-workers.¹³¹

4.1.1 Examples of assemblies containing pyrrolo-TTF

Currently pyrrolo-annelated TTF derivatives of type **146** are successfully being used as redox active moieties in rotaxanes and molecular-based electronically switchable devices,¹³² however, we were more interested in examples where **146** had been used in cyclophane synthesis. The triple-bridged pyrrolo-TTF cyclophane **148** could be made from the pyrrolo-TTF building block **149** in only 4 steps and in excellent yields.¹³³ The flexible oxyethylene linkers were designed to allow an interplanar distance between the two pyrrolo-TTF moieties of up to *ca.* 7 Å (see the X-ray crystal structure Figure 53), which is the optimal distance for CT and/or π - π interaction upon inclusion of an electron deficient guest molecule to be sandwiched between the TTF moieties.¹³⁴ Complexes with the good electron acceptor TCNQ **13**⁹ were studied both in solution and in the solid state. Two CT bands were observed in its

solution UV-vis absorption spectrum, at $\lambda_{\text{max}} = 749$ and 849 nm, respectively. However, an X-ray crystal structure of the CT complex **148**·TCNQ later revealed that the TCNQ molecule was located between two different cyclophanes, *i.e.* not acting as a guest in a host-guest complex.¹³³



Scheme 26: The triple-bridged pyrrolo-TTF cyclophane **148** could be made in 4 steps from the building block **149**.¹³³

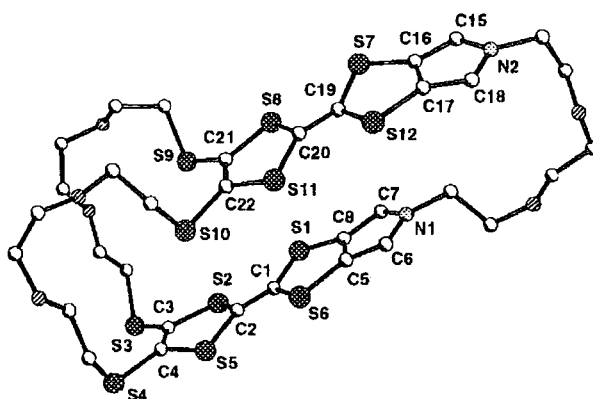
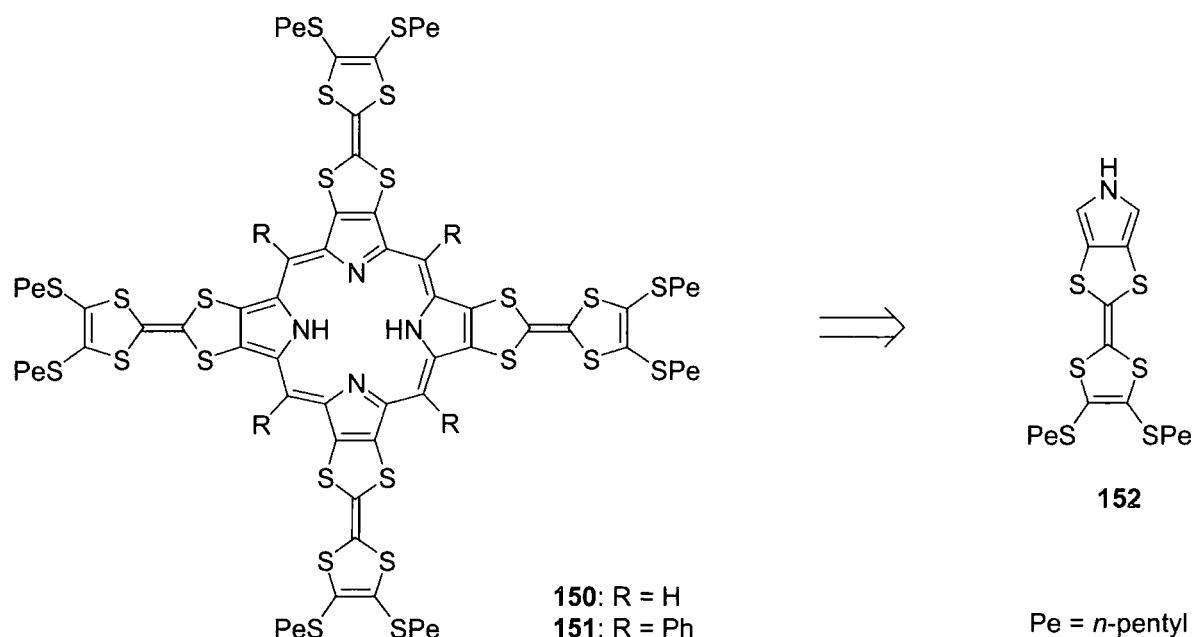


Figure 53: The X-ray crystal structure of the pyrrolo-TTF cyclophane **148**.¹³⁵

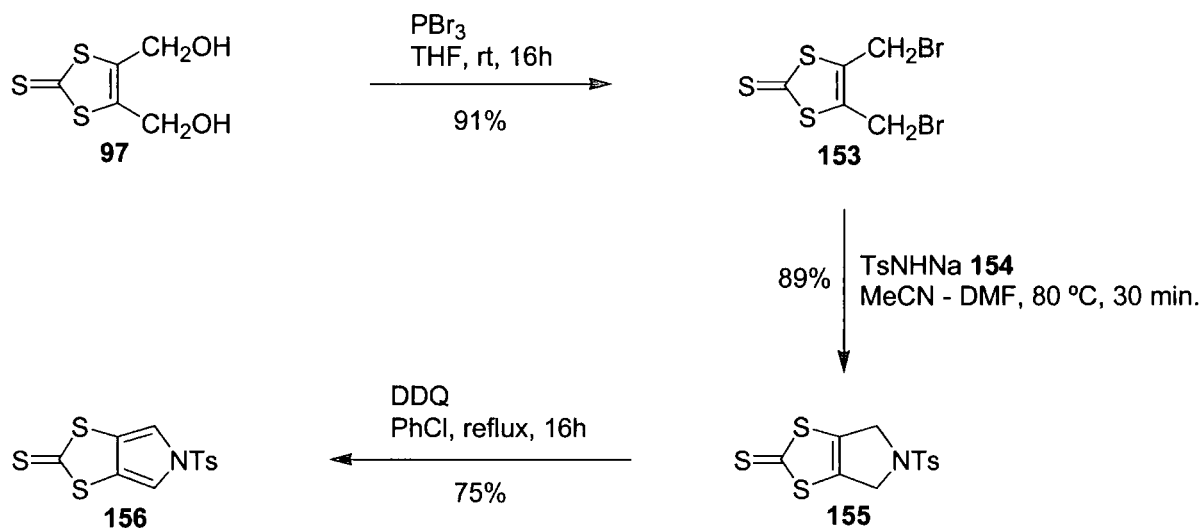
Related work in Becher's group involves the formation of porphyrins from pyrrolo-TTF derivatives of type **146**. The synthesis of tetrathiafulvaleno-annelated porphyrins **150** and **151** were achieved from the pyrrolo-TTF **152** in good yields using two different routes.¹³⁶ However, the porphyrins were difficult to characterise since they could only be obtained as a 4:1 mixture of the neutral and the cation radical species, which made ^1H NMR spectroscopy inapplicable. High resolution matrix-assisted laser-desorption/ionisation mass spectroscopy finally afforded good evidence of the existence of these peculiar compounds, combining the intriguing optical and metal-binding properties of the porphyrin with the favourable redox properties of TTF. The physical and metalbinding properties of **150** and **151** are currently under investigation.¹³⁶



Scheme 27: The TTF-annulated porphyrins **150** and **151** were made from pyrrolo-TTF derivative **152**.¹³⁶

4.1.2 Synthesis of the pyrrolo building block

The examples mentioned above had all been synthesised from the readily available building block **156** (Scheme 28).¹³¹



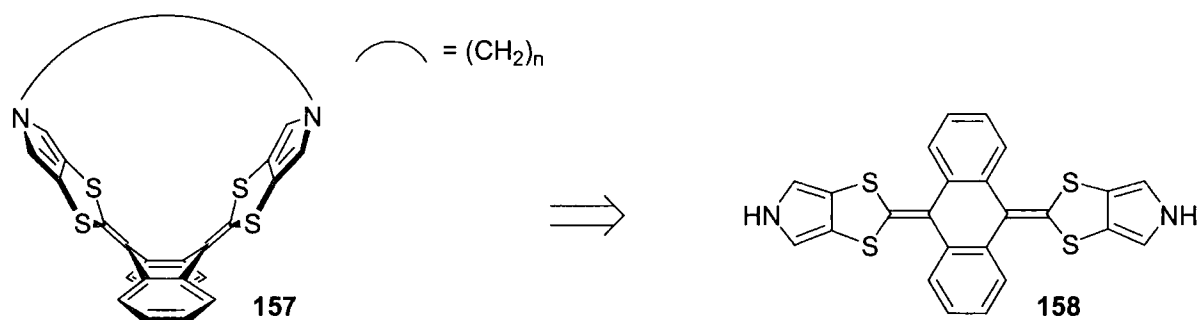
Scheme 28: Synthesis of the pyrrolo-annulated 1,3-dithiole-2-thione **156** proceeded in good yields.¹³¹

The synthesis of **156** is done in only 3 steps from 4,5-bis(hydroxymethyl)-1,3-dithiole-2-thione **97**¹²² (Scheme 13). Bromination of **97** using phosphorus tribromide afforded **153** in near quantitative yield. Cyclisation was performed by treatment of **153** with 2

equivalents of sodium tosylamide affording the dihydropyrrolo compound **155** in 89% yield and finally **155** was oxidised to the pyrrole derivative **156**, using DDQ, in 75% yield. The tosyl group serves as a protecting group in the subsequent TTF synthesis, but it is easily cleaved by reflux with excess sodium methoxide in a 1:1 (v/v) mixture of tetrahydrofuran-methanol.¹³¹

4.2 STRATEGY

Our aim was to utilise the pyrrolo-annulated 1,3-dithiole-2-thione building block **156** to synthesise bispyrrolo-TTFAQ **158**, which could be used for the preparation of TTFAQ cyclophanes **157** (Scheme 29). Bispyrrolo-TTFAQ **158** would be ideal for cyclophane synthesis by bridging the two pyrrolo-annulated 1,3-dithiole rings, since the pyrrole moieties should be easy to *N*-alkylate using a bisalkylating reagent, *i.e.* 1,6-diiodohexane. However, first task was to convert **156** to the corresponding phosphonate ester, so **158** could be formed in a subsequent Horner-Wadsworth-Emmons olefination.



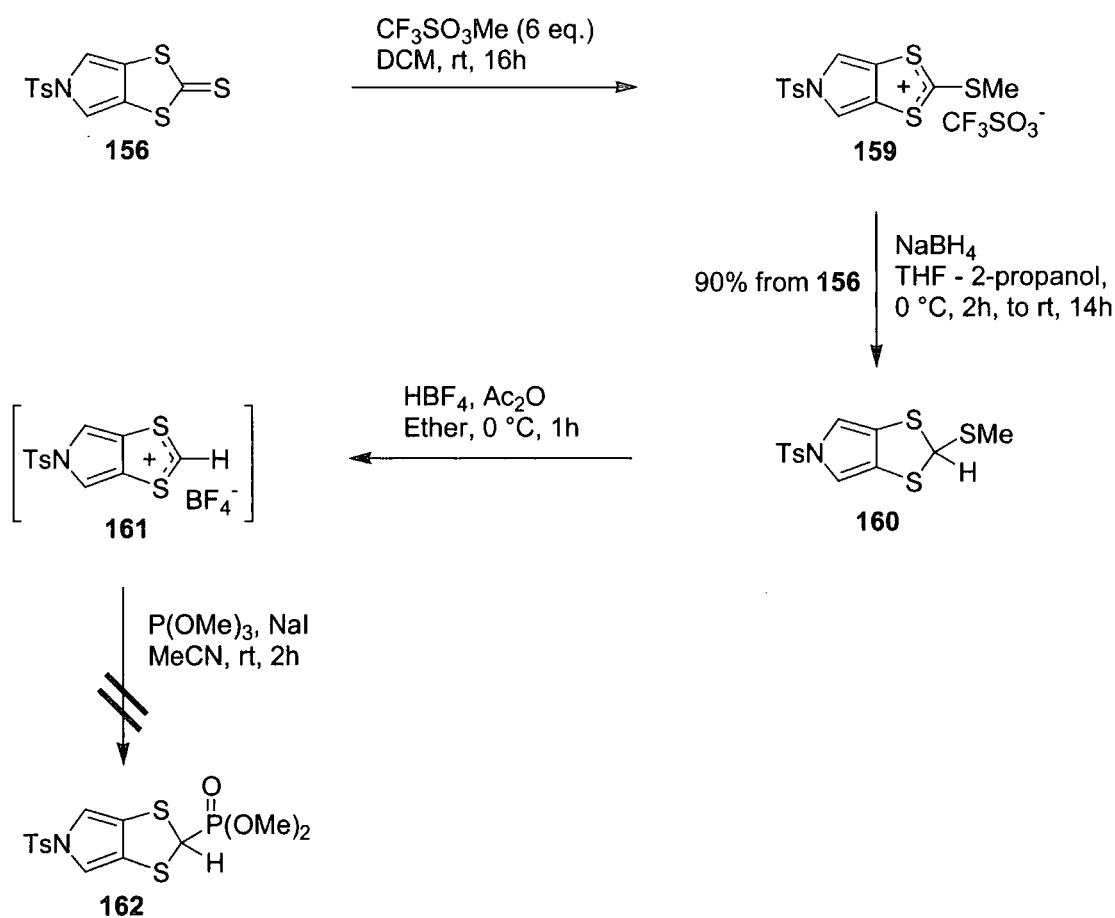
Scheme 29: From bispyrrolo-TTFAQ **158** it should be possible to synthesise new TTFAQ cyclophanes like **157**, where the two pyrrole moieties are linked by a $(\text{CH}_2)_n$ bridge.

4.3 SYNTHESIS OF PYRROLO-ANNELATED TTFAQ DERIVATIVES

The general procedure for the synthesis of phosphonate esters from 1,3-dithiole-2-thiones (see Appendix One) was applied to the conversion of **156** to the corresponding phosphonate ester reagent.

4.3.1 Synthesis of phosphonate esters containing the pyrrole moiety

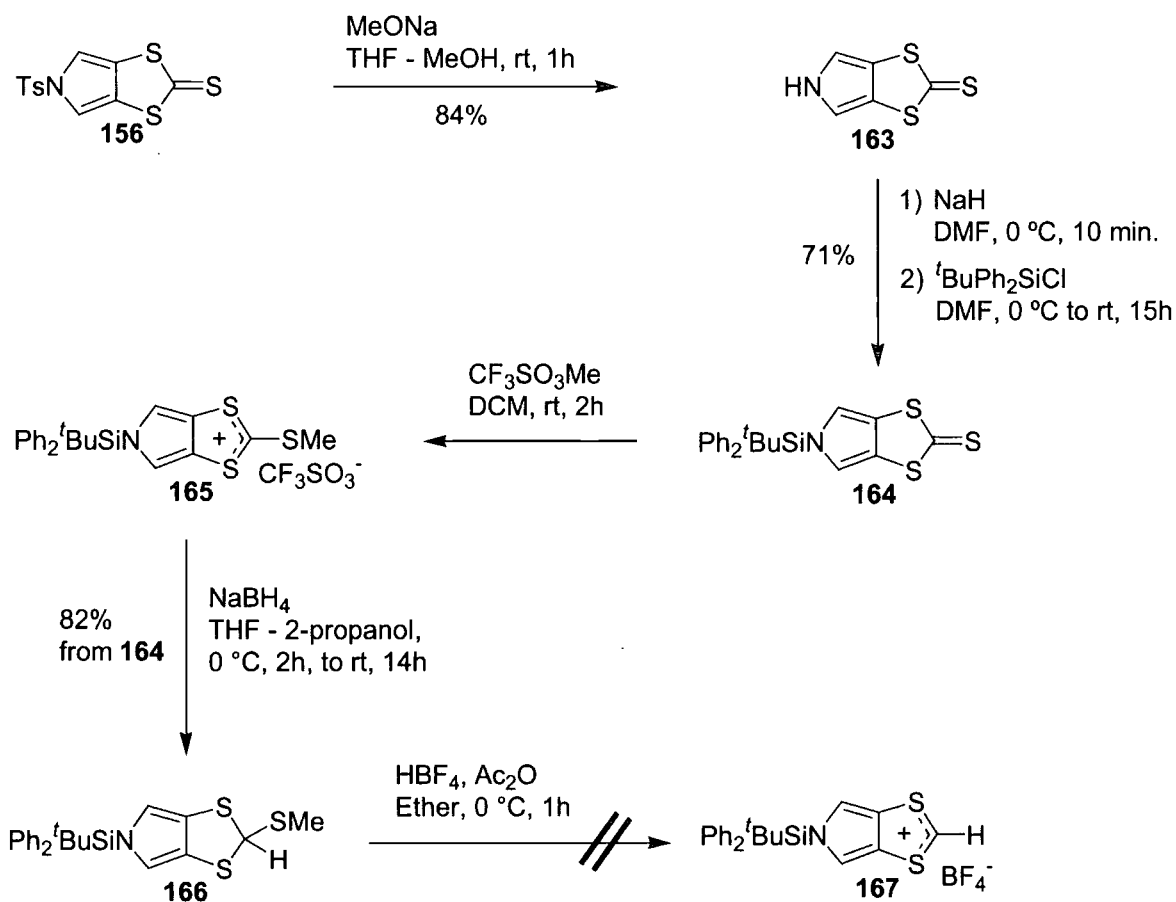
The pyrrolo-annulated 1,3-dithiole-2-thione building block **156**¹³¹ was methylated using methyl triflate under standard conditions (Scheme 30). However, whereas the methylation normally proceeds rapidly using an equimolar amount of methyl triflate, this reaction lasted 16 h and 6 equivalents of methyl triflate had to be used. This can be explained by the electron withdrawing effect of the tosyl group. The triflate salt **159** was used crude immediately upon concentration of the reaction mixture, due to its instability. Reduction of **159** using sodium borohydride in a mixture of tetrahydrofuran and 2-propanol proceeded smoothly and afforded **160** in 90% yield calculated from **156**.



Scheme 30: Attempted synthesis of a pyrrole containing phosphonate ester reagent.

The final two steps are normally done without characterisation of the intermediate 1,3-dithiolium salt, since they are generally not very stable. Thus **160** was protonated, using hydrofluoroboric acid, affording a yellow precipitate, which was reacted with trimethyl phosphite and an equimolar amount of sodium iodide in dry acetonitrile. This should have yielded the desired phosphonate ester **162**, but instead several other products had formed,

none of which were identified. The reaction was tried a few times, but the result was always the same. Probably the 1,3-dithiolium salt **161** was never formed, maybe due to the destabilisation of the electron withdrawing tosyl group, hence we decided to try another protecting group for the pyrrole moiety. Compound **156** was detosylated using the literature procedure to give **163** as a yellow powder (Scheme 31).¹³¹ The pyrrole **163** was deprotonated using sodium hydride in *N,N*-dimethylformamide and silylated with *tert*-butyldiphenylchlorosilane to give **164** in 71% yield. The methylation of **164** went smoothly, now the electron withdrawing tosyl group was no longer present, using 1 equivalent of methyl triflate under standard conditions. Again the triflate salt **165** was used crude and reduced immediately following standard conditions to give **166** in 82% yield from **164**.



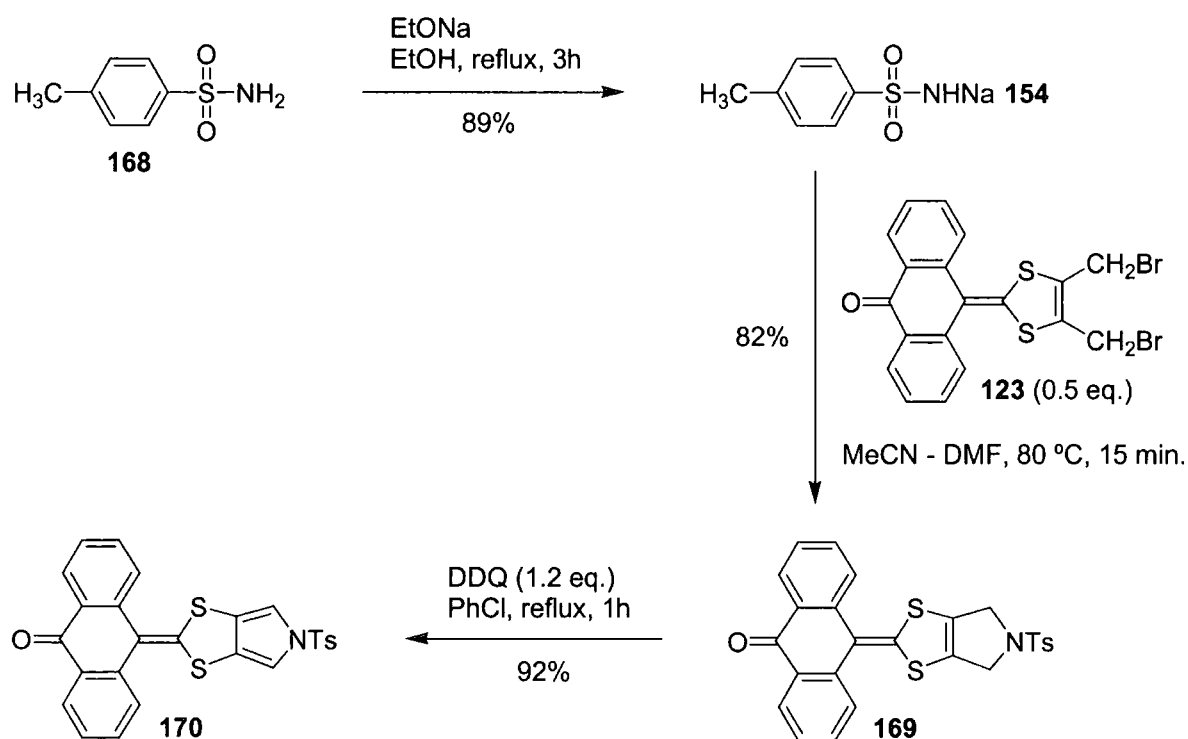
Scheme 31: Attempted synthesis of a 1,3-dithiole phosphonate ester bearing a silyl protected pyrrole.

Finally, to a solution of **166** in anhydrous diethyl ether at 0 °C was added dropwise a solution of hydrofluoroboric acid, which caused formation of a pale yellow precipitate. However, shortly after addition of the hydrofluoroboric acid, the precipitate turned orange-brown, and before the solvent could be removed so the reaction with trimethyl phosphite could proceed,

the precipitate had decomposed to black tar. Thus, using a silyl protecting group did not help to form a stable 1,3-dithiolium salt **167**. At this stage the attempts to synthesise a 1,3-dithiole-2-phosphonate ester containing a pyrrole moiety were abandoned. Alternatively, we appreciated that monopyrrolo-annulated TTFAQ derivatives should be available from the bis(bromomethyl) derivative **123** (Scheme 21), using conditions similar to the synthesis of the pyrrolo-annulated 1,3-dithiole-2-thione building block **156** (Scheme 28). These monopyrrolo-TTFAQ derivatives should be interesting in their own rights. The extension of the π -system of one of the 1,3-dithiole rings could afford interesting crystal packing, allowing increased intermolecular π - π interaction, but also the pyrrole unit could provide a new handle for the functionalisation of TTFAQ. However, the synthesis of TTFAQ cyclophanes following the initial strategy (section 4.2) could not be carried through, at least not using the methodology for TTFAQ synthesis available at the time.

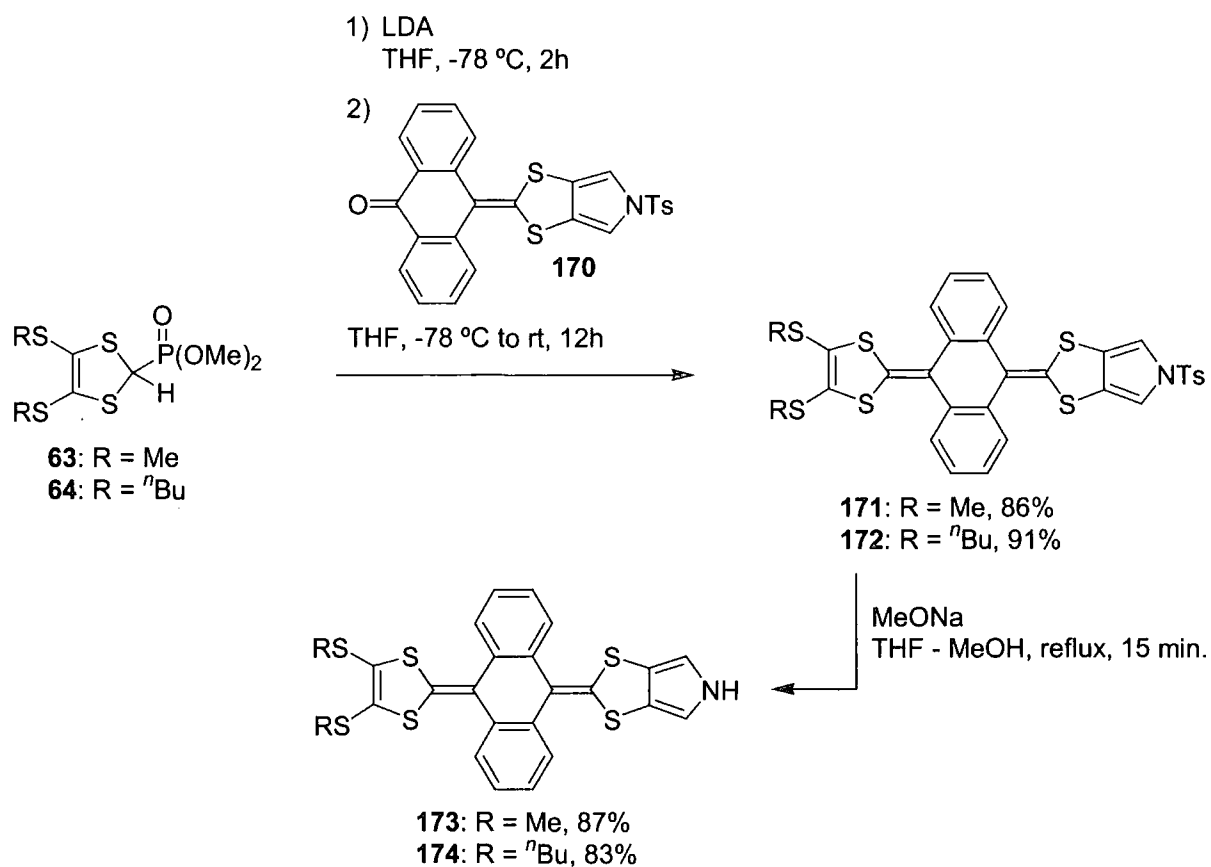
4.3.2 Synthesis of monopyrrolo-annulated TTFAQ derivatives

The dihydropyrrolo derivative **169** was made in a reaction between dibromide **123** and sodium tosylamide **154** (Scheme 32), which was made in quantitative yield from *p*-toluenesulfonamide following the literature procedure.¹³⁷



Scheme 32: Synthesis of the pyrrolo-annulated anthraquinone derivative **170**.

Two equivalents of sodium tosylamide were used, since 1 equivalent reacts with the formed HBr. The reaction conditions had to be followed very precisely to get a good yield. Too low a temperature afforded substitution by two equivalents of tosylamide on the dithiole moiety, whereas too high a temperature increased the amount of decomposition products. That is also why the reaction needed to be cooled as soon as it had gone to completion. In an optimised synthesis, **169** was obtained as an orange powder in 82% yield. Aromatisation of **169** to the pyrrolo derivative **170** was achieved by refluxing **169** in chlorobenzene in the presence of 1.2 equivalents of DDQ. This afforded the important intermediate **170** as a bright yellow powder in 92% yield. Monopyrrolo-annulated TTFAQ derivatives were now within reach by Horner-Wadsworth-Emmons olefinations using different phosphonate ester reagents.



Scheme 33: Synthesis of pyrrolo-annulated TTFAQ derivatives by a Horner-Wadsworth-Emmons olefination.

We decided to use phosphonate ester reagents **63** and **64** (see Appendix One for their synthesis) substituted with methylthio and butylthio groups, respectively, since this should afford pyrrolo-TTFAQ derivatives with different solubility and different possibilities for crystal packing. Thus, the anions generated by the reaction of phosphonate esters **63** and **64**

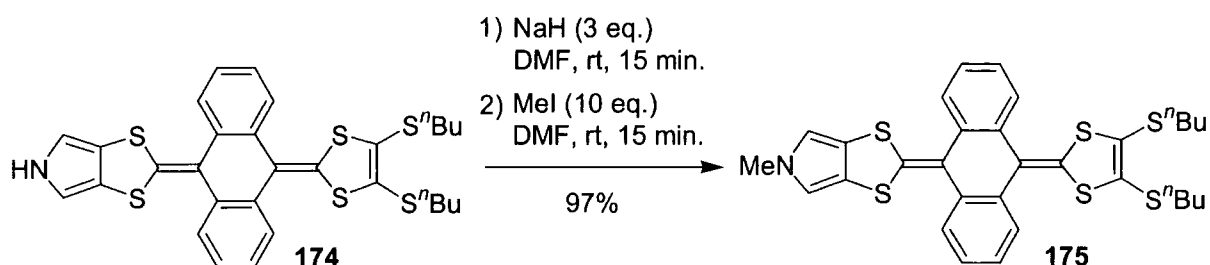
with lithium diisopropylamide at $-78\text{ }^{\circ}\text{C}$ were reacted with pyrrole derivative **170** to give the pyrrolo-annulated TTFAQ derivatives **171** and **172** in 86% and 91% yield, respectively. Compound **172** was obtained as a yellow powder which could not be recrystallized, but yellow prism-shaped single crystals of **171** were grown from dichloromethane-heptane. The crystal structure of **171** will be discussed below (section 4.5). For the detosylation of **171** and **172**, the standard conditions of Becher *et al.* were applied.¹³¹ Reflux in the presence of sodium methoxide in a 1:1 (v/v) mixture of tetrahydrofuran and methanol for 15 min afforded the unsubstituted pyrrolo-TTFAQ derivatives **173** and **174** in 87% and 83% yield, respectively. Some decomposition was observed during the detosylation, which is normally not the case for equivalent pyrrolo-TTF derivatives, hence the completed reaction was cooled and worked up rapidly. The hexylthio substituted derivative **174** afforded beautiful yellow prism-shaped single crystals (see the X-ray crystal structure in section 4.5), whereas **173** was obtained as a yellow powder. All the pyrrolo-TTFAQ derivatives were fully characterised and very soluble in common organic solvents, and they could be synthesised on a multigram scale.

4.4 MONOPYRROLO-ANNELATED TTFAQ DERIVATIVES IN SYNTHESIS

The possibilities for further functionalisation of the pyrrole moiety of the new TTFAQ derivatives **173** and **174** were investigated.

4.4.1 Functionalisation by *N*-alkylation of monopyrrolo-TTFAQ

Monopyrrolo-TTFAQ derivative **174** was deprotonated using 3 equivalents of sodium hydride in *N,N*-dimethylformamide, whereupon methylation using excess methyl iodide proceeded in near quantitative yield to give **175** as a yellow powder.

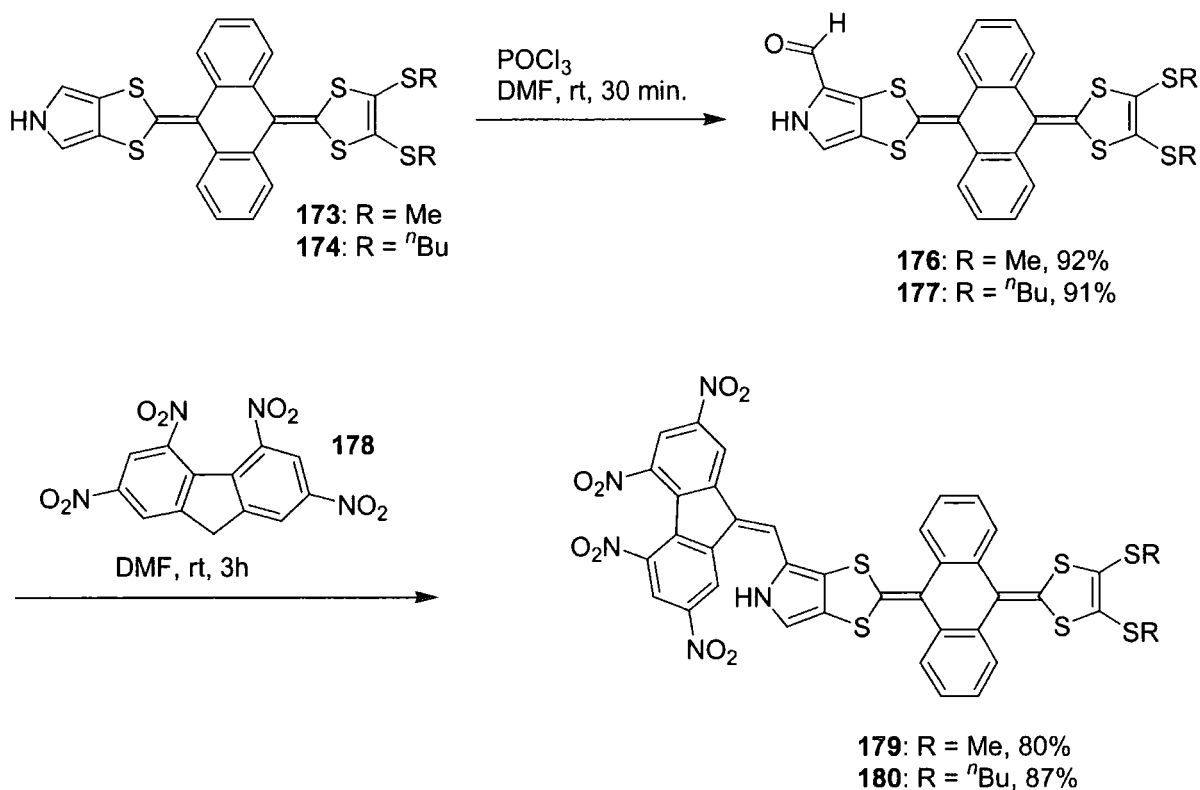


Scheme 34: *N*-alkylation of **174** using methyl iodide proceeded in near quantitative yield.

Large prism-shaped crystals were readily obtained by diffusion of heptane into a solution of **175** in dichloromethane and the structure of **175** was proven by X-ray crystallography (see section 4.5). Thus, it should be possible to functionalise the pyrrolo-TTFAQ derivatives by reaction with different electrophiles.

4.4.2 New donor-acceptor dyads from formylated pyrrolo-TTFAQ derivatives

Although a new route to formylated TTFAQ derivatives was developed in section 3.4.5, it was still very attractive to us to find an efficient and high-yielding route to formylated TTFAQ derivatives, since this could provide a new building block for future conjugated donor-donor or donor-acceptor systems (see Chapter 3) *via* condensation reactions. Vilsmeier formylation of the pyrrolo-TTF derivatives **146** had proven to be very efficient,¹³⁶ thus compounds **173** and **174** were reacted with phosphorus oxychloride and *N,N*-dimethylformamide under standard conditions to give aldehydes **176** and **177** in 92% and 91% yields, respectively (Scheme 35).

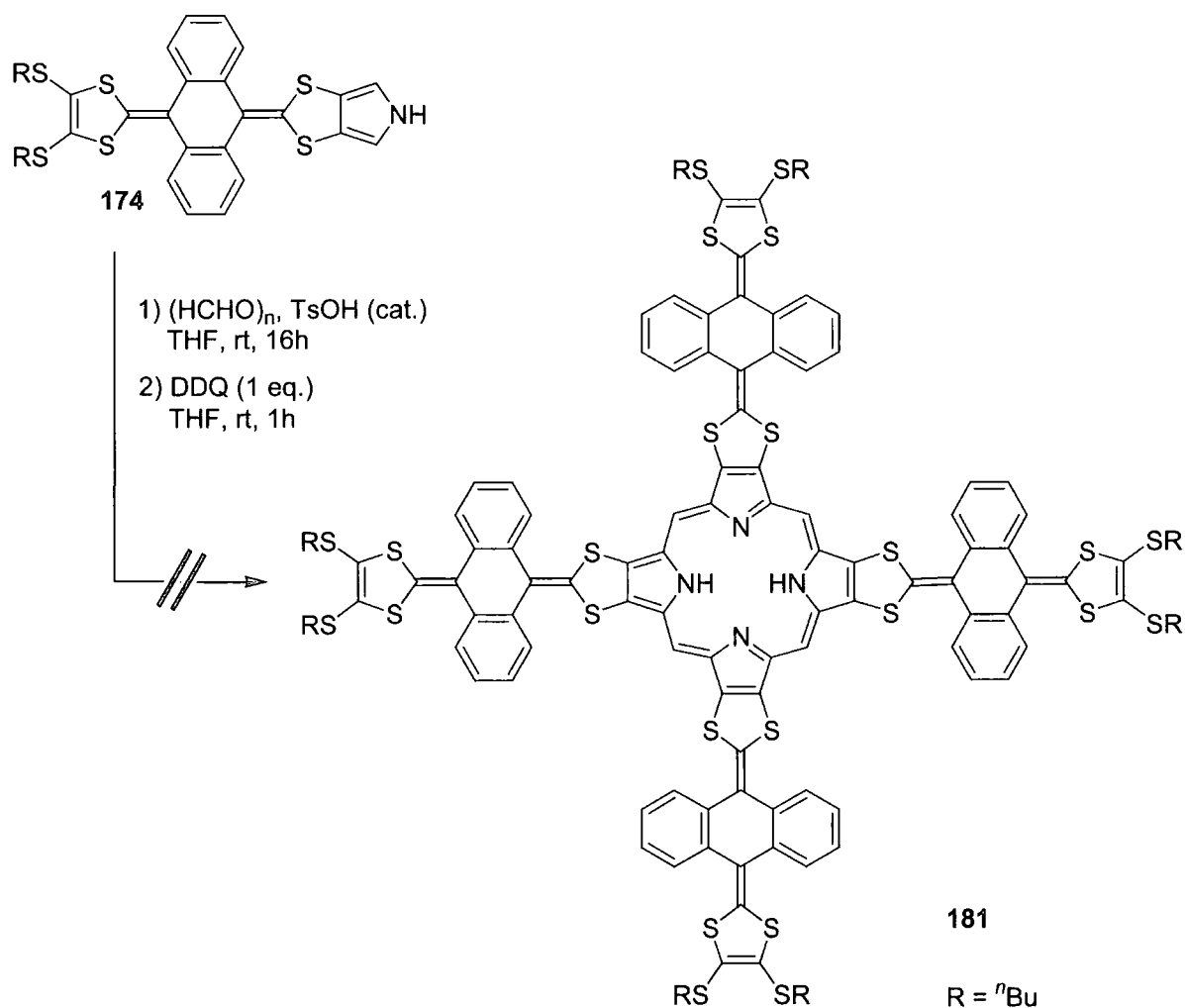


Scheme 35: Vilsmeier formylation of **173** and **174** proceeded in excellent yields, affording aldehydes which could subsequently be used for the synthesis of donor-acceptor dyads **179** and **180**, respectively.

To prove the versatility of these new formylated TTFAQ derivatives, examples of donor-acceptor dyads from **176** and **177** were synthesised. For this purpose, a sample of the acceptor 2,4,5,7-tetranitrofluorene **178**¹³⁸ was kindly donated by Dr. Dmitrii F. Perepichka. Condensation in *N,N*-dimethylformamide of donors **176** and **177** with fluorene acceptor **178** afforded dyads **179** and **180**, respectively, as black powders in good yields. Dyad **180** was very soluble in common organic solvents, whereas **179**, possessing methylthio groups, had low solubility. Their ¹H NMR spectra were affected by the ability of **179** and **180** to adopt two different conformations, which afforded two sets of broad peaks. Hence, some of the signals in the ¹H NMR spectra have non-integer integrals (see section 8.3). However, the dyads were also characterized by mass spectroscopy and elemental analysis.

4.4.3 Attempted synthesis of a TTFAQ-annelated porphyrin

During my stay in the group of Prof. Becher, the work concerning the TTF-annelated porphyrins (Scheme 27) attracted our attention, since the TTF-annelated porphyrins could only be obtained as a mixture of the neutral and the cation radical species.¹³⁶ Possibly a TTFAQ-annelated porphyrin could afford a stable species containing a TTFAQ cation radical moiety. Thus an attempt at the direct synthesis of TTFAQ-annelated porphyrin **181** from pyrrolo-TTFAQ **174** was carried out, following the procedure developed by Dr. Thomas Brimert for the synthesis of TTF-annelated porphyrins.^{136,139} Pyrrolo-TTFAQ **174** and paraformaldehyde were mixed in tetrahydrofuran together with a catalytic amount of *p*-toluenesulfonic acid and the mixture was stirred at room temperature overnight. This resulted in a black solution and DDQ was added to ensure full oxidation to the porphyrin species. After column chromatography, two amorphous black solids were isolated, which both afforded ¹H NMR spectra with broad signals where only the multiplets from the hexylthio and the anthracene moieties could be identified. Furthermore, their mass spectrum could not be obtained since they afforded no signal, something which was also observed for some of the TTF-annelated porphyrins.¹³⁹ Thus, the synthesis of TTFAQ-annelated porphyrins was not pursued any further.



Scheme 36: Attempted synthesis of TTFAQ-annulated porphyrin 181. Two black amorphous compounds were isolated, but they could not be characterised.

4.5 X-RAY CRYSTALLOGRAPHIC ANALYSIS

The molecular structures and conformations of **174** and **175** are similar (Figure 54). The TTFAQ core of the molecule adopts the usual saddle-shape, with the central ring of the dihydroanthracene moiety folded along the C(9)···C(10) vector by 39.5° and 38.1°, respectively. The pyrrole ring and the adjacent S(1) and S(2) atoms are co-planar within experimental error, and since both dithiolenyl rings are folded inward along the S(1)···S(2) and S(3)···S(4) vectors, respectively, the S(3)C(21)C(22)S(4) plane forms a slightly acute angle (82.0° in **174** and 84.5° in **175**) with the pyrrole ring system. In both structures the *n*-butyl chain at the S(5) atom is disordered between two conformations in a 10:1 (**174**) or 2:1 (**175**) ratio. The major component and the other (ordered) *n*-butyl chain adopt the planar all-*trans* conformations and lie practically parallel to the pyrrole ring. Two molecules, related *via* an

inversion centre, form a typical pseudo-dimer in which *n*-butyl chains of one molecule are engulfed between the pyrrole ring and *n*-butyl chains of the other, their separations corresponding to normal van der Waals distances.¹⁴⁰ Hence, the pseudo-dimers of **174** and **175** resemble the pseudo-dimer formed by donor-acceptor dyad **130** (Figure 41). The shortest intradimer contacts are S(6)···N' of 3.43 Å in **174** and 3.54 Å in **175**, and it is noteworthy that the NH group in **174** forms no hydrogen bond.

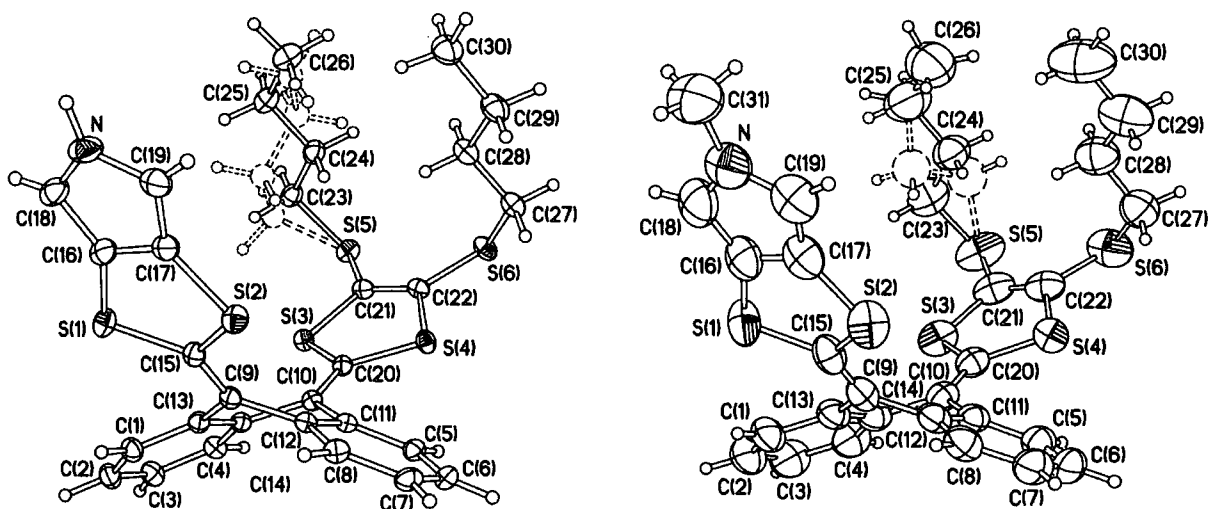


Figure 54: The X-ray crystal structures of **174** (left) and **175** (right) showing the disorder in the *n*-butyl chain at the S(5) atom.

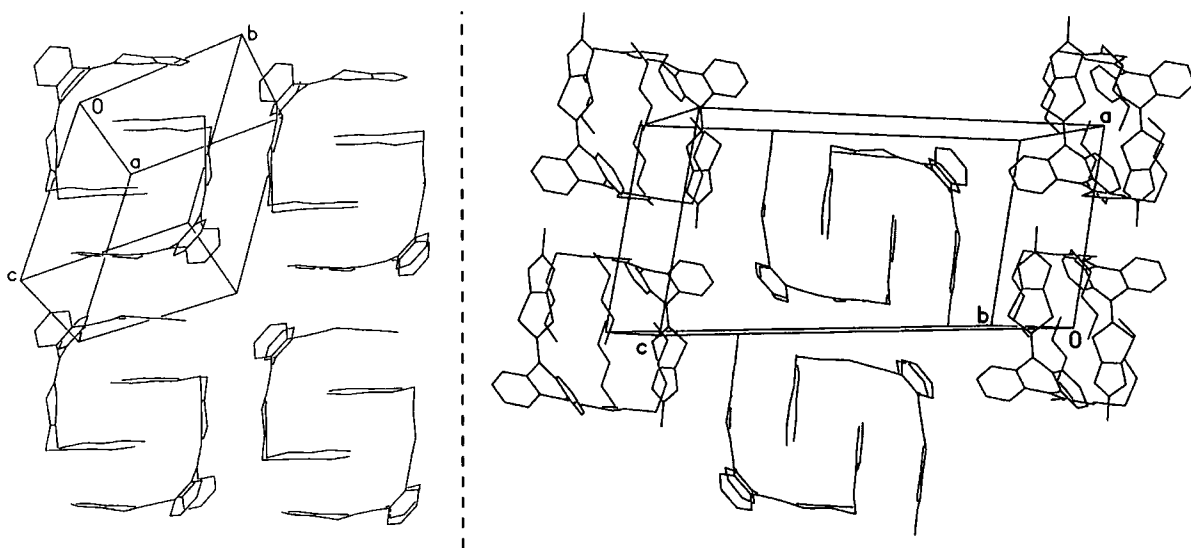


Figure 55: Crystal packing of **174** (left) and **175** (right).

Packing of pseudo-dimers in **174** and **175** is different. In the triclinic structure **174**, all pseudo-dimers have the same orientation and form a succession of layers (Figure 55, left).

Within a layer, each pseudo-dimer interacts with four others through two face-to-face contacts between dithiole rings and two face-to-face contacts between dithiole-pyrrole systems; the shortest contact distances $S\cdots S$ 3.63-3.73 Å and $S\cdots C$ 3.54-3.61 Å are close to the sums of the van der Waals radii (S, 1.81 Å; C, 1.77 Å).¹⁴⁰ In the monoclinic structure **175**, the pseudo-dimers are arranged in rows, parallel to the x axis, but dimers in adjacent layers have non-parallel (herring-bone) orientations (Figure 55, right). Thus face-to-face contacts of dithiole rings exist only within the row; the shortest distances therein ($S\cdots S$ 3.73 and $S\cdots C$ 3.69-3.72 Å) are comparable to those in **174**.

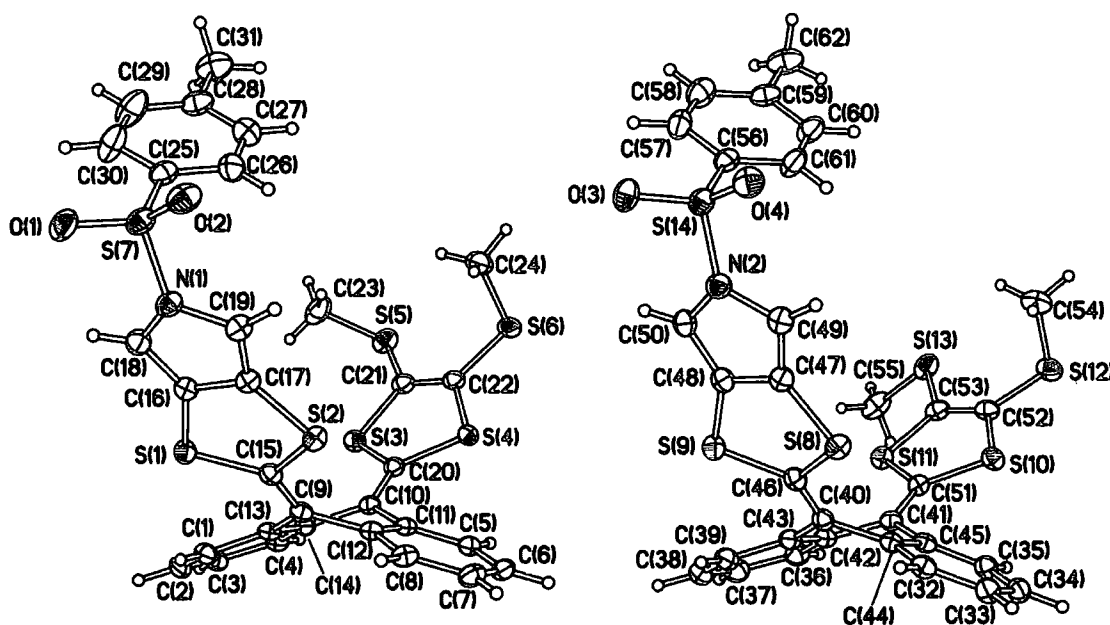


Figure 56: The X-ray crystal structure of **171** revealed two independent molecules A and B.

The asymmetric unit of **171** comprises two molecules (A and B) of broadly similar, but not identical, conformation (Figure 56). The dihydroanthracene moiety is folded along the $C(9)\cdots C(10)$ vector by 39.0° (A) and 40.0° (B), and both dithiole rings are folded inwards along the $S\cdots S$ vectors. Thus, the angle between the $S(1)C(16)C(17)S(2)$ and $S(3)C(21)C(22)S(4)$ planes in A and the corresponding angle in B is reduced to 76.0° . Whilst in **174** and **175** the pyrrole ring with immediately adjacent atoms comprise a planar system, in **171** (molecule A) the ring is folded along the $C(18)\cdots C(19)$ vector by 2.7° and the N-S bond tilts out of the $C(18)NC(19)$ plane by 20.6° (in molecule B by 2.4° and 13.5° , respectively). Each of the independent molecules and its own inversion equivalent form a mutually engulfing pseudo-dimer. In contrast with structures **174** and **175**, where the molecular cavity is occupied by the long n -butyl chains, in **171** the dithiole ring itself and its methylthio

substituents are accommodated therein, with the short intradimer contacts $S(2)\cdots S(5^{ii})$ 3.59 Å and $S(8)\cdots S(13^{iii})$ 3.60 Å for A and B, respectively. Pseudo-dimers of each type, related by the a - b translation, contact by their dithiole-pyrrole systems in a face-to-face fashion, thus forming an infinite chain (Figure 57). The contact between BB^{iii} dimers is rather close: the dithiole-pyrrole systems overlap in a nearly eclipsed manner (pyrrole over dithiole ring, and *vice versa*) with the interplanar separation of 3.52 Å. For AA^{ii} dimers the separation is larger (3.66 Å) and there is a large lateral shift between the fused systems.

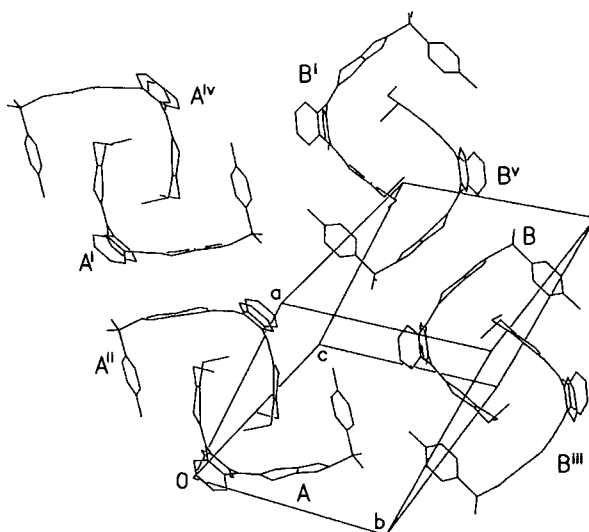


Figure 57: Crystal packing of 171.

In conclusion, pronounced intermolecular π - π interaction was indeed observed in the crystal structures of **171**, **174** and **175**, as a consequence of the extension of the π -system of one of the 1,3-dithiole rings. Attempts to get single crystals of a dication salt of the monopyrrolo-TTFAQ derivatives were unsuccessful. Complexes with TCNQ **13**⁹ were not crystalline, and the crystals obtained by electrocrystallisation were too small for an X-ray crystallographic analysis.

4.6 OPTICAL AND ELECTROCHEMICAL PROPERTIES

The cyclic voltammograms and the UV-vis absorption spectra for all the pyrrolo-annelated TTFAQ derivatives were recorded; most interesting were the spectra of the donor-acceptor dyads **179** and **180**, since intramolecular CT is most frequently manifested in the optical and electrochemical properties of donor-acceptor dyads (see section 3.1).

4.6.1 Solution electrochemical properties

The monopyrrolo-TTFAQ derivatives **171-177** all showed a single, quasi-reversible,⁶⁹ two-electron oxidation wave at potentials higher than for unsubstituted TTFAQ, which can partly be explained by the alkylthio substituents.⁶⁴ The effect of the pyrrole moiety is dependent on its substituents. Thus tosylated pyrrolo-TTFAQ derivatives **171** and **172** have oxidation potentials 130-170 mV higher than for their unsubstituted analogues, reflecting the electron withdrawing effect of the tosyl group. Alkylation of **174** to give **175** did not seem to have any significant effect, whereas formylation raised the oxidation potential by 50-90 mV.

Compound	E_{pa}^{ox}/V	E_{pc}^{ox}/V	E_{pc}^{red}/V
171	0.63	0.45	-
172	0.66	0.46	-
173	0.50	0.35	-
174	0.49	0.34	-
175	0.50	0.32	-
176	0.55	0.48	-
177	0.58	0.47	-
179^a	0.63	0.42	-0.41
180^a	0.64	0.45	-0.41

Table 3: Cyclic voltammetric data vs. Ag/AgCl. Compound *ca.* 1×10^{-3} M and electrolyte 0.1 M Bu₄NPF₆ in dichloromethane, 20 °C, scan rate 100 mV s⁻¹.¹²⁹ ^a An irreversible reduction wave was observed at E_{pc}^{red} .⁶⁹

The donor-acceptor dyads **179** and **180** showed a single, quasi-reversible, two-electron oxidation wave shifted by 130-150 mV compared to their unsubstituted precursors **173** and **174**. This can be explained by the conjugatively linked acceptor moiety, indicating a donor-acceptor interaction. In addition, the cyclic voltammograms of **179** and **180** displayed a single, irreversible, presumably one-electron reduction wave at -0.41 V, from the fluorene moiety (see the CV of **180**, Figure 58). Normally 9-substituted fluorene derivatives show reversible reduction waves. However, similar irreversible behaviour upon reduction, which is not fully understood, was observed for other condensed fluorene adducts (containing the fluorene=CH-R fragment).¹⁴¹

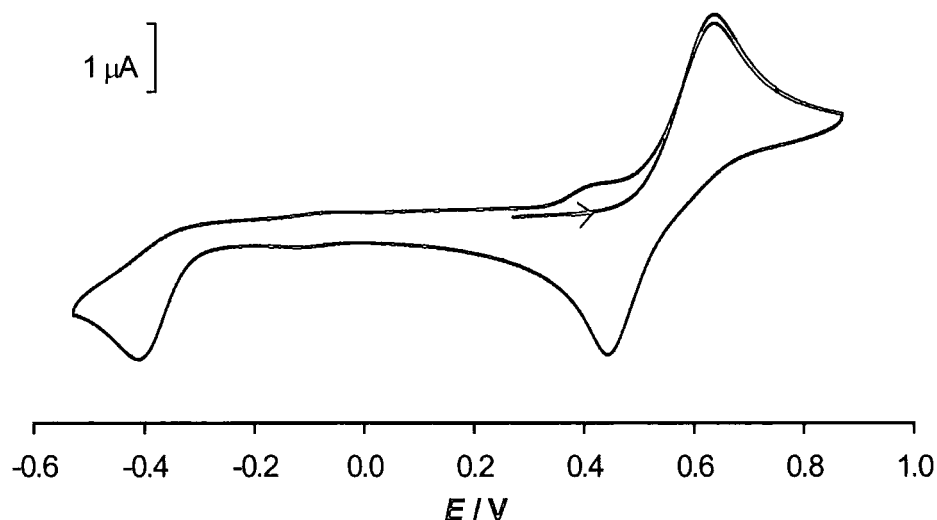


Figure 58: CV of donor-acceptor dyad 180. Experimental conditions as listed in Table 3.

4.6.2 UV-vis absorption spectra of dyads 179 and 180

The donor-acceptor dyads 179 and 180 were black powders having an intensely dark red colour in solution, clearly different from typical yellow TTFAQ derivatives. Thus a charge-transfer band was expected in the UV-vis absorption spectrum.

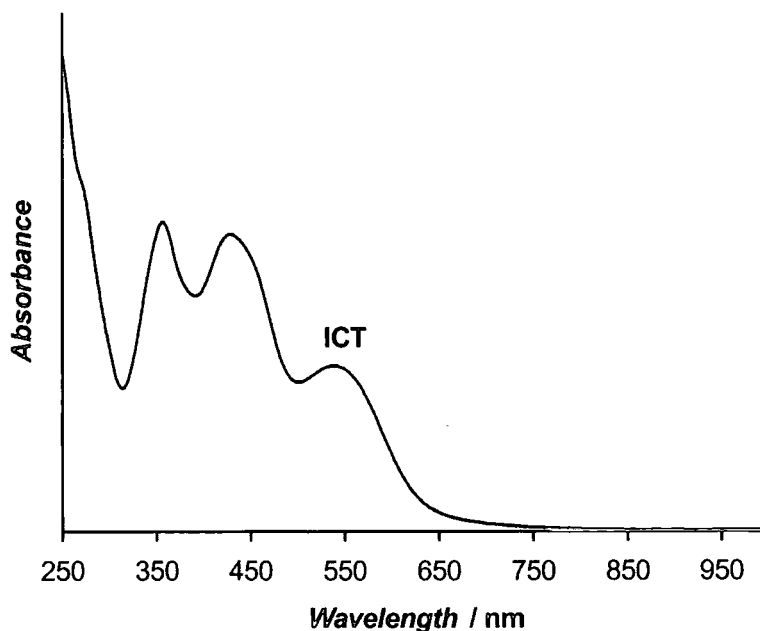


Figure 59: The UV-vis absorption spectrum of a solution of conjugated donor-acceptor dyad 180 in dichloromethane displaying an ICT band at $\lambda_{\text{max}} = 538$ nm.

The spectra of **179** and **180** were almost identical, hence the spectrum of **180** (see Figure 59) will be used as an example in this section. The absorption spectrum of **180** showed two bands typical for TTFAQ derivatives at $\lambda_{\text{max}} = 357$ nm and 428 nm, respectively. However, a third long-wavelength band was present at $\lambda_{\text{max}} = 538$ nm, indicating a significant charge-transfer interaction. Since the intensity of this band, relative to the two high-energy bands, was independent of concentration, we assign this to an intramolecular charge-transfer (ICT) band. Thus, having the donor and acceptor moiety in conjugation again proved to be beneficial for ICT (see section 3.1). Indeed, similar ICT bands have been observed for other conjugatively linked donor-acceptor dyads containing the tetranitrofluorene moiety.¹⁴²

4.7 CONCLUSIONS

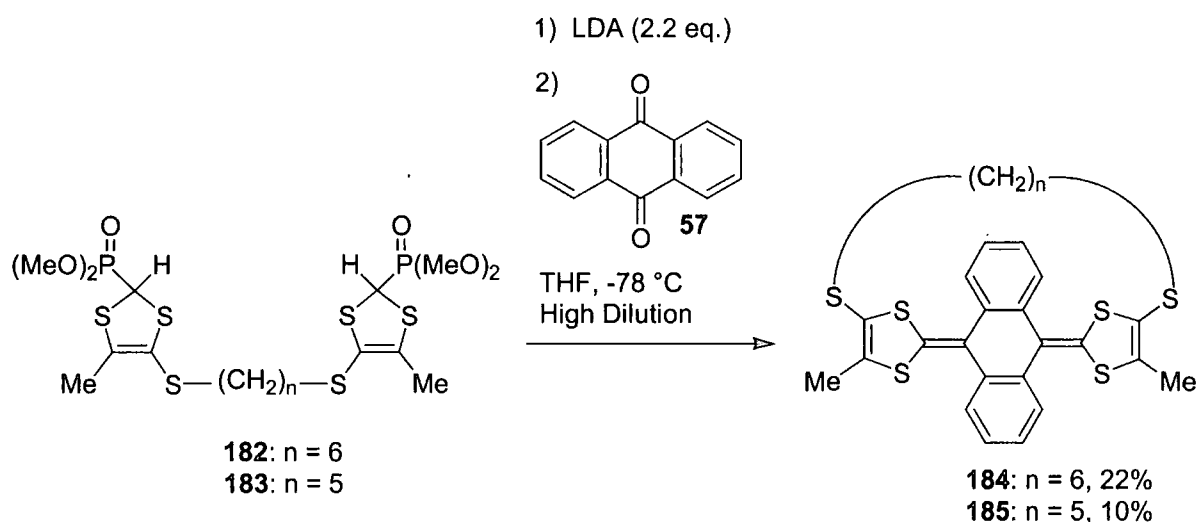
A series of monopyrrolo-annulated TTFAQ derivatives were successfully synthesised and fully characterized. This provides new TTFAQ building blocks, since the pyrrole moiety was easily *N*-alkylated. More importantly, the monopyrrolo-TTFAQ derivatives could be formylated in near quantitative yields, affording new donors for conjugatively linked donor-donor and donor-acceptor systems. Thus, conjugated donor-acceptor dyads **179** and **180**, containing a fluorene acceptor moiety, were synthesised in good yields. A significant ICT band was present in the UV-vis absorption spectrum of dyads **179** and **180**, and also the oxidation potentials were affected by the conjugatively linked acceptor. The solid state conformations of both unsubstituted **174**, tosylated **171** and methylated **175** pyrrolo-TTFAQ derivatives were studied by X-ray crystallography, showing pronounced intermolecular π - π interaction in the crystal structure, as a consequence of the extension of the π -system of one of the 1,3-dithiole rings. However, an initial aim of synthesising a bispyrrolo-annulated TTFAQ derivative **158** was not achieved, since a pyrrolo-annulated phosphonate ester reagent could not be generated. Hence, the strategy of making TTFAQ cyclophanes from **158** could not be tested. Furthermore, the synthesis of cyclophanes containing pyrrolo-TTFAQ moieties will not be possible unless a new methodology for the synthesis of TTFAQ derivatives is developed (see Chapter 6).

5 CYCLOPHANES FROM 2,6-BISFUNCTIONALISED TTFAQ BUILDING BLOCKS

This chapter describes the design and synthesis of a set of very versatile TTFAQ building blocks and their use in cyclophane synthesis. The solid state properties and the solution electrochemistry of the cyclophanes will be described, as will the synthesis of a novel donor-acceptor triad, which could also be easily obtained from the TTFAQ building blocks.

5.1 BACKGROUND AND STRATEGY

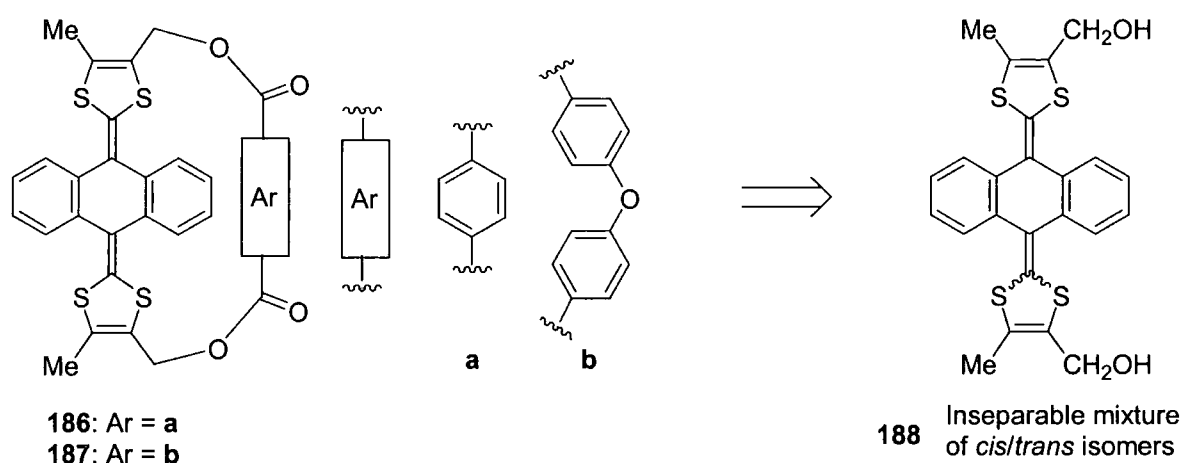
The conformational change of TTFAQ **49** upon oxidation (Scheme 6) makes it an interesting unit to incorporate into redox active cyclophanes. Especially interesting would be the solution electrochemical behaviour and the solid state structure of the TTFAQ moiety upon oxidation, when conformationally locked in a cyclophane structure. However, the synthesis of more elaborate TTFAQ cyclophanes containing a second active moiety (*e.g.* for ion recognition) would present an even bigger, but interesting challenge.



Scheme 37: Synthesis of the first TTFAQ cyclophanes 184 and 185. The shortest bridge between the two 1,3-dithiole moieties of the TTFAQ unit was pentamethylenedithio.¹⁴³

The first TTFAQ cyclophanes **184** and **185** were synthesised by Finn in our group, by a two-fold olefination reaction of anthraquinone **57** using reagents **182** and **183** (Scheme 37).¹⁴³ The

bridge increased the oxidation potential significantly relative to non-bridged analogues,¹⁴⁴ an effect which was also seen for short-bridged TTF cyclophanes (see section 1.2.4). Unfortunately, the route was low yielding and not very versatile, because a new bis(1,3-dithiole-2-phosphonate) reagent had to be synthesised for each different cyclophane. Furthermore, only a limited number of functionalities could be built into the cyclophane structure, due to the harsh reaction conditions for making the bis(1,3-dithiole-2-phosphonate) reagents. Hence, new methodology was sought. The next step was taken by Godbert in our group, alongside the work presented in this chapter. Godbert used a single pre-made TTFAQ building block, bis(hydroxymethyl) derivative **188**, to synthesise a series of cyclophanes *e.g.* **186** and **187** (Scheme 38).¹⁴⁵ A limitation was that compound **188** is isolated as an inseparable 50:50 mixture of *cis/trans* isomers and since the isolated cyclophanes were always only *cis*, the *trans* isomer was wasted and probably polymerised during the macrocyclisation reaction, resulting in a lower overall yield.



Scheme 38: Cyclophanes **186** and **187** were both made from TTFAQ building block **188**.¹⁴⁵

Although the TTFAQ cyclophanes of Finn and Godbert were synthesised in two very different ways, they had one feature in common, they were made by bridging the two 1,3-dithiole rings. Alternatively, we recognised that the saddle-shaped TTFAQ molecule could be bridged across the dihydroanthracene ring system. Thus far some TTFAQ derivatives with a monofunctionalised dihydroanthracene ring system were known,¹⁴⁶ but only a few bisfunctionalised derivatives had been reported, *e.g.* those synthesised by Marshallsay and Bryce directly from building block **189**.¹⁴⁷ However, due to solubility problems with the deprotected hydroxy analogue of **189**, compound **189** was not applied to cyclophane synthesis. The only other TTFAQ derivatives with a bisfunctionalised

dihydroanthracene ring system possessed only alkoxy groups in the 2- and 6-positions, compound **190** being an example.⁷³

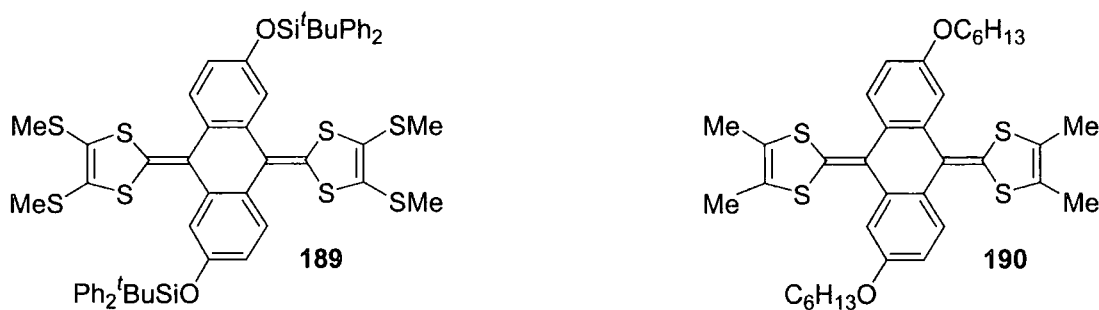
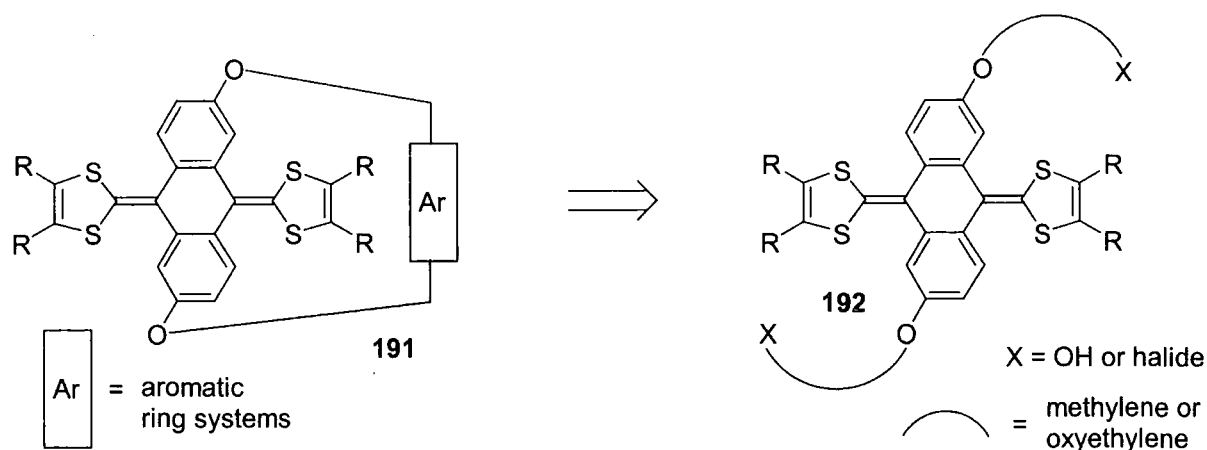


Figure 60: TTFAQ derivatives functionalised in the 2- and 6-position.

Inspired by the 2,6-bissubstituted TTFAQ derivatives **189** and **190**, we decided to synthesise TTFAQ building block **192**, which we would use for the synthesis of cyclophanes **191**. Compound **192** is symmetrical, so that isomer problems would be avoided, and has good solubility due to the linkers, which also could be varied in lengths. The linkers should possess terminal functionalities like alcohols or halides for the following cyclophane synthesis.



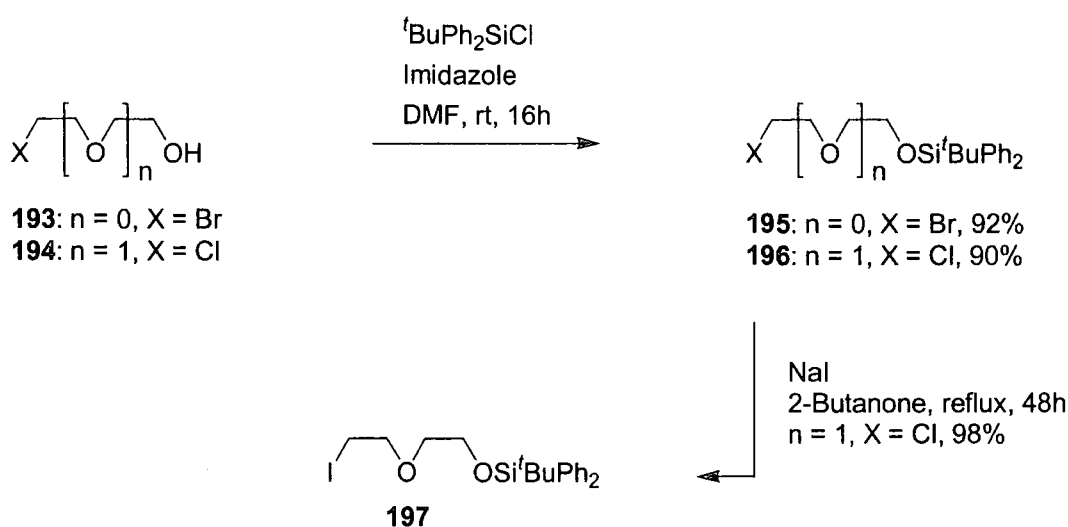
Scheme 39: Symmetric cyclophanes **191** could be made from pre-made TTFAQ building block **192**.

5.2 NOVEL CYCLOPHANES FROM 2,6-BISFUNCTIONALISED TTFAQ BUILDING BLOCKS

It was decided to make two building blocks with different linker size and with alcohols as the terminal functionality for subsequent use in the formation of cyclophanes. Oxyethylene linkers were chosen, since they would impart good solubility.

5.2.1 A new set of 2,6-bisfunctionalised TTFAQ building blocks

The backbone in the synthesis was commercially available 2,6-dihydroxyanthraquinone **198** (Scheme 41). Suitable glycol linkers **193** and **194**, both possessing a halide and an alcohol, were also commercially available. The alcohols had to be protected to survive the subsequent Horner-Wadsworth-Emmons olefination, and it proved best to do so at this early stage, since their protection could be done on a very large scale. Protection using standard conditions with *tert*-butyldiphenylsilyl chloride, which had been used successfully for the synthesis of **189** (Figure 60), gave **195** and **196** as colourless oils in 92% and 90% yield, respectively (Scheme 40). Finally chloride linker **196** was converted to the iodide **197** to increase reactivity.



Scheme 40: Synthesis of the glycol linkers.

The reaction of 2,6-dihydroxyanthraquinone **198** with halide linkers **195** and **197**, in the presence of potassium carbonate in *N,N*-dimethylformamide at 100 °C, was a messy reaction (Scheme 41), as observed by the formation of black highly polar decomposition products. Nonetheless, since the silyl protecting groups afforded good solubility, the products **199** (76% yield) and **200** (87% yield) were easily purified by column chromatography, even when made on a large scale. On the contrary, starting material **198** has a low solubility in anything but warm *N,N*-dimethylformamide and would for this reason alone be completely inapplicable in Horner-Wadsworth-Emmons olefinations without the solubilising protecting groups. Two-fold Horner-Wadsworth-Emmons olefination upon reaction with the anion generated by treatment of phosphonate ester reagent **63** (see Appendix One for the synthesis of phosphonate esters) with lithium diisopropylamide at -78 °C afforded TTFAQ derivatives **201** and **202** in good yields. Removal of the silyl protecting groups with tetrabutylammonium

that the crystals contained solvent of crystallisation. This was confirmed by the X-ray analysis, from which it was found that the asymmetric unit comprises two molecules of **203**, three CH₂Cl₂ molecules and half of a hexane molecule. It was also found that all the OH groups participate in strong (O \cdots O 2.63-2.79 Å, O-H-O 154-178 °) hydrogen bonds with each other.

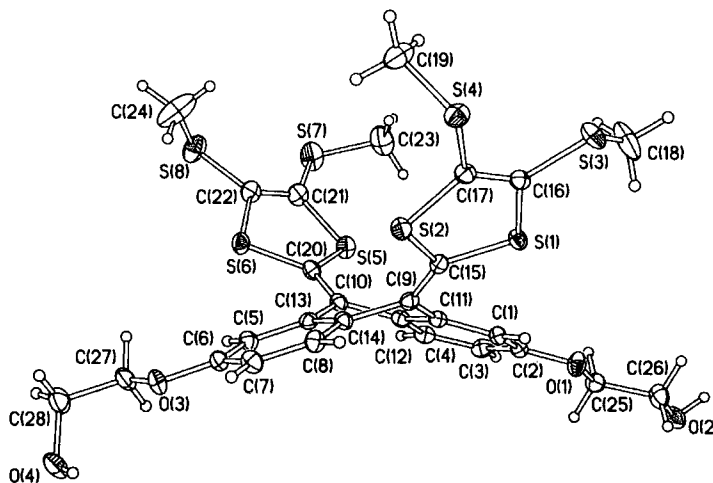


Figure 61: The X-ray crystal structure of **203** adopting the characteristic saddle-shape.

The molecular structure of **203** (Figure 61) adopts a saddle conformation similar to those previously described for TFAQ derivatives^{63,76,94} (see Table 5, section 5.2.4, for principal conformational parameters for the structure of **203**). In order to determine the conformational change accompanying oxidation, for a direct comparison to the structure of neutral **203**, a sample of **203** was electrocrystallised with perchlorate anions.⁷⁴ The dication salt was obtained under similar conditions to those described in section 2.2.4. After two weeks, 5 mm long thin red needles were harvested and submitted for X-ray analysis. The asymmetric unit of the dication salt **203**²⁺(ClO₄⁻)₂ comprises one **203**²⁺ dication, two perchlorate anions and one CH₂Cl₂ molecule (Figure 62). Intermolecular hydrogen bonds O(2)-H \cdots O(4) and O(4)-H \cdots O(1) (O \cdots O 2.93 and 2.84 Å, O-H-O 149-161°) link cations (related by the *b* translation) into an infinite chain, parallel to the *y* axis. Both dithiolium rings are planar and nearly co-planar (within 5°) and both are nearby perpendicular to the mean plane of the anthracene moiety, forming dihedral angles of 78° and 83° with it. The O(1)C(25)C(26) and O(3)C(27)C(28) side chains are essentially co-planar with the anthracene system, while the O(2)H and O(4)H hydroxy groups are oriented out of the plane on the same side of it. The asymmetric unit contains six cation-anion S \cdots O contacts shorter than the standard van der Waals distance of 3.25 Å, the shortest being S(6) \cdots O(8) 3.01 Å and S(2) \cdots O(9) 3.08 Å.

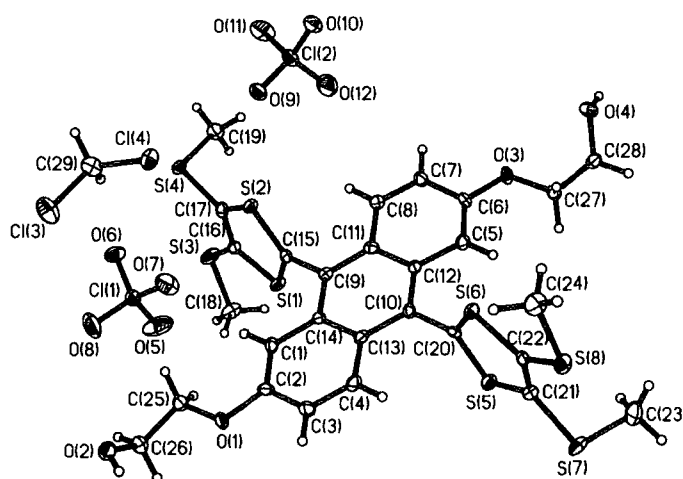


Figure 62: The asymmetric unit of $203^{2+}(\text{ClO}_4^-)_2 \cdot \text{CH}_2\text{Cl}_2$. The oxidised species 203^{2+} is not saddle-shaped.

	203	203^{2+}	
i	1.417(4)	1.435(6)	
ii	1.482(4)	1.405(6)	
iii	1.361(4)	1.487(6)	
iv	1.769(3)	1.686(5)	
v	1.759(3)	1.719(5)	
vi	1.343(4)	1.376(6)	
vii	1.753(3)	1.733(5) ^a	1.760(5) ^b
viii	1.805(4)	1.797(5) ^a	1.814(5) ^b

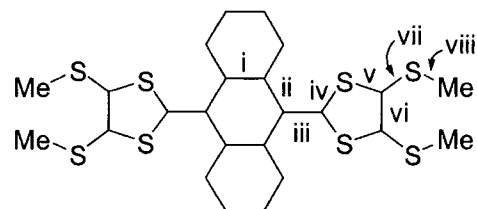
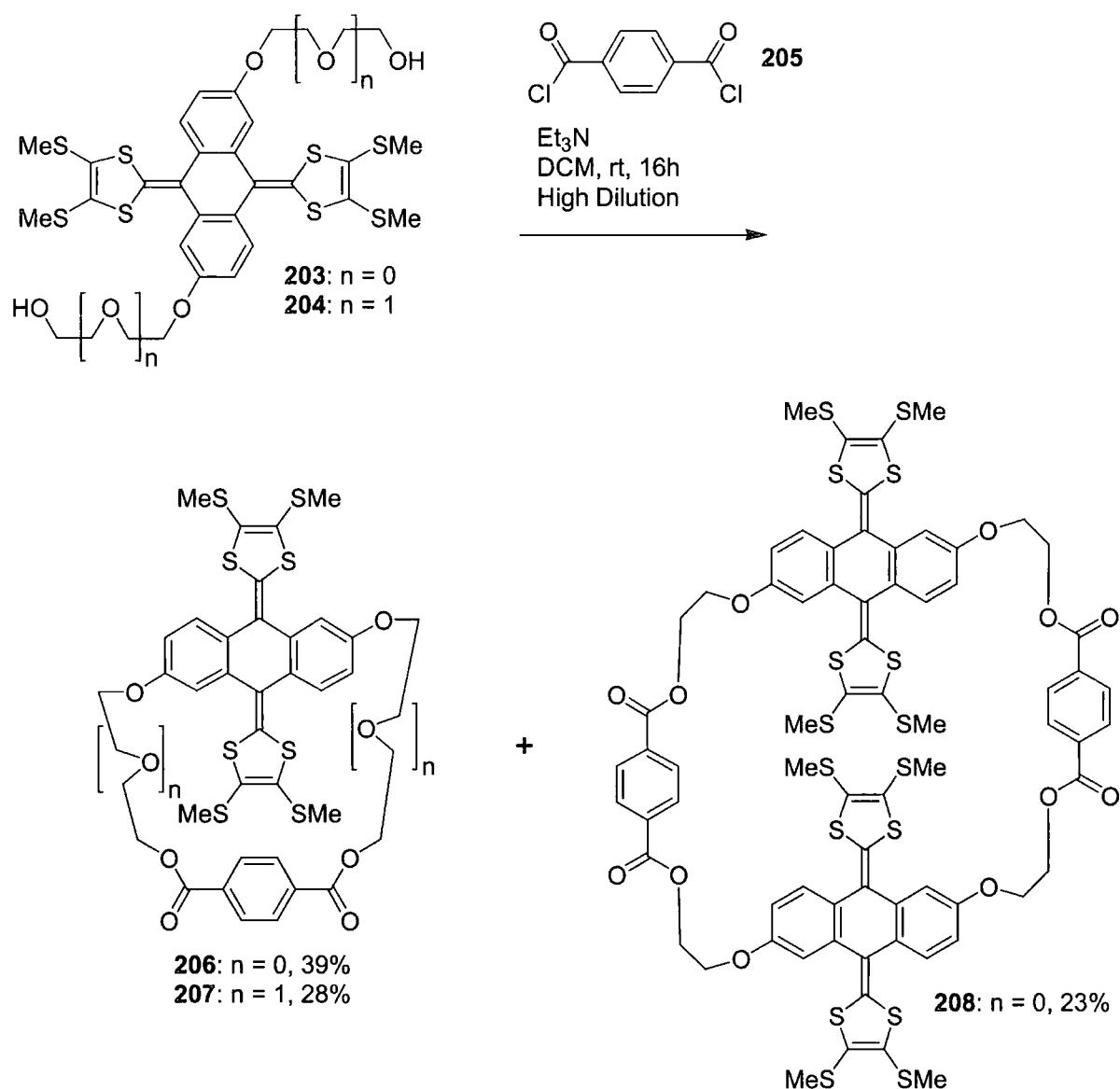


Table 4: Average bond distances (Å). ^a In-plane SMe group. ^b Out-of-plane SMe group.

As would be expected, bond iii becomes longer and ii shorter upon oxidation, as iii changes from a double bond to a single bond and ii becomes part of an aromatic system (Table 4). The C-S bonds in the dithiole rings are shortened, and the C=C bond lengthened on oxidation, as the ring acquires more aromatic character. It is interesting that while in the neutral system the inner C-S bonds iv are longer than the outer ones v, for the cation the opposite is true. The conformations of the SMe groups in 203^{2+} are noteworthy. One SMe substituent at each dithiolium ring is co-planar with the ring and the other nearly perpendicular to it (torsion angles 9.4°, 2.1°, 82.7° and 85.2° respectively); bonds vii for the in-plane substituents are substantially shorter (and viii slightly shorter) than for the out-of-plane ones, indicating uneven conjugation.

5.2.3 Synthesis of TTFAQ cyclophanes

To test the new TTFAQ building blocks as precursors for cyclophanes and to probe the effects of steric constraints on the redox and structural properties, it was decided to react **203** and **204** with 1,4-benzenedicarbonyl chloride **205** under high dilution conditions in dichloromethane in the presence of triethylamine (Scheme 42).

Scheme 42: Synthesis of TTFAQ cyclophanes **206**, **207** and **208**.

The reaction of short-linked building block **203** afforded two products which could be isolated after column chromatography, but other products which stayed at the baseline, presumably higher oligomers, were also observed. The first band off the column was isolated in 39% yield and identified as the cyclophane **206**. The second band was isolated in 23% yield

and all the initial data supported the 2+2 cyclophane structure **208**. From the macrocyclisation of the long-linkered building block **204** only one compound was isolated, in 28% yield, but a lower yield for the formation of the larger macrocycle **207** seemed reasonable. All cyclophanes **206-208** were air-stable yellow solids. The yields are very good when compared to the yields for the other TTFAQ cyclophanes described earlier (see section 5.1), which were formed in 8-22% yield.^{143,145} The use of a pre-made symmetric TTFAQ building block had proved the right choice for cyclophane synthesis. Mass spectroscopy, elemental analysis, ¹H NMR, ¹³C NMR and X-ray crystallography (see section 5.2.4) confirmed the structures of the cyclophanes **206-208**, but more interesting information was to be deduced from the ¹H NMR spectra.

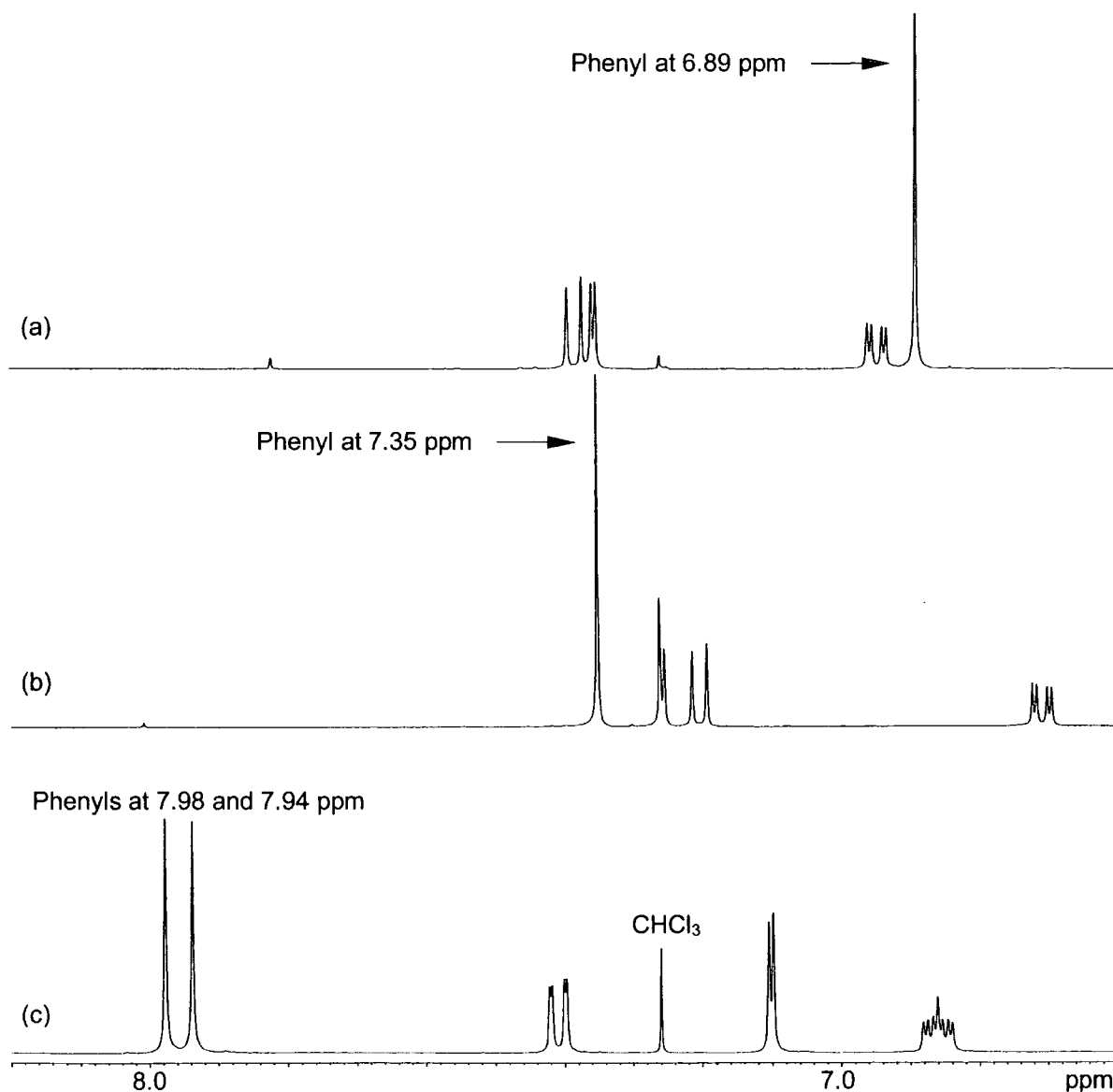


Figure 63: Parts of the ¹H NMR spectra (at 400 MHz) of (a) short-bridged cyclophane **206**, (b) long-bridged cyclophane **207** and (c) 2+2 cyclophane **208**.

The ^1H NMR spectrum shows that the 2 + 2 cyclophane **208** is present as two conformers, clearly seen from the two singlets (each integrating to 4 protons) arising from the phenyl protons at 7.98 and 7.94 ppm, respectively (Figure 63c). Also the doublets and doublet of doublets, characteristic of 2,6-bisubstituted anthraquinone derivatives, are seen as pairs, indicative of the two conformers. Another interesting feature of the ^1H NMR spectra of the cyclophanes is the chemical shift of the singlet arising from the phenyl protons. For **206**, the short-bridged cyclophane, the singlet is observed at 6.89 ppm and for **207** it is at 7.35 ppm (Figure 63a and b). Hence the chemical shift of the phenyl protons is indicative of the length of the bridge, and, consequently, how close the phenyl ring is positioned to the anthraquinonoid ring system, with a change of 1 ppm from the short-bridged **206** to the longest-bridged 2 + 2 cyclophane **208**, in which the phenyl rings can be far removed from the anthraquinonoid ring system.

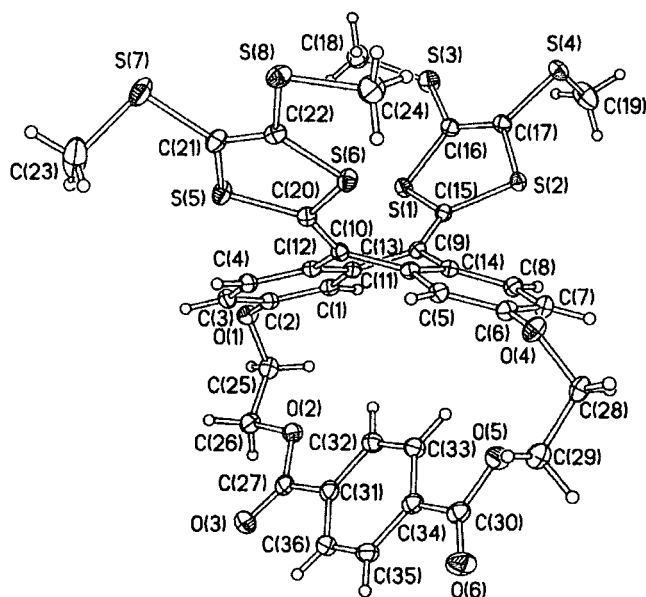
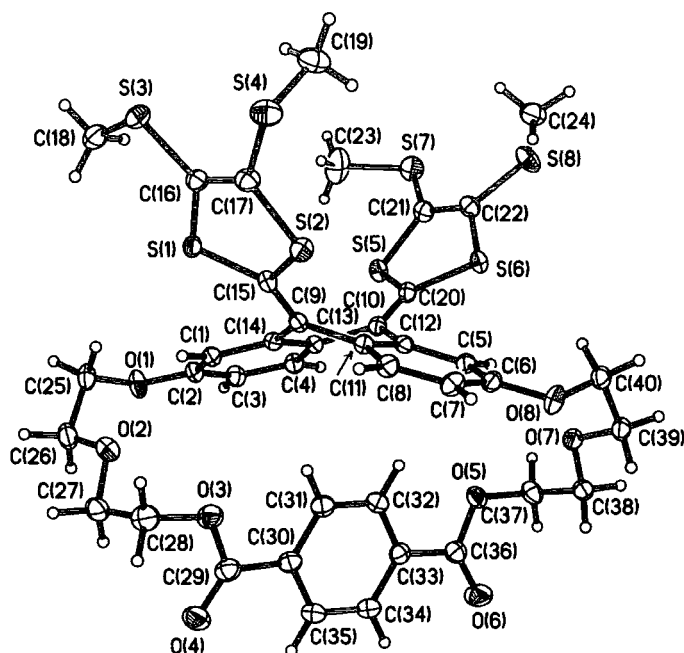
5.2.4 X-ray crystallographic analysis of the cyclophanes and a dication salt

To probe the effects of steric constraints on the structural properties, crystals of the cyclophanes were grown and submitted for X-ray analysis.

	203	206	207	208	208	208
φ	36.4	39.2	35.7	37.1	34.6	37.3
δ_1	8.4	17.9	19.3	16.6	15.6	19.4
δ_2	2.8	19.4	0	22.1	13.7	11.3
θ	79.1	87.6	83.7	61.1	73.4	73.1

Table 5: Dihedral angles (deg) in the neutral molecules. The angles are defined in the text.

The molecular structures for **206** and **207** are shown in Figure 64 and Figure 65, respectively, and principal conformational parameters are given in Table 5. Crystals of **206** and **207** contained no solvent of crystallisation. The cyclophanes **206** and **207** have saddle-like conformations similar to those described for non-bridged analogues^{63,76,94} and those with a bridge between the dithiole rings,^{143,145} and folding (φ) of the dihydroanthracene moiety along the C(9)···C(10) vector is not affected significantly by the bridge.

Figure 64: The X-ray crystal structure of cyclophane **206**.Figure 65: The X-ray crystal structure of cyclophane **207**.

Both structures show the usual packing motif^{63,76,94} of pseudo-dimers of molecules with mutually engulfing TTF AQ moieties (see packing of **206** as an example, Figure 66). However, the folding of these moieties in **206** and **207** is significantly different. The overall measure of the U-bend, the dihedral angle (θ) between the S(1)C(16)C(17)S(2) and S(5)C(21)C(22)S(6) planes in **206** (83.7°) is within the range ($76-92^\circ$) observed in

non-bridged systems^{63,76,94} including **203**. In contrast, for **207** this angle (61.1°) is almost as narrow as in **184** and **185** ($46\text{--}54^\circ$, Scheme 37). This illustrates the flexibility of the saddle conformation and its dependence on the packing.

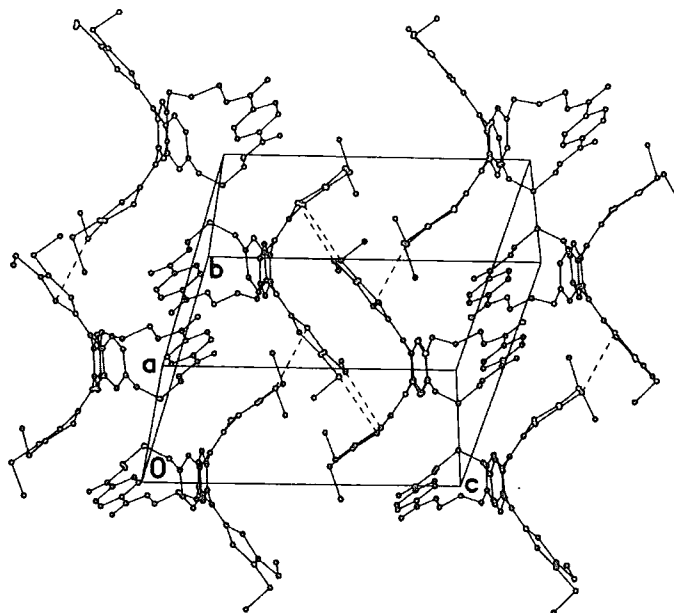


Figure 66: Crystal packing of cyclophane **206**, showing short S...S contacts ($3.55\text{--}3.64 \text{ \AA}$).

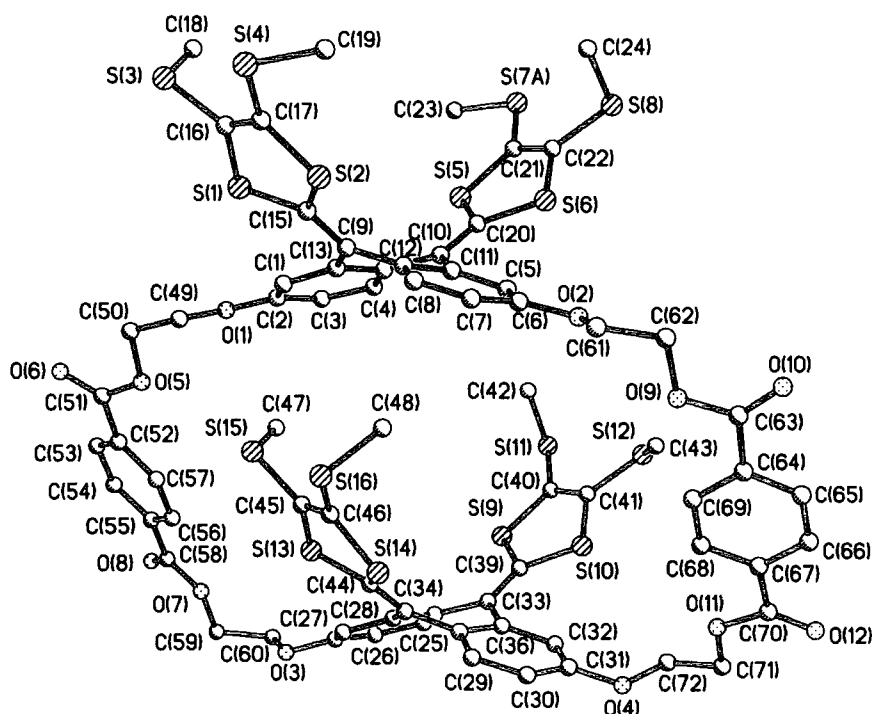


Figure 67: The X-ray crystal structure of **2 + 2** cyclophane **208**. The minor position of the disordered S(7) atom and all H atoms have been omitted.

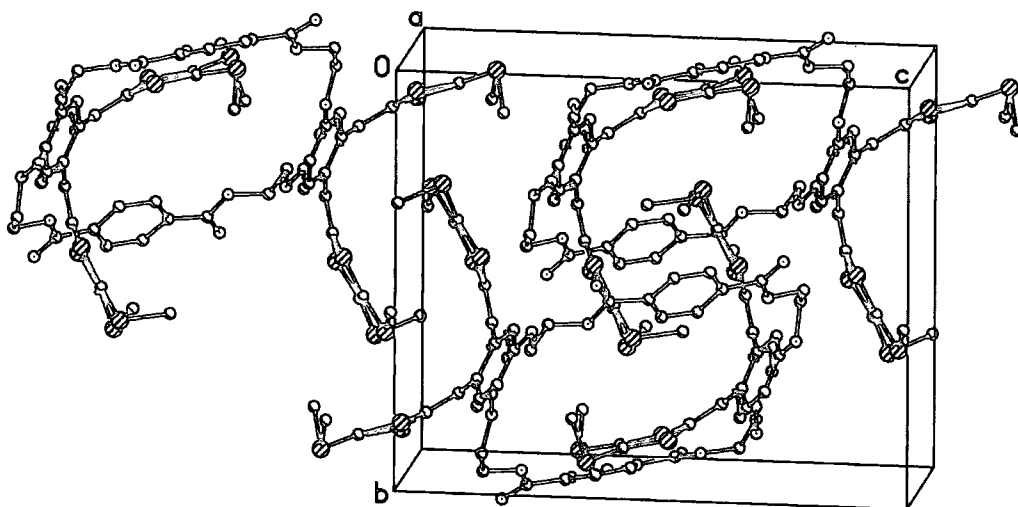


Figure 68: Crystal packing of 2 + 2 cyclophane 208.

The 2 + 2 cyclophane **208** (Figure 67) contains two saddle units (in approximately parallel orientation) forming mutually engulfing interactions with two other molecules, related to the first *via* different inversion centres (Figure 68). Intramolecular self-engulfing does not occur. The conformations of the two saddle units are very similar; one of the SMe groups shows a disorder of the sulfur atom. The structure contains infinite channels, running along the *y* axis and filled with chaotically disordered solvent of crystallisation, which we believe to be a mixture of CH₂Cl₂ and hexane, partially sharing the same sites. The volume of the channel and the electron density distribution are in agreement with a **208**:CH₂Cl₂:hexane stoichiometry of 1:1:1.

	206	206 ²⁺	207	208
i	1.420(2)	1.45(1)	1.412(2)	1.415(8)
ii	1.481(2)	1.41(1)	1.483(2)	1.462(8)
iii	1.364(2)	1.50(1)	1.359(2)	1.352(8)
iv	1.772(1)	1.678(8)	1.774(2)	1.762(6)
v	1.757(1)	1.717(7)	1.763(2)	1.752(7)
vi	1.347(2)	1.38(1)	1.346(2)	1.328(9)
vii	1.753(1)	1.740(8)	1.757(2)	1.749(8)
viii	1.812(2)	1.799(9)	1.811(2)	1.793(9)

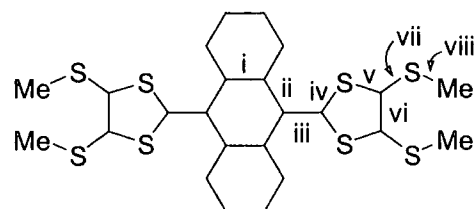


Table 6: Average bond distances (Å).

Although none of the bridges in **206** and **207** were short enough to impart any folding (φ) of the neutral cyclophanes, the short bridge in **206** could maybe alter the structure of the dication species $\mathbf{206}^{2+}$ from that of the usual structure of TTFAQ dications (see Figure 26 and Figure 62). To investigate the conformational change of the short-bridged cyclophane **206** upon oxidation, a sample of **206** was electrocrystallised with the aim of getting crystals of X-ray quality. Several solvents and electrolytes were used, but no crystals were obtained. Instead a solution of **206** in dichloromethane was oxidised by diffusion of iodine vapour, to give precipitation of black plate-shaped crystals of an iodide salt.

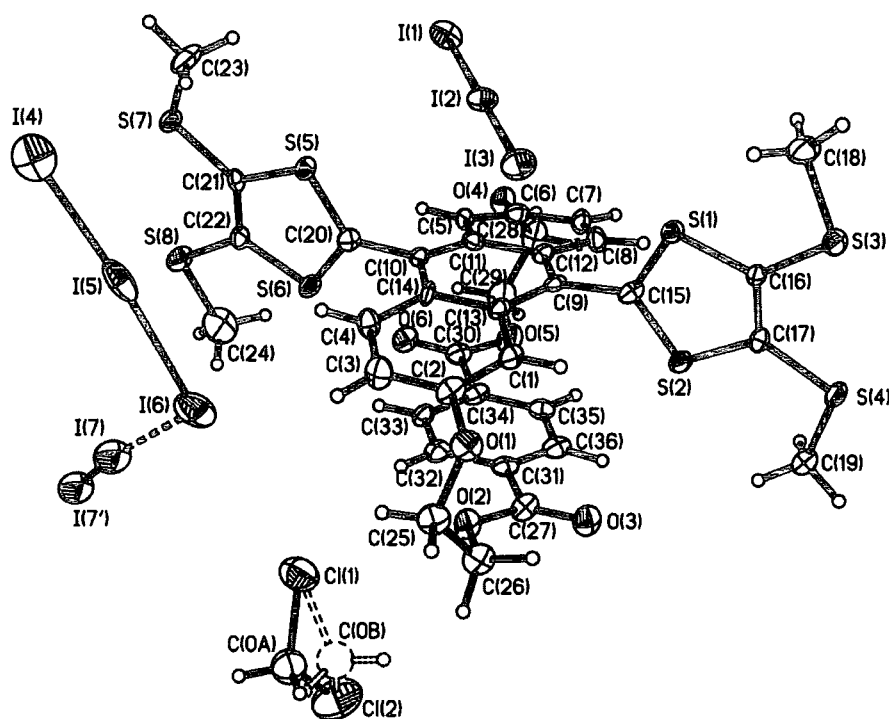


Figure 69: The asymmetric unit of $\mathbf{206}^{2+}(\text{I}_3^-)_2 \cdot (\text{I}_2)_{0.5} \cdot \text{CH}_2\text{Cl}_2$ showing 50% thermal ellipsoids. Angles in degrees: I(1)-I(2)-I(3) 176.94(3), I(4)-I(5)-I(6) 175.19(3), I(5)-I(6)-I(7) 107.66(4), I(6)-I(7)-I(7') 168.29(6).

The asymmetric unit of the iodide salt of **206** comprises one $\mathbf{206}^{2+}$ dication, two triiodide anions, half of an I_2 molecule (which is situated at an inversion centre), and one disordered CH_2Cl_2 molecule (Figure 69). The iodine molecule has a I(7)-I(7') bond distance of 2.766 Å and forms secondary bonds I(6)⋯I(7) 3.378(2) Å with two anions, causing considerable asymmetric bond distances therein: I(4)-I(5) 2.873(2) Å vs. I(5)-I(6) 2.988(2) Å. The shortest I⋯I contact formed by the other independent anion, I(3)⋯I(7) of 4.30 Å, is equal to double the van der Waals radius. Correspondingly, the I(1)-I(2) and I(2)-I(3) bonds in it are practically equal, 2.930(1) Å and 2.918(1) Å. There is no continuous polyiodide motif.

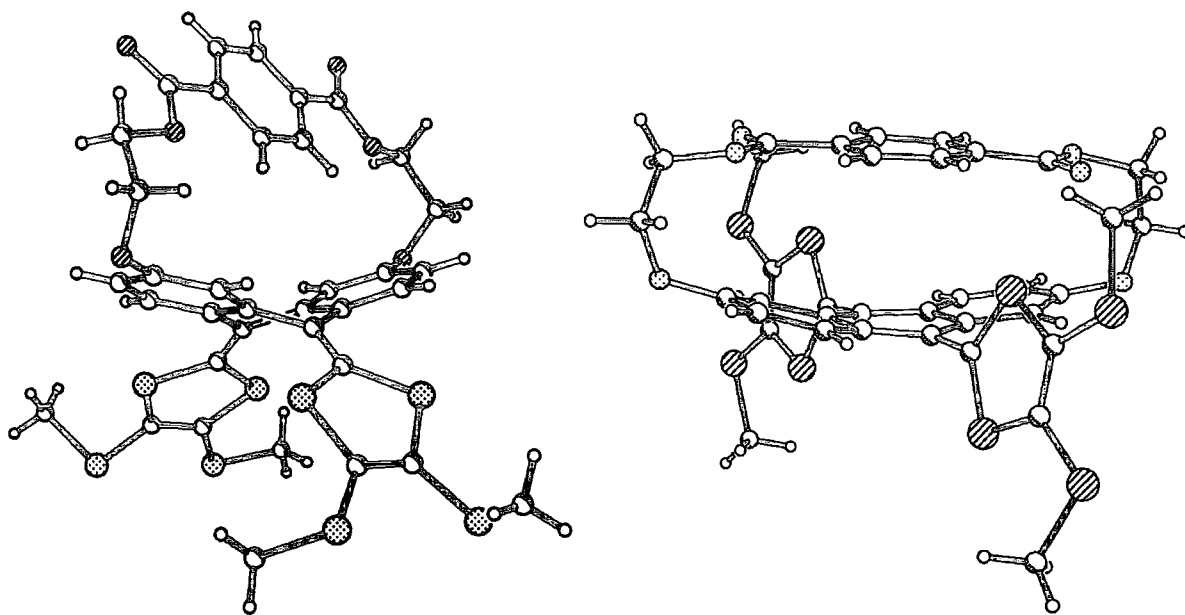


Figure 70: Cyclophane **206** in its neutral (left) and dication (right) state. Solvent of crystallisation and counter ions have been omitted for clarity. The major change in conformation upon oxidation is clear.

Oxidation of **206** to **206**²⁺ results in a profound electronic and conformational rearrangement (Figure 70), as in non-bridged analogues^{63,72,73} including precursor **203** (see discussion in section 5.2.2). The dithiolium rings in **206**²⁺ are planar and nearly perpendicular to the anthracene system, but significantly different from other TTFAQ dications, the planarity of the aromatic anthracene system is perturbed by the bridge. Two modes of distortion of an anthracene system have been observed earlier. In 9,10-bridged anthracene cyclophanes¹⁴⁸ the anthracene system is folded (by φ angle) along the C(9)–C(10) vector, with the central anthracene ring adopting a boat conformation. Non-bridged anthracene systems, which are overcrowded with substituents, adopts an “end-to-end twist”, measured by the angle τ between the C(2)–C(3) and C(6)–C(7) bonds ($\tau = 0$ for the planar anthracene).¹⁴⁹ In TTFAQ cyclophane dication **187**²⁺ of Godbert *et al*, the bridge between the dithiole rings effects only a minor ($\varphi = 6^\circ$) folding and practically no end-to-end twist of the anthracene system.¹⁴⁵ In **206**²⁺ on the other hand, both the twist ($\tau = 7^\circ$) and folding ($\varphi = 22^\circ$) are substantial. The bridging benzene ring is practically parallel and eclipsed with the central anthracene ring, resulting in intramolecular contacts C(13)–C(31) 3.58 Å, C(10)–C(33) 3.60 Å and C(11)–C(34) 3.56 Å, while in neutral **206** and **207** this benzene ring is inclined to the C(11)C(12)C(13)C(14) plane by 60° and 79° , respectively. Thus, for the conformation of the dication species **206**²⁺ the bridge exerts a major influence.

5.2.5 Solution electrochemical properties

Solution electrochemical data, obtained by cyclic voltammetry, are collated in Table 7. All the non-bridged systems **201-204** showed the quasi-reversible⁶⁹ two-electron oxidation wave typical for TTFAQ derivatives. Comparison of cyclophanes **206** and **207** with the precursors **203** and **204** reveals some interesting trends. The oxidation potential ($E^{\text{ox}}_{\text{pa}}$) is raised by 50 mV for **206**, but no increase is seen for **207**. This is consistent with the shorter bridge of **206** obstructing the marked conformational change which accompanies oxidation to the dication (Figure 70) whereas the longer bridge of **207** allows free conformational change. These observations are in good agreement with the oxidation potentials of TTFAQ cyclophanes **186** and **187** reported by Godbert *et al.* (Scheme 38).¹⁴⁵ An increase of 300 mV was observed for the short-bridged system **186**, whereas only a slight increase was seen for **187** incorporating the longer bridge. The shift in oxidation potential is obviously more significant when the two dithiole rings are bridged, since upon oxidation they undergo a greater conformational change than the anthracene ring system. Consistent with this, $\Delta E = E^{\text{ox}}_{\text{pa}} - E^{\text{ox}}_{\text{pc}}$ is significantly reduced for compound **186** (*i.e.* increased reversibility of the oxidation process) due to the short bridge restricting conformational change, whereas no significant difference in ΔE is observed for cyclophanes **206** or **207** compared to their precursors.

Compound	$E^{\text{ox}}_{\text{pa}}/\text{V}$	$E^{\text{ox}}_{\text{pc}}/\text{V}$	$\Delta E/\text{V}^a$
201	0.47	0.34	0.13
202	0.46	0.37	0.09
203	0.47	0.29	0.18
204	0.46	0.36	0.10
206	0.52	0.41	0.11
207	0.47	0.33	0.14
208	0.51	0.37	0.14

Table 7: Cyclic voltammetric data. Compound *ca.* 2×10^{-3} M, vs. Ag/AgCl, electrolyte $\text{Bu}_4\text{N}^+\text{PF}_6^-$, acetonitrile, 20 °C, scan rate 100 mV s⁻¹. ^a $\Delta E = E^{\text{ox}}_{\text{pa}} - E^{\text{ox}}_{\text{pc}}$.¹²⁹

The 2 + 2 cyclophane **208** showed one, slightly broadened, quasi-reversible oxidation wave, which we assign to a four-electron process forming the **208**⁴⁺ species. Hence, the two TTFAQ moieties in **208** behave independently, which was expected, since the redox active moieties

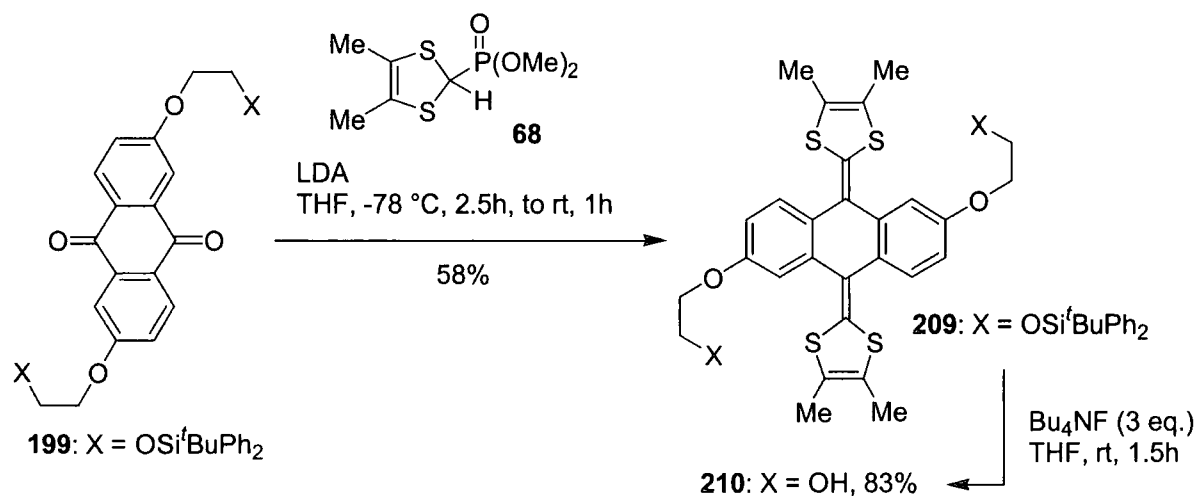
are not in conjugation (see section 3.5.1). The Coulombic repulsion between the two dication units, combined with the steric constraints in the oxidised cyclophane system, could explain the increase by 40 mV of the oxidation potential compared to that of its precursor **203**. In conclusion, the redox properties of the TTFAQ moieties are only altered to a lesser degree when bridged across the dihydroanthracene ring system.

5.3 DONOR-ACCEPTOR TRIADS FROM 2,6-BISFUNCTIONALISED TTFAQ

This part of the work was carried out in collaboration with Dr. Igor F. Perepichka, Dr. Svetlana B. Lyubchik and Dr. Dmitrii F. Perepichka in our group, and further established the versatility of the TTFAQ building blocks presented in this chapter.¹⁵⁰

5.3.1 A novel TTFAQ fluorene charge-transfer salt

In order to make both new charge-transfer salts and new donor-acceptor triads, it was decided to synthesise a building block similar to **203**, but with better donor properties. Hence, instead a TTFAQ derivative **210** with electron donating methyl groups was synthesised (Scheme 43). The reaction used the phosphonate ester **68**⁹⁵ to afford the protected alcohol **209** in 58% yield, and deprotection using fluoride yielded the diol **210** (83%). It soon became clear that **210** oxidised very easily, as a pure sample of yellow powder of **210** became brown overnight upon exposure to the air in a closed sample vial. This behaviour was never observed for any of the methylthio substituted TTFAQ derivatives presented in this thesis.



Scheme 43: Synthesis of the TTFAQ building block **210** possessing excellent donor abilities.



Beautiful single crystals of **210** were grown from dichloromethane-hexane, but within minutes after being liberated from the solvent, they degraded to a powder, suggesting the crystals were highly solvated, as was the case for the crystals of the analogue **203** (section 5.2.2). Instead, crystals of **210** suitable for X-ray crystallography were grown from toluene by Dr. Lyubchik. These crystals also contained solvent of crystallisation, but were more stable.

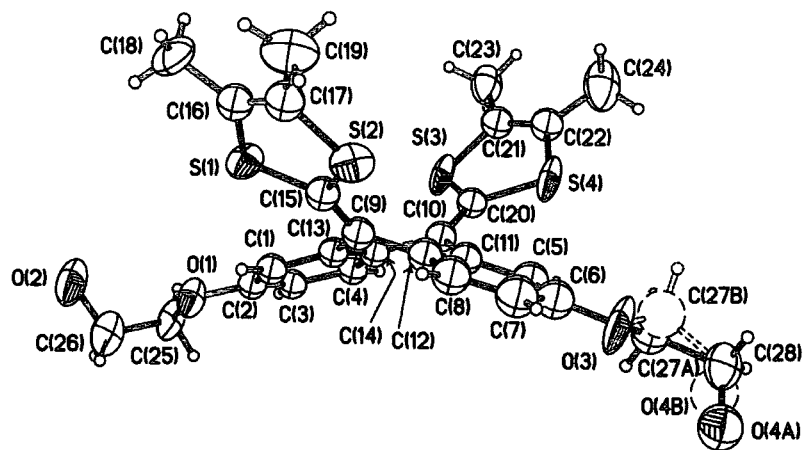


Figure 71: The X-ray crystal structure of **210**.

The asymmetric unit of $\mathbf{210} \cdot (\text{PhMe})_{1/2}$ contains two molecules of **210** and one of toluene. Molecule **210** adopts the usual saddle conformation (Figure 71). The dihydroanthracene moiety is folded along the C(9)···C(10) vector by 37° and the dithiole rings are folded (inward) by $7\text{--}15^\circ$ along the S···S vectors. Thus the outer S(1)C(16)C(17)S(2) and S(3)C(21)C(22)S(4) moieties form a dihedral angle of 83° .

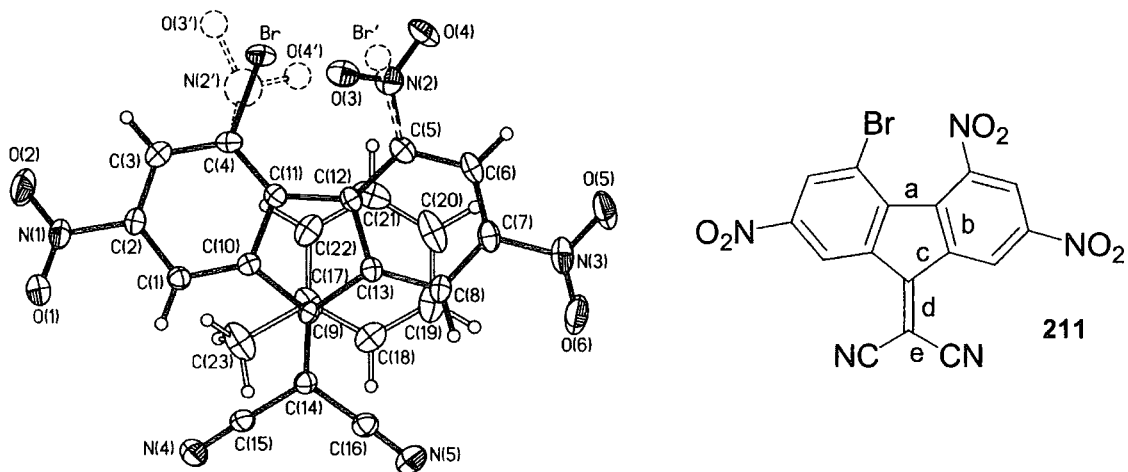


Figure 72: X-ray crystal structure of the electron acceptor **211** (black bonds) crystallised with toluene (white bonds).¹⁵¹

New donor **210** was mixed with a range of fluorene acceptors and Dr. Lyubchik obtained crystals of $210 \cdot (211)_2 \cdot (\text{MeCN})_2$, by mixing **210** with fluorene acceptor **211** (see Figure 72 for the structure of neutral acceptor **211**) in hot acetonitrile.

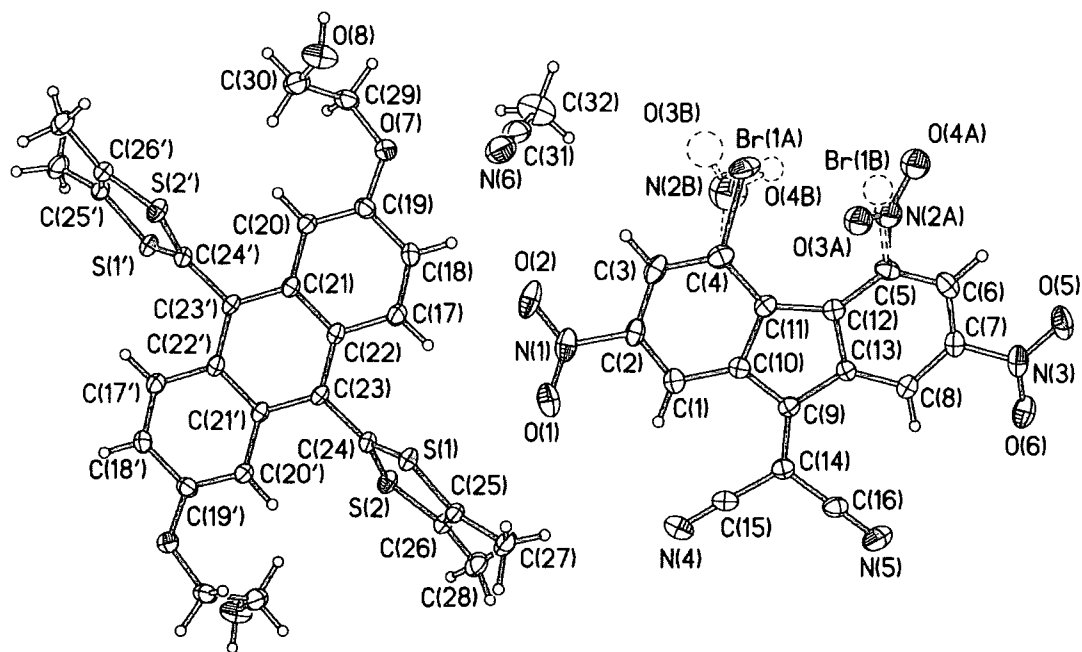


Figure 73: Molecular structure of $210 \cdot (211)_2 \cdot (\text{MeCN})_2$. Atoms, generated by inversion centre, are primed. Selected bond distances: S(1)-C(24) 1.678(3) Å, S(2)-C(24) 1.688(3) Å, S(1)-C(25) and S(2)-C(26) 1.716(3) Å, C(25)-C(26) 1.360(4) Å.

Full electron transfer was observed in the crystal structure of $210 \cdot (211)_2 \cdot (\text{MeCN})_2$, resulting in formation of the dication 210^{2+} and two anion radicals 211^- , making this the first example of an ionic fluorene charge-transfer complex.^{141a,152} Dication 210^{2+} has crystallographic C_i symmetry, while the fluorene anion radicals and the acetonitrile molecules occupy general positions (Figure 73). As with **54** (Figure 26), the conformation of **210** drastically changes upon oxidation: the folded anthracenediylidene moiety is converted into a planar (within ± 0.03 Å), fully aromatic anthracene system. Each dithiole ring acquires a +1 charge, which is manifested in the shortening of C-S bonds and lengthening of the C=C bonds, as well as planarisation of the ring. The dithiolium rings form a dihedral angle of 62° with the anthracene ring system and are connected by the essentially single C(23)-C(24) bond of 1.488(4) Å. The anion radical 211^- shows a 4/5-disorder, in a 85:15 ratio. Comparison of 211^- with the neutral molecule (Table 8) shows the shortening of the previously single bonds (a, c and e) and lengthening of the previously double bonds (b and d), resulting in a nearly

uniform delocalisation of π -electron density in the 5-membered fluorene ring and the dicyanomethylene group. These changes resemble those which occur on reduction of TCNQ **13** to the anion radical.¹⁵³

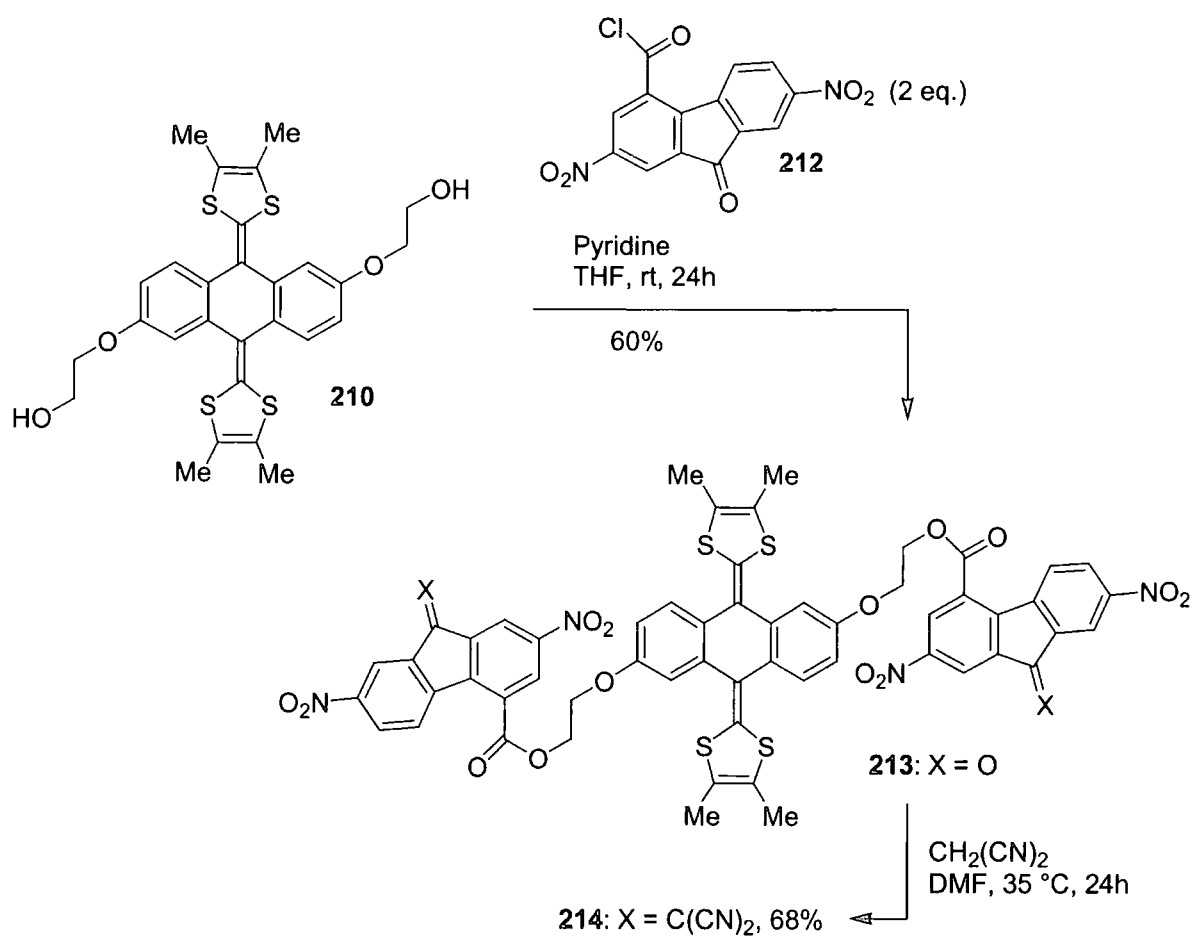
	a	b	c	d	e
211 ·PhMe	1.478(4)	1.414(4)	1.483(4)	1.359(4)	1.440(4)
210 ·(211) ₂ ·(MeCN) ₂	1.455(4)	1.436(4)	1.445(4)	1.414(4)	1.422(4)

Table 8: Average bond lengths (Å) in acceptor **211** (see Figure 72 for numeration).

Charge-transfer could not be observed for the complex **210**·(**211**)₂·(MeCN)₂ in solution (*i.e.* no long wavelength CT band was present in the absorption spectrum) as a result of the complex dissociation. Instead the results from the X-ray analysis were confirmed by IR studies of the solid state (in KBr pellets), where the C≡N stretching frequency of the complex ($\nu_{\text{C}\equiv\text{N}} = 2180 \text{ cm}^{-1}$) is significantly lowered as compared to that in neutral fluorene **211** ($\nu_{\text{C}\equiv\text{N}} = 2233 \text{ cm}^{-1}$). The complex also gave a sharp EPR signal in the solid state. A single line from the fluorene radical anion was found, $g = 2.0031$, indicating full electron transfer. Another manifestation of the CT character of **210**·(**211**)₂·(MeCN)₂ was its electrical conductivity. The complex showed semiconductivity of $\sigma_{\text{r}} = 10^{-6} \text{ S cm}^{-1}$ (two-probe method in compressed pellets).

5.3.2 Donor-acceptor triads

It was next decided to make a donor-acceptor triad (A- σ -D- σ -A). This and the following reaction (Scheme 44) was carried out by Dr. Igor F. Perepichka. Double esterification with fluorenone acid chloride **212** yielded triad **213** in 60%. To increase the strength of the acceptors, they were converted to the dicyanomethylene derivative, using malonitrile in *N,N*-dimethylformamide, affording A- σ -D- σ -A triad **214** in 68% yield. Although the acceptor strength of the fluorene groups in **214** have been increased compared to **213**, the acceptor moieties of **214** have a lower electron affinity than the acceptor **211** possessing an extra electron withdrawing nitro group. Hence, no charge-transfer band is seen in the absorption spectrum of **214** and only a small lowering of the C≡N stretching ($\nu_{\text{C}\equiv\text{N}} = 2227 \text{ cm}^{-1}$) is observed in the solid state IR spectrum.



Scheme 44: Synthesis of a TTFAQ donor-acceptor triad.

5.3.3 Solution electrochemistry

Cyclic voltammograms were recorded for the new donors **209** and **210** and the donor-acceptor triads **213** and **214** in dichloromethane using Ag/AgCl as reference electrode (see Table 9 for redox potentials).

Compound	$E_{\text{pa}}^{\text{ox}}/\text{V}$	$E_{\text{pc}}^{\text{ox}}/\text{V}$	$E_{\text{red},1}^{1/2}/\text{V}$	$E_{\text{red},2}^{1/2}/\text{V}$	$E_{\text{red},3}^{1/2}/\text{V}$
209	0.36	0.10	-	-	-
210	0.28	0.17	-	-	-
213	0.38	0.06	-0.56	-0.75	-
214	0.38	0.06	-0.12	-0.66	-1.28

Table 9: Redox potentials in a 0.1 M Bu_4NPF_6 solution in dichloromethane at room temperature using Ag/AgCl as reference. Concentration of the redox active species *ca.* 10^{-4} M, scan rate 100 mV s^{-1} .¹²⁹

The CV of TTFAQ derivative **209** with protected alcohols shows a higher oxidation potential and a considerably more quasi-reversible⁶⁹ wave than the corresponding diol **210**, presumably due to a steric effect which is not fully understood (*cf.* section 3.6.2). The instability of **210**, which was seen as rapid decomposition when exposed to air, is also reflected in its very low oxidation potential of only 0.28 V. This TTFAQ derivative, with 6 electron donating substituents, is a very good electron donor as well as a versatile building block. Donor-acceptor triads **213** and **214** show clear amphoteric multiredox behaviour, consisting of two, **213**, or three, **214**, reversible⁶⁹ reduction waves, corresponding to the fluorene moieties, and one quasi-reversible oxidation wave from the TTFAQ moiety (see CV of **214** in Figure 74). Thus, for **214** five redox states have been observed: neutral ($A^0/D^0/A^0$), dication ($A^0/D^{2+}/A^0$), diradical dianion ($A^{\cdot-}/D^0/A^{\cdot-}$), tetraanion ($A^{2-}/D^0/A^{2-}$) and diradical hexaanion ($A^{\cdot 3-}/D^0/A^{\cdot 3-}$), but for **213** the diradical hexaanion is not stable due to the lower electron affinity of the fluorenone moieties. The oxidation/reduction current ratio was 1:1, consistent with all the redox waves being two-electron waves. The oxidation potentials of the TTFAQ moieties in **213** and **214** are exactly the same, although the strength of the acceptor units are very different, as seen by the difference in the reduction potentials, indicating only little interaction between the redox active moieties in the donor-acceptor triads. Thus, the 100 mV difference in the oxidation potentials of **210** and the triads **213** and **214** is probably a combination of an intramolecular donor-acceptor interaction and a steric effect similar to what was seen for the protected diol derivative **209**.

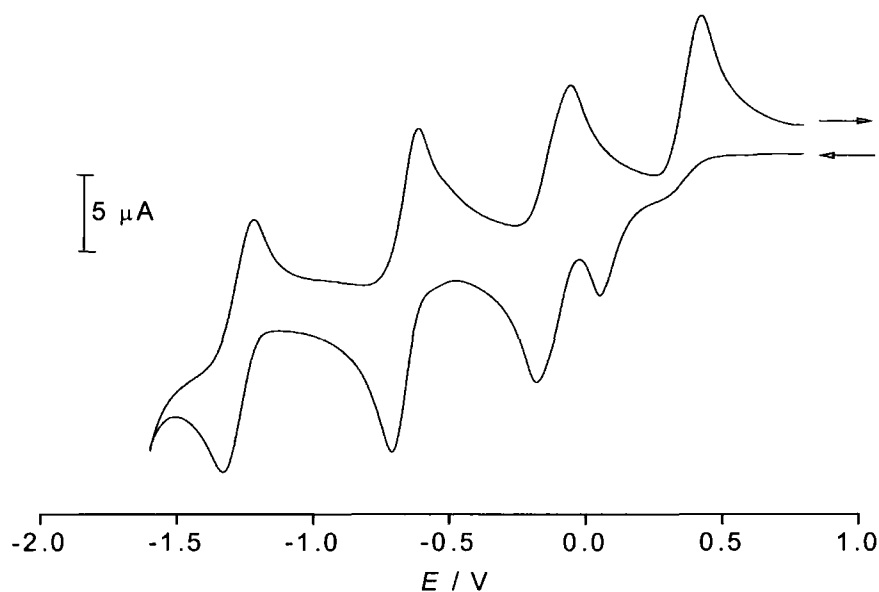


Figure 74: CV of compound **214** (*ca.* 10^{-4} M) in a 0.1 M Bu_4NPF_6 solution in acetonitrile at room temperature using Ag/AgCl as reference and a scan rate of 100 mV s^{-1} .

5.4 FUTURE PROJECTS: PHENANTHROLINE CYCLOPHANES AND CATENATES

Having established the versatility of the TTFAQ building blocks 203, 204 and 210, both for the synthesis of TTFAQ cyclophanes and donor-acceptor triads, it was decided to synthesise more elaborate TTFAQ cyclophanes which for future projects could be used for complexation studies and formation of catenates.

5.4.1 Background

The inspiration came from the work of Becher *et al.*, who synthesised a range of TTF phenanthroline cyclophanes and catenates. The strategy of using the templating abilities of Cu^+ to coordinate two phenanthroline ligands in a tetrahedral complex, originally developed by Sauvage and co-workers,¹⁵⁴ was employed to prepare first the catenate 215¹⁵⁵ and later a series of precatenates with 216¹⁵⁶ being an example (Figure 75).

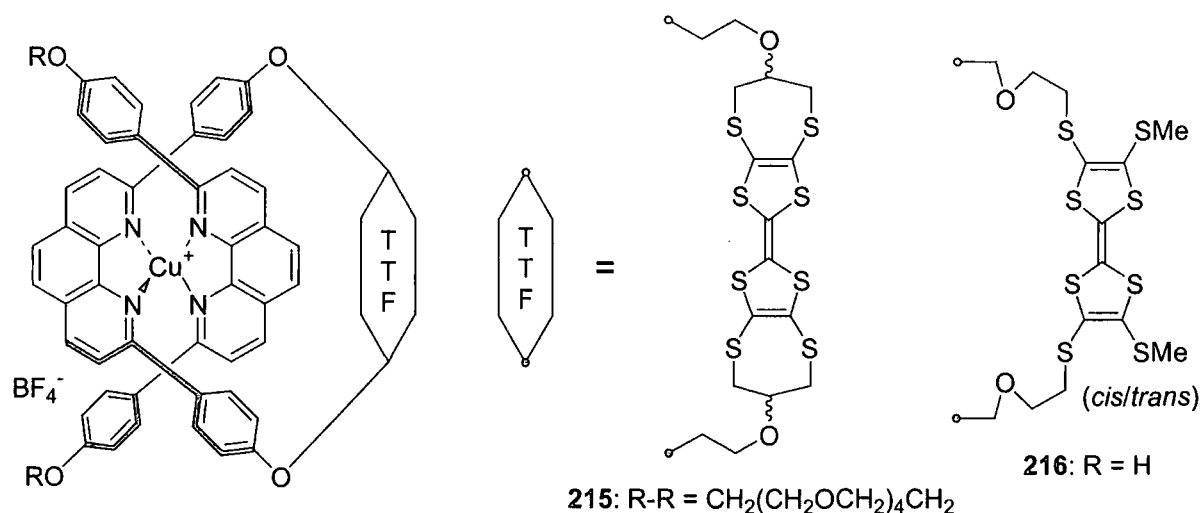
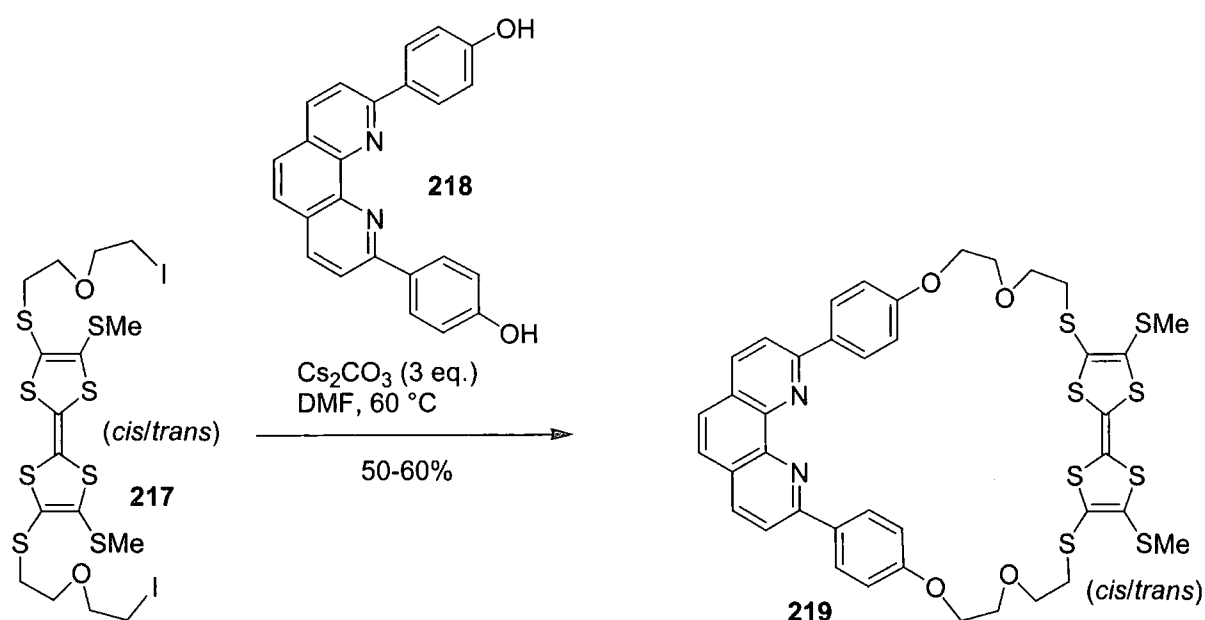


Figure 75: Examples of TTF-phenanthroline catenates and precatenates synthesised by Becher *et al.*^{155,156}

The first TTF phenanthroline catenate 215 was made as a test compound for the ultimate goal of synthesising a photoactive donor-acceptor catenate (D-P-A) where the copper(I) complex is the photoactive moiety (P), since it is a strong reductant in its excited state.¹⁵⁵ The catenate 215 is lacking the acceptor, but proved that the methodology developed by Sauvage *et al.*¹⁵⁴ worked well for the incorporation of TTF units into catenates. Later such D-P-A catenates were synthesised by Becher and co-workers,¹⁵⁷ and their properties are currently being investigated. However, the precatenates have been reported, because of their ability to work as electroactive sensors, being able to recognise different metal ions like Cu^+ , Ag^+ and Li^+ .

Hence, the oxidation potentials of precatenate **216** were anodically shifted by 70 mV for both the first and the second one-electron oxidation of the TTF moiety, compared to the precursor cyclophane **219** (Scheme 45), as monitored by cyclic voltammetry. This indicates that the Cu^+ ion was not completely expelled after the first oxidation wave of the TTF unit.¹⁵⁶ The two-electron oxidation wave of a TTFAQ moiety would therefore possibly be shifted even more, for similar precatenates made from the TTFAQ building blocks **203** and **204**. Thus, it would be worthwhile synthesising TTFAQ phenanthroline cyclophanes, even if only precatenates could be formed. Complexation studies would possibly reveal even better electroactive sensors than for the TTF precatenates.



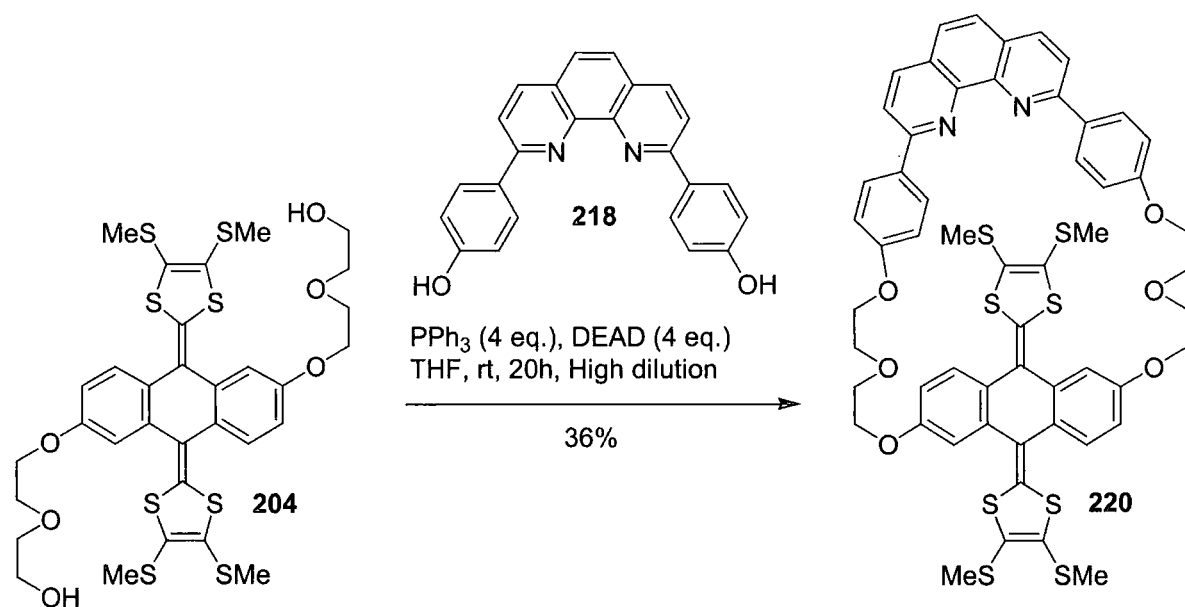
Scheme 45: Macrocyclisation to form TTF phenanthroline cyclophane **219**, by Becher and co-workers.¹⁵⁶

Precatenate **216** was made from cyclophane **219** and 2,9-di(*p*-phenol)-1,10-phenanthroline **218**, and cyclophane **219** was synthesised from reaction of TTF derivative **217** with **218** under high dilution conditions, in the presence of cesium carbonate, in 50-60% yield (Scheme 45).¹⁵⁶ We thought it should be possible to synthesise similar TTFAQ cyclophanes from TTFAQ building blocks **203** and **204**, and the 1,10-phenanthroline derivative **218**.

5.4.2 Synthesis of TTFAQ phenanthroline cyclophanes

A sample of 2,9-di(*p*-phenol)-1,10-phenanthroline **218** was kindly donated by the group of Prof. Becher, Odense University.¹⁵⁷ We decided to investigate if it was possible to

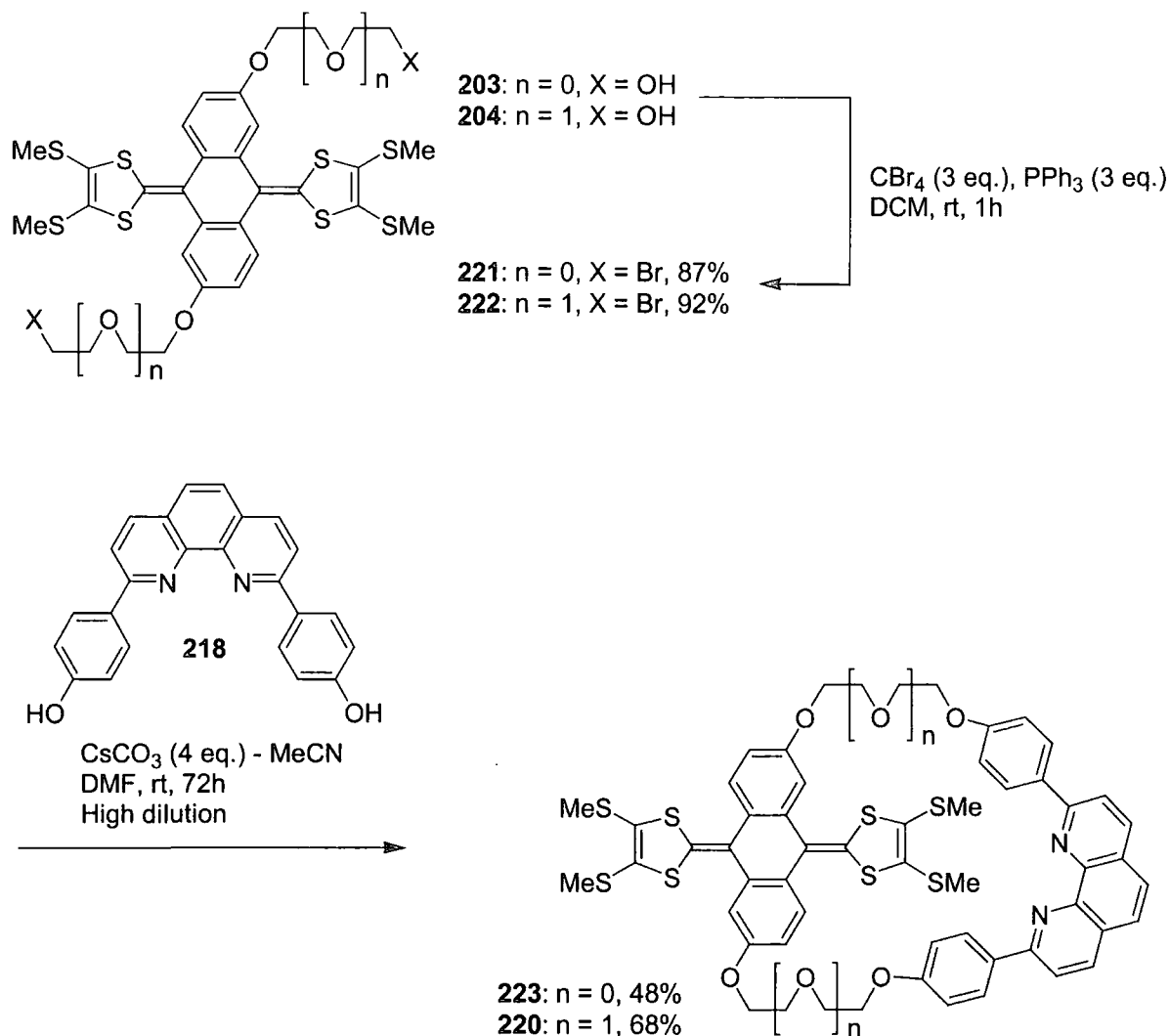
macrocyclise the TTFAQ building block **204** directly by reaction with **218** using the Mitsunobu reaction¹⁵⁸ under high dilution conditions. To a solution of 4 equivalents of diethyl azodicarboxylate (DEAD) in tetrahydrofuran was added dropwise a solution of TTFAQ diol **204**, phenanthroline derivative **218** and 4 equivalents of triphenylphosphine in tetrahydrofuran over 8 h, to ensure high dilution conditions, but still at a concentration high enough for the reactive species to be formed (Scheme 46). Subsequently TLC showed formation of one major product, but also several by-products and impurities from degraded Mitsunobu reagent. TTFAQ phenanthroline cyclophane **220** was isolated in 36% yield, but as purification was difficult, we sought another route to compound **220**, especially since a larger portion was needed if complexation experiments and catenate synthesis was to be carried out.



Scheme 46: Synthesis of a TTFAQ phenanthroline cyclophane using the Mitsunobu reaction.

We then turned to the conditions originally used by Sauvage *et al.*¹⁵⁴ and later also by Becher and co-workers.^{155,156} For this we needed to convert the TTFAQ diols **203** and **204** to the corresponding dihalides. We decided to synthesise the dibromides **221** and **222** using the mild bromination conditions mentioned earlier (section 3.4.4). Treatment of **203** and **204** with carbon tetrabromide and triphenylphosphine afforded the dibromides **221** and **222** in almost quantitative yields (Scheme 47). Dibromide TTFAQ **222** was reacted with 2,9-di(*p*-phenol)-1,10-phenanthroline **218** in the presence of cesium carbonate under high dilution conditions, by the means of a perfusor pump. The two reactants were pumped to a suspension of the excess cesium carbonate over 48 h, after which time the reaction mixture was left to stir for

another 24 h. This time the formation of cyclophane **220** was much cleaner, with only a few very polar decomposition products, which made the workup straightforward. Compound **220** was isolated as a yellow powder in 68% yield, which is excellent for this type of reaction (see Scheme 45 for comparison). The overall yield from the diol **204** was 63%, compared to 36% using the direct route under Mitsunobu conditions (Scheme 46).



Scheme 47: Synthesis of TTFAQ phenanthroline cyclophanes in two steps from diols **203** and **204**.

It should be possible to synthesise the smaller cyclophane **223** from the dibromide **221** in even higher yield, but due to very poor solubility of **221** the macrocyclisation had to be carried out under simple high dilution conditions, *i.e.* the reactants were suspended in a large volume of *N,N*-dimethylformamide and stirred at 70 °C for 72 h. Hence the yield of **223** was only 48% compared to 68% for the larger cyclophane **220**. Both cyclophanes **220** and **223** were fully characterised and especially **220** possessed good solubility in a wide range of

organic solvents, which is important for its potential use in complexation studies and catenate synthesis.

5.4.3 X-ray crystallographic analysis

We were unable to grow crystals of the larger cyclophane **220**, but crystals of **223** suitable for X-ray crystallographic analysis were grown by slow evaporation of a solution of **223** in chlorobenzene.

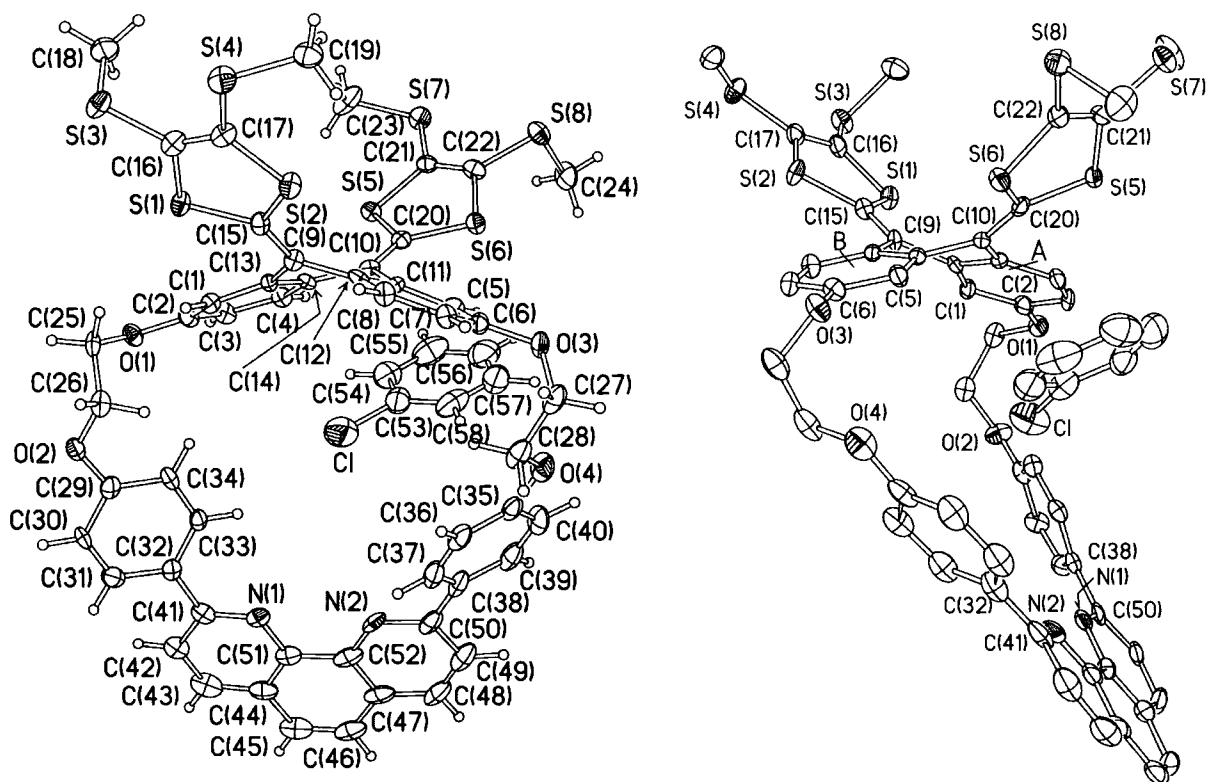


Figure 76: The X-ray crystal structure of TTFAQ phenanthroline cyclophane **223** viewed from two different directions.

Cyclophane **223** crystallised as a **223**·PhCl solvate (Figure 76). The TTFAQ system adopts the usual saddle-shaped conformation and the two dithiole rings are bent inward along the S(1)···S(2) and S(5)···S(6) vectors by 10.1° and 17.9°, respectively. Thus, the dihedral angle between the S(1)C(16)C(17)S(2) and S(5)C(21)C(22)S(6) planes (81°) is within the range observed in non-bridged TTFAQ systems (73-101°). The dihydroanthracene ring system is folded along the C(9)···C(10) vector and its peripheral benzene rings (A and B, see Figure 76 right) are inclined to each other by 39°. This usual folding is complicated by a twisting

distortion induced by the bridge. Thus, the C(9) and C(10) atoms are tilted out of the ring plane A by -0.15 and 0.14 Å, and out of plane B by 0.14 and -0.05 Å, respectively. Within the bridge, the phenanthroline system is slightly distorted. The two outer rings are non-parallel by 6° , but otherwise the macrocycle shows rather little steric strain. Twists around the C(32)-C(41) and C(38)-C(50) bonds are 29° and 37° , respectively. Overall, the macrocycle adopts a concave shape, with the chlorobenzene molecule occupying its recess and the Cl atom directed into the centre of the macrocycle. Molecules of **223**, related by an inversion centre, form pseudo-dimers with mutually engulfing TTFAQ moieties (Figure 77), which is the usual packing motif for TTFAQ systems (see other examples section 4.5 and 5.2.4).

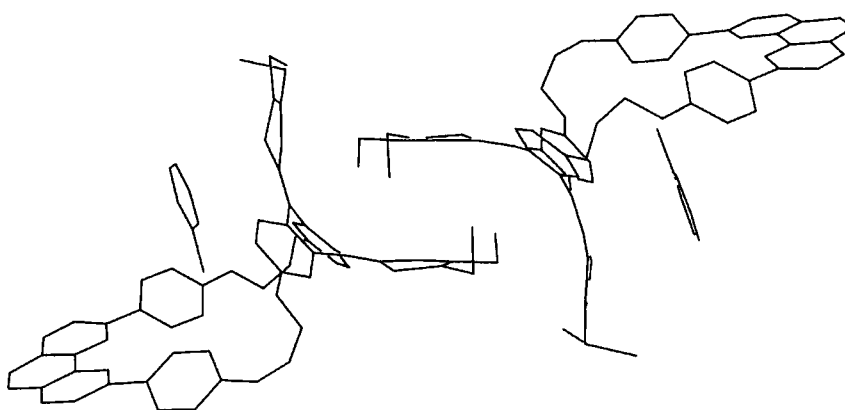


Figure 77: Packing of TTFAQ phenanthroline cyclophane **223**.

5.4.4 Future projects

For future projects, the incorporation of **220** and **223** into precatenates, for complexation studies and catenate synthesis, should be very interesting. Bryce *et al.* recently synthesised the bis-crown annelated TTFAQ derivative **224**¹⁵⁹ inspired by the analogous TTF derivative **225**¹⁶⁰ synthesised by Becher and co-workers. Both **224** and **225** sense Ag^+ and Na^+ ions, which is manifested by a positive shift of the first oxidation potentials in the cyclic voltammogram. However, the oxidation potential for **224** is shifted more than for the TTF derivative **225**, and **224** is significantly more sensitive than **225**. For **224** saturation is achieved with < 10 equivalents of Na^+ (causing a shift of 100 mV), whereas 250 equivalents of Na^+ was required to shift the oxidation potential of **225** by 80 mV. An explanation could be that the two-electron wave of **224**, rather than the one-electron wave of **225**, serves to enhance the Coulombic repulsion with the bound metal cations. Thus, one could anticipate the TTFAQ phenanthroline cyclophanes **220** and **223** to be part of even better sensors (precatenates) than

the TTF phenanthroline precatenate **216** of Becher *et al.*¹⁵⁶ (Figure 75), especially since the Cu^+ ion was not expelled until the second one-electron oxidation wave of precatenate **216** (see section 5.4.1).

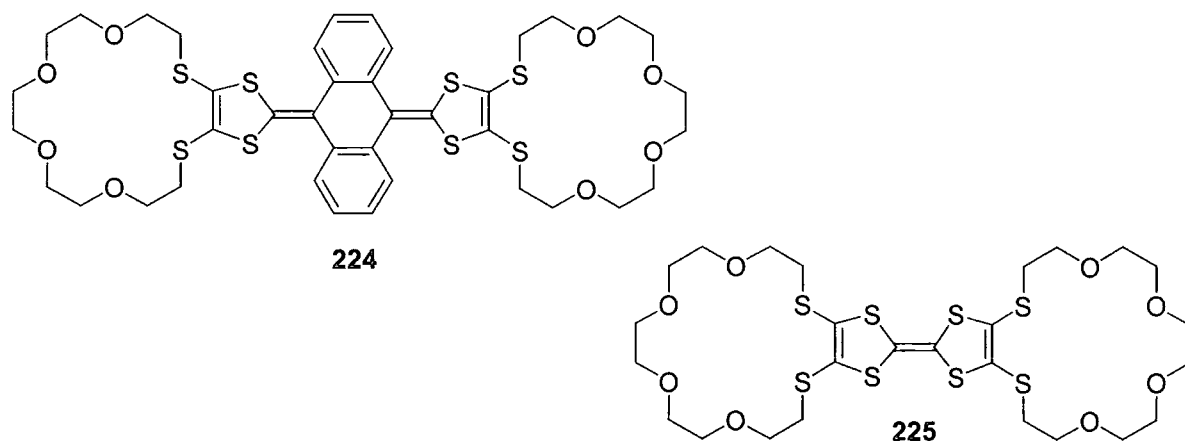


Figure 78: The Ag^+ and Na^+ sensing TTFAQ derivative **224**¹⁵⁹ and the corresponding TTF derivative **225**.¹⁶⁰

5.5 CONCLUSIONS

An efficient synthesis of a new set of TTFAQ building blocks, functionalised in the 2- and 6-positions, has been developed. Their symmetry makes them ideal for cyclophane synthesis, as shown by the high yielding synthesis of **206** and **207**, and the 2 + 2 cyclophane **208**. The cyclophanes were characterised by X-ray crystallography, which also revealed the structure of the oxidised cyclophane **206**²⁺ to be distorted from the normal conformation of TTFAQ dication species, due to the strain imposed by the bridge. The redox properties of the cyclophanes were only altered to a minor degree, when compared to TTFAQ cyclophanes having the 1,3-dithiole rings bridged. The TTFAQ building blocks proved to be very versatile for the synthesis of TTFAQ phenanthroline cyclophanes and also a donor-acceptor triad. Thus, this work paves the way for the incorporation of TTFAQ into more elaborate structures and supramolecular assemblies like catenates and compounds for ion recognition.

6 A NOVEL ROUTE TO HIGHLY FUNCTIONALISED TTFAQ DERIVATIVES

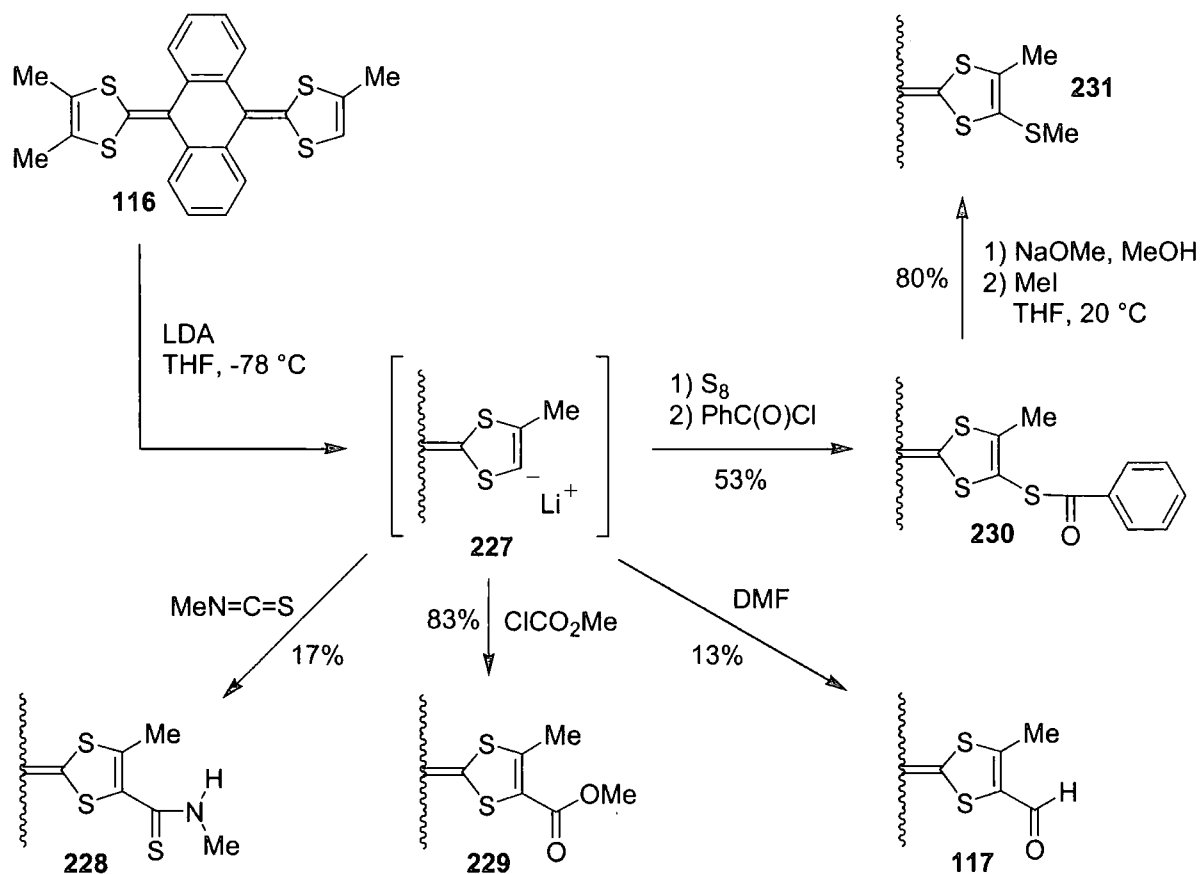
Although the well-known methodology for TTFAQ synthesis (section 2.3) had proven efficient and versatile, we were limited by the harsh reaction conditions in our effort to incorporate TTFAQ into more complicated molecular structures. This chapter describes a new synthetic route, affording highly functionalised TTFAQ building blocks, together with a few examples of their use.

6.1 BACKGROUND

Apart from the TTFAQ derivatives referred to and synthesised in Chapter 5, which were made by functionalising the dihydroanthracene ring system, TTFAQ derivatives have traditionally been made by functionalising the 1,3-dithiole rings.

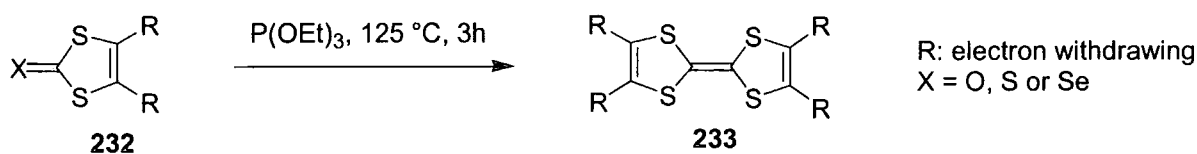
6.1.1 TTFAQ derivatives by lithiation of the 1,3-dithiole rings

Functionalisation of the 1,3-dithiole rings of TTFAQ has mainly been done by lithiation.⁹⁶ Finn in our group used the trimethyl derivative **116**, which could only be lithiated in one position, to monofunctionalise TTFAQ, using lithium diisopropylamide, followed by trapping of the transient lithium salt **227** by several electrophiles (Scheme 48).^{94,125} Aldehyde and thioamide derivatives **117** and **228**, respectively, were obtained in poor yield (13-17%), whereas the trapping with methylchloroformate gave ester **229** in good yield (83%). Thus, the derivative **229** has found the widest use.^{66,161} Sulfur insertion into the lithiated species followed by reaction of the resulting transient thiolate anion with benzoyl chloride, afforded the thioester **230** in 53% yield. Compound **230** could then be used as a shelf-stable precursor for other TTFAQ derivatives like **231**.^{94,125} Bisfunctionalisation has been done in a similar fashion by Godbert in our group, by lithiation of dimethyl TTFAQ derivatives.^{66,145} This has led to the building block **188** (Scheme 38), which was used for cyclophane synthesis.

Scheme 48: Functionalisation of the 1,3-dithiole rings of TFAQ by lithiation.^{94,125}

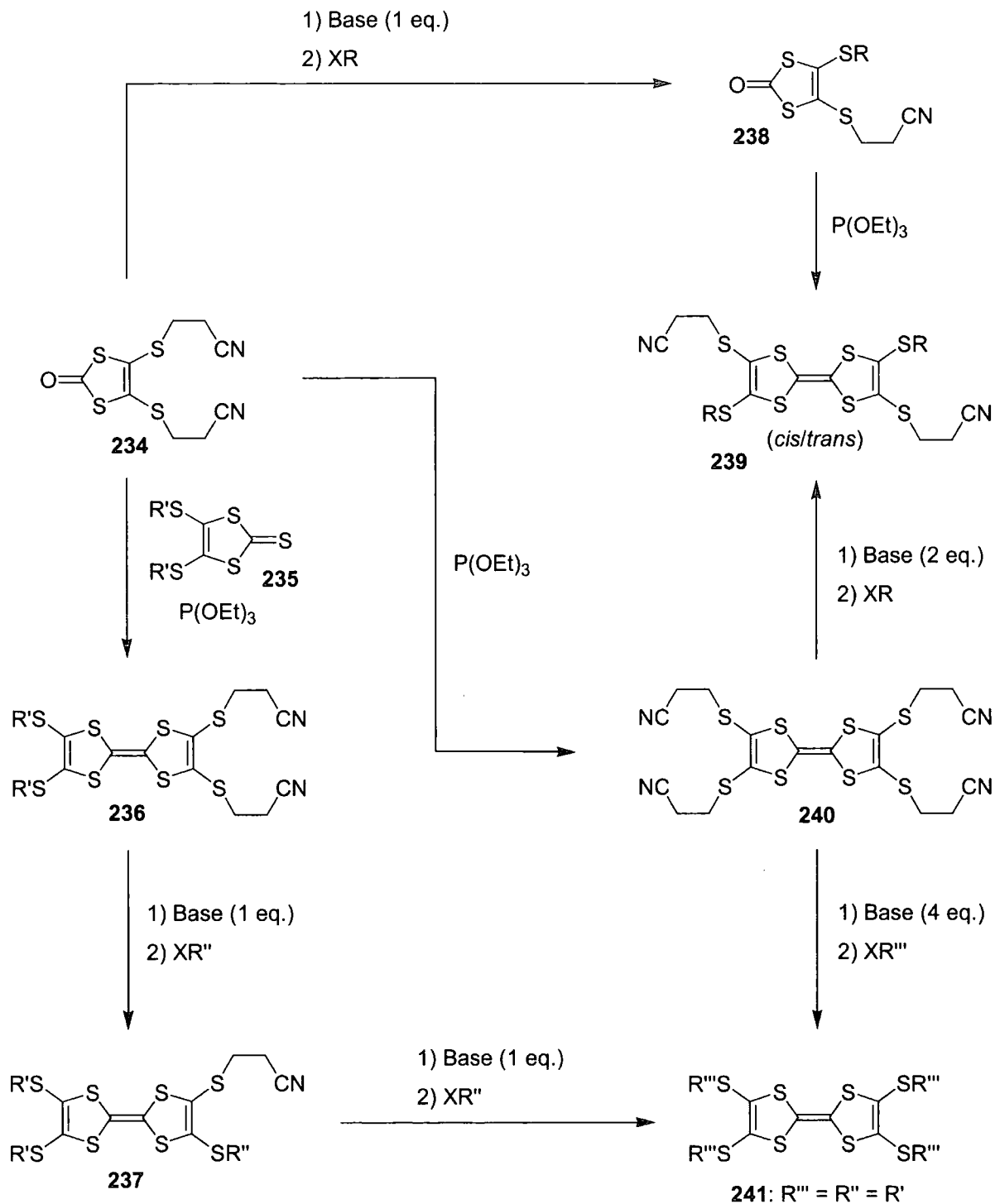
6.1.2 Cyanoethyl protected TTF thiolates

Traditionally TTF has been structurally modified by coupling reactions of 1,3-dithiole derivatives already functionalised with different substituents or by lithiation of TTF followed by reaction with electrophiles.⁶ One of the most widely used coupling reactions is the phosphite mediated coupling of 1,3-dithiole-2-chalcogenones.¹⁶² However, this reaction only proceeds for 1,3-dithiole-2-chalcogenones **232** substituted with electron withdrawing groups, e.g. alkylthio groups, and most systems containing alcohol-, thioester-, urethane- or carbonyl functional groups cannot survive the reaction conditions (Scheme 49). Generally both oxones and selenones give higher yields than the corresponding thiones.⁶



Scheme 49: Phosphite mediated coupling of 1,3-dithiole-2-chalcogenones to give TTF derivatives.

A break-through in functionalising TTF came in the group of Becher in 1993,¹⁶³ when a precursor **240** for TTF tetrathiolate was made from 4,5-bis(2-cyanoethylthio)-1,3-dithiole-2-one **234** by a phosphite mediated coupling reaction (Scheme 50).¹⁶⁴



Base = CsOH or MeONa, X = halide, R = alkyl

Scheme 50: Synthesis and reaction of the 4 important TTF building blocks **236**, **237**, **239** and **240**.

The 2-cyanoethyl group is ideal for the purpose of protecting the 1,3-dithiole-4,5-dithiolates, since it can be easily removed by a β -elimination, using bases like cesium hydroxide or sodium methoxide, and most importantly, the protecting group can survive the phosphite coupling. The TTF thiolates generated by deprotection are very reactive nucleophiles, which can be easily alkylated, and this makes **240** an ideal building block for the incorporation of TTF into macro- and supramolecular assemblies.¹⁶³ After the synthesis of **240**, the concept of TTF derivatives possessing one or more 2-cyanoethyl protected thiolates was successfully developed, which can be seen from Scheme 50. Cross-coupling of bisprotected 1,3-dithiole-2-one **234** with other alkylthio substituted 1,3-dithiole-2-thiones **235** afforded TTF **236** possessing two protected thiolates. Next it was found that both bisprotected **234** and bisprotected TTF thiolates **236** could be sequentially deprotected and realkylated to give first monoprotected derivatives **238** and **237**, respectively, and then bisalkylated derivatives like **235** and **241**, respectively, in quantitative yield.¹⁶⁵ The sequential deprotection/realkylation protocol can be explained by the unfavourable Coulombic repulsion between negatively charged thiolate groups on the same dithiole ring, an explanation which has been supported by theoretical calculations. They also explain why addition of 2 equivalents of base to compound **240**, followed by realkylation, exclusively affords bisprotected TTF derivative **239** as a *cis/trans* mixture.¹⁶⁶ Compound **239** can also be made in a phosphite coupling of 1,3-dithiole-2-one **238**.¹⁶⁵

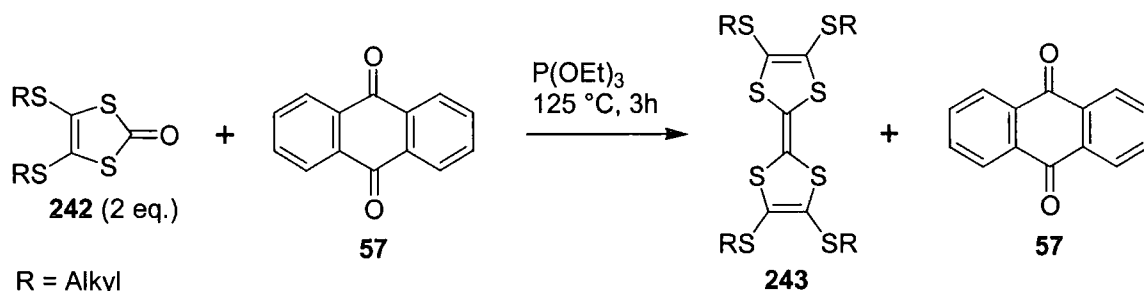
TTF derivatives **236**, **237**, **239** and **240** makes up a complete set of very versatile building blocks for incorporating TTF into supramolecular assemblies.^{163,167} During the writing of this thesis, a literature search using Beilstein Cross Fire afforded more than 60 hits and over 150 derivatives of TTF containing one or several cyanoethyl protected thiolates. Since the first paper was published in 1994,¹⁶⁴ they have been used for the synthesis of not only the cyclophanes reviewed in section 1.2.7 and 1.2.8, but also for the synthesis of catenanes,^{27,168} rotaxanes,^{168,169} dendrimers,¹⁷⁰ molecular switches¹⁷¹ and other complicated assemblies.^{167,172}

6.2 THE PHOSPHITE COUPLING – A NEW ROUTE TO TTFAQ DERIVATIVES

It was clear that TTFAQ analogues of the TTF derivatives **236**, **237**, **239** and **240** would be of great synthetic use, complimenting the lithiation methodology for the functionalisation of the dithiole rings of TTFAQ (section 6.1.1). However, even if a phosphonate ester derivative **254**

possessing two 2-cyanoethyl protected thiolates could be made (see Scheme 55, or for the detailed synthesis of phosphonate esters from 4,5-bis(alkylthio)-1,3-dithiole-2-thiones see Appendix One), the protecting groups would never survive the basic conditions in the subsequent Horner-Wadsworth-Emmons olefination, which should otherwise have afforded the desired TTFAQ derivative **246** (Scheme 55). A Wittig salt of **234** had been reported,¹⁷³ but it could only be used in a special pseudo-Wittig reaction, and only when triethylamine was used as base, and therefore a reaction with anthraquinone was excluded. Alternatively the sulfur insertion reaction of Scheme 48 could be expanded to a quadruple insertion, to give a tetrakisprotected TTFAQ thiolate, but the mono-insertion could only be done on a small scale in moderate yields, so a quadruple sulfur insertion was not realistic.

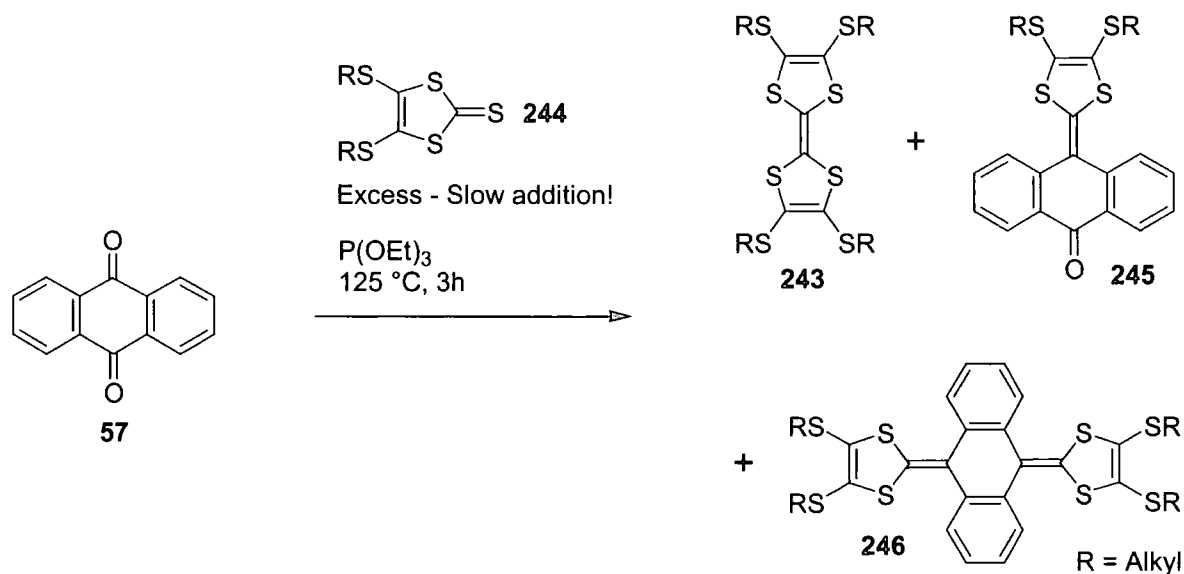
All problems could be solved, if it was possible to cross-couple two 1,3-dithiole-2-one units with anthraquinone in a phosphite mediated reaction. Indeed this had already been tried in our group.¹⁷⁴ From the reaction of 1,3-dithiole-2-one **242** and anthraquinone **57** in a 2:1 ratio, heated in neat triethyl phosphite over 3 h, only the symmetrical TTF derivative **243** and unreacted anthraquinone was isolated (Scheme 51). Hence, for several years the reaction was not investigated further, but the search for new TTFAQ building blocks made us return to the phosphite coupling.



Scheme 51: Early attempts at synthesising TTFAQ derivatives by a phosphite mediated cross-coupling reaction afforded only the symmetrical TTF derivative **243** and unreacted anthraquinone **57**.

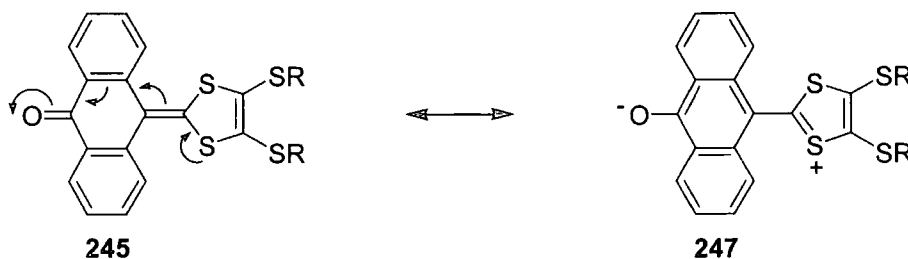
To minimize the formation of the symmetrical TTF derivative **243**, we carried out reactions where anthraquinone **57** was heated in triethyl phosphite and an excess of 1,3-dithiole-2-thione derivative **244**, which is less reactive than the corresponding ketone, was added in small portions over 3 hours (Scheme 52). This would favour a coupling of the thione **244** with anthraquinone, compared to self-coupling of **244**, since the concentration of **244** would be low at any time and anthraquinone would be in large excess at least until a major fraction of it had reacted. The reaction was monitored by TLC, and formation of 3 major products was

observed concomitantly with the consumption of the anthraquinone. Also it was found that an added small portion of 1,3-dithiole-2-thione **244** had all reacted within 15 min of addition, which supported the observations of the early attempt (Scheme 51). Apart from a range of minor by-products,¹⁷⁵ the 3 major compounds were identified as the TTF derivative **243**, the ketone **245** and the TTFAQ derivative **246** (Scheme 52).



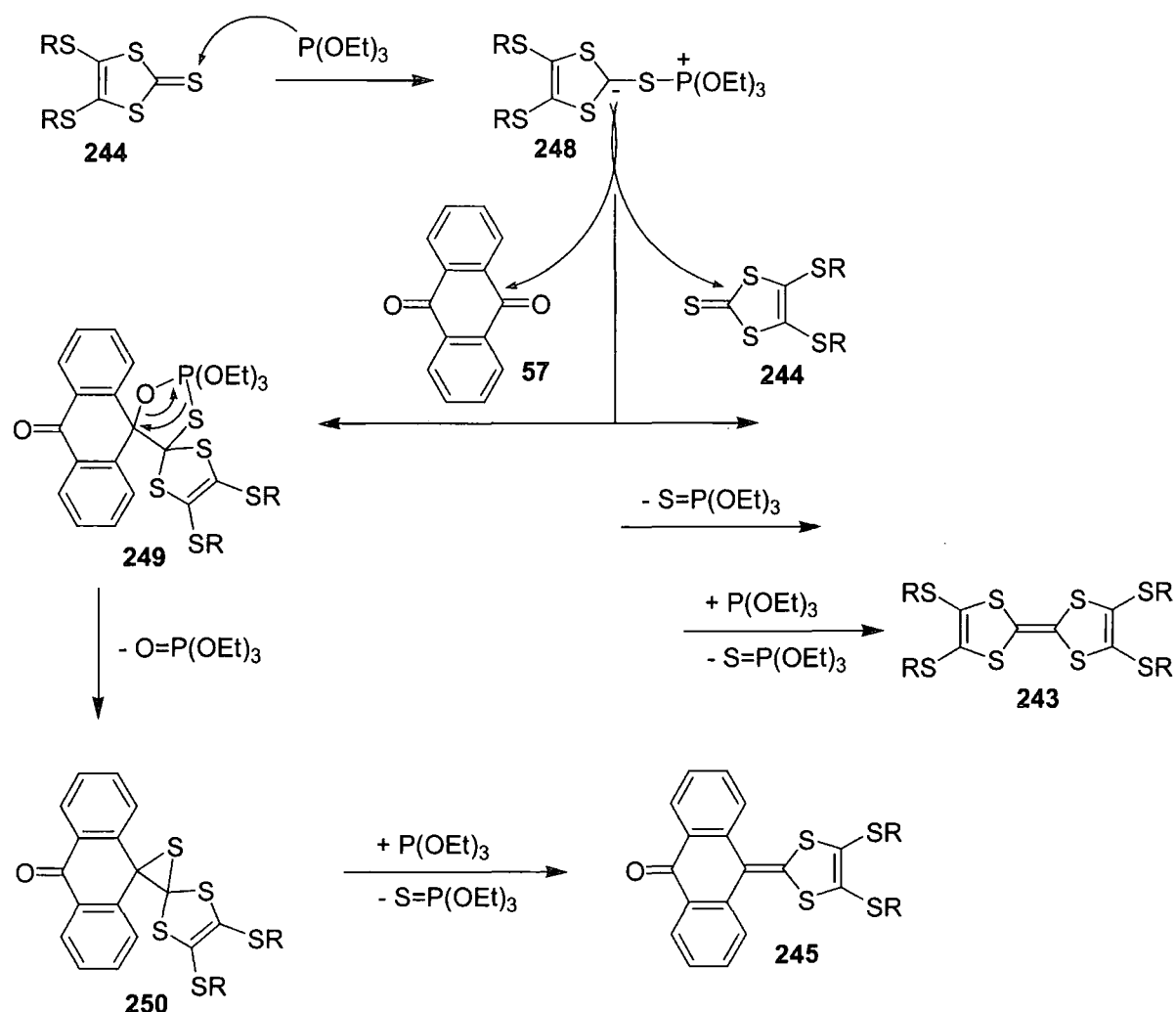
Scheme 52: By slow addition of the 1,3-dithiole-2-thione **244**, TTFAQ derivative **246** could be synthesised in a phosphite mediated cross-coupling reaction with anthraquinone. The corresponding symmetrical TTF derivative **243** and the ketone **245** were also formed.

Importantly, further self-coupling of ketone **245** did not take place, which would have otherwise lowered the yield of the TTFAQ derivative **246** considerably. This is possibly due to a significant contribution from the resonance form **247** (Scheme 53), which would not stimulate the attack of triethyl phosphite at the oxygen, necessary for self-coupling of **245** (see the proposed mechanism, Scheme 54).



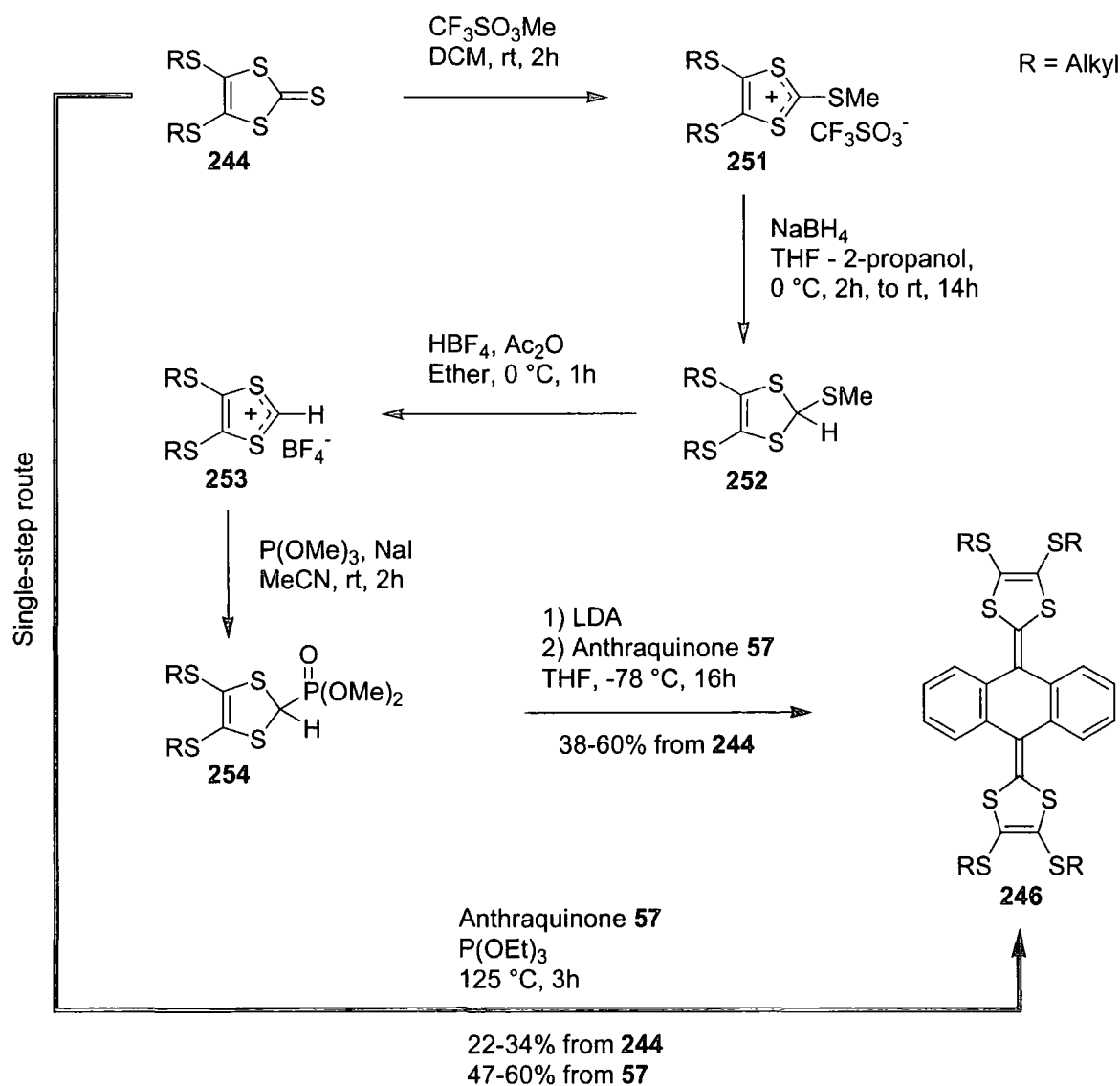
Scheme 53: A significant contribution from the resonance form **247** might be what prevents the self-coupling of ketone **245** in the phosphite mediated coupling reaction.

A closer look at the mechanism can help to explain why our new methodology for the synthesis of TTFAQ derivatives works so well. Upon addition of a small portion of thione **244**, presumably most of **244** will be subject to a thiophilic attack of triethyl phosphite, since the phosphite is present in large excess as the solvent. Thus not much thione **244** is left to react with the formed 1,3-dipolar intermediate **248**, and the competition from a large excess of anthraquinone **57** is strong. The part of the 1,3-dipolar intermediate **248** which is not used in the formation of the symmetric TTF derivative **243**, should react in a similar way with anthraquinone. ¹⁶² Nucleophilic attack of **248** on a carbonyl group of the anthraquinone **57** forms the transient species **249**, which collapses to give the episulfide **250**. Reaction of epoxides and episulfides with triethyl phosphite is well-known to give olefins. ¹⁷⁶ In this case reaction of **250** with 1 equivalent of triethyl phosphite leads to the ketone **245**, possibly *via* a betaine intermediate.



Scheme 54: The proposed mechanism for the formation of either the ketone **245** or the symmetrical TTF derivative **243**, *via* one of the two competing pathways.

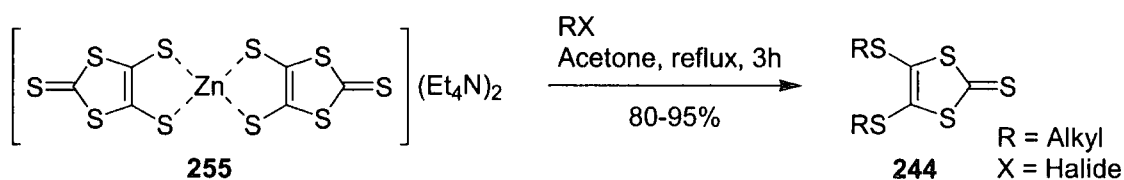
The reaction conditions for our new synthesis of TTFAQ derivatives were optimised and the results can be found in section 6.3, 6.6, 7.1.3 and 7.2.1. However, several general points should be mentioned. Since the reactivity of the ketone **245** varies with the electron withdrawing ability of the substituents on the 1,3-dithiole moiety, with electron withdrawing groups increasing the reactivity of **245**, the number of equivalents of thione **244** needed varies considerably (see section 6.6 and 7.2.1). Thus, the reactions should always be monitored by TLC, so they can be stopped when so little anthraquinone and ketone **245** is left, that further addition of thione **244** would almost exclusively lead to the formation of TTF derivative **243**.



Scheme 55: The classic multi-step synthesis of TTFAQ derivatives **246** from 4,5-bis(alkylthio)-1,3-dithiole-2-thiones **244** vs. the single-step phosphite mediated cross-coupling. The general yields are based on the reactions carried out for the work presented in this thesis.

The coupling reactions can be carried out on a multi-gram scale, but unfortunately anthraquinone is only moderately soluble in even hot triethyl phosphite. To overcome this problem, a mixture of triethyl phosphite-chlorobenzene 1:3 (v/v) was found to be ideal. However, further dilution of the phosphite leads to a significant increase in reaction time, which would require an even slower addition of the 1,3-dithiole-2-thione derivative **244**.

Not only does the phosphite mediated cross-coupling reaction allow us to synthesise TTFAQ derivatives bearing more elaborate functionalities, it is also labour and cost efficient. The classic five-step synthesis of TTFAQ derivatives **246** from 4,5-bis(alkylthio)-1,3-dithiole-2-thiones **244** (Scheme 55. For the detailed synthesis of phosphonate esters see Appendix One) takes 4-5 working days and involves 3 purifications by column chromatography. In contrast, the phosphite coupling can be carried out in a single step and be worked up within 1 day. However, calculating the yields from the thiones **244**, which are used in large excess in the phosphite coupling, the new methodology compares badly with the classic five-step synthesis (22-34% vs. 38-60%, Scheme 55). But, 4,5-bis(alkylthio)-1,3-dithiole-2-thiones **244** can easily be obtained in multi-gram batches by alkylation of 1,3-dithiole-2-thione-4,5-dithiolate,¹⁷⁷ using its zinc complex **255** (Scheme 56. See also Appendix One for experimental details), and **255** can be made in 200 g batches in just 2 days.¹⁷⁸ Thus, the lower over-all yield calculated from the 4,5-bis(alkylthio)-1,3-dithiole-2-thiones **244**, is more than out-balanced by the ease of the phosphite coupling, not even taking the possible synthesis of cyanoethyl protected TTFAQ derivatives into account.



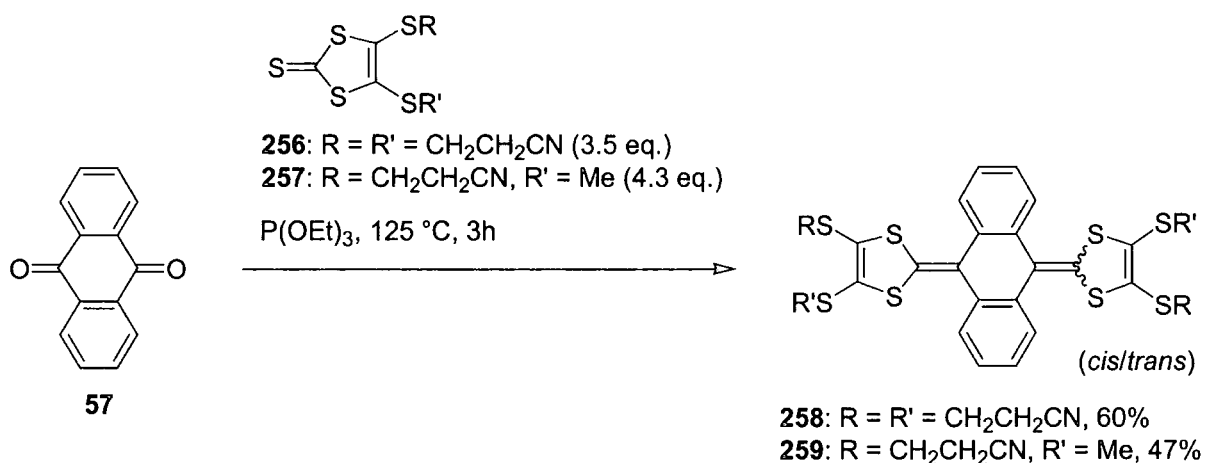
Scheme 56: The zinc complex **255**¹⁷⁸ is a readily available source for alkylthio substituted 1,3-dithiole-2-thiones.¹⁷⁷ The yields are based on the reactions carried out for the work presented in this thesis.

6.3 SYNTHESIS OF NEW TTFAQ BUILDING BLOCKS

Having developed the synthesis of TTFAQ derivatives by a phosphite mediated coupling reaction, we could now achieve the goal of synthesising TTFAQ building blocks similar to TTF derivatives **236**, **237**, **239** and **240** (Scheme 50).

6.3.1 Synthesis of symmetrical TTFAQ derivatives

Two symmetrical⁸⁷ TTFAQ derivatives were synthesised by a phosphite mediated cross-coupling of anthraquinone **57** with 1,3-dithiole-2-thione **256** and **257**, respectively (Scheme 57). Slow addition of **256**¹⁶⁴ to a heated solution of anthraquinone afforded 2-cyanoethyl protected TTFAQ tetrathiolate **258**, as monitored by TLC. The reaction was stopped after 3.5 equivalents of thione **256** were added, since further addition of thione only increased the formation of the corresponding self-coupled TTF derivative **240** (Scheme 50). Upon cooling to 0 °C and addition of methanol a yellow precipitate formed, which could be filtered and purified by column chromatography to give **258** as a yellow solid in 60% yield.



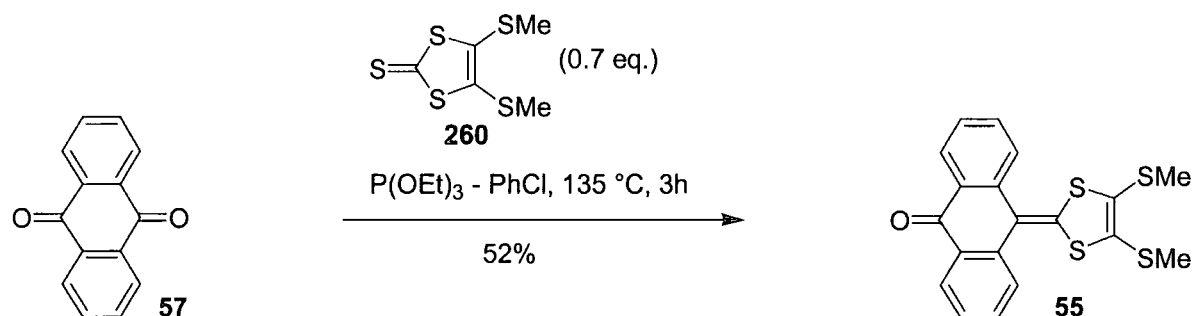
Scheme 57: Slow addition of 1,3-dithiole-2-thione derivatives **256** and **257** to a heated solution of anthraquinone **57** in triethyl phosphite afforded TTFAQ building blocks **258** and **259**, respectively.

The TTFAQ building block **259** was synthesised similarly to **258**, from thione **257**^{165b} and anthraquinone, except that **259** could not be precipitated by addition of methanol. Instead the smelly product mixture was purified directly by column chromatography. Pure TTFAQ derivative **259** was obtained in only 47% yield, by using 4.3 equivalents of thione **257**, but this was due to difficulties separating **259** from the self-coupled TTF derivative **239**. To avoid this problem, **259** could alternatively be made by bisdeprotection of **258**, followed by methylation (similar to the synthesis of TTF derivative **239** from **240**, Scheme 50).

6.3.2 A two-step synthesis of unsymmetrical TTFAQ derivatives

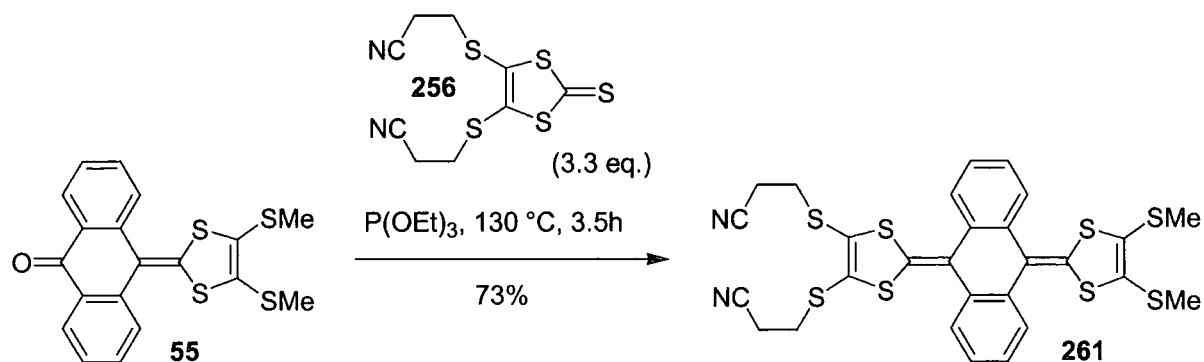
Next we investigated the synthesis of unsymmetrical TTFAQ derivatives, *i.e.* bearing two different 1,3-dithiole moieties. This would have to be done in two steps. To form ketones like

245, an excess of anthraquinone is needed, to ensure that only a minimum of **245** is coupled a second time to form the corresponding TTFAQ derivative. Since this reaction was done on a multi-gram scale, a mixture of triethyl phosphite-chlorobenzene 1:3 (v/v) was used as solvent, allowing a large amount of anthraquinone to be dissolved. Thus, to a solution of anthraquinone **57** was added 0.7 equivalents of thione **260**^{165b} in small portions, which afforded ketone **55** in 52% yield (Scheme 58). The yield is comparable with the literature procedure,⁷⁶ but this new methodology can be used to couple 1,3-dithioles bearing functional groups which would not survive the literature procedure.



Scheme 58: The ketone **55** was obtained using an excess of anthraquinone **57**.

In the second step ketone **55** was dissolved in neat triethyl phosphite and reacted with thione **256**. Addition of 3.3 equivalents of **256**¹⁶⁴ in small portions afforded building block **261** in 73% yield (Scheme 59).



Scheme 59: The second step in the synthesis of an unsymmetrical TTFAQ derivative.

6.3.3 Monodeprotection of a bisprotected TTFAQ thiolate derivative

The last building block **262** left to synthesise possessed only one cyanoethyl protected thiolate and its synthesis demonstrated the successful sequential deprotection of bisprotected TTFAQ

derivative **261**. By analogy with the quantitative synthesis of **237** (Scheme 50), which can be explained by the unfavourable Coulombic repulsion between negatively charged thiolate groups on the same dithiole ring,¹⁶⁶ it should be possible to monodeprotect and realkylate **261** in high yield. Thus, to a solution of compound **261** in *N,N*-dimethylformamide was slowly added 1 equivalent of sodium methoxide and the reaction mixture was left to stir for 1 h. This ensures that equilibrium, where only the monodeprotected species is present, is reached, before trapping of the transient thiolate by alkylation. Subsequent alkylation using methyl iodide afforded **262** in 96% yield.



Scheme 60: Monodeprotection of bisprotected TTFAQ thiolate derivative **261**, followed by realkylation using methyl iodide, proceeds in high yield.

6.4 NOVEL TTFAQ BUILDING BLOCKS IN SYNTHESIS

To prove the versatility of the protected TTFAQ thiolate derivatives **258**, **259**, **261** and **262** as building blocks for advanced redox active molecular systems, four examples are given.

6.4.1 A new TTFAQ derivative for solid state hydrogen bonding

In our group several unsuccessful attempts had been made to synthesise a TTFAQ derivative with all four positions of the dithiole rings substituted with hydroxymethyl groups (compound **263** being an example).¹⁷⁹ Such systems are interesting, since they could engage in intermolecular hydrogen bonding, thereby providing increased supramolecular order in solid state structures. The TTF derivative **264** was synthesised by Becher *et al.*¹⁶⁴ from TTF building block **240** (Scheme 50) and the X-ray crystal structure showed an interesting

coexistence of uniform π - π stacking and hydrogen-bonded $O\cdots H\cdots O$ networks.¹⁸⁰ Thus we decided to synthesise tetrakis(2-hydroxyethylthio)TTFAQ **265**, the TTFAQ analogue of **264**.

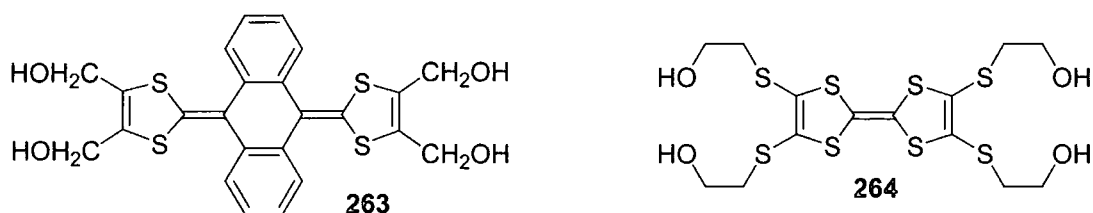
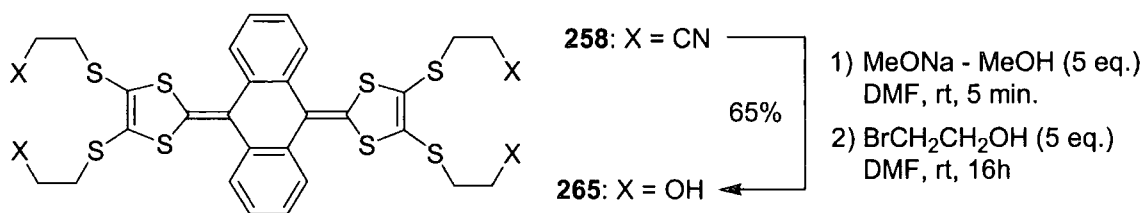


Figure 79: Synthesis of TTFAQ derivative **263** failed,¹⁷⁹ whereas compound **264** could be easily synthesised from TTF building block **240** (Scheme 50).¹⁶⁴

Deprotection of **258** using 5 equivalents of sodium methoxide generated the tetrathiolate, which was realkylated by addition of bromoethanol, and compound **265** was isolated as a yellow powder in 65% yield (Scheme 61). To investigate the hydrogen bonding properties of **265** in the solid state, crystals of **265** were grown from acetone, acetonitrile and methanol. The unsolvated crystals were too small for X-ray crystallography, but solvates **265**·MeOH_{2.5} (**265a**) and **265**·MeCN_{1.5} (**265b**) were obtained as orange blocks and prisms, respectively. They were stable under the mother liquor, but quickly decomposed if dried. Both were poor diffractors, probably because of the extensive disorder in the crystals (see below), but still suitable for X-ray crystallographic analysis.



Scheme 61: Synthesis of hydroxyethylthio derivative **265**.

Crystal structures **265a** and **265b** are very similar. In both cases the asymmetric unit contains one molecule of **265** possessing the saddle conformation typical for TTFAQ derivatives. In **265a** one of the dithiole rings of **265** shows disorder between two sets of positions, A and B, with occupancies 84% and 16%, respectively. The two hydroxyethyl chains at the ordered end of the TTFAQ unit are also ordered. These chains are both folded inward and locked in this conformation by an intramolecular hydrogen bond. As we have seen above (section 3.4.5, 3.4.8, 4.5 and 5.2.4) the crystal packing of TTFAQ derivatives usually follows a peculiar

motif: a pair of molecules, related *via* an inversion centre, form a pseudo-dimer in which each TTFAQ unit engulfs one dithiole end (or substituents thereat, if sufficiently large) of the other. Such pseudo-dimers exist in every TTFAQ containing structure studied so far, except where (as in **184-187**, section 5.1) the engulfing is prevented by a bridge between the two dithiole rings. In structure **265a** the intramolecular cavity of molecule **265** is occupied by a methanol molecule, which is hydrogen bonded to one of the ordered hydroxyethyl chains of an inversion-related molecule **265**. The resulting motif can also formally be regarded as a self-engulfing pseudo-dimer, if the hydrogen bonded methanol is considered as an 'extension' of the substituents on the dithiole ring. The pseudo-dimers pack in chess-board order (Figure 80) and form a layer, parallel to the crystallographic (1 1 0) plane. The layers are pierced by continuous channels running parallel to the *z* axis and occupied by disordered methanol molecules. The remaining two hydroxyethyl chains of the molecule, *i.e.* those on the 'non-engulfed' end, display a complicated disorder of their own. These chains are adjacent to the channels and, in some cases, share crystal space with the disordered methanol.

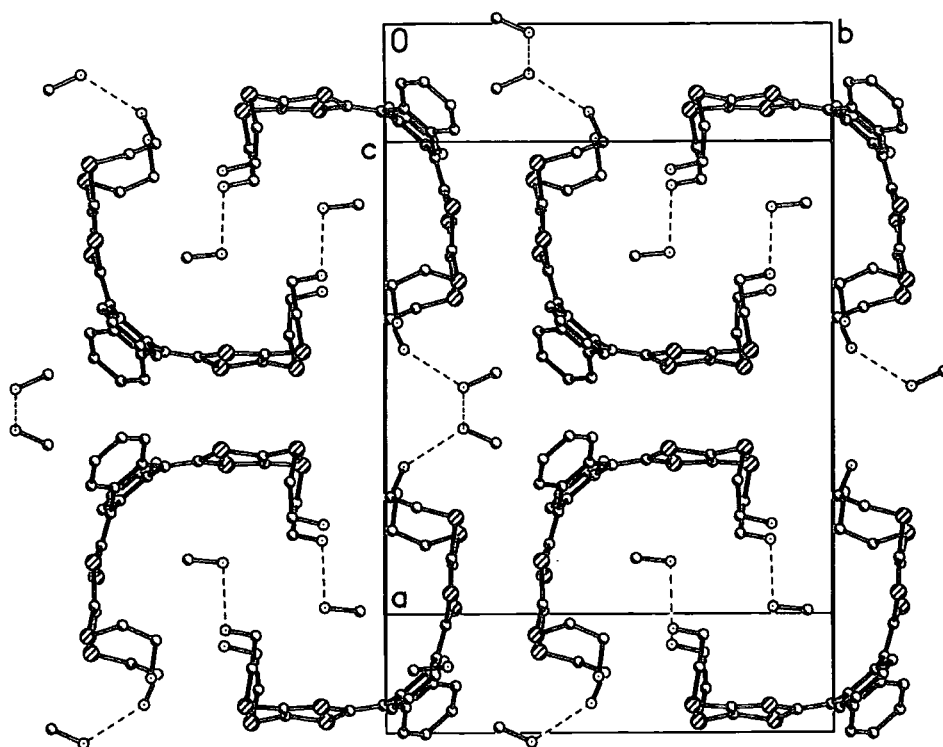


Figure 80: Crystal packing of **265a**, showing intermolecular hydrogen bonds (dashed lines). Minor positions of the disordered atoms and all hydrogens are omitted. Projection on the (1 1 0) plane.

In **265b**, the TTFAQ core of **265** is ordered, but the substituents are heavily disordered. In one end, the hydroxyethyl chains are disordered between two conformations, but in either case

both chains are folded inward and linked by an intramolecular hydrogen bond. The hydroxyethyl chains attached to the other end of the TTFAQ moiety are disordered between three possible conformations, two of them folded inwards and forming an intramolecular O-H...O hydrogen bond (as described above) and the third stretched outwards.

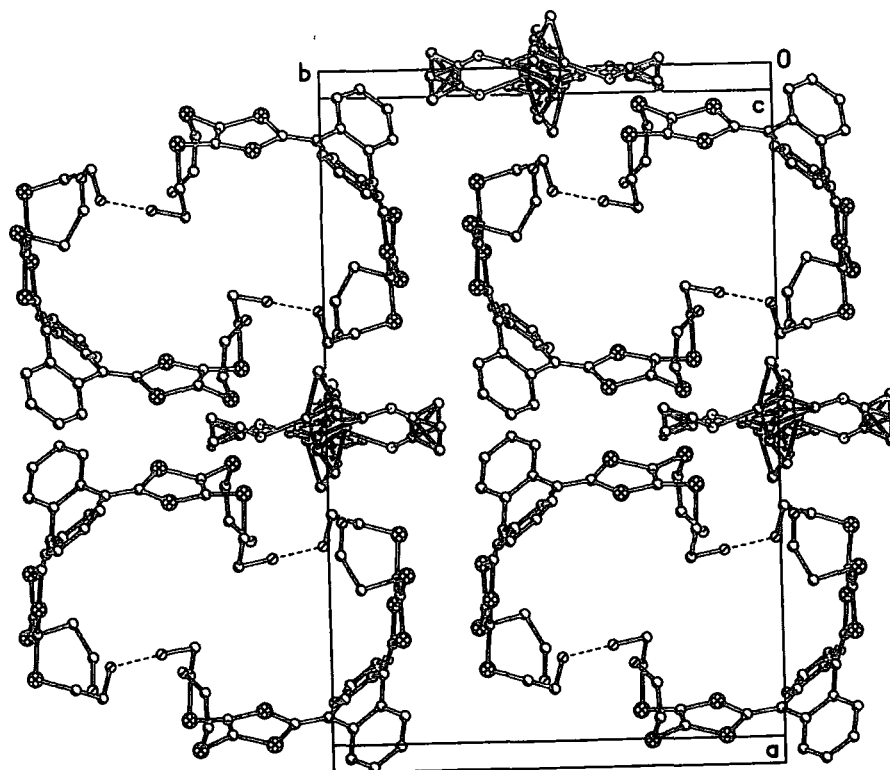


Figure 81: Crystal packing of **265b**, showing intermolecular hydrogen bonds (dashed lines) and the chaotically disordered solvent inside intermolecular channels. Minor positions of the disordered hydroxyethyl chains and all hydrogens are omitted. Projection on the (1 1 0) plane.

In **265b** two molecules of **265**, related by an inversion centre, form a pseudo-dimer similar in configuration to that in structure **265a**, but containing no solvent molecules within its cavity. There is also *no mutual engulfing* of the molecules, instead the dimer is held together by intermolecular hydrogen bonds between inward-oriented hydroxyls (Figure 81). As in **265a**, the pseudo-dimers form a layer parallel to the (1 1 0) plane and pierced by infinite channels parallel to the *z* axis. However, in **265b** the solvent (acetonitrile) is found only within these channels and is continuously and practically randomly distributed along their length. This distribution was approximated by a succession of arbitrary atomic positions with fractional occupancies; the amount of the solvent was estimated from the free volume of the channels and the level of residual electron density therein. The cavity of each molecule **265** is 'plugged' from both sides by parts of two other molecules (belonging to two adjacent layers):

a benzene ring of one and a hydroxyethyl chain (in an outstretched conformation) of another. Such plugging, prevented in **265a** by the intracavity methanol, results in the *c* parameter of **265b** being *ca.* 1.2 Å shorter than in **265a**. Thus, **265b** is the first example of a non-bridged TTFAQ derivative *not* forming a *mutually engulfing* pseudo-dimer in the solid state.

6.4.2 A high-yielding synthesis of a single-bridged TTFAQ cyclophane

The first TTFAQ cyclophanes **184** and **185** were synthesised by Finn in our group¹⁴³ (see section 5.1), but the strategy used was low-yielding (Scheme 37). To make a direct comparison, we synthesised cyclophane **266** as a close analogue of the most strained TTFAQ cyclophane **185** synthesised by Finn, having a single pentamethylenedithio bridge (Figure 82).

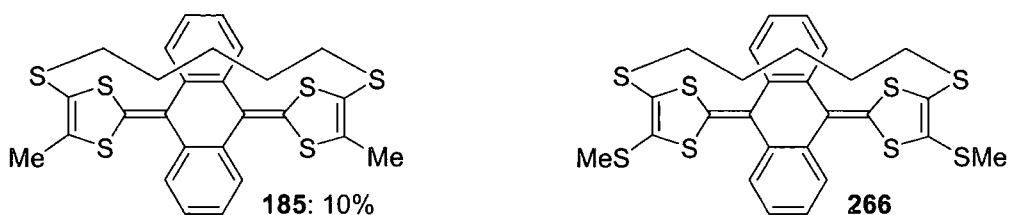
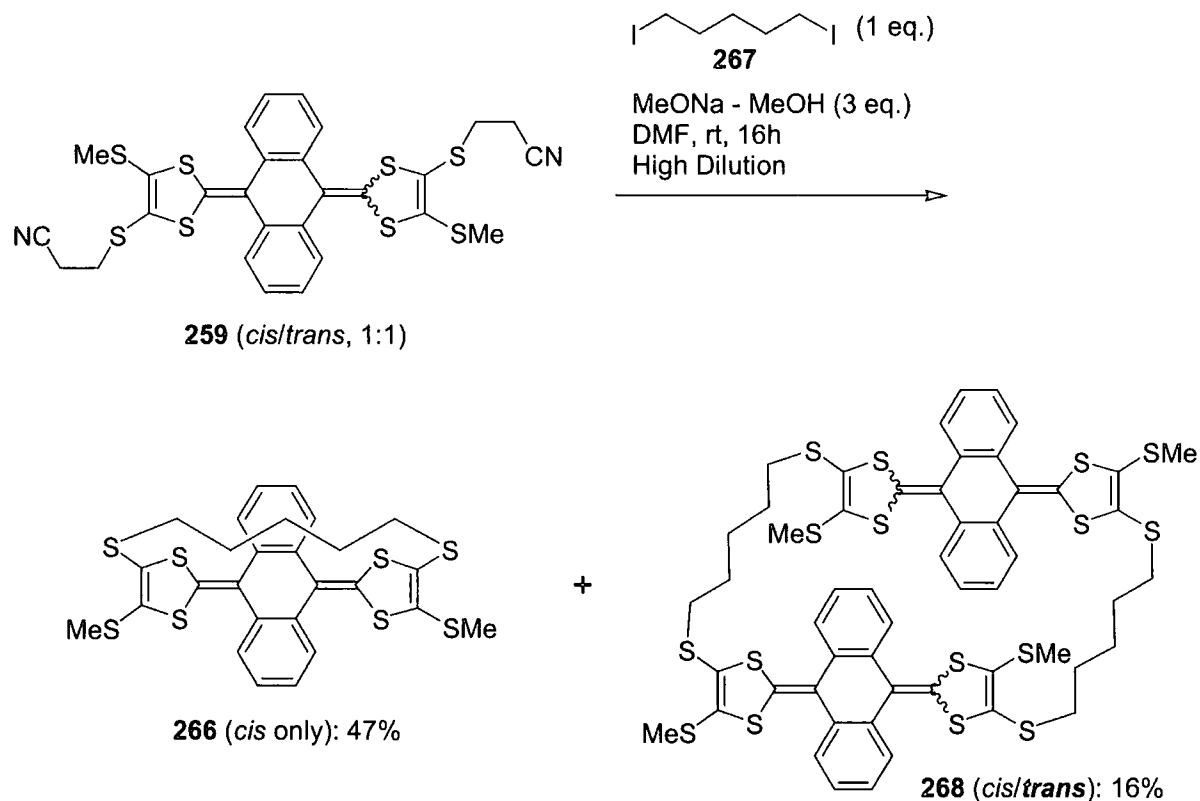


Figure 82: The first TTFAQ cyclophane **185** was synthesised by Finn in 10% yield.¹⁴³ For direct comparison, **266** was synthesised using the new TTFAQ building block **259**.

A solution of **259** and 1 equivalent of 1,5-diiodopentane **267** was mixed with a solution of 3 equivalents of sodium methoxide under high dilution conditions, by the means of a perfusor pump. Generation of the corresponding TTFAQ bisthiolate *in situ* and rapid trapping by the reactive diiodo linker, afforded two compounds in 47% and 16% yield, respectively (Scheme 62). The major compound was very soluble and analysed correctly for either the *cis*- or *trans*-bridged cyclophane, and ¹H NMR showed it was not a *cis/trans* mixture. An X-ray crystal structure (Figure 83, right) confirmed it to be the *cis*-bridged isomer **266**. The minor product **268**, when obtained pure, was nearly insoluble in every solvent, including carbon disulfide, toluene, chloroform and dimethylsulfoxide, which made ¹H NMR characterisation very difficult. However, other analysis soon excluded the *trans*-bridged cyclophane, even though the elemental analysis showed the right percentage of carbon and hydrogen. The melting point of **268** was above 280 °C (compared to 239-240 °C for **266**) and a mass spectrum revealed that it was a 2 + 2 adduct (the cyclic voltammogram also showed that **268** was a non-strained TTFAQ derivative, see section 6.5).



Scheme 62: The single-bridged TTFAQ cyclophane **266** was synthesised in 47% yield from the TTFAQ building block **259**. Also the 2 + 2 adduct **268** was isolated.

The yield of cyclophane **266** (47%) is far better than that obtained by Finn *et al.* for cyclophane **185** (10%),¹⁴³ showing the strength of using the pre-made building block **259**. However, since only 50% of **259** was the *cis* isomer, almost quantitative conversion of the *cis* building block to cyclophane **266** takes place. The situation is similar to the syntheses of Godbert *et al.*, in which a *cis/trans* mixture of the precursor only afforded the *cis*-bridged cyclophanes (in 8-15% yield).¹⁴⁵ Thus, even though two very different methodologies were used in the work of Finn *et al.* and Godbert *et al.*, always only the *cis* isomer was isolated, and it seemed that the synthesis of cyclophane **266** followed this trend. Indeed, formation of the *trans*-bridged analogue of **266** is so disfavoured that even a small amount was never detected. Contrary to this, the 2 + 2 adduct **268**, which statistically should be made almost entirely of the *trans* isomer of **259** (based on the yield of the *cis*-bridged cyclophane **266**, but not proved by analysis), is isolated in 16% yield, even though it requires the formation of 4 bonds to give a 34-membered macrocycle! An explanation could be the dynamic properties of TTFAQ derivatives in solution. As described earlier (section 2.2.2), the TTFAQ molecule in solution is flipping between two conformations, which should suppress reaction to take place *trans*.

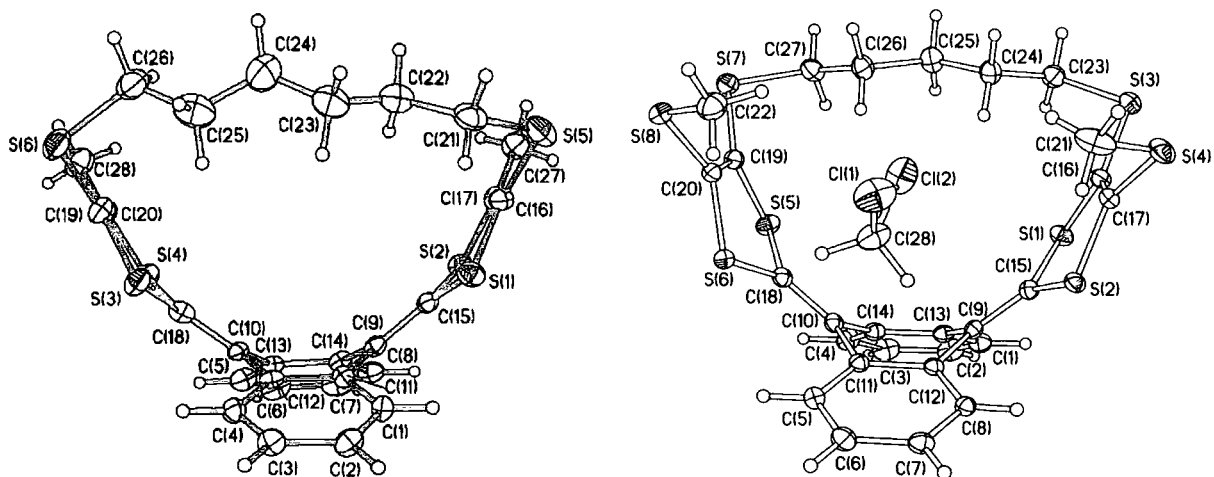


Figure 83: The X-ray crystal structures of single-bridged cyclophanes **185**¹⁸¹ (left) and **266** (right). The crystal structure of **266** is solvated with one molecule of dichloromethane situated in the cavity. The dichloromethane molecule is disordered between two orientations; only the major one (89%) is shown.

Crystallisation of compound **266** from dichloromethane-hexane yielded two different solvates, **266**·CH₂Cl₂ (**266a**) and **266**·(CH₂Cl₂)_{1.5} (**266b**), both as yellow blocks. The asymmetric unit of **266a** comprises one molecule of **266** and one disordered molecule of dichloromethane, fitting into the molecular cavity of **266** (Figure 83, right). The asymmetric unit of **266b** comprises two molecules of **266**, each of them containing an intensely disordered dichloromethane molecule in the cavity, and two other dichloromethane molecules, which occupy inter-molecular voids and are disordered around inversion centres (*i.e.* their independent positions have occupancies of 50%). The addition of this ‘outer’ solvent actually loosens the crystal packing: the unit cell volume of **266b** exceeds that of **266a** by 241 Å³, or 120.5 Å³ per extra dichloromethane molecule, while the volume per molecule in pure solid dichloromethane is only 82 Å³ (at 153 K).¹⁸² The molecular structures of **266** in both solvates are similar to that of **185** (Figure 83, left),¹⁸¹ which has two methyl substituents instead of methylthio groups. As in the latter, the pentamethylene bridge in **266** adopts a nearly planar all-*trans* conformation (S-C-C-C and C-C-C-C torsion angles are in the range 160 to 180°). Its pulling effect is manifested in the asymmetry of the transannular distances C(16)···C(19) and C(17)···C(20), which was *not* observed in **185**, as well as S(3)···S(7) and S(4)···S(8) distances (Table 10). The TTFAQ system adopts the usual saddle-shaped conformation, enhanced by the short bridge. The dithiole rings are folded inward along the S(1)···S(2) and S(5)···S(6) vectors (angles δ_1 and δ_2 , respectively. The dihedral angles of the TTFAQ moiety in cyclophane **266** are collated in Table 10). The dihedral angle (θ) between the S(1)C(16)C(17)S(2) and S(5)C(19)C(20)S(6) moieties, which gives a good measure of the

overall U-bending, is considerably wider in **266** than in **185**, but much smaller than in non-bridged saddle molecules (73-101°).^{66,73,94} This is probably due to the solvated dichloromethane molecule situated in the molecular cavity of **266**. The dihydroanthracene ring system is folded along the C(9)···C(10) vector, but the folding angle (φ) is not significantly larger than in non-bridged systems (35-41°).^{66,73,94}

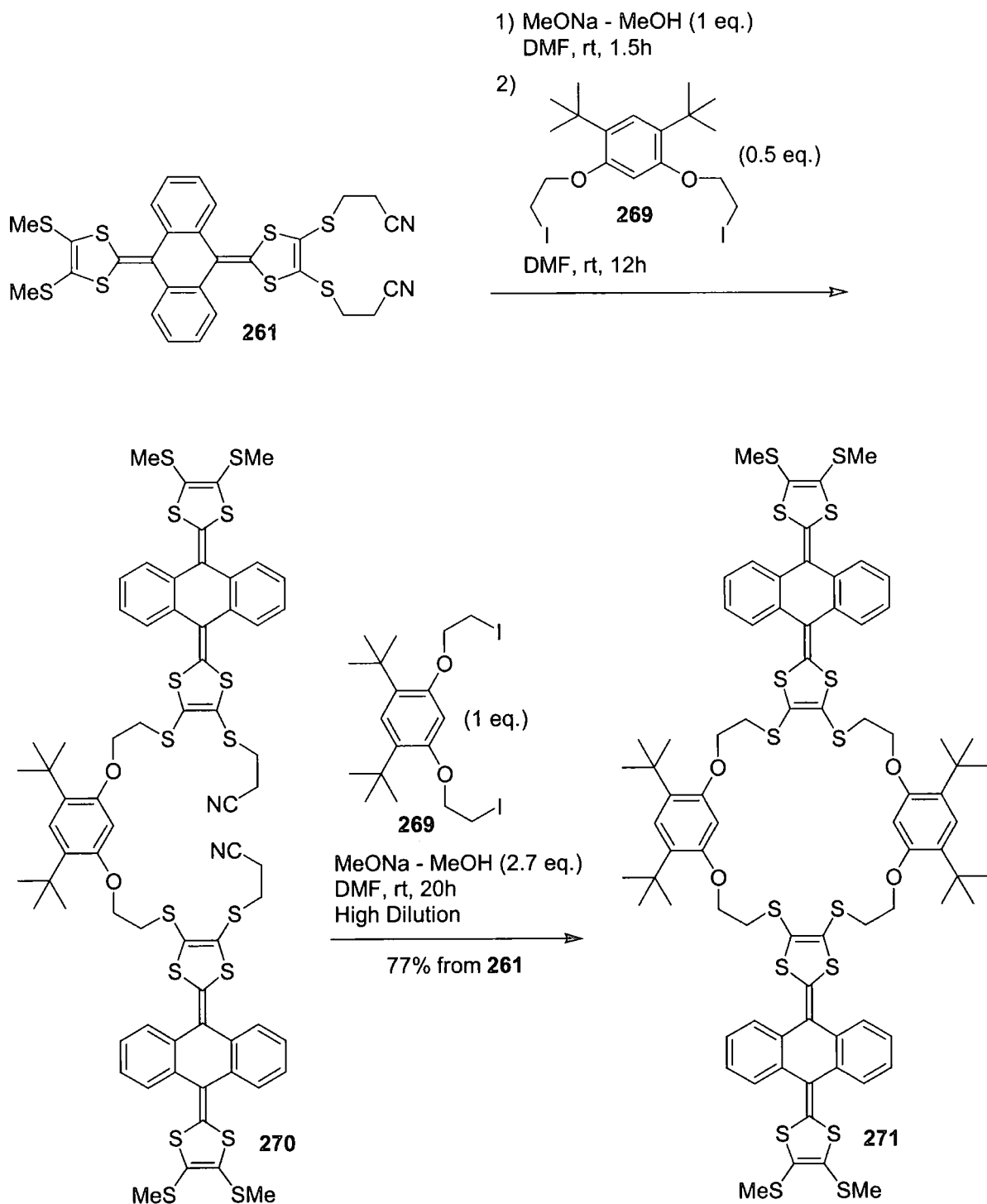
	266a	266b^a	266b^a	185
C(16)···C(19) / Å	7.27	7.27	7.32	7.06
C(17)···C(20) / Å	7.60	7.59	7.63	7.01
S(3)···S(7) / Å	8.13	8.13	8.16	-
S(4)···S(8) / Å	9.24	9.33	9.32	-
$\delta_1 / ^\circ$	23.3	22.0	26.2	29.4
$\delta_2 / ^\circ$	28.6	27.2	23.8	22.6
$\theta / ^\circ$	44.1	45.4	45.2	34.7
$\varphi / ^\circ$	41.7	40.3	39.8	43.4

Table 10: Molecular geometry. ^a Two independent molecules.

6.4.3 A one-pot synthesis of a novel dimeric TTFAQ cyclophane

Dimeric TTFAQ cyclophane **268** was synthesised in only 16% yield as a by-product in the synthesis of cyclophane **266** (Scheme 62). We thought it should be possible to synthesise similar structures using TTFAQ building block **261**. The strategy applied has been used by Becher *et al.* to synthesise a wide range of TTF cyclophanes (see examples Figure 9).³³⁻³⁶ The synthesis benefits greatly from the sequential deprotection of **261**, which was demonstrated in the synthesis of compound **262** (Scheme 60). Since the reaction of TTFAQ thiolates with good electrophiles are quantitative, they are ideal for the performance of a series of reactions all in one pot. Thus **261** was monodeprotected using 1 equivalent of sodium methoxide followed by reaction with ½ equivalent of the linker **269**. To ensure complete reaction, the mixture was left overnight, whereupon inspection by TLC revealed formation of only one product. Confident the formed product was **270**, the reaction was not worked up at this stage, but rather the next synthetic step was carried out. A second portion of linker **269** was added to the reaction mixture, which was then reacted with a solution of sodium methoxide under high

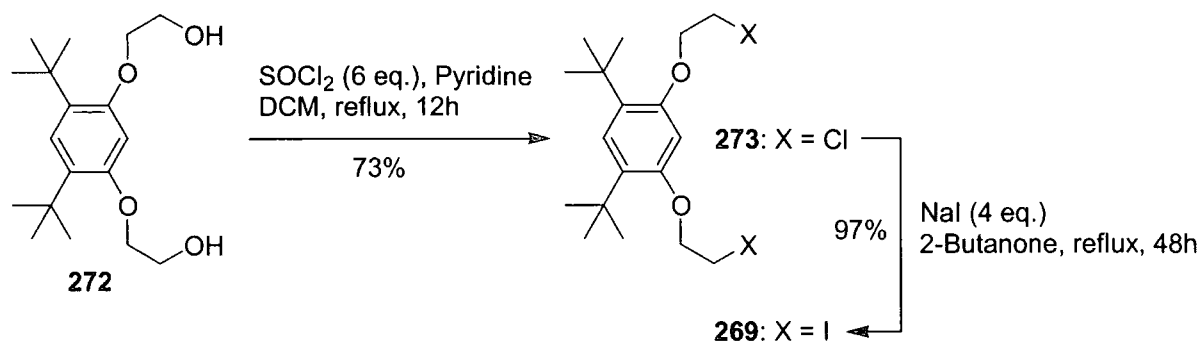
dilution conditions. This afforded dimeric TTFAQ cyclophane **271** in 77% yield, which is remarkably high for a one-pot synthesis of a macrocycle in which 4 bonds are formed.



Scheme 63: Synthesis of dimeric TTFAQ cyclophane **271** in a one-pot synthesis.

The linker was not only chosen because of its very reactive iodides, but also since its two *tert*-butyl groups should ensure good solubility of the cyclophane. Insolubility of these

products is known to be a problem, but the corresponding bromide linker had been used previously by Becher and co-workers for the synthesis of TTF cyclophanes **32j** and **38b**.^{36,46} Linker **272**¹⁸³ was chlorinated to give **273**, using thionyl chloride, and a subsequent Finkelstein reaction afforded the linker **269** in good yield (Scheme 64).



Scheme 64: Halogenation of linker **272** to form first the dichloride **273** and finally diiodide **269**.

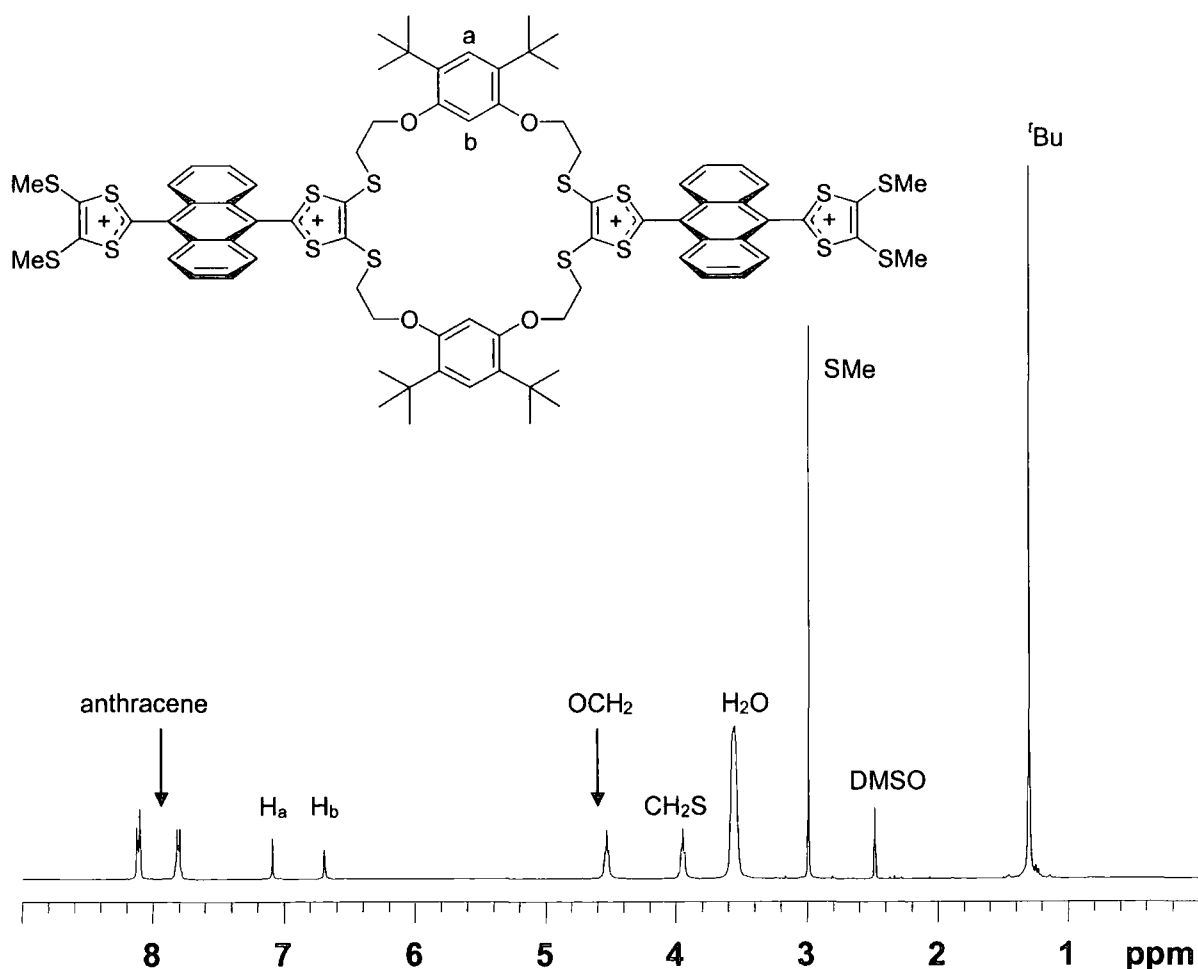
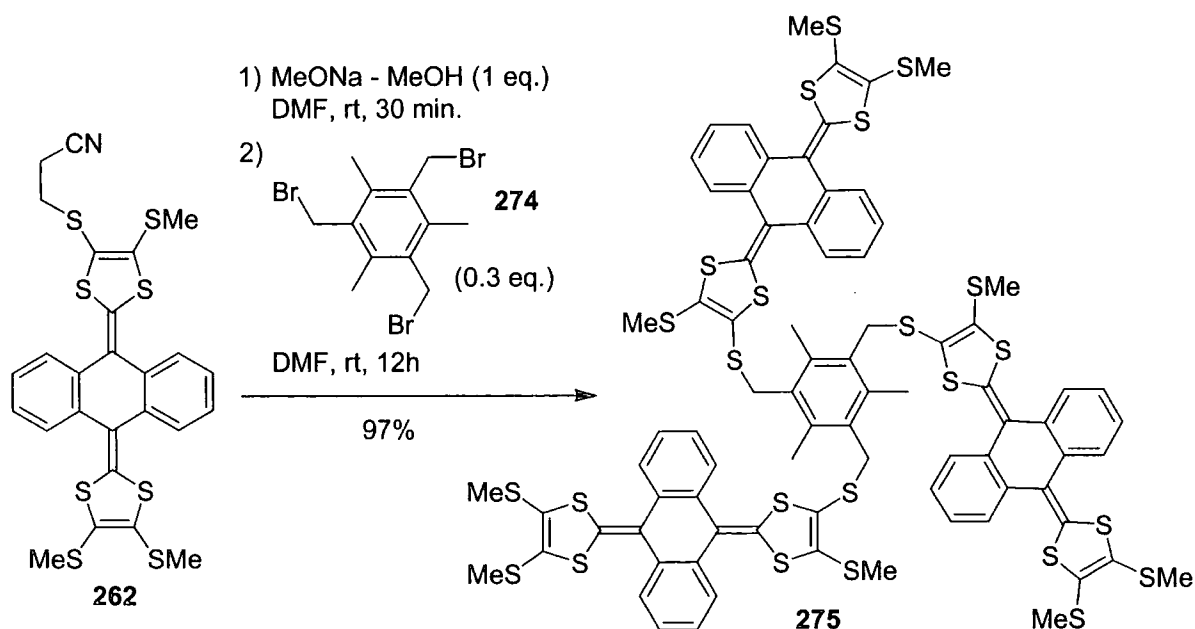


Figure 84: The ^1H NMR spectrum (at 500 MHz in $\text{DMSO-}d_6$) of the tetracation of dimeric TTFAQ cyclophane **271** was very simple due to the symmetry gained upon the oxidation of the TTFAQ moieties.

In spite of the four *tert*-butyl groups, characterisation of cyclophane **271** was troublesome due to low solubility. Elemental analysis and a mass spectrum confirmed the structure of **271**, but the ^1H NMR spectrum was rather weak and further complicated by the ability of **271** to adopt two different conformations. As for conjugated TTFAQ dimer **143** (Scheme 25), cyclophane **271** possesses two TTFAQ moieties locked in positions relative to each other. This leads to two different conformers, even though **271** is made of symmetric building blocks. In one conformer each TTFAQ moiety is flipped up ([up, up] = [down, down]) and in the other conformer one TTFAQ moiety is flipped up and the other flipped down ([up, down] = [down, up]). The solution was to oxidise **271**, using iodine, as for the conjugated dimer **143** (section 3.5.3). This had the added benefit of increasing the strength of the NMR signal, due to the good solubility of $\mathbf{271}^{4+}$ in dimethylsulfoxide. The ^1H NMR spectrum (Figure 84) reflects the high symmetry of $\mathbf{271}^{4+}$ consisting of planar symmetric moieties. None of the peaks is broadened or split, which was the case for the weak spectrum of the neutral molecule. Hence the structure of **271** was also confirmed by ^1H NMR spectroscopy.

6.4.4 Synthesis of a TTFAQ trimer - towards novel TTFAQ dendrimers

The final example is the use of **262** to form the TTFAQ trimer **275** (Scheme 65). Our group has recently published the synthesis of the first dendrimers incorporating TTFAQ units,¹⁶¹ placed at the periphery of a dendritic aryl system, using the hydroxymethyl derivative **53** (Figure 24).



Scheme 65: Synthesis of TTFAQ trimer **275** in high yield from building block **262**.

Earlier we had successfully synthesised TTF dendrimers using TTF building blocks like **237** (Scheme 50), and compound **274** proved perfect as a very reactive dendrimer core.¹⁷⁰ In the TTF series, the first test reaction, prior to the synthesis of a TTF₂₁ dendrimer,^{170c} was the formation of a trimer using core reagent **274**. Hence, TTFAQ **262** was tested for its potential use in the synthesis of TTFAQ dendrimers. A small excess of the thiolate, generated by the deprotection of **262** using 1 equivalent of sodium methoxide, easily displaced the benzylic bromides of **274**, to furnish the TTFAQ trimer **275** in near quantitative yield. The solubility of **275** was low, but the compound was fully characterised and thus this work paves the way for the synthesis of a new series of dendritic macromolecules incorporating the TTFAQ unit.

6.5 SOLUTION ELECTROCHEMICAL PROPERTIES

Cyclic voltammetry was performed for all the new TTFAQ derivatives, and their oxidation potentials are collated in Table 11.

Compound	E_{pa}^{ox}/V	E_{pc}^{ox}/V	$\Delta E/V^a$
258	0.66	0.54	0.12
259	0.61	0.45	0.16
261	0.60	0.50	0.10
262	0.57	0.44	0.13
265	0.54	0.43	0.11
266	0.90	0.84	0.06
268	0.59	0.41	0.18
271	0.60	0.42	0.18
275	0.55	0.45	0.10
54	0.55	0.43	0.12

Table 11: Cyclic Voltammetric Data vs. Ag/AgCl. Compound *ca.* 1×10^{-3} M and electrolyte 0.1 M Bu₄NPF₆ in dichloromethane, 20 °C, scan rate 100 mV s⁻¹. ^a $\Delta E = E_{pa}^{ox} - E_{pc}^{ox}$.¹²⁹

As expected for tetrakis(alkylthio) substituted TTFAQ derivatives, the oxidation potentials are raised relative to unsubstituted TTFAQ.⁶⁴ Also, for the cyanoethyl bearing derivatives, an additive effect of *ca.* 30 mV for each cyanoethyl group seems to be the case. Thus,

tetrakis(2-cyanoethylthio)TTFAQ **258**, bissubstituted derivatives **259** and **261**, monosubstituted derivative **262** and tetrakis(methylthio)TTFAQ **54** have oxidation potentials E_{pa}^{ox} of 0.66, 0.60, 0.57 and 0.55 V, respectively. However, the most interesting CV data was obtained for TTFAQ cyclophane **266**. The cyclic voltammogram of cyclophane **266** showed the single two-electron oxidation wave to be considerably anodically shifted; 290 mV compared to its precursor **259** (Figure 85) and 350 mV compared to tetrakis(methylthio)-TTFAQ **54**. These are similar shifts to those found for the short-bridged TTFAQ cyclophanes **185** and **186** reported by Finn and Godbert *et al*, respectively,^{143,145} and can be explained by the obstruction of the marked conformational change, which accompanies oxidation, and the destabilisation of the dication imposed by the short bridge. Consistent with this, ΔE for **266** is only 60 mV, and thereby significantly reduced compared to the typical values for TTFAQ derivatives (see Table 11), but in agreement with data for cyclophanes **185** and **186**.^{143,145} Again, this increased reversibility of the oxidation process must be due to the conformation of the cyclophane dication **266**²⁺, which should be closer to the saddle-shape than non-bridged TTFAQ dications, and thus only a small overpotential is needed for the reduction back to the neutral state. However, we still had not synthesised a TTFAQ cyclophane where the cation radical state was stabilised enough for it to be visible in the cyclic voltammogram.

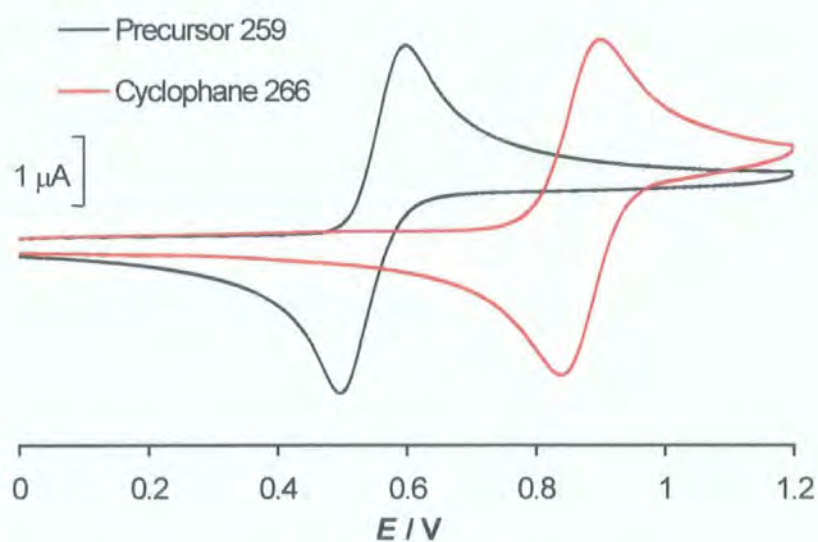


Figure 85: Cyclic voltammograms of **266** and its precursor **259**. Conditions are given in Table 11.

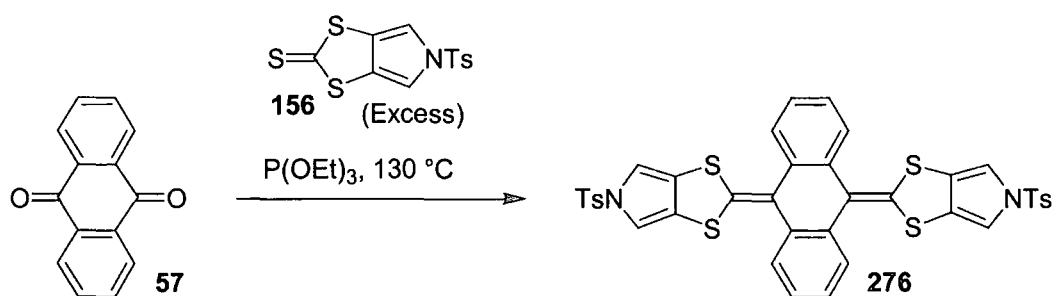
The CV of dimeric cyclophane **268** was similar to typical cyclic voltammograms of non-bridged tetrakis(alkylthio)TTFAQ derivatives, *e.g.* its precursor **259** (Figure 85), thus this was the first evidence that **268** was indeed a non-strained TTFAQ derivative and *not* the *trans*-

bridged analogue of cyclophane **266**. The other oligo TTFAQ derivatives (**271** and **275**), like dimeric cyclophane **268**, showed only a single, quasi-reversible, oxidation wave at typical oxidation potentials. Thus no intramolecular electronic interaction was observed in the cyclic voltammograms of oligo TTFAQ systems **268**, **271** and **275**.

The UV-vis absorption spectra of the alkylthio substituted TTFAQ derivatives presented in this chapter showed two strong absorption bands characteristic of TTFAQ. Only the spectrum of strained cyclophane **266** deserves further comments and will be discussed in section 7.3.1.

6.6 FUTURE PROJECTS

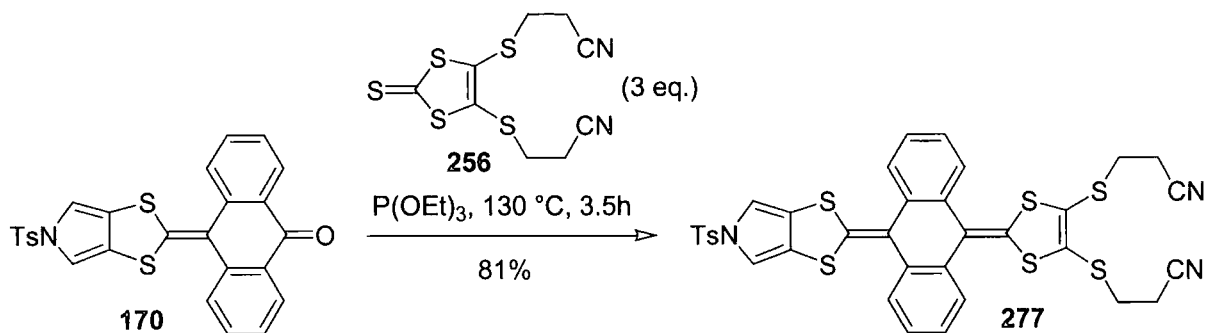
The first future project would be to solve the problems encountered in the attempted synthesis of bispyrrolo-annelated TTFAQ derivative **158** (Scheme 29, Chapter 4) arising from the failure to synthesise a phosphonate ester reagent containing the pyrrole moiety. However, applying the phosphite mediated cross-coupling reaction between 1,3-dithiole-2-thione **156**¹³¹ and anthraquinone **57** should afford bispyrrolo-TTFAQ derivative **276** (Scheme 66). Detosylation of **276** using standard conditions should afford the desired unsubstituted bispyrrolo-TTFAQ **158** and hence a new range of TTFAQ cyclophanes **157** should be within reach (Scheme 29).



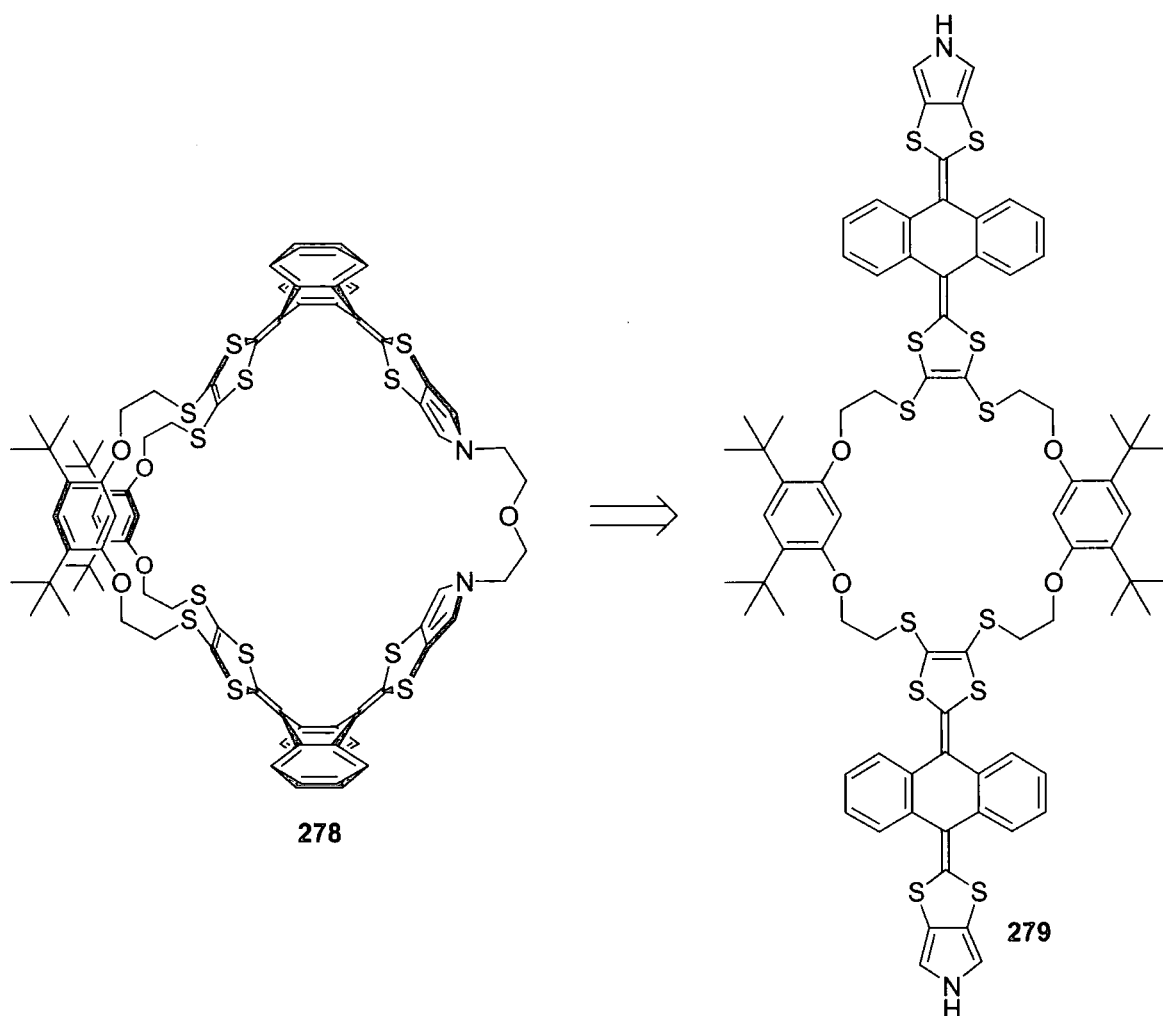
Scheme 66: It should be possible to synthesise the bispyrrolo-TTFAQ derivative **276** by a phosphite coupling between anthraquinone **57** and pyrrolo-annelated thione **156**.

Pyrrolo-TTFAQ building block **277** would supplement **258**, **259**, **261** and **262** presented above. Indeed, slow addition of 3 equivalents of thione **256** to a heated solution of ketone **170** in triethyl phosphite afforded the pyrrolo-annelated TTFAQ derivative **277** in 81% yield (Scheme 67), which makes **170** the most reactive ketone used in the phosphite coupling reactions. This could be explained by the strongly electron withdrawing tosyl group, which

was also reflected in the oxidation potentials of the tosylated pyrrolo-TTFAQ derivatives presented in Chapter 4 (Table 3).



Scheme 67: The TTFAQ building block 277, possessing both a protected pyrrole moiety and two cyanoethyl protected thiolates, could be synthesised in high yield from ketone 170 and thione 256 in a phosphite mediated cross-coupling reaction.



Scheme 68: Dimeric pyrrolo-TTFAQ cyclophane 278 should be available *via* the intermediate 279 from the new building block 277.

With pyrrolo-TTFAQ derivative **277** in our possession, a range of interesting TTFAQ cyclophanes should be accessible. Following the strategy of Becher *et al.* for the synthesis of triple-bridged pyrrolo-TTF cyclophane **148** (Scheme 26),¹³³ could lead to dimeric pyrrolo-TTFAQ cyclophanes like **278** (Scheme 68). It should be noted that one of the intermediates in the synthesis of **278** from building block **277**, is double-bridged dimeric TTFAQ cyclophane **279**, similar to the cyclophane **271** which was described above (Scheme 63). Thus, the synthesis of **278** looks like a promising project.

6.7 CONCLUSIONS

By expanding the well-known phosphite mediated coupling reaction, used for the synthesis of TTF derivatives, to also include cross-couplings of 1,3-dithiole-2-thiones with anthraquinone, a new route to highly functionalised TTFAQ derivatives has been developed. This new methodology not only allows the synthesis of TTFAQ derivatives possessing functional groups which would never survive the Horner-Wadsworth-Emmons reaction, but also cuts the classic five-step synthesis of TTFAQ derivatives from 1,3-dithiole-2-thiones bearing electron withdrawing groups, down to a single step. A complete set of TTFAQ building blocks, possessing one or more cyanoethyl protected thiolates, was successfully synthesised using the phosphite coupling reaction. The equivalent TTF derivatives have in less than 10 years from their discovery afforded more than 60 publications presenting novel macromolecular and supramolecular assemblies incorporating TTF, structures which could otherwise not have been synthesised. Thus, the synthesis of **258**, **259**, **261** and **262** should likewise revolutionise the incorporation of TTFAQ moieties into large structurally challenging assemblies. Indeed, 4 examples showing their versatility afforded a novel TTFAQ derivative for the study of hydrogen bonding in the solid state **265**, a highly efficient synthesis of a single-bridged cyclophane **266**, a high-yielding one-pot synthesis of a dimeric TTFAQ cyclophane **271** and finally a trimer **275**.

7 MULTIPLE-BRIDGED TTFAQ CYCLOPHANES

This chapter describes the synthesis and solid state conformations of novel multiple-bridged TTFAQ cyclophanes, and explores their remarkable optical and electrochemical properties.

7.1 DOUBLE-BRIDGED TTFAQ CYCLOPHANES

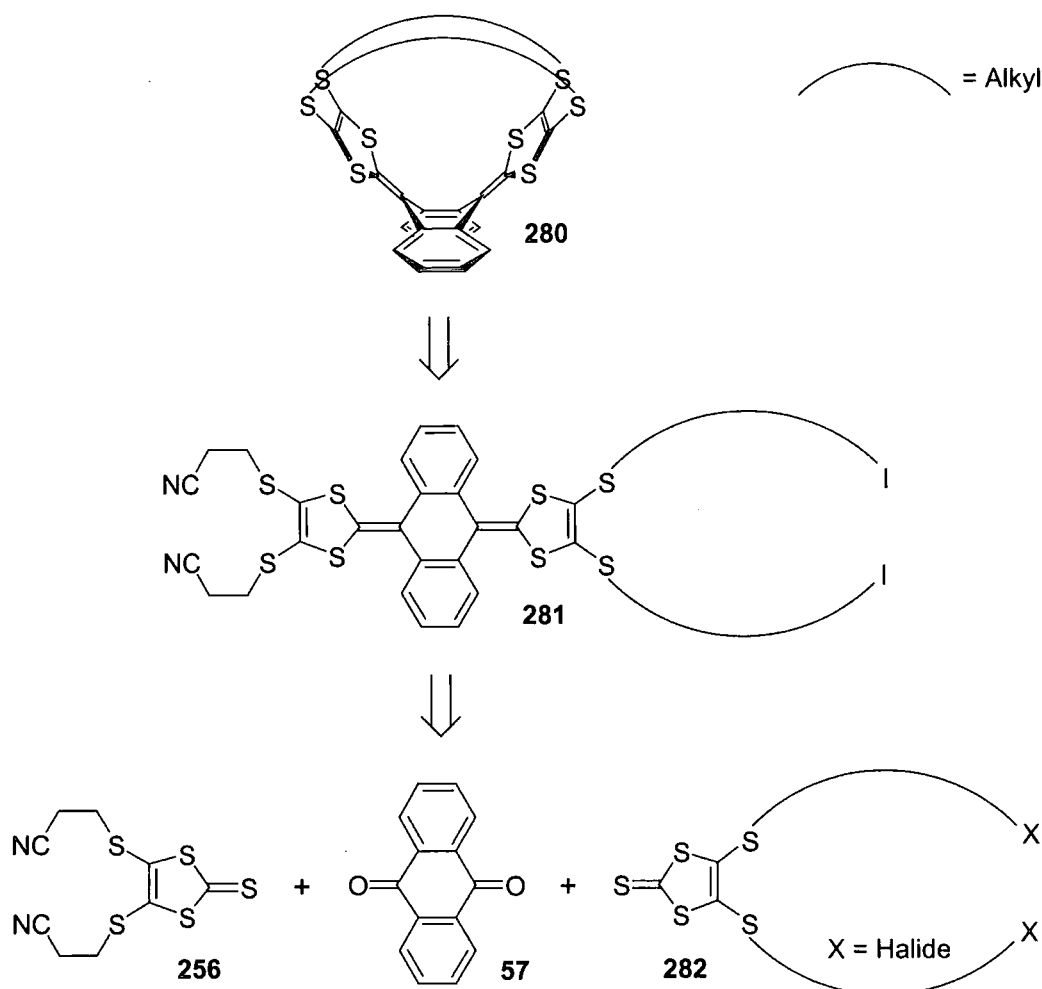
Encouraged by the efficient synthesis of **266** (Scheme 62) we decided to attempt double-bridging of the 1,3-dithiole rings of TTFAQ, something which hitherto had been impossible. This should provide rigid TTFAQ cyclophanes with unique electrochemical properties.

7.1.1 Background for bridging the 1,3-dithiole rings of TTFAQ

The first TTFAQ cyclophanes (see section 5.1) involved linking the 1,3-dithiole rings of TTFAQ with a single bridge.^{143,145} These derivatives were harder to oxidise and with increased reversibility, results which were confirmed by the electrochemical properties of cyclophane **266**, as discussed in section 6.5. The reason was strain imposed by the bridge, which obstructed the TTFAQ system from changing conformation and also destabilised the dication. However, we still had not synthesised a TTFAQ cyclophane for which the destabilisation of the dication was making the cation radical stable with respect to the dication. A considerable conformational change of the single-bridged TTFAQ cyclophanes still occurred upon oxidation,¹⁴⁵ so we were interested in synthesising even more strained and rigid TTFAQ cyclophanes, since gain of aromaticity upon oxidation for a conformationally locked TTFAQ moiety would be difficult, and thus the dication state would not be energetically favourable relative to the cation radical state. Ultimately, this could make the isolation of a TTFAQ cation radical salt possible. A TTFAQ cyclophane with two short bridges, both in a *cis* conformation, connecting the two 1,3-dithiole rings (**280**, Scheme 69), was our target. Unfortunately, the methodologies of both Finn *et al.*¹⁴³ and Godbert *et al.*¹⁴⁵ had proved unsuccessful in attempts to synthesise double-bridged TTFAQ cyclophanes, so a new strategy, based upon the synthesis of TTFAQ cyclophane **266** (Scheme 62), had to be developed.

7.1.2 Designing the synthesis

A possible precursor for the double-bridged TTFAQ cyclophane **280** was derivative **281** (Scheme 69). When deprotected under dilute conditions, the resulting thiolates should preferably displace the iodides intramolecularly to give **280**, thereby avoiding too much polymerisation by intermolecular reaction. Building block **281** should be available in three steps from the thiones **256**¹⁶⁴ and **282**, and anthraquinone **57**, using the two-step methodology for the synthesis of unsymmetrical TTFAQ derivatives by phosphite mediated cross-coupling reactions (see section 6.3.2). The third and final step would be a halogen exchange, since alkyl iodides are too reactive to survive a phosphite coupling (see the proposed mechanism, Scheme 54).



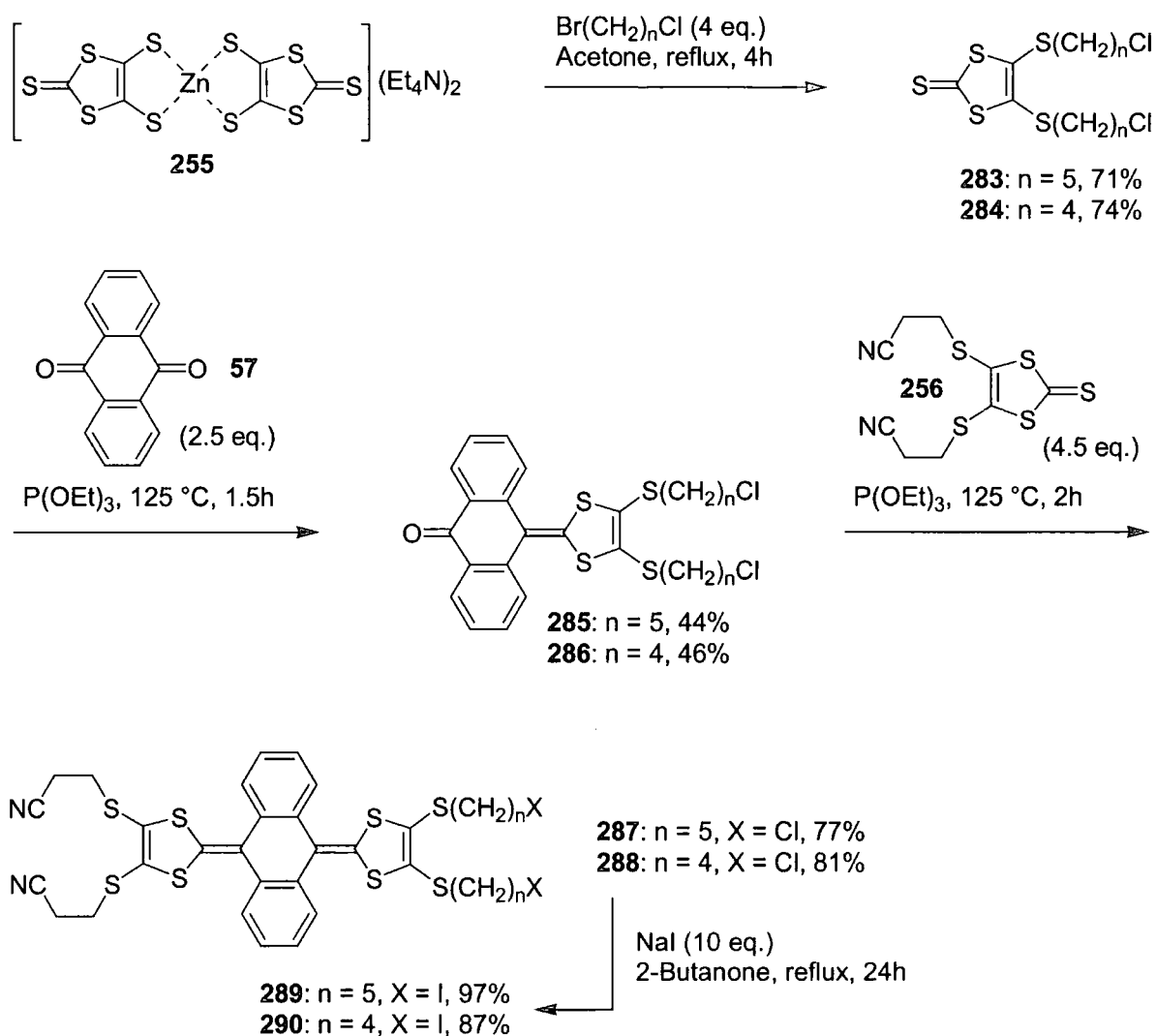
Scheme 69: Retro synthesis of double-bridged TTFAQ **280**.

In order to minimize the risk of *trans*-bridging, since this would block the possibility for the second bridge to be formed and hence cause polymerisation, and to get as strained a

cyclophane as possible, the shortest possible bridge was chosen. From the work of Finn *et al.*¹⁴³ and the synthesis of single-bridged cyclophane **266**, we learned that a pentamethylenedithio bridge was thus far the shortest possible and that no *trans*-bridged cyclophanes were formed using this bridge. Hence a pentamethylenedithio bridge was chosen.

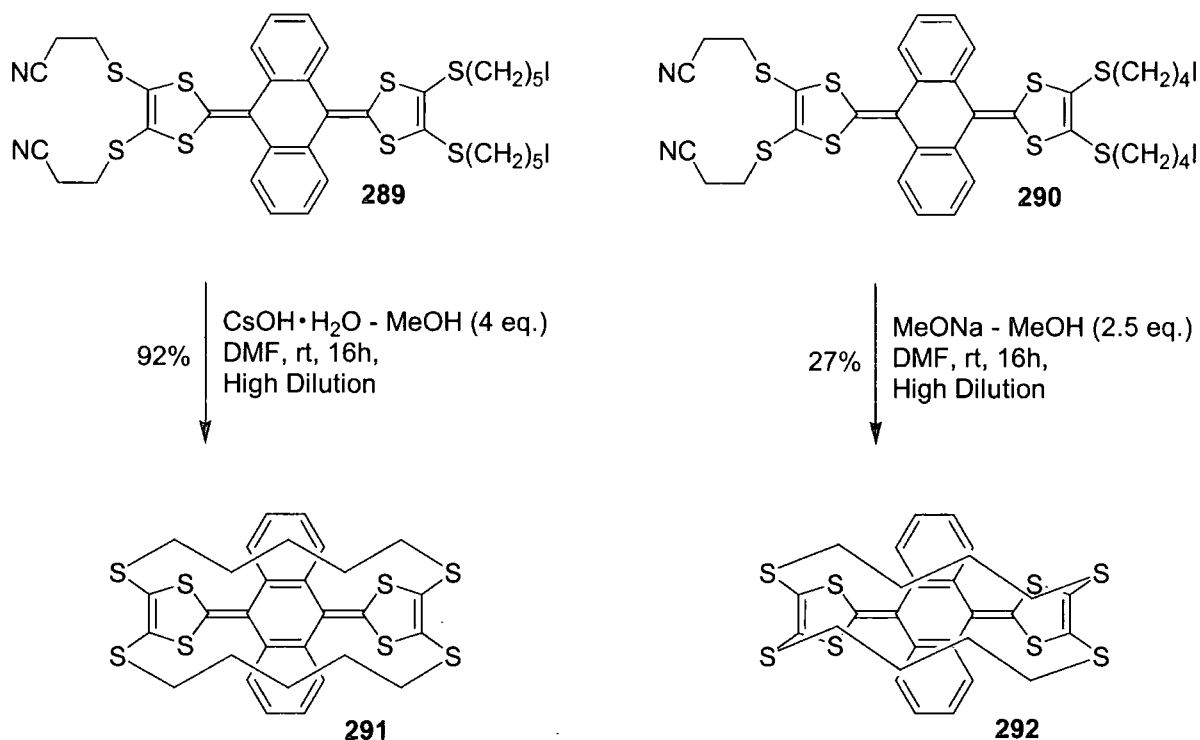
7.1.3 Synthesis of double-bridged TTFAQ cyclophanes

The dichloride thione **283** was almost the sole product when zincate **255**¹⁷⁸ was refluxed with 4 equivalents of 1-bromo-5-chloropentane as reported earlier by Takimiya *et al.*⁴⁰ Slow addition of **283** to an excess of anthraquinone **57** in triethyl phosphite at 125 °C afforded the ketone **285** in 44% yield.



Scheme 70: Synthesis of TTFAQ cyclophane building blocks **289** and **290**.

The second phosphite coupling yielded TTFAQ derivative **287**. After 4.5 equivalents of the thione **256**¹⁶⁴ had been added in small portions, 77% of the ketone **285** had been converted to **287**, and it was decided to stop the reaction. Finally a halogen exchange in refluxing 2-butanone afforded the diiodide **289**, in almost quantitative yield.



Scheme 71: Intramolecular reaction is favoured for the synthesis of **291** whilst the opposite is true for **292**.

The building block **289**, possessing both two protected thiolates and two alkyl iodides, was added slowly to a solution of 4 equivalents of cesium hydroxide monohydrate in *N,N*-dimethylformamide under high dilution conditions, to afford the desired doubled-bridged TTFAQ cyclophane **291** as tiny pale yellow crystals in 92% yield, which is remarkably efficient for a double macrocyclisation. Contrary to its precursors, which all possessed flexible alkyl chains, the solubility of the rigid cyclophane **291** in common organic solvents was relatively poor. However, the solubility was sufficient for NMR studies in CDCl_3 . From the ^{13}C NMR spectrum of the bulk product, it can be seen that the *cis/cis* isomer was the sole product. Only this isomer **291** possesses a symmetry high enough to afford the simple ^{13}C NMR spectrum shown in Figure 86. In total agreement with the structure of **291**, 9 different carbons (6 aromatic and 3 aliphatic) were observed. The X-ray crystal structure (see Figure 89) later confirmed the structure of **291**. The formation of only the *cis/cis* isomer can be explained not only by the careful choice of linkers, but also because the TTFAQ molecule

in solution is flipping between two conformations (see section 2.2.2), which presumably suppresses reaction from taking place *trans*, as discussed in section 6.4.2.

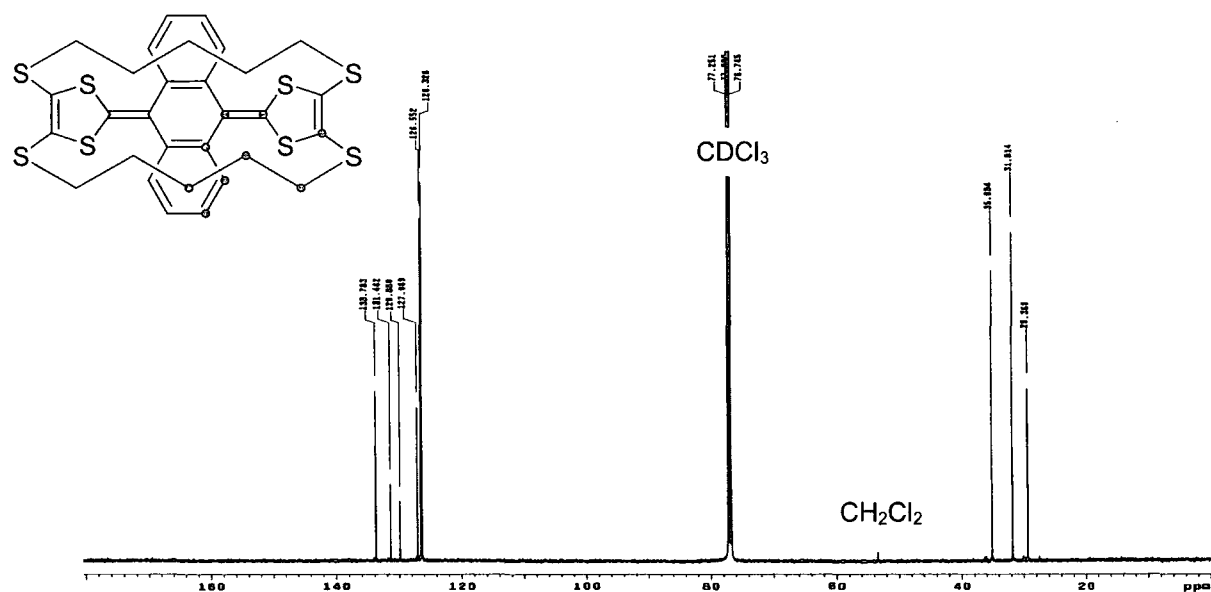


Figure 86: The ^{13}C NMR spectrum (at 100 MHz) of **291** is very simple due to the high symmetry of the double-bridged TTFAQ derivative. Only 6 aromatic and 3 aliphatic carbons are seen.

With the macrocyclisation to form **291** being so successful, it was obvious to try and shorten the linkers, and perhaps strain the molecule even more. Accordingly, thione **284**⁴⁰ was synthesised from zincate **255**¹⁷⁸ and 1-bromo-4-chloro-butane in 74% yield. The two phosphite couplings to give first ketone **286** and then TTFAQ derivative **288** were carried out as for the synthesis of **287** and in approximately the same yields. Finally, **288** was converted to building block **290**. The first attempt at synthesising cyclophane **292** was carried out exactly as the synthesis of **291**, but the result was very different. During workup an insoluble yellow powder, believed to be polymerised **290**, was removed by filtration, and after purification by column chromatography, only 16% of the cyclophane **292** was obtained. It seemed therefore, that due to ring strain the intermolecular reaction (polymerisation) was now favoured, whereas for the pentamethylenedithio bridge intramolecular reaction (macro-cyclisation) took place almost exclusively. A second synthesis, under even more dilute conditions, was carried out. Instead of adding the precursor **290** slowly to a dilute solution of excess base, a solution of **290** and a solution of 2.5 equivalents of sodium methoxide in methanol and *N,N*-dimethylformamide was added simultaneously to stirred *N,N*-dimethylformamide over 16 h. Again a considerable amount of insoluble yellow powder was filtered off, but the yield of **292** was increased to 27% (Scheme 71).

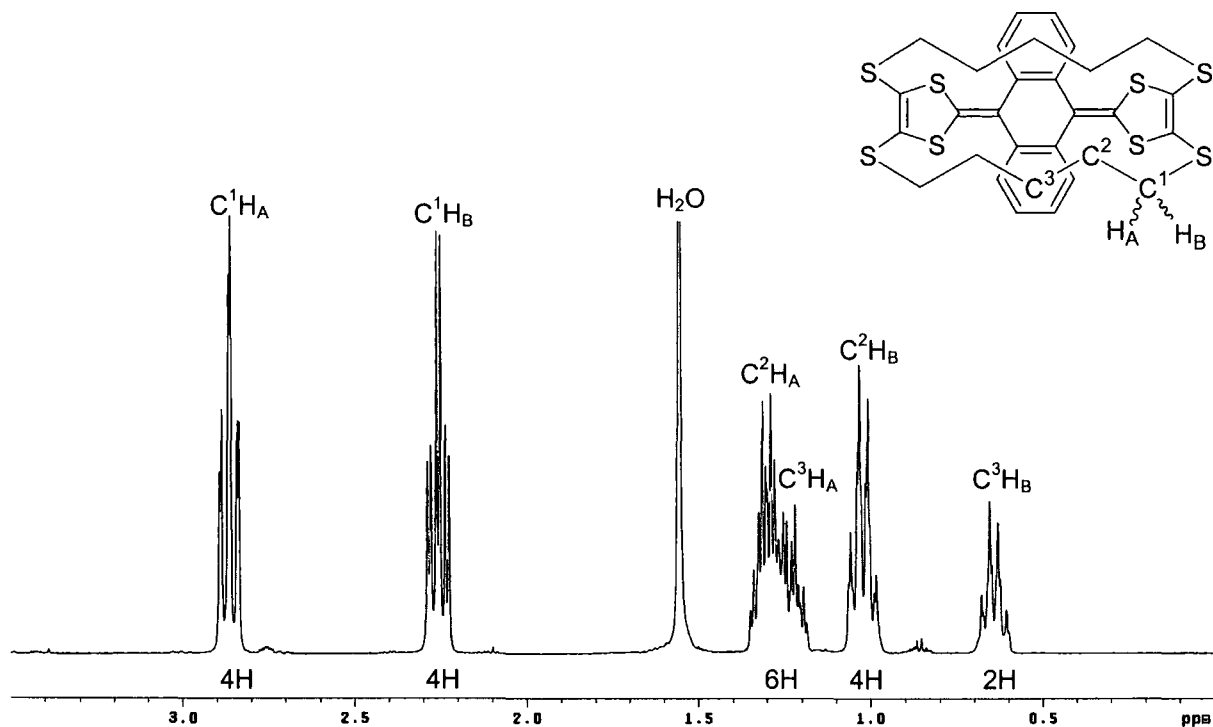


Figure 87: The low frequency (*i.e.* high-field) part of the ^1H NMR spectrum (at 400 MHz) of cyclophane 291. Differences in chemical shift for methylene protons $\Delta\delta(\text{H}_\text{A}\text{H}_\text{B})$: 0.60 ppm, 0.28 ppm and 0.58 ppm for C^1 , C^2 and C^3 , respectively.

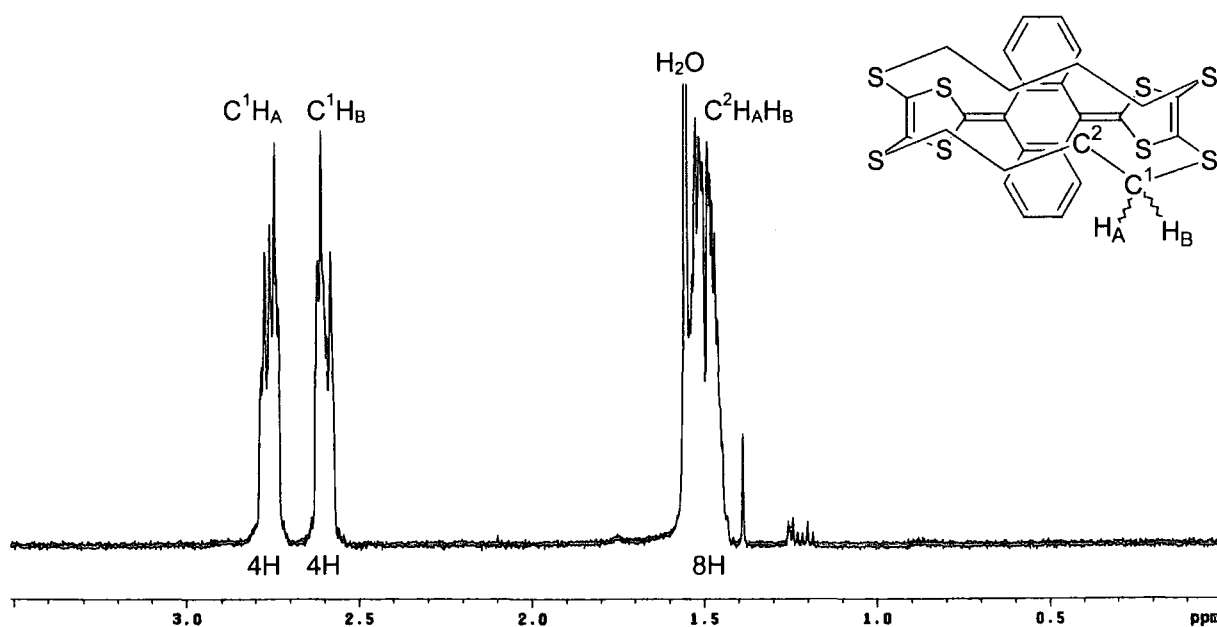


Figure 88: The low frequency part of the ^1H NMR spectrum (at 400 MHz) of cyclophane 292. Differences in chemical shift for methylene protons $\Delta\delta(\text{H}_\text{A}\text{H}_\text{B})$: 0.16 ppm and 0.04 ppm for C^1 and C^2 , respectively.

As for cyclophane **291**, a very simple ^{13}C NMR spectrum together with the mass spectrum was convincing evidence for the formation of **292**. However, the ^1H NMR spectra of the two double-bridged cyclophanes deserve some comment. The ^1H NMR spectrum of **291** was the first sign that a new rigid structure had been formed. All the methylene groups have sets of diastereotopic protons H_A and H_B (Figure 87) and the difference in chemical shift $\Delta\delta(\text{H}_\text{A}\text{H}_\text{B})$ is large. For **291** $\Delta\delta(\text{H}_\text{A}\text{H}_\text{B})$: 0.60 ppm, 0.28 ppm and 0.58 ppm for the three different methylene groups. In contrast, for its non-bridged precursors **287** and **289**, the difference in chemical shift $\Delta\delta(\text{H}_\text{A}\text{H}_\text{B})$ is *ca.* 0.10 ppm, and only for the protons α to the sulfur of the alkylsulfanyl substituents on the 1,3-dithiole rings of the TTFAQ moiety. However, one has to be careful to take the difference in chemical shift as a measure of the strain and rigidity in the system. Bigger $\Delta\delta(\text{H}_\text{A}\text{H}_\text{B})$ values do not correlate with a more strained system in this series. For cyclophane **292**, which is the most strained TTFAQ derivative ever synthesised, $\Delta\delta(\text{H}_\text{A}\text{H}_\text{B})$ are 0.16 ppm and 0.04 ppm for the two different methylene groups (Figure 88).

7.1.4 X-ray crystallographic analysis of cyclophanes **291** and **292**

Crystals of pentamethylenedithio double-bridged TTFAQ **291**, suitable for X-ray crystallographic analysis, were readily grown by slow diffusion of hexane into a solution of **291** in toluene. Three different kinds of crystals were obtained, but only two of them could be solved. X-ray quality crystals of cyclophane **292** were also obtained.

	291	291 · C_7H_8	292
φ	40.2	40.8	43.4
δ_1	18.4	30.2	30.6
δ_2	18.3	30.9	28.7
θ	42.9	33.0	4.8

Table 12: Dihedral angles (deg) in the cyclophanes. The angles are defined in the text.

In the structure of the cyclophanes **291** (Figure 89) and **292** (Figure 90), the usual saddle-like conformation of TTFAQ is aggravated by the short bridges between the dithiole rings. A good measure of the overall bending is the angle (θ) between the planar $\text{S}(1)\text{C}(16)\text{C}(17)\text{S}(2)$ and $\text{S}(5)\text{C}(19)\text{C}(20)\text{S}(6)$ moieties (the dihedral angles of the TTFAQ moiety in the cyclophanes

291 and **292** are collated in Table 12). In non-bridged TTFAQ systems (θ) ranges from 73° to 101° ,^{66,73,94} one hexamethylenedithio bridge (cyclophane **184**)¹⁴³ reduces it to 46 – 54° and one pentamethylenedithio bridge (cyclophanes **185** and **266**, see section 6.4.2) to 35 – 45° . The second pentamethylenedithio bridge in **291** adds little to the strain, but the two tetramethylenedithio bridges in **292** make these peripheral moieties of the TTFAQ unit nearly coplanar. On the other hand, folding (ϕ) of the anthracene system along the C(9)–C(10) vector does not exceed the range observed in unconstrained TTFAQ derivatives (35 – 45°),^{66,73,94} and the overall bending (θ) in **292** is enhanced mainly by stronger folding (δ) of both dithiole rings along the S–S vectors.

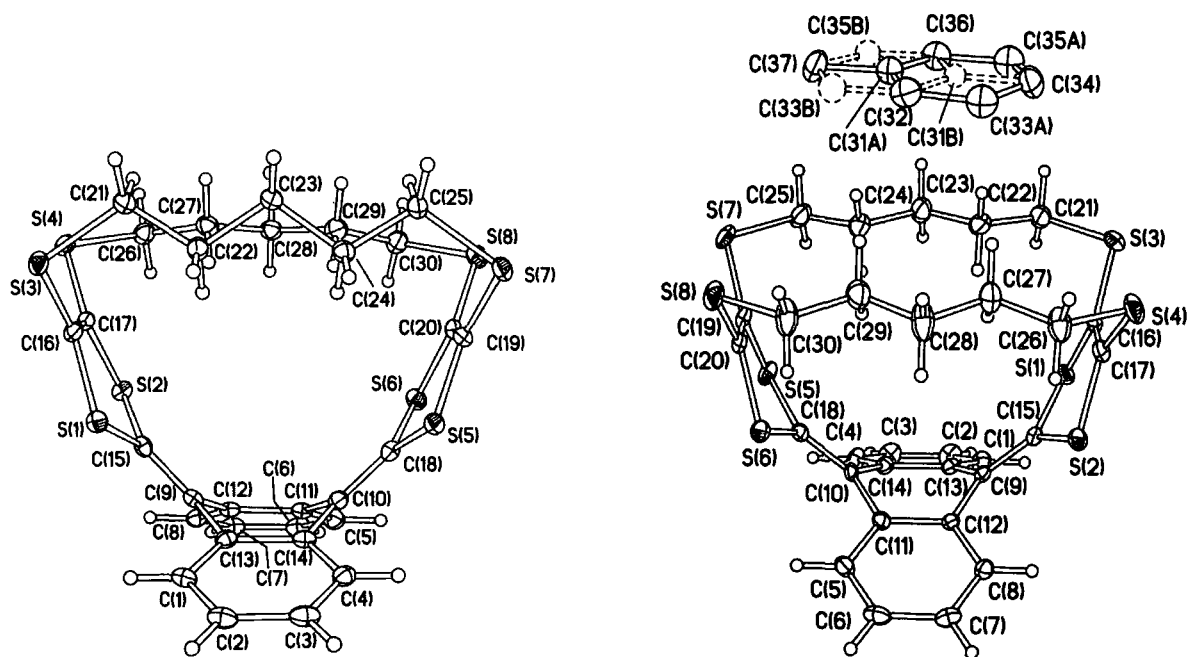


Figure 89: The X-ray crystal structures of the pentamethylenedithio double-bridged TTFAQ **291**. Both crystals of unsolvated **291** (left) and the solvate **291**·C₇H₈ (right) was solved. The toluene molecule in **291**·C₇H₈ is disordered between overlapping positions A (58%) and B (42%).

The TTFAQ moiety has local C_{2v} symmetry in both **291** and **291**·C₇H₈. The pentamethylene chains all adopt practically planar all-*trans* conformations (see Figure 91 for a different view of the structure of **291**, **291**·C₇H₈ and **292**). However, in the solvent-free crystal of **291**, the mean planes of the two bridges are nearly perpendicular (86°), inclined differently (by 18° and 76°) to the TTFAQ mirror plane which passes through the C(9), C(10), C(15) and C(18) atoms. In **291**·C₇H₈ both bridges are nearly perpendicular to this mirror plane (78 – 86°) and conform approximately to the molecular C_{2v} symmetry. The change of conformation from **291** to **291**·C₇H₈ is obviously effected by the contact with the planar toluene molecule, but it results in a substantial increase of molecular bending. This shows that in spite of the strain,

the TTFAQ unit in **291** still possesses such flexibility, that its conformation can be affected by the demands of crystal packing. In **292** both bridges have more strained conformations and the approximate molecular symmetry is reduced to C_2 , with an appreciable (chiral) twist of the TTFAQ moiety itself.

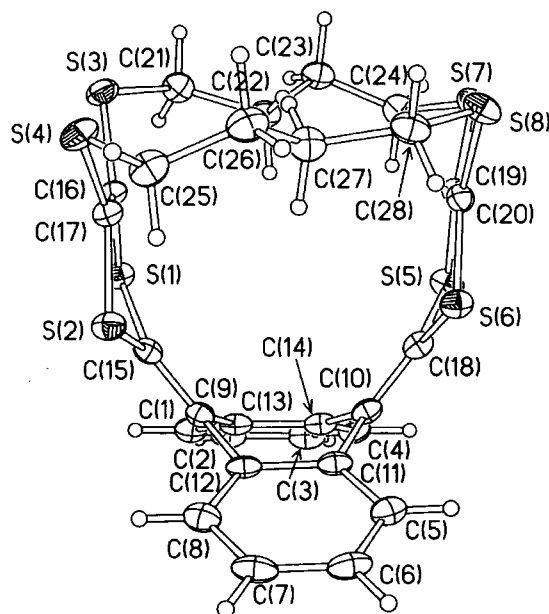


Figure 90: The X-ray crystal structure of the tetramethylenedithio double-bridged TTFAQ **292**.

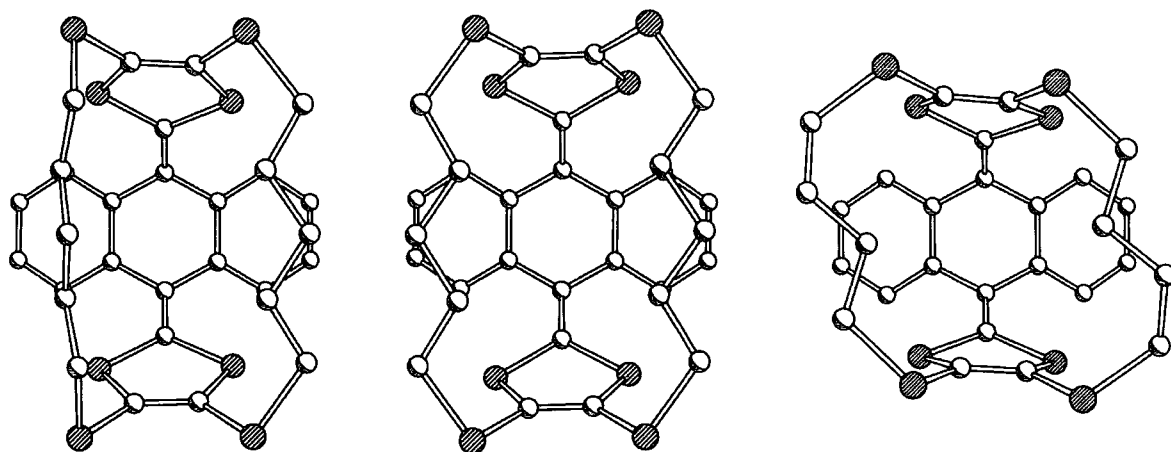


Figure 91: The X-ray crystal structures of **291**, solvated **291** and **292**; projections on the C(11)C(12)C(13)C(14) planes. Solvents have been removed for clarity.

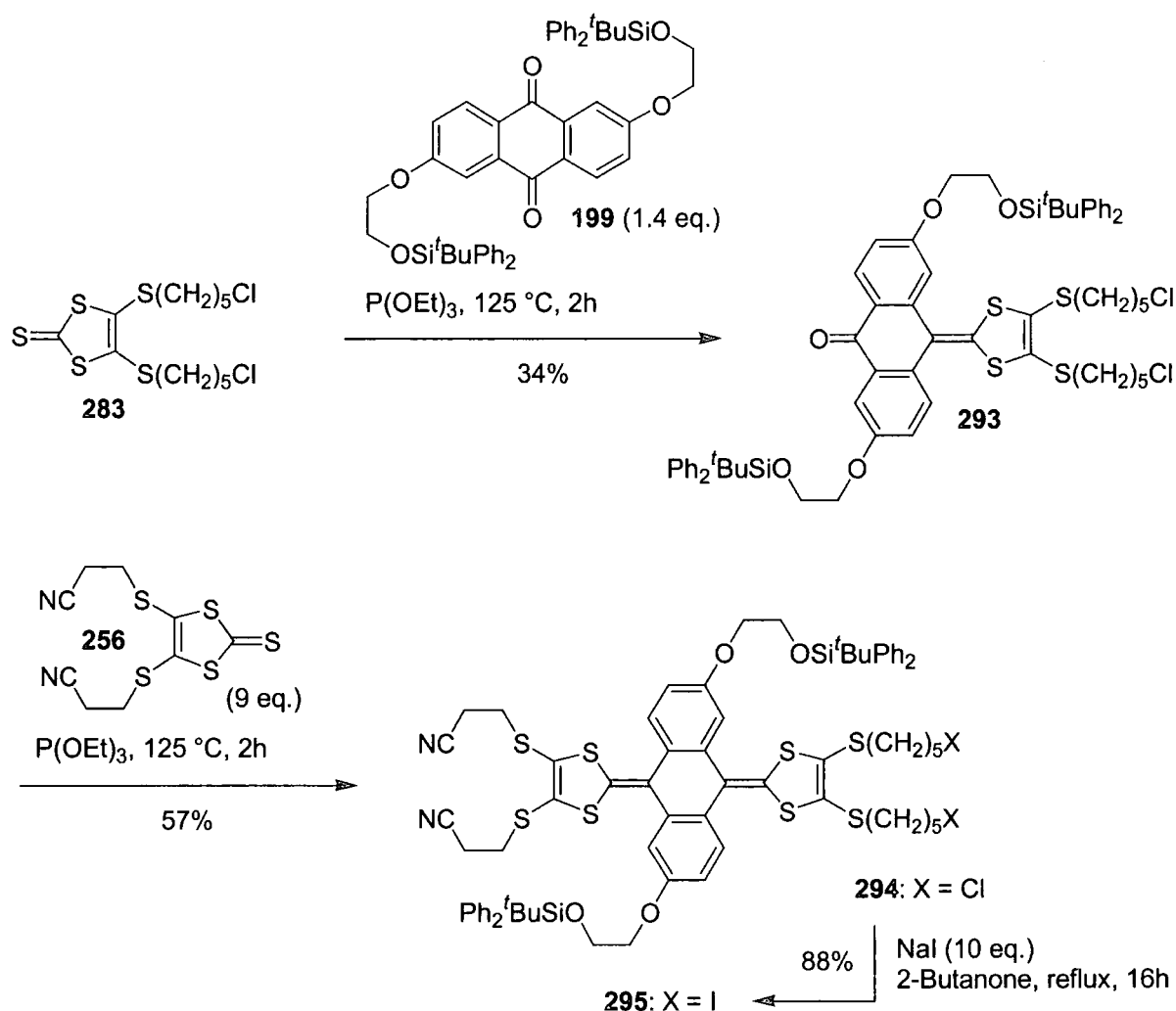
7.2 TRIPLE-BRIDGED TTFAQ CYCLOPHANES

The high yielding synthesis of double-bridged cyclophane **291** opened up the possibility to fulfil our dream of triply bridging the TTFAQ system, by combining the methodology used in

Chapter 5 with the methodology developed for the double-bridged cyclophanes. For this we needed to synthesise a pentamethylenedithio double-bridged TTFAQ cyclophane with protected alcohol linkers in the 2- and 6-positions.

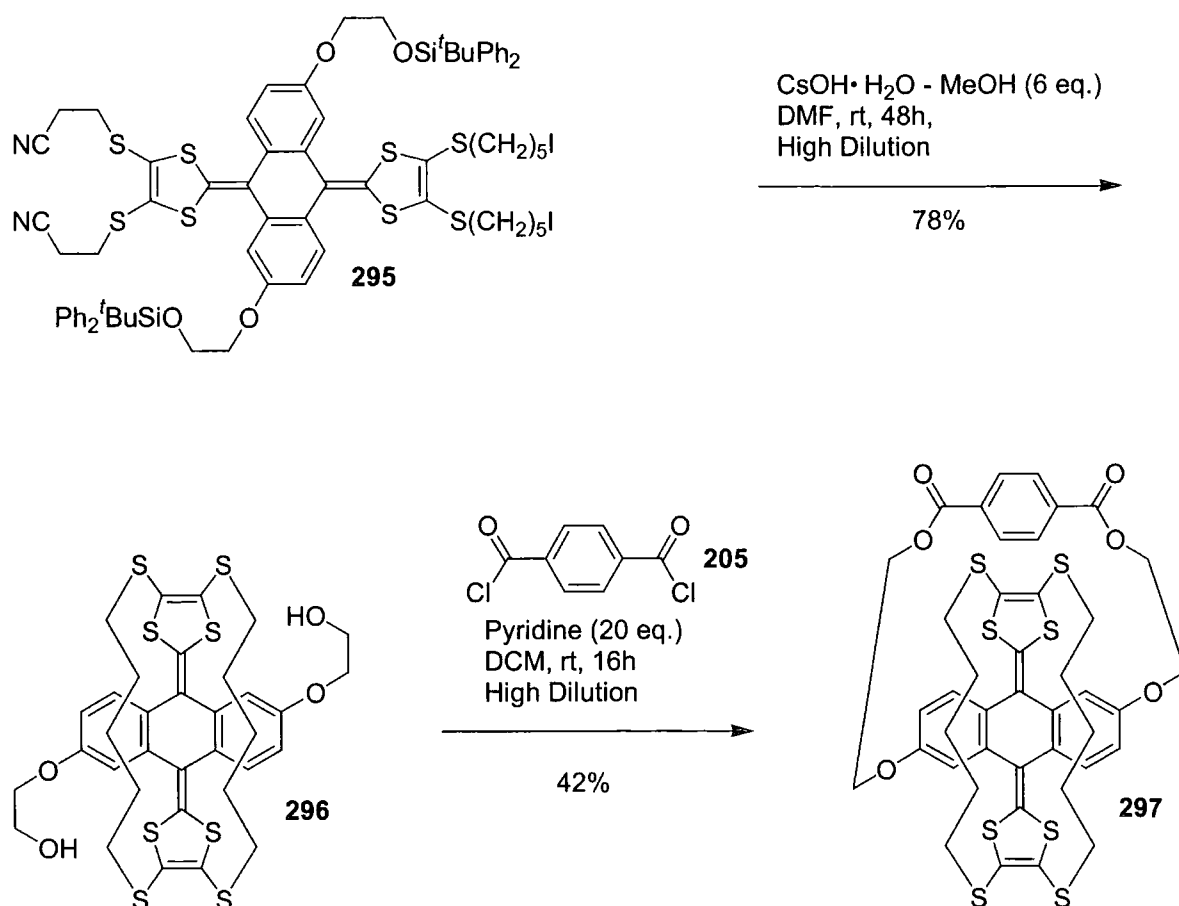
7.2.1 Synthesis of a triple-bridged TTFAQ cyclophane

First anthraquinone derivative **199** was coupled with the thione **283**. The thione was added in small portions to a solution of **199** in triethyl phosphite stirring at 125 °C. After 0.4 equivalents of **283** had been added, TLC showed that only very little of the ketone **293** had formed, and a lot of the symmetric TTF by-product was present in the reaction mixture. Thus another 0.3 equivalents of **283** were added, before the reaction was worked up, and the ketone **293** was isolated in only 34% from **283**.



Scheme 72: Synthesis of the highly functionalised TTFAQ building block **295**.

It was apparent that the anthraquinone derivative **199** is less reactive than anthraquinone itself. This was confirmed in the second phosphite coupling. As much as 9 equivalents of the thione **256** had to be added to yield 57% of the TTFAQ derivative **294**. In the similar reactions to form **287** and **288** (Scheme 70), only 4.5 equivalents of **256** was needed to yield 77% and 81% of **287** and **288**, respectively. It seemed that the electron donating effect of the alkoxy substituents in the 2- and 6-position was not to be underestimated (see also section 6.2), although a steric effect of the bulky protecting groups cannot be excluded. Finally the chlorides of **294** were converted into iodides, affording compound **295** in 88% yield. This is truly a highly functionalised TTFAQ derivative, functionalised in 6 positions with three different functionalities, which was a very ambitious goal at the beginning of this project. So even if a large excess of thiones **283** and **256** had to be used for the two phosphite couplings, it opens up possibilities to synthesise unique exotic structures which hitherto seemed unattainable.



Scheme 73: Synthesis of the triple-bridged TTFAQ cyclophane **297**.

Next step was to double-bridge the two 1,3-dithiole moieties of **295** in a reaction similar to the synthesis of **291**. From earlier work with TTF derivatives it was known that cesium hydroxide monohydrate could cleave the silyl protecting groups during the deprotection of the thiolates.¹⁸⁴ However, this undesired deprotection of the alcohols should be a lot slower than the deprotection of the thiolates which in turn are better nucleophiles than the alkoxides, so the intramolecular reaction to form a double-bridged TTFAQ cyclophane should not be harmed by the presence of some alkoxide in the reaction mixture. Thus, we used 6 equivalents of cesium hydroxide monohydrate and left the reaction mixture to stir for another 24 h after the addition of precursor **295** was completed (Scheme 73). This ensured complete deprotection of the alcohols after the macrocyclisation, thereby avoiding a mixture of double-bridged TTFAQ cyclophanes with protected and deprotected alcohols. The double-bridged diol **296** was isolated in 78% yield, which was very satisfactory for a double macrocyclisation followed by a double deprotection, all in one pot. Cyclophane **296** can form unstable solvent containing crystals, but contrary to the unsubstituted cyclophane analogue **291**, it is still very soluble due to the 2-hydroxyethoxy substituents. The last macrocyclisation was carried out under conditions similar to the formation of cyclophane **206** (Scheme 42), by reaction of **296** with 1,4-benzenedicarbonyl chloride **205** in dichloromethane, this time in the presence of pyridine. The yield of triple-bridged cyclophane **297**, a pale yellow solid with good solubility in common organic solvents, was 42% [*cf.* **206** (39%)]. Hence two different methodologies had been successfully combined to create a TTFAQ derivative with a remarkable architecture.

The structure of **297** was confirmed by ¹H NMR, ¹³C NMR, HRMS and elemental analysis, but the NMR data alone left no doubt about the structure. Due to C₂ symmetry the ¹³C NMR spectrum of **297** was very simple. The ¹H NMR spectrum of **297** (Figure 92) looks very much like the low frequency part of the spectrum for **291** (Figure 87) combined with the high frequency part of the spectrum for **206** (Figure 63a). Most diagnostic for the phenyl bridge is the up-field shift of the phenyl protons (singlet at 6.91 ppm), due to the ring current of the dihydroanthracene ring system, which was characteristic for cyclophane **206** (singlet at 6.89 ppm). Characteristic for the double-bridged compound **291** were the diastereotopic protons of the methylene groups, which had a large difference in chemical shift $\Delta\delta(\text{H}_A\text{H}_B)$. This pattern is easily recognized for triple-bridged cyclophane **297**, since although **297** has five different methylene groups (and not three like **291**) the signals from the protons on C^{1*} and C^{2*} coincide with the signals from the protons on C¹ and C², respectively.

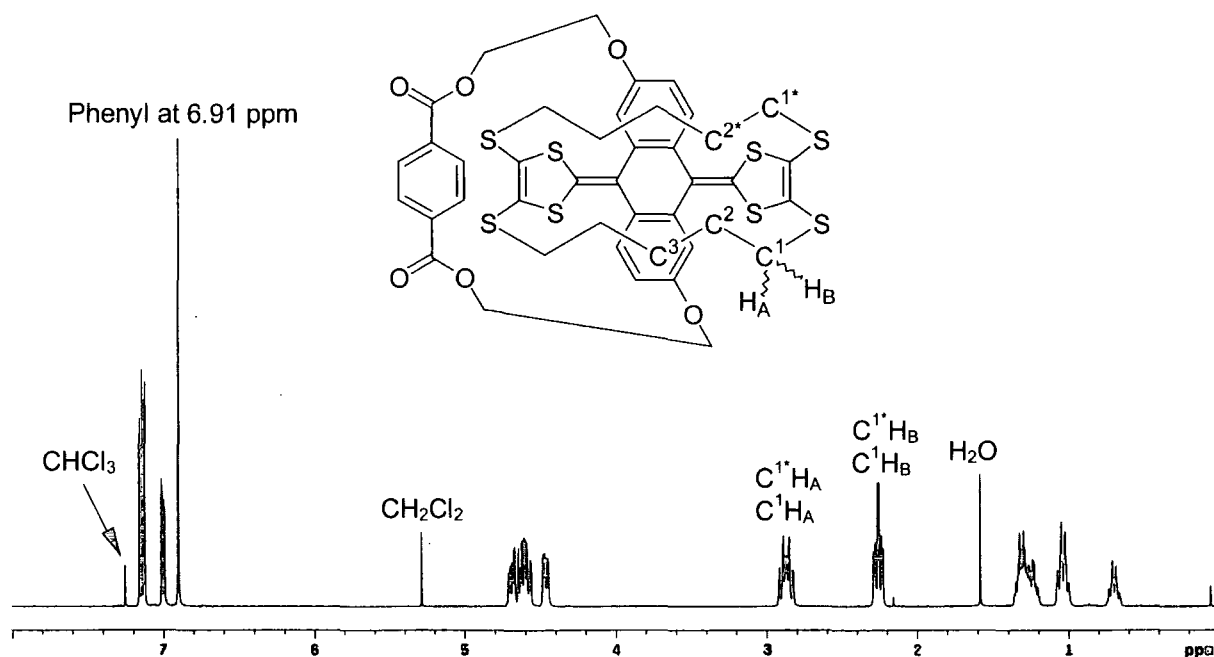


Figure 92: The ^1H NMR spectrum (at 400 MHz) of triple-bridged cyclophane **297**. Most characteristic is the up-field shifted phenyl protons (the singlet at 6.91 ppm) and the diastereotopic protons, with a large difference in chemical shift $\Delta\delta(\text{H}_\text{A}\text{H}_\text{B})$, of the methylene groups (the multiplets from diastereotopic protons for C^1 and $\text{C}^{1'}$ have been labelled as examples).

7.2.2 X-ray crystallographic analysis of triple-bridged cyclophane **297**

Crystals of **297**· $(\text{CH}_2\text{Cl}_2)_2$ afforded an X-ray structure showing the beautiful architecture of the triple-bridged cyclophane (Figure 93 and Figure 94). The conformation of the TTFAQ moiety is very similar to that in the crystal structure of **291**· C_7H_8 (Figure 89, right). The saddle-like conformation is bent by the short bridges between the dithiole rings, making the angle (θ) between the planar $\text{S}(1)\text{C}(16)\text{C}(17)\text{S}(2)$ and $\text{S}(5)\text{C}(19)\text{C}(20)\text{S}(6)$ moieties only 31.7° . However, as for **291**· C_7H_8 this is mainly due to strong folding (δ) of both dithiole rings along the $\text{S}\cdots\text{S}$ vectors ($\delta_1 = 31.9^\circ$, $\delta_2 = 32.4^\circ$). In spite of the phenyl bridge, bridging the dihydroanthracene moiety, the folding ($\phi = 40.6^\circ$) along the $\text{C}(9)\cdots\text{C}(10)$ vector does not exceed the range observed in unconstrained TTFAQ derivatives ($35\text{--}45^\circ$),^{66,73,94} as was the case for cyclophane **206** (Figure 64), possessing the same phenyl bridge. The pentamethylene chains both adopt practically planar all-*trans* conformations, which are nearly perpendicular to the plane passing through the $\text{C}(9)$, $\text{C}(10)$, $\text{C}(15)$ and $\text{C}(18)$ atoms, similar to the pentamethylenedithio bridges in the solvated crystals of **291** (Figure 89, right). Disorder was

observed for atoms O(1) and C(31) in the bridge across the dihydroanthracene moiety, and for Cl(4) in one of the dichloromethane molecules.

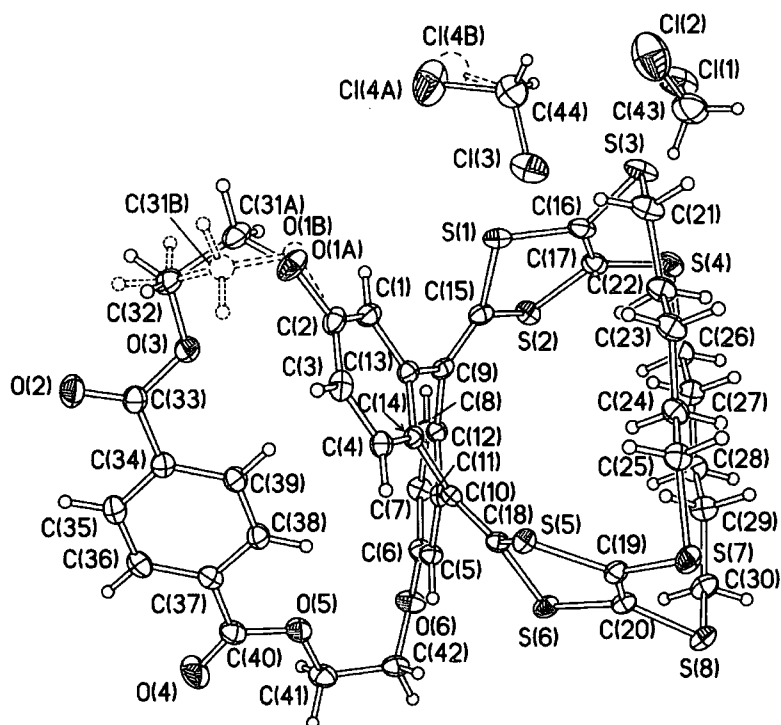


Figure 93: The X-ray crystal structure of triple-bridged cyclophane 297. Atoms O(1) and C(31) are disordered between positions A (72%) and B (28%), Cl(4) between positions A (90%) and B (10%).

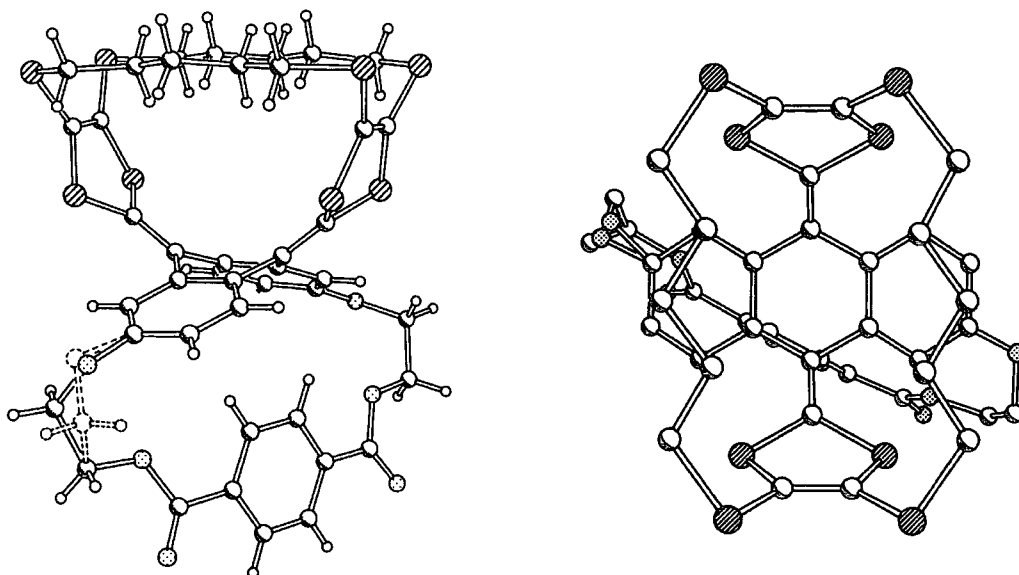


Figure 94: The X-ray crystal structure of 297 viewed from two different angles. The atom labels and solvent of crystallisation has been omitted for clarity.

7.3 OPTICAL AND ELECTROCHEMICAL PROPERTIES

7.3.1 UV-vis absorption spectra

The UV-vis spectra of the TTFAQ cyclophanes and their precursors were recorded in dichloromethane. The values of λ_{\max} (lg ϵ) for all the compounds, including the single-bridged cyclophane **266** (Scheme 62), are listed in Table 13.

Compound	λ_{\max}/nm (lg ϵ)	λ_{\max}/nm (lg ϵ)	λ_{\max}/nm (lg ϵ)	λ_{\max}/nm (lg ϵ)
266	421 (4.32)	363 (4.14)	271 (4.41)	
287	432 (4.44)	362 (4.20)		
288	431 (4.43)	362 (4.19)		
289	432 (4.44)	362 (4.21)		
290	432 (4.45)	362 (4.20)		
291	414 (4.35)	372 (4.11)	351 (4.15)	269 (4.44)
292	398 (4.08)	370 (4.08)	340 (4.07)	267 (4.40)
294	428 (4.44)	361 (4.21)		
295	428 (4.43)	361 (4.20)		
296	411 (4.32)	353 (4.22)		
297	414 (4.26)	353 (4.16)		

Table 13: Values of λ_{\max} (lg ϵ) in the UV-vis region for cyclophanes and precursors. The spectra were all recorded in dichloromethane at 20 °C.

All the precursors **287-290** showed two bands typical for tetrakis(alkylthio)TTFAQ derivatives, at 432 and 362 nm, respectively. However, the incorporation of methylenedithio bridges in cyclophanes **266**, **291** and **292** changes the spectrum significantly (see their spectra and the spectrum of precursor **289** in Figure 95), with a blue-shift of the longest wavelength absorption band, indicating loss of π -conjugation.⁶⁴ Incorporation of a single pentamethylenedithio bridge (cyclophane **266**) decreases the extinction coefficient and the longest wavelength band shifts from 432 nm to 421 nm, whereas a second pentamethylenedithio bridge (cyclophane **291**) shifts the band further to 414 nm. Shortening of the bridges to two

tetramethylenedithio linkers (cyclophane **292**) has an even greater impact. The extinction coefficient of the longest wavelength band is halved (relative to **289**) and shifted to 398 nm, where it has almost completely merged with bands at 370 and 340 nm, respectively. Thus, the blue-shift and the decrease of the extinction coefficient of especially the longest wavelength band is a direct measure of the bend of the TTFAQ moieties in the strained cyclophanes, an observation also reported by Finn *et al.*¹⁴³ A similar behaviour was observed for strained TTF cyclophanes **24** and **26** (section 1.2.4) and the same trend is seen for double-bridged cyclophane **296** and triple-bridged cyclophane **297**, although the third bridge across the dihydroanthracene system makes little difference to the spectrum, which is in agreement with the UV-vis absorption spectra for cyclophane **206** and its precursors (see experimental, section 8.4).

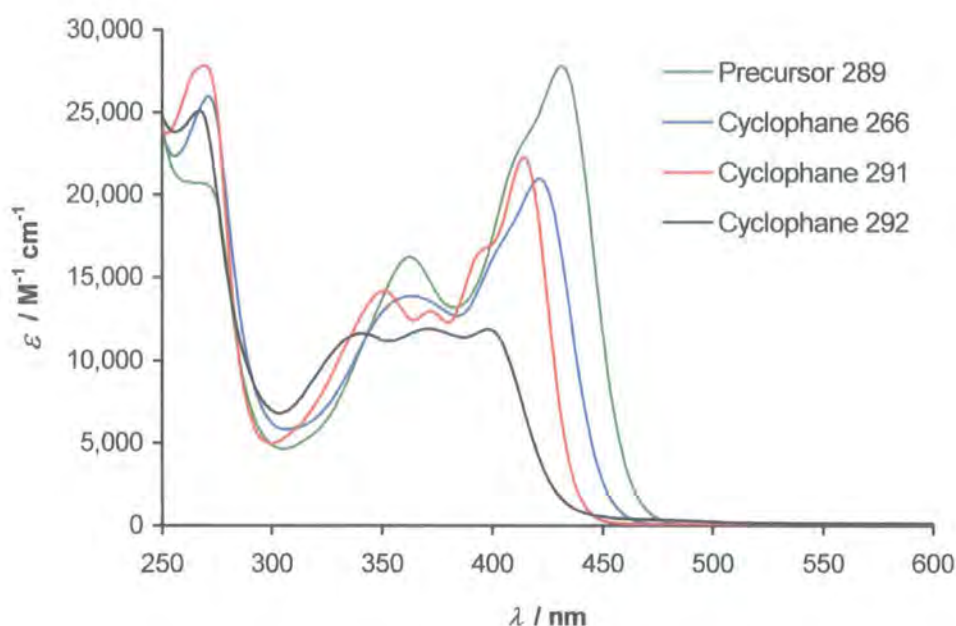


Figure 95: UV-vis spectra of cyclophanes 266, 291 and 292, and the precursor 289 recorded in dichloromethane at 20 °C.

7.3.2 Solution electrochemical properties

Cyclic voltammetry was carried out on all the new TTFAQ derivatives (the oxidation potentials are collated in Table 14). As expected, the precursors **287-290** show a single, quasi-reversible, two-electron oxidation wave at 0.60-0.61 V, values consistent with the data obtained for tetrakis(alkylthio) substituted TTFAQ building blocks in section 6.5. More unpredictable are the oxidation potentials for the 2,6-bissubstituted precursors **294** and **295**.

The bulky silyl protecting groups increase the quasi-reversibility (ΔE increases) and raise the oxidation potential slightly compared to precursors 287-290, even though the electron donating groups in the 2,6-positions were expected to lower the oxidation potential. This unexpected effect, which must be due to steric reasons not fully understood, was also seen for other TTFAQ derivatives bearing the same protecting group (see section 3.6.2 and 5.3.3).

Compound	$E^{\text{ox}}_{\text{pa}}/\text{V}$		$E^{\text{ox}}_{\text{pc}}/\text{V}$		$\Delta E/\text{V}^a$	
287	0.60		0.51		0.09	
288	0.61		0.49		0.12	
289	0.60		0.51		0.09	
290	0.61		0.49		0.12	
291	1.01	1.25	0.95	1.19	0.06	0.06
292 ^b	0.99	1.26	0.92	1.18	0.07	0.08
294	0.63		0.41		0.22	
295	0.63		0.41		0.22	
296	0.92	1.13	0.86	1.08	0.06	0.05
297	0.98	1.20	0.92	1.14	0.06	0.06

Table 14: Cyclic Voltammetry data vs. Ag/AgCl. Compound *ca.* 1×10^{-3} M and electrolyte 0.1 M Bu₄NPF₆ in dichloromethane, 20 °C, scan rate 100 mV s⁻¹.¹²⁹ ^a $\Delta E = E^{\text{ox}}_{\text{pa}} - E^{\text{ox}}_{\text{pc}}$. ^b Scan rate 5000 mV s⁻¹ due to some deposition of oxidised species on the electrode at lower scan rates.

The remarkable results are clearly seen in the oxidation potentials of the double-bridged cyclophanes 291 and 292. As expected from our experience with cyclophanes 185,¹⁴³ 186,¹⁴⁵ and 266 (Scheme 62), the oxidation potentials of the cyclophanes are raised considerably compared to their precursors, in this case by *ca.* 400 mV (see also discussion in section 6.5). However, contrary to all other TTFAQ cyclophanes, the oxidation occurs in *two*, reversible,⁶⁹ one-electron oxidation waves instead of a single, quasi-reversible, two-electron oxidation wave (Figure 96). Hence, these TTFAQ derivatives are the first for which the formation of the cation radical species is visible in the cyclic voltammograms. The reason must be that little or no conformational change can accompany the oxidation of the double-bridged TTFAQ cyclophanes, due to their very rigid structures. Hence the second oxidation does not allow the cyclophane to change into a conformation where the dication is significantly stabilised due to

increased aromaticity, which makes the cation radical stable in respect to the dication. Furthermore, the dication is not stabilised by minimisation of Coulombic repulsion to the same degree as non-bridged TTFAQ derivatives, since the strained double-bridged cyclophanes positions the 1,3-dithiolium rings in closer proximity almost parallel to each other, and not further removed, perpendicular to a flat anthracene plane. Thus, our strategy to structurally manipulate the redox properties of TTFAQ to yield the cation radical state had proved to be successful.

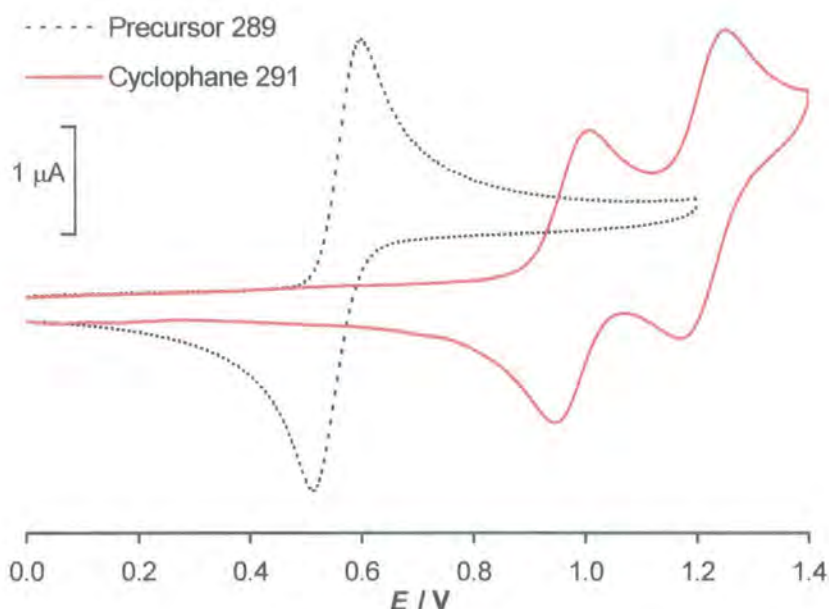


Figure 96: Cyclic voltammetry of cyclophane 291 and its precursor 289.

For all the cyclophanes **291**, **292**, **296** and **297** it is appropriate to quote the half-wave potentials (Table 15), just as for other reversible redox systems, instead of the oxidation potentials. We can then compare the splitting ($E_2^{1/2} - E_1^{1/2}$) of the two reversible oxidation waves with the values for **9**, **47** and **298**, known from the literature. The splitting for the multiple-bridged cyclophanes are 0.22-0.26 V, which is smaller than for TTF **9**, but still larger than for the extended TTF **47** and for the planar donor **298**. For **298** no steric interaction plays a role in the oxidation processes, but it gains aromaticity for the central quinonoid ring upon oxidation. This indicates little gain of aromaticity for the TTFAQ cyclophanes and presumably also a through-space interaction between the charged moieties, upon oxidation. The half-wave potentials of the 2,6-bissubstituted double-bridged cyclophane **296** are lowered by 90-110 mV compared to the potentials for unsubstituted analogue **291**. This can be explained by the electron donating effect of the substituents, which for this compound are

non-bulky 2-hydroxyethoxy groups, and hence the picture is not altered by any steric effect from bulky protecting groups, as for the non-bridged precursors. The effect of the third bridge is seen as an increase in the half-wave potential of *ca.* 60 mV, an increase similar to that found for cyclophane **206** (section 5.2.5).

Compound	$E_1^{1/2}/V$	$E_2^{1/2}/V$	$(E_2^{1/2} - E_1^{1/2})/V$
291 ^a	0.98	1.22	0.24
292 ^a	0.96	1.22	0.26
296 ^a	0.89	1.11	0.22
297 ^a	0.95	1.17	0.22
9 ^b	0.34	0.71	0.37
47 ^b	0.20	0.36	0.16
298 ^c	-0.11	-0.04	0.07

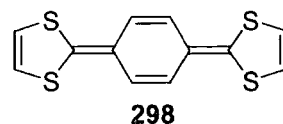
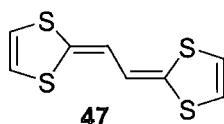
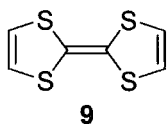


Table 15: Half-wave potentials for cyclophanes 291, 292, 296 and 297 and for some reference compounds.
^a Conditions as in Table 14. ^b 0.1 M Tetraethylammonium perchlorate, acetonitrile, vs. Ag/AgCl.⁵⁷ ^c 0.1 M Tetraethylammonium perchlorate, acetonitrile, vs. standard calomel electrode (SCE).⁶²

An X-ray crystal structure of any of these oxidised species could help to shed some light on what happens upon oxidation of the multiple-bridged cyclophanes, but unfortunately both electrocrystallisation and chemical oxidation using iodine vapour or bromine failed to give any crystals. Alternatively the absorption spectra of the oxidised species of the double-bridged cyclophanes could give us more information.

7.3.3 Spectroelectrochemical studies – the hunt for the cation radical

So far, investigation of the cation radical of TTFAQ derivatives had been limited to the studies of transient species obtained either by flash photolysis⁷⁸ or pulse radiolysis,⁸⁴ or to the studies of the transient charge-separated species generated by photoinduced charge-transfer in TTFAQ-C₆₀ dyads.⁸⁵ These transient species only had life-times of a few hundred

microseconds, whereas the CV experiments of the multiple-bridged cyclophanes showed the cation radical species to be stable for at least a few minutes. However, to get good spectroelectrochemical data, the cation radical species needed to be stable for a few hours.

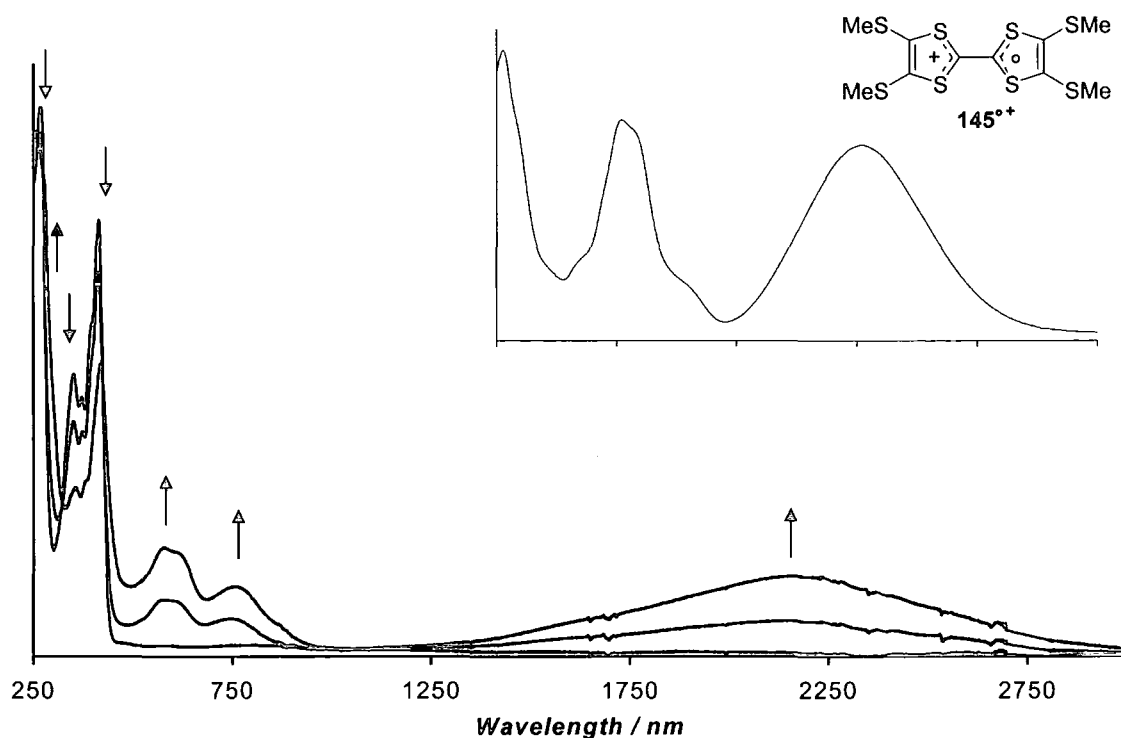


Figure 97: Spectroelectrochemistry of cyclophane **291** in dichloromethane at 20 °C. The figure shows the oxidation of **291** to the cation radical species **291**^{•+}. Inset is the absorption spectrum of the cation radical **145**^{•+} of tetrakis(methylthio)TTF in dichloromethane solution ($\lambda_{\text{max}} = 460$ and 850 nm, respectively).

Spectroelectrochemical studies of both unsubstituted **291** and bisubstituted **296** double-bridged cyclophanes were undertaken.⁸³ Upon oxidation, the strong bands characteristic of neutral **291** at $\lambda_{\text{max}} = 351$ and 414 nm give way to a sharp band at $\lambda_{\text{max}} = 423$ nm and two broad bands at $\lambda_{\text{max}} = 580$ and 760 nm, respectively (Figure 97). Finally a very broad band stretching from 1300 nm to 2900 nm, with $\lambda_{\text{max}} = 2175$ nm, makes the spectrum of the cyclophane cation radical **291**^{•+} most unusual. The two broad bands at $\lambda_{\text{max}} = 580$ and 760 nm are similar to those of the cation radical of alkylthio substituted TTF derivatives.¹⁸⁵ We did spectroelectrochemistry of tetrakis(methylthio)TTF for comparison, and the spectrum of the cation radical **145**^{•+} is inset in Figure 97 (spectra of **145** and **145**²⁺ can be found in Appendix Two). However, the very broad low-energy band ($\lambda_{\text{max}} = 2175$ nm) is reminiscent of the partly oxidised dimeric TTF cyclophane **32h** (Figure 9, Chapter 1), synthesised by Becher *et al*, for

which a similar absorption (with $\lambda_{\max} = 2300$ nm) was unambiguously assigned as being a mixed valence band, resulting from *intermolecular* interaction.³⁶ In the case of cyclophane **291**, we assign the low-energy band to a mixed valence band arising from the interaction between the neutral and the oxidised dithiole rings. The ratio of the low-energy band and the other bands seemed unaffected by the concentration, and noteworthy the ratio was the same for the cation radical of bisubstituted double-bridged TTFAQ cyclophane **296** (Figure 98). Hence, in our case the interaction causing the mixed valence band should be *intramolecular*.

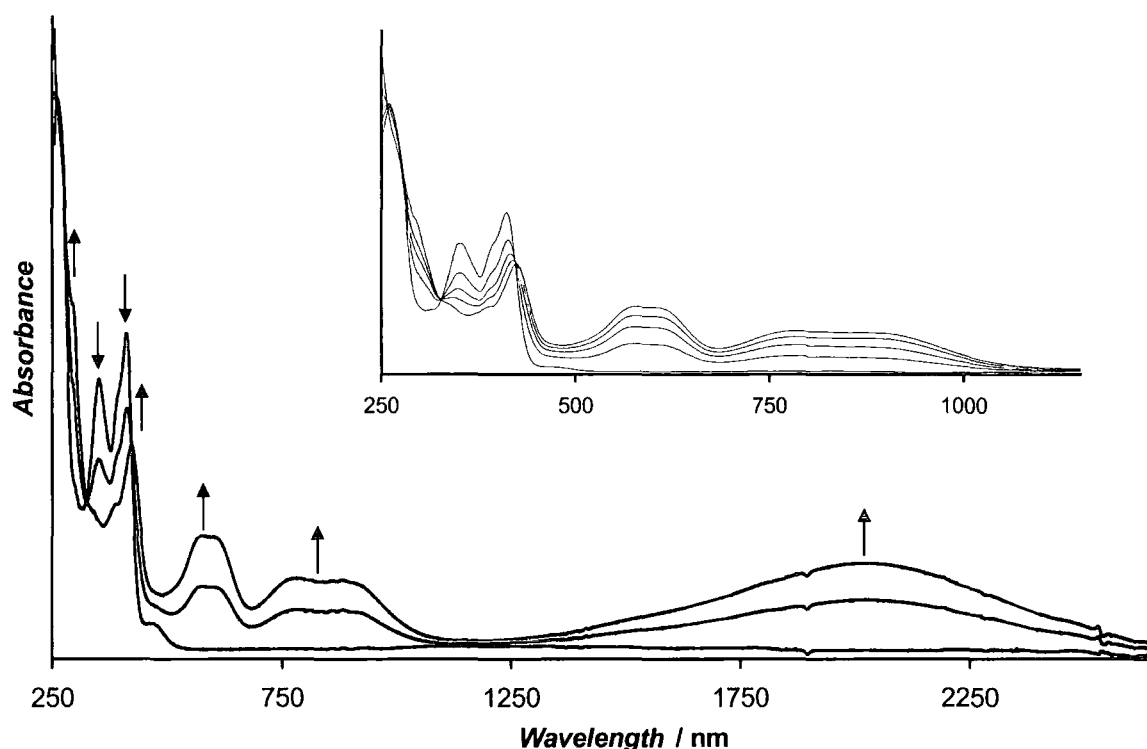


Figure 98: Spectroelectrochemistry of cyclophane **296** in dichloromethane at 20 °C. The figure shows the oxidation of **296** to the cation radical species $296^{\bullet+}$. Inset the short-wavelength part, showing two isosbestic points.

Changes in the absorption spectrum upon oxidation of the bisubstituted double-bridged TTFAQ cyclophane **296** are very similar to the oxidation of **291**. New bands at 423 and 580 nm appear together with a mixed valence band at $\lambda_{\max} = 2040$ nm (Figure 98), and the mixed valence band is slightly less broadened and a little blue-shifted compared to the spectrum of $291^{\bullet+}$. However, the long-wavelength intrinsic cation radical band seems to be split into two bands ($\lambda_{\max} = 775$ and 890 nm), forming a broad superposition of bands stretching over 300 nm. This could be explained by the ability of **296** to adopt two slightly different thermodynamically stable conformations in solution.

For both **291** and **296** the cation radical was stable on the spectroelectrochemical time-scale, since the spectra of the neutral species could be completely recovered upon reduction of the cation radical species. Furthermore, clean isosbestic points were seen in the formation of **291**^{•+} and **296**^{•+} (see the expanded part of the spectrum inset in Figure 98 as an example). However, further oxidation to form the dication species **291**²⁺ and **296**²⁺ caused decomposition and neither the spectra of the cation radicals nor the spectra of the neutral species could be recovered upon reduction (spectra showing the formation of the decomposition products for **291** and **296** can be found in Appendix Two). Thus, prolonged oxidation over 1 hour was too harsh conditions. The decomposition products were not identified, but the instability of the dication species could explain the failed attempts to isolate any salts by electrocrystallisation of the multiple-bridged cyclophanes.

7.4 CONCLUSIONS

Using the new methodology described in Chapter 6, highly functionalised TTFAQ building blocks **289**, **290** and **295** were obtained. Reaction of **289** and **295** afforded double-bridged cyclophanes in near quantitative yields. Also highly strained cyclophane **292** and a triple-bridged cyclophane **297** were synthesised, and their beautiful architectures were studied using X-ray crystallography. The crystal structures revealed increased strain in the series of bridged cyclophanes, which was accompanied by a characteristic blue-shift in the UV-vis absorption spectra. However, the most remarkable result was that the oxidation of the multiple-bridged cyclophanes occurs in *two*, reversible, one-electron oxidation waves. This is the first and only time that the cation radical of a TTFAQ derivative has been observed using cyclic voltammetry and spectroelectrochemistry. Hence the aim of this project has been achieved. However, further characterisation and investigation into these novel cation radical species should prove very interesting. Also the highly functionalised building blocks presented in this chapter, and related TTFAQ derivatives, should be very useful for the synthesis of other structurally challenging redox systems.

8 EXPERIMENTAL PROCEDURES

This final chapter provides the experimental procedures for the novel compounds presented in this thesis. Included will also be compounds **55** and **195**, which are known from the literature, but for this work they have been synthesised in a different manner.

8.1 GENERAL METHODS

All reactions which required inert or dry atmospheres, were carried out under a blanket of argon, which was dried by passage through a column of phosphorus pentoxide. All reagents employed were of standard reagent grade and purchased from Aldrich, Avocado, Fluka or Merck and used as supplied unless otherwise stated. The following solvents were dried and distilled immediately prior to use: Acetone, over Drierite (CaSO_4); Acetonitrile and dichloromethane, over calcium hydride; diethyl ether and toluene, over sodium metal; tetrahydrofuran, over potassium metal. *N,N*-Dimethylformamide was dried by standing over 4Å molecular sieves for at least 48 h and was not distilled prior to use. Ethanol and methanol were dried and distilled over magnesium turnings and stored under dry argon over 3Å molecular sieves. Pyridine was dried by standing over potassium hydroxide overnight followed by vacuum distillation and stored under dry argon over 3Å molecular sieves. 2-Butanone, carbon disulfide, chlorobenzene, cyclohexane, ethyl acetate, hexane, heptane and petroleum ether were used without prior purification.

Column chromatography was carried out using either Prolabo silica (70-230 mesh) or Merck alumina (activity I to II, 70-230 mesh); the latter was neutralised by pre-soaking in ethyl acetate for 24 h prior to use. Solvents used for chromatography were distilled prior to use, with the exception of dichloromethane and chloroform which were used as supplied. Analytical Thin Layer Chromatography (TLC) was performed on Merck DC-Alufolien Silica gel, 60 F₂₅₄ 0.2 mm thickness or Merck DC-Alufolien Aluminum oxide neutral (Type E), 60 F₂₅₄ 0.2 mm thickness precoated TLC plates.

Cyclic voltammetry data were measured using a BAS CV50 electrochemical analyser with internal resistance compensation. Cyclic voltammetry experiments were performed in a

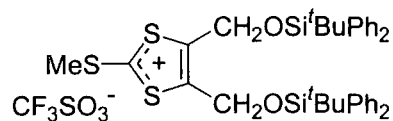
one-compartment cell with a platinum disc working electrode, a platinum counter electrode and an aqueous Ag/AgCl electrode as reference. The experiments were carried out using a 10^{-4} - 10^{-3} M solution of the redox active species in an anhydrous and degassed 0.1 M solution of tetrabutylammonium hexafluorophosphate in dichloromethane, unless otherwise stated. The sweep rate for the data listed in this chapter was 100 mV s^{-1} . Spectroelectrochemical data were recorded using an optically transparent thin-layer electrode (OTTLE) cell with a platinum gauze working electrode, platinum wire counter electrode and a platinum wire pseudo reference electrode. The cell was driven by a home-built potentiostat.⁸³

^1H NMR spectra were recorded on a Varian Unity 300 at 300 MHz, a Varian VXR 400s at 400 MHz or a Varian Inova 500 at 500 MHz using the deuterated solvent as lock. Chemical shifts are quoted in ppm, relative to tetramethylsilane (TMS), using TMS or the residual solvent as internal reference. ^{13}C NMR were recorded using broad band decoupling, at the Varian VXR 400s or Varian Inova 500 at 100 MHz and 125 MHz, respectively. The following abbreviations are used in listing NMR spectra: s = singlet, d = doublet, t = triplet, q = quartet, br = broad.

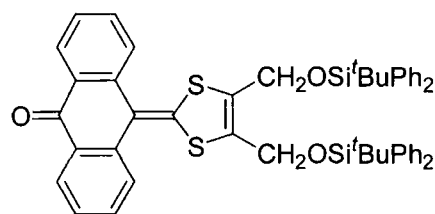
Electron Impact (EI) and Chemical Ionisation (CI) mass spectra were recorded on a Micromass AutoSpec spectrometer operating at 70 eV with the ionisation mode as indicated. Electrospray (ES) mass spectra were recorded on a Micromass LCT spectrometer. Plasma Desorption (PD) mass spectra were obtained on a Bio-ion 20K time of flight instrument from Applied Biosystem on the basis of 500 000 fission events (Odense University). Matrix Assisted Laser Desorption/Ionisation (MALDI) time of flight mass spectra were recorded on a Kompact Maldi 2, Kratos Analytical instrument using 2,5-dihydroxybenzoic acid as matrix (Odense University).

UV-vis spectra were recorded using a Varian Cary 5 spectrophotometer at ambient temperature. This spectrophotometer was also used for recording the spectra when spectroelectrochemistry was performed. Elemental analyses were obtained on an Exeter Analytical Inc. CE-440 elemental analyzer. Melting points were recorded on a Stuart Scientific SMP3 melting point apparatus and are uncorrected.

8.2 EXPERIMENTAL PROCEDURES TO CHAPTER 3

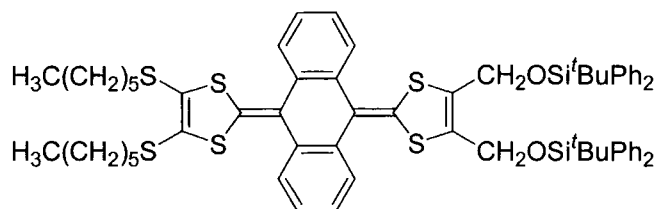
4,5-Bis(*tert*-butyldiphenylsiloxymethyl)-2-methylthio-1,3-dithiolium triflate (**102**)

4,5-Bis(*tert*-butyldiphenylsiloxymethyl)-1,3-dithiole-2-thione **101** (1 equivalent) was dissolved in dry degassed dichloromethane (10 mL/g of **101**) and stirred under argon at room temperature. Methyl triflate (1.1 equivalents) was added in one portion and the stirring was continued for 1 h, whereupon the colour changed from yellow to almost colourless. Concentration *in vacuo* afforded a pale yellow salt **102**, which was used without further purification, mp 90-91 °C. ¹H NMR (CDCl₃): δ 7.57-7.52 (8H, m), 7.44-7.35 (12H, m), 4.66 (4H, s), 3.17 (3H, s), 1.04 (18H, s).

10-[4,5-Bis(*tert*-butyldiphenylsiloxymethyl)-1,3-dithiol-2-ylidene]anthracene-9(10H)-one (**104**)

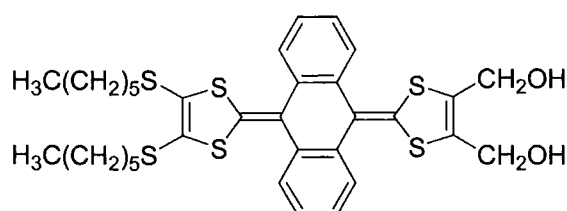
The triflate salt **102** (from 28.50 g, 42.47 mmol of **101**) and anthrone **60** (8.24 g, 42.4 mmol) were dissolved in a 3:1 (v/v) mixture of pyridine-acetic acid (400 mL) and stirred under argon at 60 °C for 3 h and then at 120 °C for another 3 h. The dark red mixture was concentrated under reduced pressure, redissolved in dichloromethane (500 mL), washed with water (2 x 400 mL) and brine (400 mL), dried (MgSO₄) and concentrated *in vacuo*. The residue was chromatographed (silica gel, dichloromethane-hexane, 3:1 v/v) affording **104** as an orange powder (32.00 g, 91% from **101**), mp 128-129 °C (from chloroform-methanol). ¹H NMR (CDCl₃): δ 8.32 (2H, d, *J* = 8.0 Hz), 7.93 (2H, d, *J* = 8.0 Hz), 7.67-7.63 (2H, m), 7.59-7.56 (8H, m), 7.46-7.30 (14H, m), 4.19 (s, 4H), 1.02 (s, 18H). ¹³C NMR (CDCl₃): δ 183.6, 143.9, 139.1, 135.5, 132.4, 131.5, 130.5, 129.9, 129.2, 127.8, 127.0, 126.3, 126.1, 116.6, 59.0, 26.6, 19.2. MS (PD): *m/z* = 831.2 (theory: 831.2). Anal. Calcd. for C₅₁H₅₀O₃S₂Si₂ (MW 831.24): C, 73.69; H, 6.06. Found C, 73.45; H, 6.22.

9-[4,5-Bis(*tert*-butyldiphenylsiloxymethyl)-1,3-dithiol-2-ylidene]-10-[4,5-bis(hexylthio)-1,3-dithiol-2-ylidene]-9,10-dihydroanthracene (105)



To a solution of the phosphonate ester **65** (1.35 g, 3.05 mmol) in dry tetrahydrofuran (100 mL) at $-78\text{ }^{\circ}\text{C}$ under argon was added lithium diisopropylamide (2.23 mL of a 1.5 M solution in cyclohexane, 3.35 mmol) *via* syringe and the resultant cloudy yellow mixture was stirred for 2 h. The ketone **104** (2.11 g, 2.54 mmol) was added to the mixture as a solid, against a positive pressure of argon, which afforded an orange suspension. The suspension was stirred at $-78\text{ }^{\circ}\text{C}$ for another 2 h, whereupon it was allowed to slowly attain room temperature overnight. Evaporation of the solvent gave a red residue which was dissolved in dichloromethane (200 mL), washed with water (200 mL) and brine (200 mL), dried (MgSO_4) and concentrated *in vacuo*. Purification by column chromatography (silica gel, dichloromethane-hexane, 1:3 v/v) afforded **105** as an analytically pure yellow foam (2.26 g, 77%), mp $56\text{--}58\text{ }^{\circ}\text{C}$. $^1\text{H NMR}$ (CDCl_3): δ 7.72–7.70 (2H, m), 7.60–7.56 (10H, m), 7.39–7.28 (16H, m), 4.18 (2H, d, $J = 12.8\text{ Hz}$), 4.11 (2H, d, $J = 13.2\text{ Hz}$), 2.88–2.73 (4H, m), 1.65–1.58 (4H, m), 1.41–1.34 (4H, m), 1.31–1.23 (8H, m), 1.01 (18H, s), 0.87 (6H, t, $J = 6.8\text{ Hz}$). $^{13}\text{C NMR}$ (CDCl_3): δ 135.54, 135.52, 135.3, 134.7, 133.8, 132.6, 132.5, 130.4, 129.8, 128.4, 127.7, 126.1, 126.0, 125.7, 125.4, 125.2, 123.4, 121.1, 59.1, 36.2, 31.3, 29.7, 28.2, 26.6, 22.5, 19.2, 14.0. UV-vis (CH_2Cl_2): λ_{max} (lg ϵ) 366 (4.19), 438 (4.43) nm. CV: $E_{\text{pa}}^{\text{ox}} = 0.54\text{ V}$, $E_{\text{pc}}^{\text{ox}} = 0.23\text{ V}$. MS (PD): $m/z = 1148.6$ (theory: 1149.9). Anal. Calcd. for $\text{C}_{66}\text{H}_{76}\text{O}_2\text{S}_6\text{Si}_2$ (MW 1149.88): C, 68.94; H, 6.66. Found C, 68.86; H, 6.73.

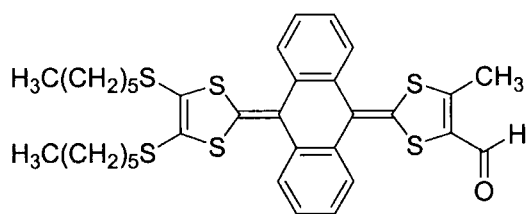
9-[4,5-Bis(hexylthio)-1,3-dithiol-2-ylidene]-10-[4,5-bis(hydroxymethyl)-1,3-dithiol-2-ylidene]-9,10-dihydroanthracene (106)



The protected bis(hydroxymethyl) derivative **105** (2.21 g, 1.93 mmol) was dissolved in dry tetrahydrofuran (25 mL) and stirred under argon at room temperature. A solution of tetrabutylammonium fluoride (5.78 mL of a

1.0 M solution in tetrahydrofuran, 5.78 mmol) was added dropwise *via* syringe over 15 min, making the reaction mixture change colour from yellow to light brown. Further stirring for 1.5 h, followed by addition of a few drops of water (0.1 mL) and evaporation of the solvent afforded a brown residue. The residue was dissolved in dichloromethane (200 mL), washed with water (200 mL) and brine (200 mL), dried (MgSO₄) and concentrated *in vacuo*. Chromatography using a short column (silica gel, dichloromethane until no more traces of by-products were visible on the column, then dichloromethane-ethyl acetate, 2:1 v/v) afforded **106** as an analytically pure yellow solid (1.14 g, 88%), mp 110-111 °C. ¹H NMR (CDCl₃): δ 7.62-7.55 (4H, m), 7.28-7.26 (4H, m), 4.27-4.17 (4H, m), 2.93 (2H, t, *J* = 5.6 Hz), 2.80-2.75 (4H, m), 1.63-1.56 (4H, m), 1.40-1.33 (4H, m), 1.29-1.24 (8H, m), 0.87 (6H, t, *J* = 6.8 Hz). ¹³C NMR (CDCl₃): δ 134.8, 134.5, 131.9, 131.4, 129.9, 126.1(2C), 125.9, 125.5, 125.1, 123.1, 122.6, 56.8, 36.2, 31.3, 29.6, 28.2, 22.5, 14.0. UV-vis (CH₂Cl₂): λ_{max} (lg ε) 269 (4.24), 364 (4.20), 432 (4.45) nm. CV: *E*^{ox}_{pa} = 0.45 V, *E*^{ox}_{pc} = 0.32 V. MS (PD): *m/z* = 672.2 (theory: 673.1). Anal. Calcd. for C₃₄H₄₀O₂S₆ (MW 673.08): C, 60.67; H, 5.99. Found C, 60.51; H, 5.99.

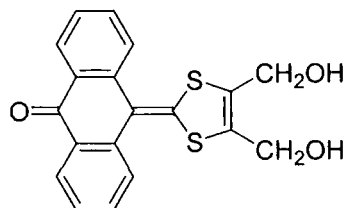
9-(4-Formyl-5-methyl-1,3-dithiol-2-ylidene)-10-[4,5-bis(hexylthio)-1,3-dithiol-2-ylidene]-9,10-dihydroanthracene (108)



To a stirred solution of **106** (0.101 g, 0.15 mmol) and carbon tetrabromide (0.150 g, 0.45 mmol) in dichloromethane (50 mL) at room temperature under argon was added a solution of triphenylphosphine (0.118 g, 0.45 mmol) in dichloromethane (10 mL) over 2 h. The reaction mixture was stirred for 16 h and concentrated under reduced pressure. The residue was column chromatographed (silica gel, dichloromethane-hexane, 2:1 v/v) to give **108** as a brown solid (0.060 g, 61%). Brown prism shaped crystals suitable for X-ray crystallography were grown by slow evaporation of a solution of **108** in a mixture of dichloromethane and hexane, mp 178-179 °C. ¹H NMR (CDCl₃): δ 9.70 (1H, s), 7.65-7.56 (4H, m), 7.33-7.30 (4H, m), 2.84-2.74 (4H, m), 2.43 (3H, s), 1.63-1.53 (4H, m), 1.40-1.37 (4H, m), 1.28-1.26 (8H, m), 0.89-0.85 (6H, m). UV-vis (CH₂Cl₂): λ_{max} (lg ε) 359 (4.19), 424 (4.46) nm. CV: *E*^{ox}_{pa} = 0.62 V, *E*^{ox}_{pc} = 0.50 V. MS (EI):

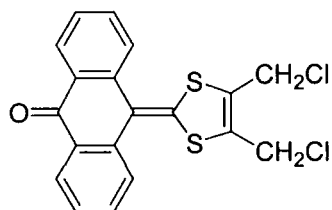
m/z (%) 654 (100, M^+). Anal. Calcd. for $C_{34}H_{38}OS_6$ (MW 655.06): C, 62.34; H, 5.85. Found C, 62.24; H, 5.89.

10-[4,5-Bis(hydroxymethyl)-1,3-dithiol-2-ylidene]anthracene-9(10H)-one (118)



To a stirred solution of the protected alcohol **104** (32.00 g, 38.50 mmol) in dry tetrahydrofuran (200 mL) was added a solution of tetrabutylammonium fluoride (115 mL of a 1.0 M solution in tetrahydrofuran, 115 mmol) over 15 min. Stirring under argon at room temperature was continued for 2 h, whereupon water (500 mL) was added to afford a red precipitate. The precipitate was filtered, washed with water (40 mL) and methanol (3 x 40 mL), and dried in vacuum over phosphorus pentoxide to give **118** as an orange powder sufficiently pure for further reaction (11.48 g, 84%). Compound **118** could be recrystallised from ethanol-hexane to give pure **118** as small red needles, mp 245-247 °C (decomp.). 1H NMR ($DMSO-d_6$): δ 8.13 (2H, d, $J = 7.6$ Hz), 7.94 (2H, d, $J = 7.6$ Hz), 7.78 (2H, t, $J = 7.6$ Hz), 7.50 (2H, t, $J = 7.6$ Hz), 5.61 (2H, t, $J = 5.6$ Hz), 4.33 (4H, d, $J = 5.6$ Hz). ^{13}C NMR ($CDCl_3$): δ 182.1, 144.5, 138.4, 132.3, 130.6, 129.5, 126.5, 126.44, 126.43, 115.6, 56.0. MS (EI): m/z (%) 354 (45, M^+), 336 (100). Accurate Mass Calcd. for $C_{19}H_{14}O_3S_2$: 354.03844. HRMS (EI): 354.03791 (-1.5 ppm).

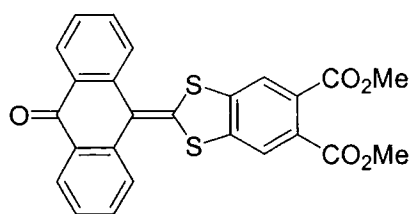
10-[4,5-Bis(chloromethyl)-1,3-dithiol-2-ylidene]anthracene-9(10H)-one (119)



To a stirred solution of bis(hydroxymethyl) derivative **118** (0.210 g, 0.59 mmol) in dry *N,N*-dimethylformamide (7 mL) at 0 °C under argon was added thionyl chloride (0.13 mL, 0.211 g, 1.78 mmol) dropwise *via* syringe, whereupon the colour changed from dark red to pale brown. The reaction mixture was stirred for 30 min, slowly warming to room temperature, and diluted with dichloromethane (100 mL). The organic phase was washed with water (3 x 100 mL), dried ($MgSO_4$) and concentrated *in vacuo*. Purification of the residue by column chromatography (silica gel, dichloromethane-hexane, 2:1 v/v) afforded **119** as small yellow crystals (0.192 g, 83%), mp 230 °C (decomp.). 1H NMR ($CDCl_3$): δ 8.27 (2H, d, $J = 8.0$ Hz), 7.83 (2H, d, $J = 8.0$ Hz),

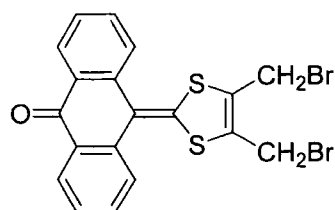
7.67 (2H, t, $J = 7.5$ Hz), 7.46 (2H, t, $J = 7.5$ Hz), 4.36 (4H, s). ^{13}C NMR (CDCl_3): δ 183.5, 138.6, 138.2, 131.9, 130.7, 129.3, 127.3, 127.0, 126.1, 119.6, 36.1. MS (EI): m/z (%) 394 (2, $[\text{M} + 4]^+$), 392 (5, $[\text{M} + 2]^+$), 390 (6, M^+), 208 (100). Anal. Calcd. for $\text{C}_{19}\text{H}_{12}\text{Cl}_2\text{OS}_2$ (MW 391.34): C, 58.31; H, 3.09. Found C, 58.35; H, 3.05.

Diels-Alder adduct 122



The dichloride **119** (0.115 g, 0.294 mmol), dimethyl acetylenedicarboxylate (0.14 mL, 0.167 g, 1.18 mmol), potassium iodide (0.146 g, 0.882 mmol) and 18-crown-6 (0.233 g, 0.882 mmol) were dissolved in dry toluene (70 mL) and stirred under argon at 100 °C for 2 h, in which time the colour changed from yellow to brown. To facilitate aromatisation, DDQ (0.133 g, 0.588 mmol) was added to the reaction mixture, which was stirred for another 1 h at 100 °C. The mixture was diluted with dichloromethane (200 mL), washed with an aqueous 0.5% sodium thiosulphate solution (3 x 200 mL) and water (200 mL), dried (MgSO_4) and filtered through a short silica column, eluting with dichloromethane-toluene, 1:1 v/v. The filtrate was concentrated *in vacuo* and the residue purified by column chromatography (silica gel, dichloromethane-ethyl acetate, 95:5 v/v) affording **122** as small golden needles (0.082 g, 61%), mp >250 °C. ^1H NMR (CDCl_3): δ 8.26 (2H, d, $J = 7.8$ Hz), 7.90 (2H, d, $J = 7.8$ Hz), 7.69 (2H, t, $J = 7.5$ Hz), 7.60 (2H, s), 7.49 (2H, t, $J = 7.5$ Hz), 3.89 (6H, s). ^{13}C NMR (CDCl_3): δ 183.6, 166.8, 138.7, 138.6, 137.8, 131.9, 131.0, 130.2, 127.5, 127.3, 126.3, 121.3, 121.2, 52.9. MS (EI): m/z (%) 460 (100, M^+). Anal. Calcd. for $\text{C}_{25}\text{H}_{16}\text{O}_5\text{S}_2$ (MW 460.52): C, 65.20; H, 3.50. Found C, 64.80; H, 3.44.

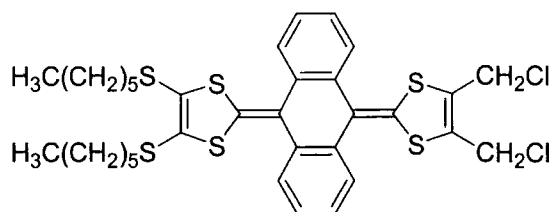
10-[4,5-Bis(bromomethyl)-1,3-dithiol-2-ylidene]anthracene-9(10H)-one (123)



Diol **118** (11.40 g, 32.16 mmol) was dissolved in dry *N,N*-dimethylformamide (150 mL) and stirred at 0 °C under argon. Phosphorus tribromide (9.07 mL, 26.12 g, 96.50 mmol) was added *via* syringe over 5 min, accompanied by a colour change from red to yellow orange. Stirring at 0 °C was

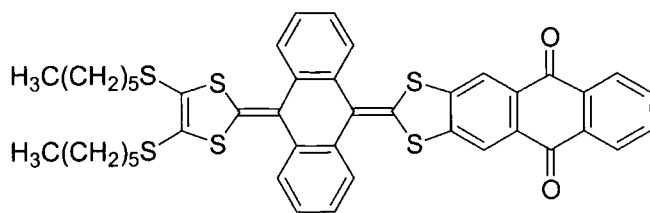
continued for 30 min followed by another 2 h at room temperature, after which a yellow precipitate was formed. Methanol (500 mL) was added to precipitate the remaining product, whereupon the reaction mixture was filtered. The yellow precipitate was washed with water (30 mL) and methanol (3 x 30 mL), and dried in vacuum over phosphorus pentoxide to give **123** as a yellow powder sufficiently pure for further reaction (13.76 g, 89%), mp 228-230 °C (from dichloromethane-hexane, decomp.). ¹H NMR (CDCl₃): δ 8.27 (2H, d, *J* = 7.2 Hz), 7.82 (2H, d, *J* = 7.6 Hz), 7.67 (2H, t, *J* = 7.6 Hz), 7.46 (2H, t, *J* = 7.6 Hz), 4.23 (4H, s). ¹³C NMR (CDCl₃): δ 183.5, 138.6, 137.8, 131.9, 130.7, 129.6, 127.3, 127.1, 126.1, 119.4, 21.3. MS (EI): *m/z* (%) 482 (4, [M + 4]⁺), 480 (7, [M + 2]⁺), 478 (4, M⁺), 320 (100). Anal. Calcd. for C₁₉H₁₂Br₂OS₂ (MW 480.24): C, 47.52; H, 2.52. Found C, 47.70; H, 2.53.

9-[4,5-Bis(chloromethyl)-1,3-dithiol-2-ylidene]-10-[4,5-bis(hexylthio)-1,3-dithiol-2-ylidene]-9,10-dihydroanthracene (128)



To a solution of bis(hydroxymethyl) derivative **106** (0.600 g, 0.891 mmol) in dry degassed acetonitrile (10 mL) was added dry carbon tetrachloride (3.0 mL) and triphenylphosphine (0.701 g, 2.67 mmol) whereupon the reaction

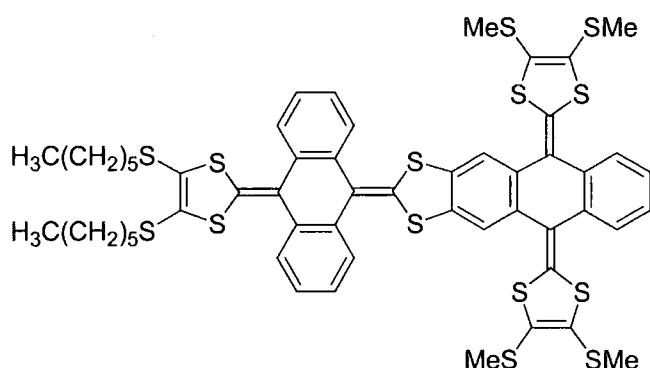
was stirred under argon at 80 °C for 20 min, in which time the colour changed from yellow to dark brown. The reaction mixture was cooled to room temperature and immediately filtered through a plug of silica, eluting with ethyl acetate, to remove the brown baseline. The yellow solution was concentrated *in vacuo* yielding a brownish yellow glass which was triturated with cyclohexane to give a yellow solid. The solid was filtered off, washed with methanol and dried, affording **128** as a yellow powder (0.415 g, 66%), mp 97-99 °C. ¹H NMR (CDCl₃): δ 7.61-7.58 (4H, m), 7.32-7.30 (4H, m), 4.31 (4H, s), 2.86-2.74 (4H, m), 1.65-1.59 (4H, m), 1.42-1.36 (4H, m), 1.30-1.26 (8H, m), 0.87 (6H, t, *J* = 7.0 Hz). ¹³C NMR (CDCl₃): δ 134.7, 134.6, 131.9, 129.0, 128.8, 126.5, 126.2 (2C), 125.4, 125.2, 123.9, 122.5, 36.5, 36.3, 31.3, 29.6, 28.2, 22.5, 14.0. UV-vis (CH₂Cl₂): λ_{max} (lg ε) 361 (4.21), 430 (4.47) nm. CV: *E*^{ox}_{pa} = 0.58 V, *E*^{ox}_{pc} = 0.48 V. MS (ES): *m/z* (%) = 712 (16, [M+4]⁺), 710 (84, [M+2]⁺), 708 (100, M⁺). Accurate Mass Calcd. for C₃₄H₃₈Cl₂S₆: 708.06749. HRMS (ES): 708.06777 (+0.4 ppm).

Diels-Alder adduct **130**

The dichloride **128** (0.100 g, 0.141 mmol), naphthoquinone **90** (0.089 g, 0.563 mmol), potassium iodide (0.070 g, 0.423 mmol) and 18-crown-6 (0.112 g, 0.423 mmol)

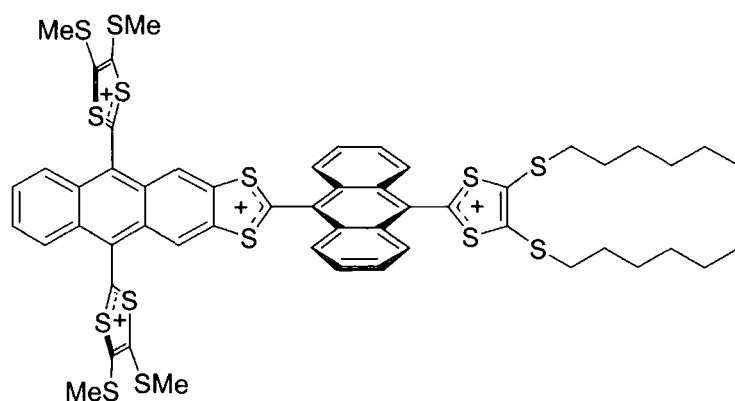
were dissolved in dry toluene (40 mL) and stirred under argon at 90 °C for 5 h, in which time the colour changed from yellow to dark brown. To complete aromatisation, DDQ (0.128 g, 0.563 mmol) was added to the reaction mixture, which was stirred for another 4 h at 90 °C. The colour changed to red-brown and a black precipitate formed. The mixture was diluted with dichloromethane (200 mL), washed with aqueous 0.5% sodium thiosulphate solutions (3 x 200 mL) and water (200 mL), dried (MgSO₄) and filtered through a short silica column, eluting with dichloromethane-toluene, 1:1 v/v. Evaporation of the solvent under reduced pressure followed by column chromatography (silica gel, dichloromethane-hexane, 1:1 v/v) afforded **130** as shiny black-red crystals (0.070 g, 63%), mp 229-230 °C. Crystals suitable for X-ray crystallography were grown by slow evaporation of a solution of **130** in a mixture of dichloromethane and hexane. ¹H NMR (CDCl₃): δ 8.28-8.26 (2H, m), 8.08 (2H, s), 7.80-7.77 (2H, m), 7.73-7.70 (2H, m), 7.65-7.63 (2H, m), 7.39-7.37 (4H, m), 2.84-2.71 (4H, m), 1.62-1.53 (4H, m), 1.39-1.32 (4H, m), 1.28-1.21 (8H, m), 0.83 (6H, t, *J* = 6.8 Hz). ¹³C NMR (CDCl₃): δ 181.9, 143.7, 134.9, 134.4, 134.2, 133.2, 132.7, 131.4, 128.7, 127.2, 127.0, 126.3, 126.22, 126.19, 125.5 (2C), 122.1, 118.8, 36.2, 31.2, 29.6, 28.1, 22.5, 14.0. UV-vis (CH₂Cl₂): λ_{max} (lg ε) 350 (4.55), 427 (4.50) nm. CV: *E*^{ox}_{pa} = 0.71 V, *E*^{ox}_{pc} = 0.61 V, *E*^{red}_{pc} = -0.85 V, *E*^{red}_{pa} = -0.79 V. MS (EI): *m/z* (%) = 792 (M⁺, 78), 502 (100). Accurate Mass Calcd. for C₄₄H₄₀O₂S₆: 792.13526. HRMS (EI): 792.13524 (+0.0 ppm).

TTFAQ dimer 143



To a stirred solution of phosphonate ester **63** (0.183 g, 0.60 mmol) in dry tetrahydrofuran (50 mL) at $-78\text{ }^{\circ}\text{C}$ under argon was added lithium diisopropylamide (0.44 mL of a 1.5 M solution in cyclohexane, 0.66 mmol) and the resultant cloudy yellow mixture was stirred for 2 h at $-78\text{ }^{\circ}\text{C}$.

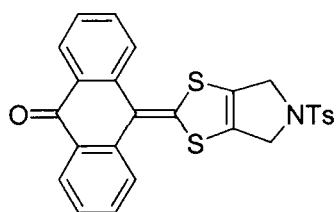
Anthraquinone derivative **130** (0.045 g, 0.057 mmol) was dissolved in dry tetrahydrofuran (100 mL) by sonication and added to the reaction mixture *via* syringe over 1 h. The reaction mixture was stirred at $-78\text{ }^{\circ}\text{C}$ for another 1 h, whereupon it was allowed to slowly attain room temperature for 12 h. Evaporation of the solvent afforded a red residue which was dissolved in dichloromethane (100 mL), washed with water, dried (MgSO_4) and concentrated *in vacuo*. Column chromatography (silica gel, dichloromethane-hexane, 1:1 v/v) afforded an impure orange powder. The crude product was purified using a short column (silica gel, carbon disulfide) to give **143** as a yellow powder (0.058 g, 88%), mp $154\text{--}156\text{ }^{\circ}\text{C}$. $^1\text{H NMR}^{186}$ (CDCl_3): δ 7.80-7.78 (0.6H, m), 7.71-7.69 (1.4H, m), 7.62-7.60 (2H, m), 7.49-7.47 (2H, m), 7.38-7.27 (8H, m), 2.85-2.71 (4H, m), 2.43 (1.9H, s), 2.39 (1.9H, s), 2.35 (4.1H, s), 2.31 (4.1H, s), 1.63-1.54 (4H, m), 1.41-1.31 (4H, m), 1.29-1.20 (8H, m), 0.85 (4.1H, t, $J = 7.0\text{ Hz}$), 0.81 (1.9H, t, $J = 7.0\text{ Hz}$). UV-vis (CH_2Cl_2): λ_{max} ($\lg \epsilon$) 275 (4.74), 377 (4.51), 440 (4.73) nm. CV: $E^{\text{ox}}_{\text{pa}} = 0.54\text{ V}$, $E^{\text{ox}}_{\text{pc}} = 0.45\text{ V}$; $E^{\text{ox}}_{\text{pa}} = 0.67\text{ V}$, $E^{\text{ox}}_{\text{pc}} = 0.62\text{ V}$. MS (ES): m/z (%) 1187 (100, $[\text{M}+\text{K}]^+$), 1171 (31, $[\text{M}+\text{Na}]^+$), 1148 (28, M^+). Accurate Mass Calcd. for $\text{C}_{54}\text{H}_{52}\text{S}_{14}$: 1148.0159. HRMS (ES): 1148.0148 (-1.0 ppm).

Generation and ^1H NMR spectrum of the TTFAQ dimer tetracation 143^{4+} 

To half the volume of the NMR sample of **143** was added a solution of iodine (excess) in CDCl_3 after which a red precipitate formed. The precipitate was filtered, dried *in vacuo*, dissolved in $\text{DMSO-}d_6$ and the ^1H NMR spectrum of 143^{4+} was

recorded. ^1H NMR ($\text{DMSO-}d_6$): δ 8.15 (2H, s), 8.03-8.01 (2H, m), 7.76-7.74 (4H, m), 7.65-7.64 (2H, m), 7.50-7.43 (4H, m), 2.99 (12H, s), 2.81 (4H, t, $J = 7.5$ Hz), 1.54-1.47 (4H, m), 1.35-1.29 (4H, m), 1.23-1.17 (8H, m), 0.78 (6H, t, $J = 7.0$ Hz).

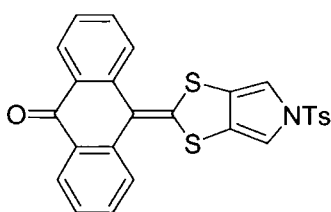
8.3 EXPERIMENTAL PROCEDURES TO CHAPTER 4

10-{4,6-Dihydro-*N*-tosylpyrrolo[3,4-d]-1,3-dithiol-2-ylidene}anthracene-9(10H)-one (169)

Sodium tosylamide **154**¹³⁷ (2.68 g, 13.9 mmol) was suspended in dry acetonitrile (50 mL) and stirred under argon at 80 °C. The dibromide **123** (3.33 g, 6.93 mmol) was dissolved in a minimum of dry *N,N*-dimethylformamide (200 mL) stirred at 80 °C and transferred to the sodium tosylamide suspension over 10 min using a double ended needle and a positive pressure of argon. The dark brown reaction mixture was stirred for another 5 min at 80 °C before it was cooled to 0 °C, using an ice bath, and concentrated under reduced pressure. To the residue was added water (150 mL) and the mixture was extracted with dichloromethane (3 x 100 mL). The combined organic phases were dried (MgSO_4), filtered through a plug of silica and concentrated *in vacuo*. Column chromatography (silica gel, dichloromethane until two minor by-products were off the column, then dichloromethane-ethyl acetate, 95:5 v/v) afforded **169** as an orange powder

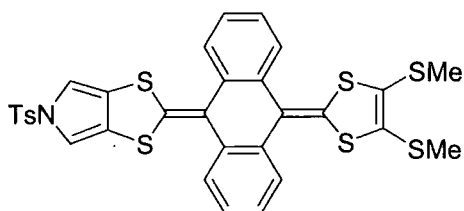
(2.77 g, 82%), mp 218-220 °C (decomp.). ^1H NMR (CDCl_3): δ 8.21 (2H, d, $J = 7.5$ Hz), 7.76 (2H, d, $J = 8.0$ Hz), 7.68 (2H, d, $J = 8.0$ Hz), 7.61 (2H, t, $J = 7.5$ Hz), 7.42 (2H, t, $J = 7.5$ Hz), 7.30 (2H, d, $J = 8.5$ Hz), 4.25 (4H, s), 2.39 (3H, s). ^{13}C NMR (CDCl_3): δ 183.4, 147.8, 144.3, 138.5, 133.3, 131.8, 130.6, 130.1, 127.3, 127.2, 127.1, 126.3, 126.0, 121.0, 52.4, 21.5. MS (EI): m/z (%) 489 (14, M^+), 91 (100). Accurate Mass Calcd. for $\text{C}_{26}\text{H}_{19}\text{NO}_3\text{S}_3$: 489.05271. HRMS (EI): 489.05200 (-1.5 ppm).

10-{*N*-Tosylpyrrolo[3,4-*d*]-1,3-dithiol-2-ylidene}anthracene-9(10H)-one (170)



To a suspension of **169** (8.70 g, 17.8 mmol) in chlorobenzene (200 mL) was added DDQ (4.84 g, 21.3 mmol) and the mixture was refluxed for 1 h. The reaction mixture was cooled to room temperature and reduced to 50 mL *in vacuo*. The resulting suspension was applied to a column (silica gel, dichloromethane) and chromatographed to give **170** as a yellow powder (7.98 g, 92%), mp 250-251 °C (decomp.). ^1H NMR (CDCl_3): δ 8.21 (2H, d, $J = 7.5$ Hz), 7.90 (2H, d, $J = 8.0$ Hz), 7.69 (2H, d, $J = 8.5$ Hz), 7.64 (2H, t, $J = 7.5$ Hz), 7.46 (2H, t, $J = 7.5$ Hz), 7.26 (2H, d, $J = 8.0$ Hz), 6.94 (2H, s), 2.38 (3H, s). ^{13}C NMR (CDCl_3): δ 183.9, 146.9, 145.6, 139.1, 135.2, 131.7, 131.1, 130.1, 127.4, 127.1, 126.9, 126.7, 125.7, 122.4, 110.8, 21.6. MS (PD): $m/z = 486.6$ (theory: 487.6). Anal. Calcd. for $\text{C}_{26}\text{H}_{17}\text{NO}_3\text{S}_3$ (MW 487.62): C, 64.04; H, 3.51; N, 2.87. Found C, 63.80; H, 3.35; N, 2.92.

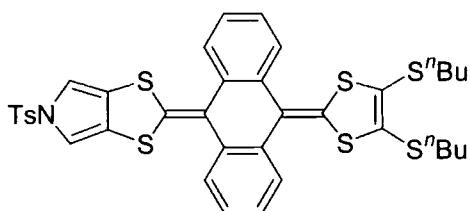
9-{*N*-Tosylpyrrolo[3,4-*d*]-1,3-dithiol-2-ylidene}-10-{4,5-bis(methylthio)-1,3-dithiol-2-ylidene}-9,10-dihydroanthracene (171)



To a solution of the phosphonate ester **63** (0.359 g, 1.18 mmol) in dry tetrahydrofuran (50 mL) at -78 °C under argon was added lithium diisopropylamide (0.86 mL of a 1.5 M solution in cyclohexane, 1.30 mmol) *via* syringe and the resultant cloudy yellow mixture was stirred for 1.5 h at -78 °C. Ketone **170** (0.500 g, 1.03 mmol) was dissolved in dry tetrahydrofuran (25 mL) and added to the reaction mixture *via* syringe over

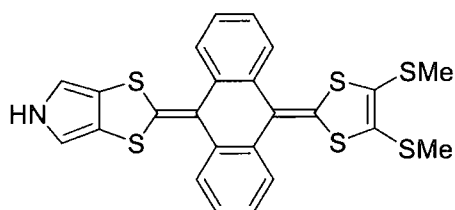
30 min. The reaction mixture was stirred at $-78\text{ }^{\circ}\text{C}$ for another 2 h, whereupon it was allowed to slowly attain room temperature for 12 h. Evaporation of the solvent afforded a red residue which was dissolved in dichloromethane (100 mL), washed with brine, dried (MgSO_4) and concentrated *in vacuo*. Column chromatography (silica gel, dichloromethane-cyclohexane, 2:1 v/v) afforded **171** as a yellow powder. Recrystallisation from dichloromethane-heptane gave yellow prisms, some of which were suitable for X-ray crystallography (0.590 g, 86%), mp $259\text{--}260\text{ }^{\circ}\text{C}$. ^1H NMR (CDCl_3): δ 7.69 (2H, d, $J = 8.4$ Hz), 7.66-7.64 (2H, m), 7.56-7.54 (2H, m), 7.33-7.30 (4H, m), 7.25 (2H, d, $J = 8.4$ Hz), 6.85 (2H, s), 2.38 (3H, s), 2.35 (6H, s). ^{13}C NMR (CDCl_3): δ 145.3, 138.8, 135.3, 134.9, 134.8, 131.5, 130.1, 126.9, 126.7, 126.6, 126.5, 126.3, 125.9, 125.7, 125.3, 123.3, 110.5, 21.6, 19.1. UV-vis (CH_2Cl_2): λ_{max} (lg ϵ) 353 (4.31), 422 (4.42) nm. CV: $E^{\text{ox}}_{\text{pa}} = 0.63$ V, $E^{\text{ox}}_{\text{pc}} = 0.45$ V. MS (PD): $m/z = 665.0$ (theory: 666.0). Anal. Calcd. for $\text{C}_{31}\text{H}_{23}\text{NO}_2\text{S}_7$ (MW 665.98): C, 55.91; H, 3.48; N, 2.10. Found C, 55.93; H, 3.42; N, 2.09.

9- $\{N$ -Tosylpyrrolo[3,4- d]-1,3-dithiol-2-ylidene}-10- $\{4,5$ -bis(butylthio)-1,3-dithiol-2-ylidene}-9,10-dihydroanthracene (172**)**



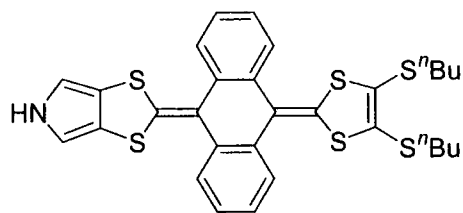
This procedure is similar to the synthesis of **171**. The phosphonate ester **64** (0.427 g, 1.10 mmol) in dry tetrahydrofuran (50 mL) was deprotonated using lithium diisopropylamide (0.81 mL of a 1.5 M solution in cyclohexane, 1.21 mmol) and reacted with ketone **170** (0.400 g, 0.82 mmol) in dry tetrahydrofuran (20 mL). Purification by column chromatography (silica gel, dichloromethane-cyclohexane, 1:1 v/v) afforded **172** as a yellow powder (0.560 g, 91%), mp $191\text{--}192\text{ }^{\circ}\text{C}$. ^1H NMR (CDCl_3): δ 7.69 (2H, d, $J = 8.5$ Hz), 7.66-7.64 (2H, m), 7.60-7.58 (2H, m), 7.33-7.30 (4H, m), 7.26 (2H, d, $J = 7.5$ Hz), 6.85 (2H, s), 2.84-2.72 (4H, m), 2.38 (3H, s), 1.61-1.55 (4H, m), 1.44-1.36 (4H, m), 0.89 (6H, t, $J = 7.5$ Hz). ^{13}C NMR (CDCl_3): δ 145.3, 138.6, 135.3, 135.0, 134.9, 132.0, 130.0, 126.9, 126.7, 126.62, 126.57, 126.2 (2C), 125.9, 125.2, 122.4, 110.5, 35.9, 31.7, 21.61, 21.58, 13.6. UV-vis (CH_2Cl_2): λ_{max} (lg ϵ) 353 (4.30), 423 (4.41) nm. CV: $E^{\text{ox}}_{\text{pa}} = 0.66$ V, $E^{\text{ox}}_{\text{pc}} = 0.46$ V. MS (EI): m/z (%) 749 (100, M^+). Accurate Mass Calcd. for $\text{C}_{37}\text{H}_{35}\text{NO}_2\text{S}_7$: 749.0713. HRMS (ES): 749.0725 (+1.6 ppm).

9-{Pyrrolo[3,4-d]-1,3-dithiol-2-ylidene}-10-{4,5-bis(methylthio)-1,3-dithiol-2-ylidene}-9,10-dihydroanthracene (173)



The tosylate **171** (0.500 g, 0.751 mmol) was dissolved in dry degassed tetrahydrofuran-methanol, 2:1 v/v (50 mL). Sodium methoxide (2.2 mL of a 30% solution in methanol, 11.3 mmol) was added to the solution and the reaction refluxed for 15 min under argon, in which time the colour changed from yellow to brown. The reaction mixture was cooled to room temperature, water was added (10 mL) and the mixture was concentrated to 10 mL under reduced pressure. The residue was taken into dichloromethane (100 mL), washed with water and brine, dried (MgSO₄) and concentrated *in vacuo*. Column chromatography (silica gel, dichloromethane-cyclohexane, 2:1 v/v) afforded **173** as a yellow powder which darkens upon standing (0.334 g, 87%), mp > 280 °C. ¹H NMR (CDCl₃): δ 8.17 (1H, br s), 7.78-7.76 (2H, m), 7.54-7.53 (2H, m), 7.35-7.29 (4H, m), 6.56 (2H, d, *J* = 2.5 Hz), 2.36 (6H, s). ¹³C NMR (CDCl₃): δ 142.2, 135.4, 134.9, 130.6, 126.2 (2C), 126.0, 125.8, 125.3, 124.6, 124.1, 119.1, 109.0, 19.2. UV-vis (CH₂Cl₂): λ_{max} (lg ε) 362 (4.21), 428 (4.46) nm. CV: *E*_{pa}^{ox} = 0.50 V, *E*_{pc}^{ox} = 0.35 V. MS (EI): *m/z* (%) 511 (100, M⁺). Anal. Calcd. for C₂₄H₁₇NS₆ (MW 511.79): C, 56.32; H, 3.35; N, 2.74. Found C, 56.54; H, 3.46; N, 2.76.

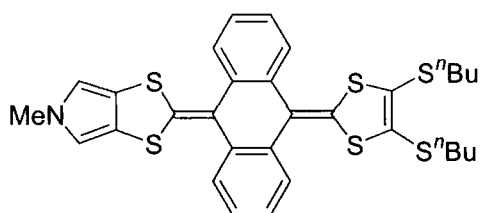
9-{Pyrrolo[3,4-d]-1,3-dithiol-2-ylidene}-10-{4,5-bis(butylthio)-1,3-dithiol-2-ylidene}-9,10-dihydroanthracene (174)



By a procedure similar to the conversion of **171** to **173**, tosylate **172** (1.60 g, 2.13 mmol) in dry degassed tetrahydrofuran-methanol, 2:1 v/v (100 mL) was treated with sodium methoxide (4.8 mL of a 30% solution in methanol, 25 mmol) to form **174**. Purification by column chromatography (silica gel, dichloromethane-cyclohexane, 1:2 v/v) afforded **174** as a yellow solid. Recrystallisation from dichloromethane-heptane gave yellow-brown prisms, some of which were suitable for X-ray crystallography, (1.05 g, 83%), mp 221-222 °C. ¹H NMR (CDCl₃): δ 8.13 (1H, br s), 7.77-7.75 (2H, m), 7.58-7.57 (2H, m), 7.34-7.29 (4H, m), 6.52 (2H, d, *J* = 2.5 Hz), 2.84-2.79 (2H, m), 2.77-2.71 (2H, m), 1.61-1.55 (4H,

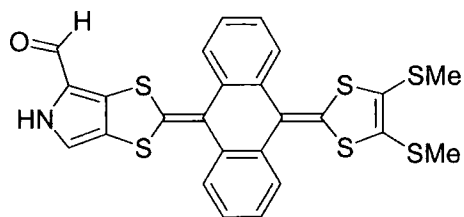
m), 1.44-1.36 (4H, m), 0.88 (6H, t, $J = 7.5$ Hz). ^{13}C NMR (CDCl_3): δ 142.0, 135.4, 135.0, 131.1, 126.2 (2C), 126.1, 126.0, 125.2, 124.6, 123.0, 119.0, 109.0, 36.0, 31.7, 21.6, 13.6. UV-vis (CH_2Cl_2): λ_{max} ($\lg \epsilon$) 368 (4.21), 429 (4.45) nm. CV: $E_{\text{pa}}^{\text{ox}} = 0.49$ V, $E_{\text{pc}}^{\text{ox}} = 0.34$ V. MS (PD): $m/z = 596.7$ (theory: 596.0). Anal. Calcd. for $\text{C}_{30}\text{H}_{29}\text{NS}_6$ (MW 595.95): C, 60.46; H, 4.90; N, 2.35. Found C, 60.17; H, 4.87; N, 2.27.

9- $\{N$ -Methylpyrrolo[3,4-d]-1,3-dithiol-2-ylidene}-10-\{4,5-bis(butylthio)-1,3-dithiol-2-ylidene}-9,10-dihydroanthracene (175)



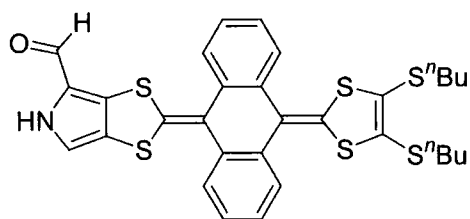
To a stirred suspension of sodium hydride (0.020 g of a 60% dispersion in mineral oil, 0.50 mmol) in dry degassed N,N -dimethylformamide (20 mL) under nitrogen was added a degassed solution of pyrrole **174** (0.100 g, 0.168 mmol) in dry N,N -dimethylformamide (10 mL) over 5 min, whereupon the reaction mixture turned red. The reaction was stirred for another 15 min at room temperature followed by addition of methyl iodide (0.10 mL, 0.227 g, 1.60 mmol) which caused the colour to turn yellow. Stirring was kept for a further 15 min after which time the reaction mixture was concentrated, taken into dichloromethane (50 mL), washed with water and dried (MgSO_4). Purification by column chromatography (silica gel, dichloromethane-cyclohexane, 1:1 v/v) afforded **175** as a yellow powder. Recrystallisation from dichloromethane-heptane gave yellow prisms, some of which were suitable for X-ray crystallography (0.099 g, 97%), mp 214-215 °C. ^1H NMR (CDCl_3): δ 7.77-7.75 (2H, m), 7.58-7.56 (2H, m), 7.33-7.28 (4H, m), 6.37 (2H, s), 3.60 (3H, s), 2.85-2.79 (2H, m), 2.77-2.72 (2H, m), 1.62-1.54 (4H, m), 1.45-1.37 (4H, m), 0.89 (6H, t, $J = 7.5$ Hz). ^{13}C NMR (CDCl_3): δ 141.9, 135.5, 135.0, 131.0, 126.2, 126.1, 126.0 (2C), 125.1, 124.4, 123.0, 118.0, 112.8, 37.1, 36.0, 31.7, 21.6, 13.6. UV-vis (CH_2Cl_2): λ_{max} ($\lg \epsilon$) 267 (4.32), 366 (4.19), 433 (4.46) nm. CV: $E_{\text{pa}}^{\text{ox}} = 0.50$ V, $E_{\text{pc}}^{\text{ox}} = 0.32$ V. MS (PD): $m/z = 611.4$ (theory: 610.0). Anal. Calcd. for $\text{C}_{31}\text{H}_{31}\text{NS}_6$ (MW 609.98): C, 61.04; H, 5.12; N, 2.30. Found C, 60.92; H, 5.17; N, 2.32.

9-{4-Formylpyrrolo[3,4-d]-1,3-dithiol-2-ylidene}-10-{4,5-bis(methylthio)-1,3-dithiol-2-ylidene}-9,10-dihydroanthracene (176)



Phosphorus oxychloride (0.042 mL, 0.069 g, 0.450 mmol) was added to dry *N,N*-dimethylformamide (2 mL) under nitrogen and stirred for 10 min at room temperature. A solution of pyrrolo-annelated TFAQ 173 (0.150 g, 0.293 mmol) in dry *N,N*-dimethylformamide (2 mL) was added dropwise over 5 min, whereupon the resulting dark violet reaction mixture was stirred for another 20 min. A 10% aqueous solution of sodium acetate (15 mL) and water (10 mL) was added to the reaction mixture, which caused precipitation of a yellow solid. The solid was filtered and redissolved in dichloromethane (50 mL), washed with water, dried (MgSO_4) and concentrated under reduced pressure. The crude product was columned (silica gel, dichloromethane-ethyl acetate, 1:1 v/v) to give **176** as a yellow powder (0.145 g, 92%), mp > 280 °C (yellow microcrystals from chlorobenzene-heptane, decomp.). ^1H NMR (CDCl_3): δ 9.45 (1H, s), 9.07 (1H, br s), 7.76-7.76 (2H, m), 7.60-7.56 (2H, m), 7.39-7.34 (4H, m), 6.83 (1H, d, $J = 2.8$ Hz), 2.37 (6H, s). UV-vis (CH_2Cl_2): λ_{max} (lg ϵ) 306 (4.36), 358 (4.18), 425 (4.45) nm. CV: $E^{\text{ox}}_{\text{pa}} = 0.55$ V, $E^{\text{ox}}_{\text{pc}} = 0.48$ V. MS (EI): m/z (%) 539 (100, M^+). Accurate Mass Calcd. for $\text{C}_{25}\text{H}_{17}\text{NOS}_6$: 538.96345. HRMS (EI): 538.96323 (-0.4 ppm).

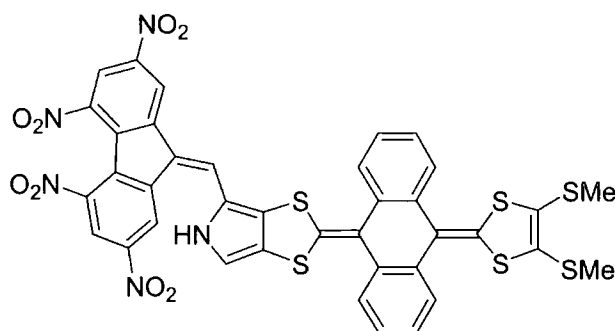
9-{4-Formylpyrrolo[3,4-d]-1,3-dithiol-2-ylidene}-10-{4,5-bis(butylthio)-1,3-dithiol-2-ylidene}-9,10-dihydroanthracene (177)



This procedure is similar to the synthesis of aldehyde **176**. Phosphorus oxychloride (0.036 mL, 0.059 g, 0.385 mmol) in dry *N,N*-dimethylformamide (2 mL) was reacted with a solution of **174** (0.153 g, 0.257 mmol) in dry *N,N*-dimethylformamide (2 mL). Purification by column chromatography (silica gel, dichloromethane-ethyl acetate, 1:1 v/v) afforded **177** as a yellow powder (0.146 g, 91%), mp 169-170 °C. ^1H NMR (CDCl_3): δ 9.86 (1H, br s), 9.32 (1H, s), 7.73-7.59 (4H, m), 7.36-7.31 (4H, m), 6.74 (1H, br s), 2.83-2.69 (4H, m), 1.59-1.50 (4H, m), 1.41-1.33 (4H, m), 0.88-0.85 (6H, m). UV-vis

(CH₂Cl₂): λ_{\max} (lg ϵ) 306 (4.37), 359 (4.20), 427 (4.46) nm. CV: $E^{\text{ox}}_{\text{pa}} = 0.58$ V, $E^{\text{ox}}_{\text{pc}} = 0.47$ V. MS (PD): $m/z = 622.9$ (theory: 624.0). Anal. Calcd. for C₃₁H₂₉NOS₆ (MW 623.96): C, 59.67; H, 4.68; N, 2.24. Found C, 59.82; H, 4.75; N, 2.23.

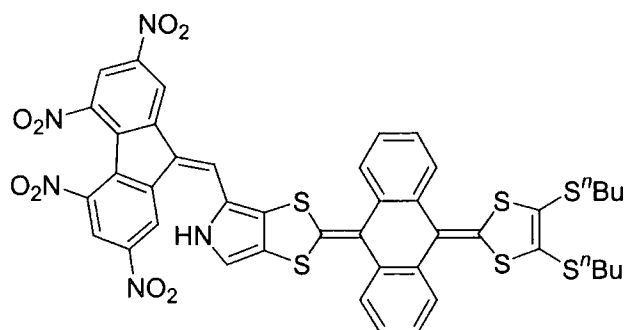
PyrroloTTFAQ fluorene adduct **179**



TTFAQ Aldehyde **176** (0.038 g, 0.070 mmol) and 2,4,5,7-tetranitrofluorene **178**¹³⁸ (0.029 g, 0.084 mmol) were dissolved in dry degassed *N,N*-dimethylformamide (2 mL) and stirred at room temperature under argon for 2.5 h. The black mixture was concentrated *in vacuo* and the residue

purified by column chromatography (silica gel, dichloromethane) to give **179** as a black powder (0.049 g, 80%), mp > 280 °C. ¹H NMR (DMSO-*d*₆): δ 12.32 (1H, s), 9.57 (1H, s), 9.16 (1H, s), 8.77-8.66 (2H, m), 7.74-7.65 (3H, m), 7.58-7.55 (3H, m), 7.48-7.41 (4H, m), 2.36-2.33 (6H, m). UV-vis (CH₂Cl₂): λ_{\max} (lg ϵ) 356 (4.51), 427 (4.47), 539 (4.22) nm. CV: $E^{\text{ox}}_{\text{pa}} = 0.63$ V, $E^{\text{ox}}_{\text{pc}} = 0.42$ V, $E^{\text{red}}_{\text{pc}} = -0.41$ V. MS (PD): $m/z = 867.8$ (theory: 868.0). Accurate Mass Calcd. for C₃₈H₂₁N₅O₈S₆: 866.97144. HRMS (EI): 866.97188 (+0.5 ppm).

PyrroloTTFAQ fluorene adduct **180**



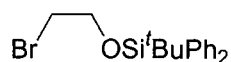
This procedure is similar to the synthesis of **179**. TTFAQ Aldehyde **177** (0.025 g, 0.040 mmol) and 2,4,5,7-tetranitrofluorene **178**¹³⁸ (0.015 g, 0.043 mmol) were reacted in dry degassed *N,N*-dimethylformamide (2 mL) to give a black residue. Purification by column

chromatography (silica gel, dichloromethane) afforded **180** as a black powder (0.033 g, 87%), mp 192-194 °C (decomp.). ¹H NMR (CDCl₃): δ 9.05 (0.2H, s), 8.91 (0.2H, s), 8.83 (0.8H, s),

8.74 (0.8H, s), 8.70 (2H, s), 8.52 (1H, br s), 7.64-7.58 (4H, m), 7.48-7.41 (3H, m), 7.31-7.19 (2H, m), 6.87 (1H, s), 2.73-2.70 (4H, m), 1.53-1.47 (4H, m), 1.39-1.29 (4H, m), 0.89-0.81 (6H, m).¹⁸⁷ UV-vis (CH₂Cl₂): λ_{\max} (lg ϵ) 357 (4.50), 428 (4.48), 538 (4.23) nm. CV: $E^{\text{ox}}_{\text{pa}} = 0.64$ V, $E^{\text{ox}}_{\text{pc}} = 0.45$ V, $E^{\text{red}}_{\text{pc}} = -0.41$ V. MS (PD): $m/z = 951.2$ (theory: 952.2). Anal. Calcd. for C₄₄H₃₃N₅O₈S₆ (MW 952.16): C, 55.50; H, 3.49; N, 7.36. Found C, 55.51; H, 3.67; N, 7.22.

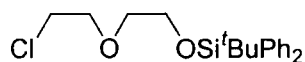
8.4 EXPERIMENTAL PROCEDURES TO CHAPTER 5

1-Bromo-2-[(*tert*-butyldiphenylsilyl)oxy]ethane (**195**)¹⁸⁸



To a solution of 2-bromoethanol **193** (10.62 g, 85.0 mmol) and imidazole (27.2 g, 400 mmol) in dry *N,N*-dimethylformamide (50 mL) was added *tert*-butyldiphenylchlorosilane (21.99 g, 80.0 mmol) and the reaction was stirred for 16 h at room temperature. The solution was poured onto water (500 mL) and extracted with hexane (3 x 150 mL). The combined organic phases were washed with brine, dried (MgSO₄) and concentrated *in vacuo* to give a yellow oil. Purification by chromatography using a short column (silica gel, dichloromethane-hexane, 1:3 v/v) afforded **195** as a colourless oil (26.64 g, 92%). ¹H NMR (CDCl₃): δ 7.72-7.69 (4H, m), 7.46-7.38 (6H, m), 3.95 (2H, t, $J = 6.6$ Hz), 3.44 (2H, t, $J = 6.6$ Hz), 1.10 (9H, s).

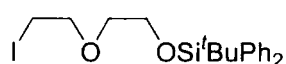
1-Chloro-2-{2-[(*tert*-butyldiphenylsilyl)oxy]ethoxy}ethane (**196**)



This procedure is similar to the synthesis of **195**. 2-(2-Chloroethoxy)-ethanol **194** (9.97 g, 80.0 mmol) and *tert*-butyldiphenylchlorosilane (20.61 g, 75.0 mmol) were reacted in dry *N,N*-dimethylformamide (50 mL) in the presence of imidazole (27.2 g, 400 mmol). Purification by chromatography using a short column (silica gel, dichloromethane-hexane, 1:3 v/v) afforded **196** as a colourless oil (24.47 g, 90%). ¹H NMR (CDCl₃): δ 7.72-7.70 (4H, m), 7.44-7.40 (6H, m), 3.84 (2H, t, $J = 5.6$ Hz), 3.77 (2H, t, $J = 6.0$ Hz), 3.64 (2H, t, $J = 5.6$ Hz),

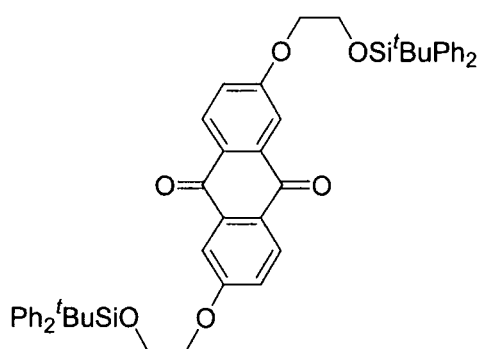
3.61 (2H, t, $J = 6.0$ Hz), 1.08 (9H, s). ^{13}C NMR (CDCl_3): δ 135.6, 133.5, 129.6, 127.6, 72.5, 71.4, 63.5, 42.8, 26.8, 19.2. MS (CI): m/z (%) 380 (67, MNH_4^+), 285 (100). Anal. Calcd. for $\text{C}_{20}\text{H}_{27}\text{ClO}_2\text{Si}$ (MW 362.97): C, 66.18; H, 7.50. Found C, 66.04; H, 7.45.

1-Iodo-2-[(*tert*-butyldiphenylsilyl)oxy]ethane (**197**)



To a solution of compound **196** (24.30 g, 67 mmol) in dry 2-butanone (100 mL) was added sodium iodide (15.0 g, 100 mmol). The suspension was refluxed under argon for 48 h, concentrated *in vacuo*, and redissolved in dichloromethane (300 mL). The solution was washed with water and brine, dried (MgSO_4) and filtered through a plug of silica. Evaporation of the solvent *in vacuo* afforded **197** as a colourless oil (29.80 g, 98%). ^1H NMR (CDCl_3): δ 7.72-7.70 (4H, m), 7.44-7.38 (6H, m), 3.83 (2H, t, $J = 5.0$ Hz), 3.77 (2H, t, $J = 6.5$ Hz), 3.63 (2H, t, $J = 5.0$ Hz), 3.23 (2H, t, $J = 6.5$ Hz), 1.08 (9H, s). ^{13}C NMR (CDCl_3): δ 135.6, 133.5, 129.6, 127.6, 72.1, 72.0, 63.5, 26.8, 19.1, 3.1. MS (CI): m/z (%) 472 (48, MNH_4^+), 251 (100). Anal. Calcd. for $\text{C}_{20}\text{H}_{27}\text{IO}_2\text{Si}$ (MW 454.42): C, 52.86; H, 5.99. Found C, 52.95; H, 5.98.

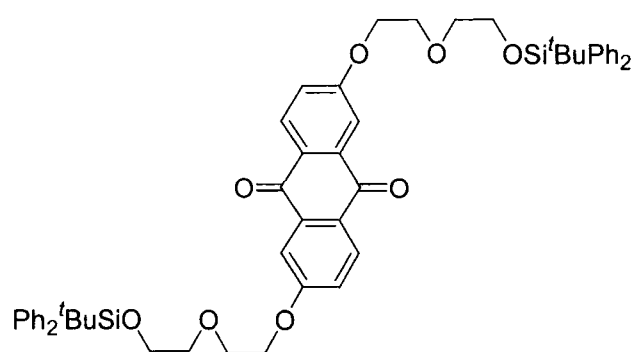
2,6-Bis{2-[(*tert*-butyldiphenylsilyl)oxy]ethoxy}anthraquinone (**199**)



To a mixture of 1-bromo-2-[(*tert*-butyldiphenylsilyl)oxy]ethane **195** (16.35 g, 45.0 mmol) and potassium carbonate (4.15 g, 30.0 mmol) in dry degassed *N,N*-dimethylformamide (20 mL) was added anthraflavic acid **198** (3.60 g, 15.0 mmol). The reaction mixture was stirred under argon at 100 °C for 16 h, which made the colour change from yellow to dark red, diluted with dichloromethane (300 mL) and washed with brine. The organic phase was dried (MgSO_4) and filtered through a plug of silica to give a yellow solution, which was concentrated *in vacuo*. The oily residue was purified by column chromatography (silica gel, dichloromethane-hexane, 1:1 v/v) and concentration *in vacuo* of the first yellow fraction afforded **199** as a pale yellow solid (9.18 g, 76%), mp 133-134 °C. ^1H NMR (CDCl_3): δ 8.23 (2H, d, $J = 8.8$ Hz), 7.80-7.78 (8H, m), 7.72

(2H, d, $J = 2.4$ Hz), 7.47-7.42 (12H, m), 7.19 (2H, dd, $J_1 = 2.4$ Hz, $J_2 = 8.8$ Hz), 4.29 (4H, t, $J = 4.8$ Hz), 4.10 (4H, t, $J = 4.8$ Hz), 1.14 (18H, s). ^{13}C NMR (CDCl_3): δ 181.8, 163.6, 135.6, 135.5, 133.2, 129.7, 129.5, 127.6, 126.9, 120.7, 110.5, 69.6, 62.3, 26.7, 19.1. MS (CI): m/z (%) 805 (13, MH^+), 729 (100). Anal. Calcd. for $\text{C}_{50}\text{H}_{52}\text{O}_6\text{Si}_2$ (MW 805.12): C, 74.59; H, 6.51. Found C, 74.32; H, 6.56.

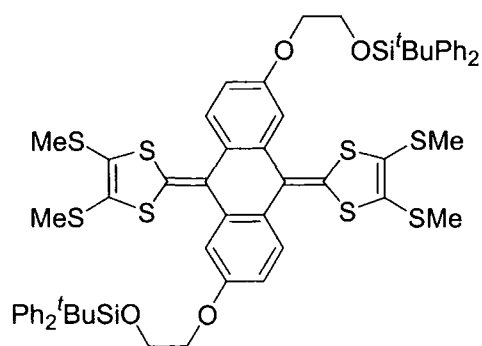
2,6-Bis{2-[2-[(*tert*-butyldiphenylsilyl)oxy]ethoxy]ethoxy}anthraquinone (200)



By a procedure similar to the synthesis of **199**, compound **200** was obtained from the reaction of anthraflavic acid **198** (3.60 g, 15.0 mmol) with linker **197** (20.45 g, 45.0 mmol) in the presence of potassium carbonate (4.15 g, 30.0 mmol). Purification by column chromatography (silica gel, dichloromethane) afforded

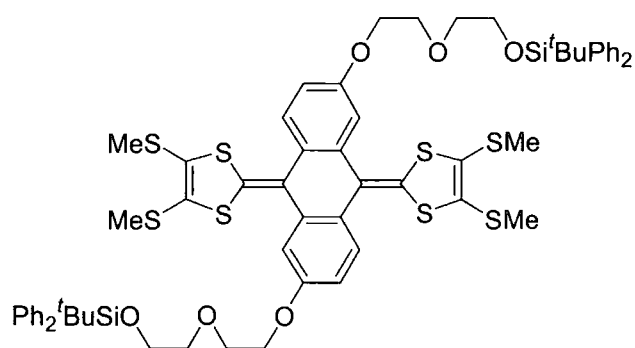
200 as a pale yellow solid (11.64 g, 87%), mp 103-104 °C. ^1H NMR (CDCl_3): δ 8.22 (2H, d, $J = 8.8$ Hz), 7.72 (2H, d, $J = 2.8$ Hz), 7.70-7.68 (8H, m), 7.42-7.34 (12H, m), 7.24 (2H, dd, $J_1 = 2.8$ Hz, $J_2 = 8.8$ Hz), 4.26 (4H, t, $J = 4.6$ Hz), 3.91 (4H, t, $J = 4.6$ Hz), 3.85 (4H, t, $J = 5.2$ Hz), 3.69 (4H, t, $J = 5.2$ Hz), 1.05 (18H, s). ^{13}C NMR (CDCl_3): δ 182.2, 163.7, 135.7, 135.6, 133.6, 129.6, 129.6, 127.6, 127.2, 121.2, 110.5, 72.7, 69.4, 68.2, 63.5, 26.8, 19.2. MS (CI): m/z (%) 910 (10, MNH_4^+), 61 (100). Anal. Calcd. for $\text{C}_{54}\text{H}_{60}\text{O}_8\text{Si}_2$ (MW 893.22): C, 72.61; H, 6.77. Found C, 72.52; H, 6.76.

2,6-Bis{2-[(*tert*-butyldiphenylsilyl)oxy]ethoxy}-9,10-bis[4,5-bis(methylthio)-1,3-dithiol-2-ylidene]-9,10-dihydroanthracene (201)



To a solution of phosphonate ester **63** (1.72 g, 5.66 mmol) in dry tetrahydrofuran (100 mL) at $-78\text{ }^{\circ}\text{C}$ under argon was added lithium diisopropylamide (4.14 mL of a 1.5 M solution in cyclohexane, 6.22 mmol) *via* syringe and the resultant cloudy yellow mixture was stirred for 2 h at $-78\text{ }^{\circ}\text{C}$. Compound **199** (1.90 g, 2.36 mmol) was dissolved in dry tetrahydrofuran (30 mL) and added to the reaction mixture *via* syringe over 15 min. The reaction mixture was stirred at $-78\text{ }^{\circ}\text{C}$ for another 2 h, whereupon it was allowed to slowly attain room temperature over 12 h. Evaporation of the solvent gave a red residue which was dissolved in dichloromethane (200 mL), washed with water and brine, dried (MgSO_4) and concentrated *in vacuo*. Column chromatography (silica gel, dichloromethane-hexane, 1:1 v/v) afforded **201** as a yellow foam (1.89 g, 69%), mp $82\text{--}85\text{ }^{\circ}\text{C}$. ^1H NMR (CDCl_3): δ 7.78–7.76 (8H, m), 7.48 (2H, d, $J = 8.4\text{ Hz}$), 7.46–7.40 (12H, m), 7.12 (2H, d, $J = 2.8\text{ Hz}$), 6.84 (2H, dd, $J_1 = 2.8\text{ Hz}$, $J_2 = 8.4\text{ Hz}$), 4.23–4.16 (4H, m), 4.07 (4H, t, $J = 5.2\text{ Hz}$), 2.41 (6H, s), 2.37 (6H, s), 1.12 (18H, s). ^{13}C NMR (CDCl_3): δ 157.1, 136.2, 135.6, 133.4, 129.6, 129.1, 127.7, 127.5, 126.5, 125.7, 125.5, 123.5, 111.9, 111.7, 69.2, 62.6, 26.8, 19.2, 19.04, 19.01. CV (MeCN): $E^{\text{ox}}_{\text{pa}} = 0.47\text{ V}$, $E^{\text{ox}}_{\text{pc}} = 0.34\text{ V}$. MS (CI): m/z (%) 1161 (13, MH^+), 283 (100). Anal. Calcd. for $\text{C}_{60}\text{H}_{64}\text{O}_4\text{S}_8\text{Si}_2$ (MW 1161.85): C, 62.03; H, 5.55. Found C, 61.65; H, 5.54.

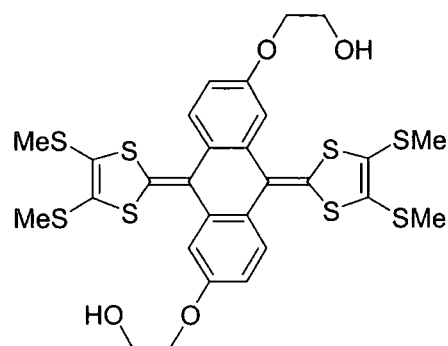
2,6-Bis{2-{2-[(*tert*-butyldiphenylsilyl)oxy]ethoxy}ethoxy}-9,10-bis[4,5-bis(methylthio)-1,3-dithiol-2-ylidene]-9,10-dihydroanthracene (202)



This procedure is similar to the synthesis of **201**. The phosphonate ester **63** (4.00 g, 13.1 mmol) was deprotonated using lithium diisopropylamide (9.60 mL of a 1.5 M solution in cyclohexane, 14.4 mmol) and reacted with compound **200** (4.70 g, 5.26 mmol).

Purification by column chromatography (silica gel, dichloromethane-hexane, 3:1 v/v) afforded **202** as a yellow foam (5.33 g, 81%), mp 51-54 °C. ¹H NMR (CDCl₃): δ = 7.71-7.68 (8H, m), 7.43 (2H, d, *J* = 8.8 Hz), 7.41-7.34 (12H, m), 7.07 (2H, d, *J* = 2.4 Hz), 6.83 (2H, dd, *J*₁ = 2.4 Hz, *J*₂ = 8.8 Hz), 4.15 (4H, t, *J* = 4.8 Hz), 3.89-3.84 (8H, m), 3.69 (4H, t, *J* = 5.2 Hz), 2.38 (6H, s), 2.34 (6H, s), 1.06 (18H, s). ¹³C NMR (CDCl₃): δ 157.1, 136.2, 135.6, 133.6, 129.6, 129.2, 127.7, 127.6, 126.6, 126.1, 125.4, 123.5, 112.2, 111.5, 72.7, 69.7, 67.7, 63.5, 26.8, 19.18, 19.16, 19.1. CV (MeCN): *E*^{ox}_{pa} = 0.46 V, *E*^{ox}_{pc} = 0.37 V. MS (CI): *m/z* (%) 1249 (14, MH⁺), 283 (100). Anal. Calcd. for C₆₄H₇₂O₆S₈Si₂ (1249.95): C, 61.50; H, 5.81. Found C, 61.23; H, 5.84.

2,6-Bis(2-hydroxyethoxy)-9,10-bis[4,5-bis(methylthio)-1,3-dithiol-2-ylidene]-9,10-dihydroanthracene (203)

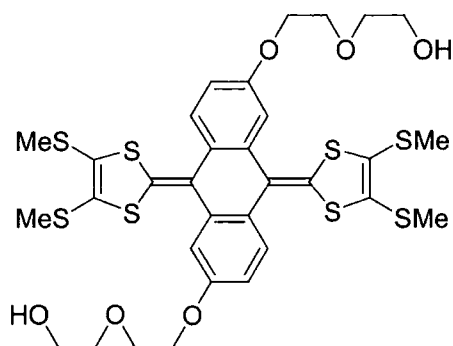


Compound **201** (1.70 g, 1.47 mmol) was dissolved in dry tetrahydrofuran (20 mL) and stirred under argon at room temperature. A solution of tetrabutylammonium fluoride (4.40 mL of a 1.0 M solution in tetrahydrofuran, 4.40 mmol) was added dropwise *via* syringe over 15 min, causing the reaction mixture to change colour from yellow to brown. Further stirring for 1.5 h, followed by addition of a few drops of water (0.1 mL)

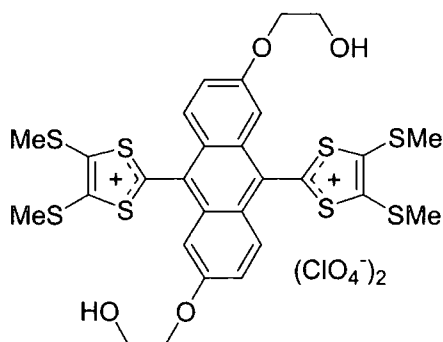
and evaporation of the solvent, afforded a brown residue. The residue was dissolved in dichloromethane (200 mL), washed with water and brine, dried (MgSO₄) and concentrated *in*

vacuo. Chromatography using a short column (silica gel, dichloromethane until no more by-products were visible on the column, then dichloromethane-ethyl acetate, 3:1 v/v) afforded **203** as a yellow solid (0.938 g, 93%), mp 147-150 °C. Yellow-brown prisms, suitable for X-ray crystallographic analysis, were grown by slow diffusion of hexane into a solution of **203** in dichloromethane. ^1H NMR (CDCl_3): δ 7.44 (2H, d, $J = 8.8$ Hz), 7.08 (2H, d, $J = 2.4$ Hz), 6.84 (2H, dd, $J_1 = 2.4$ Hz, $J_2 = 8.8$ Hz), 4.15 (4H, t, $J = 4.8$ Hz), 4.01 (4H, t, $J = 4.8$ Hz), 2.39 (12H, s), 1.94 (2H, br s). ^{13}C NMR (CDCl_3): δ 156.9, 136.3, 129.6, 128.0, 126.7, 126.3, 125.3, 123.2, 112.0, 111.6, 69.4, 61.4, 19.2, 19.1. UV-vis (CH_2Cl_2): λ_{max} (lg ϵ) 364 (4.18), 432 (4.40) nm. CV (MeCN): $E_{\text{pa}}^{\text{ox}} = 0.47$ V, $E_{\text{pc}}^{\text{ox}} = 0.29$ V. MS (EI): m/z (%) 684 (100, M^+). Anal. Calcd. for $\text{C}_{28}\text{H}_{28}\text{O}_4\text{S}_8$ (MW 685.05): C, 49.09; H, 4.12. Found C, 49.10; H, 4.20.

2,6-Bis[2-(2-hydroxyethoxy)ethoxy]-9,10-bis[4,5-bis(methylthio)-1,3-dithiol-2-ylidene]-9,10-dihydroanthracene (204)

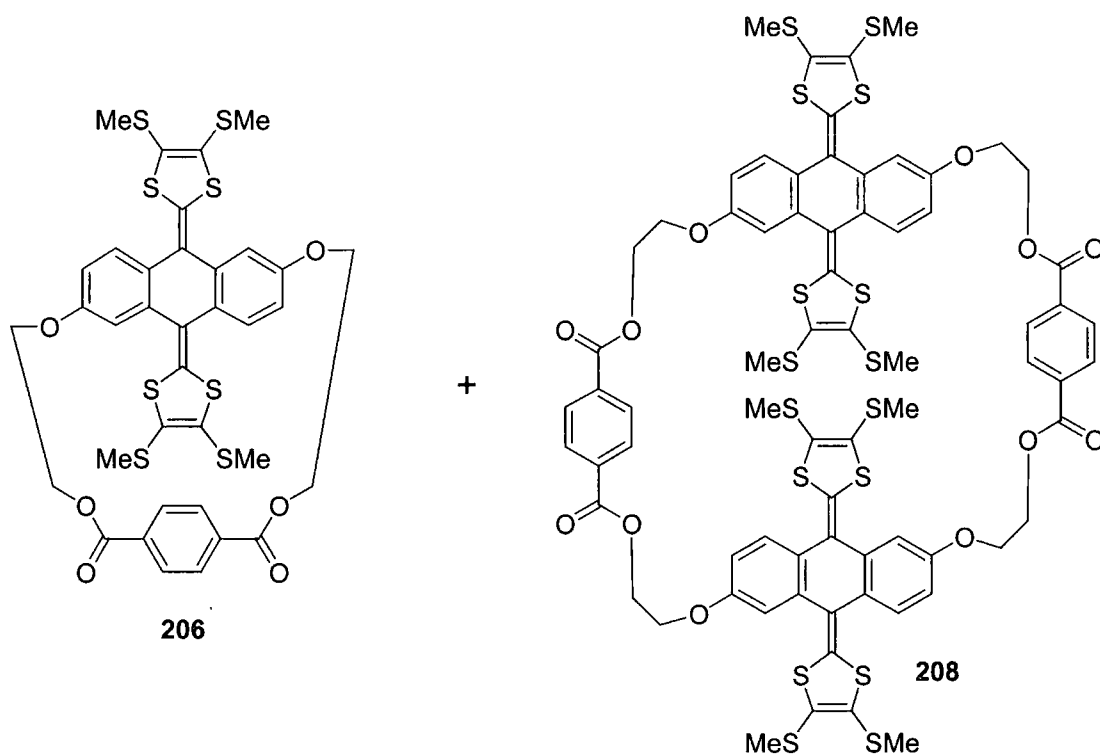


By a similar procedure to the conversion of **201** to **203**, compound **202** (5.00 g, 4.00 mmol) was treated with tetrabutylammonium fluoride (12.0 mL of a 1.0 M solution in tetrahydrofuran, 12.0 mmol) to form **204**. Purification by chromatography using a short column (silica gel, dichloromethane until no more by-products were visible on the column, then ethyl acetate) afforded **204** as a yellow solid (2.68 g, 87%), mp 204-205 °C. ^1H NMR (CDCl_3): δ 7.43 (2H, d, $J = 8.8$ Hz), 7.07 (2H, d, $J = 2.8$ Hz), 6.84 (2H, dd, $J_1 = 2.4$ Hz, $J_2 = 8.4$ Hz), 4.20 (4H, t, $J = 4.8$ Hz), 3.90 (4H, t, $J = 4.8$ Hz), 3.78 (4H, t, $J = 4.8$ Hz), 3.69 (4H, t, $J = 4.8$ Hz), 2.38 (12H, s), 1.98 (2H, br s). ^{13}C NMR (CDCl_3): δ 156.9, 136.3, 129.4, 127.8, 126.6, 126.3, 125.3, 123.3, 112.2, 111.6, 72.6, 69.6, 67.6, 61.8, 19.2, 19.1. UV-vis (CH_2Cl_2): λ_{max} (lg ϵ) 364 (4.18), 432 (4.41) nm. CV (MeCN): $E_{\text{pa}}^{\text{ox}} = 0.46$ V, $E_{\text{pc}}^{\text{ox}} = 0.36$ V. MS (EI): m/z (%) 772 (100, M^+). Anal. Calcd. for $\text{C}_{32}\text{H}_{36}\text{O}_6\text{S}_8$ (MW 773.15): C, 49.71; H, 4.69. Found C, 49.77; H, 4.73.

Preparation of $203^{2+}(\text{ClO}_4^-)_2$ 

Dry tetrabutylammonium perchlorate (50 mg) was added to each chamber of a glass electrocrystallisation cell, in which the two chambers were separated by a glass frit, and the cell was flushed with argon. Compound **203** (5 mg) was placed in the anodic chamber and dry degassed dichloromethane (7 mL) was added to each chamber of the cell. The platinum electrodes were mounted, sealing the solutions from

the atmosphere. A potential of 1.0 V was applied, which provided an initial current of 1.0 μA . The cell was stored in the dark for 14 days at 20 $^\circ\text{C}$, during which time the current dropped to 0.2 μA and red needles of $203^{2+}(\text{ClO}_4^-)_2$ grew on the anode. The crystals, which were suitable for X-ray crystallography, were harvested and washed with dry dichloromethane.

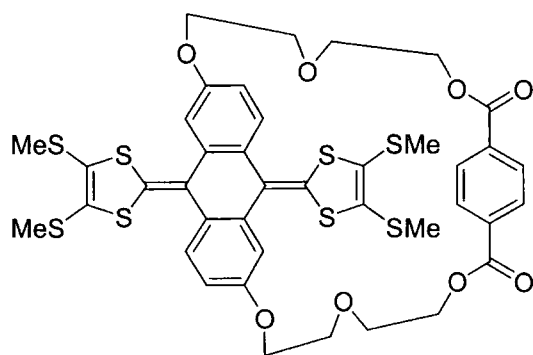
TTFAQ cyclophane **206** and TTFAQ cyclophane **208**

To a solution of diol **203** (0.300 g, 0.438 mmol) and 1,4-benzenedicarbonyl chloride **205** (0.089 g, 0.438 mmol) in dry dichloromethane (300 mL) was added triethylamine (0.50 mL,

excess) and the reaction was stirred under argon for 16 h at room temperature. The solution was concentrated *in vacuo* and the orange residue purified by column chromatography (silica gel, dichloromethane). The fractions containing the first yellow band were concentrated *in vacuo* to give **206** as a yellow powder (0.141 g, 39%). Orange-yellow prisms, suitable for X-ray crystallographic analysis, were grown by slow diffusion of hexane into a solution of **206** in dichloromethane, mp > 260 °C. ¹H NMR (CDCl₃): δ 7.38 (2H, d, *J* = 8.4 Hz), 7.36 (2H, d, *J* = 2.4 Hz), 6.95 (2H, dd, *J*₁ = 2.4 Hz, *J*₂ = 8.4 Hz), 6.89 (4H, s), 4.67-4.55 (6H, m), 4.47-4.41 (2H, m), 2.39 (6H, s), 2.38 (6H, s). ¹³C NMR (CDCl₃): δ 165.0, 158.3, 136.6, 132.9, 130.1, 128.8, 128.7, 126.6, 125.9, 125.6, 122.5, 115.3, 114.2, 67.0, 66.2, 19.1, 19.0. UV-vis (CH₂Cl₂): λ_{max} (lg ε) 368 (4.36), 436 (4.55) nm. CV (MeCN): *E*^{ox}_{pa} = 0.52 V, *E*^{ox}_{pc} = 0.41 V. MS (EI): *m/z* (%) 814 (100, M⁺). Anal. Calcd. for C₃₆H₃₀O₆S₈ (MW 815.15): C, 53.04; H, 3.71. Found C, 52.81; H, 3.68.

The second yellow broad band was collected, concentrated *in vacuo* and rechromatographed (silica gel, dichloromethane-ethyl acetate 98:2 v/v) affording **208** as a yellow powder (0.083 g, 23%), mp 222-227 °C (decomp.). Orange prisms, suitable for X-ray crystallographic analysis, were grown by slow diffusion of hexane into a solution of **208** in dichloromethane. ¹H NMR (CDCl₃): δ 7.98 (4H, s), 7.94 (4H, s), 7.412 (2H, d, *J* = 8.4 Hz), 7.408 (2H, d, *J* = 8.8 Hz), 7.10 (4H, d, *J* = 2.4 Hz), 6.87 (2H, dd, *J*₁ = 2.8 Hz, *J*₂ = 8.4 Hz), 6.85 (2H, dd, *J*₁ = 2.8 Hz, *J*₂ = 8.4 Hz), 4.76-4.68 (8H, br m), 4.42-4.38 (8H, br m), 2.34-2.33 (24H, m). UV-vis (CH₂Cl₂): λ_{max} (lg ε) 368 (4.53), 432 (4.73) nm. CV (MeCN): *E*^{ox}_{pa} = 0.51 V, *E*^{ox}_{pc} = 0.37 V. MS (EI): *m/z* (%) 1628 (1, M⁺), 182 (100). Anal. Calcd. for C₇₂H₆₀O₁₂S₁₆ (MW 1630.30): C, 53.04; H, 3.71. Found C, 52.77; H, 3.67.

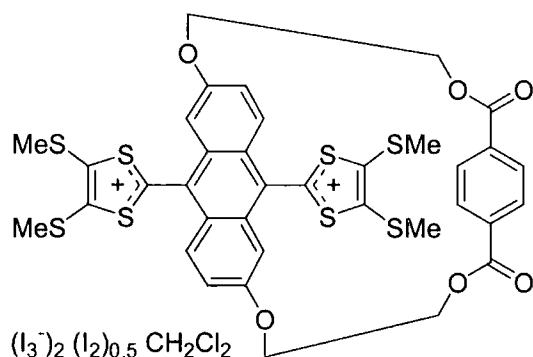
TTFAQ cyclophane **207**



By a similar procedure to the conversion of **203** to **206**, diol **204** (0.250 g, 0.320 mmol) was reacted with 1,4-benzenedicarbonyl chloride **205** (0.066 g, 0.320 mmol) in the presence of excess triethylamine. Purification by column chromatography (silica gel, dichloromethane-ethyl acetate, 95:5 v/v) afforded **207** as a

yellow powder (0.083 g, 28%). Yellow prisms, suitable for X-ray crystallographic analysis, were grown by slow diffusion of hexane into a solution of **207** in dichloromethane, mp 209-211 °C. ^1H NMR (CDCl_3): δ 7.35 (4H, s), 7.26 (2H, d, $J = 3.2$ Hz), 7.20 (2H, d, $J = 8.4$ Hz), 6.70 (2H, dd, $J_1 = 2.4$ Hz, $J_2 = 8.4$ Hz), 4.58-4.54 (2H, m), 4.41-4.37 (2H, m), 4.31-4.28 (4H, m), 4.06-4.02 (2H, m), 3.92-3.83 (6H, m), 2.373 (6H, s), 2.367 (6H, s). ^{13}C NMR (CDCl_3): δ 165.6, 157.3, 136.0, 133.0, 129.0, 128.9, 127.5, 126.3, 126.2, 125.3, 123.6, 113.2, 111.9, 70.1, 69.6, 69.2, 64.8, 19.2, 19.0. UV-vis (CH_2Cl_2): λ_{max} ($\lg \epsilon$) 364 (4.37), 432 (4.58) nm. CV (MeCN): $E^{\text{ox}}_{\text{pa}} = 0.47$ V, $E^{\text{ox}}_{\text{pc}} = 0.33$ V. MS (EI): m/z (%) 902 (100, M^+). Anal. Calcd. for $\text{C}_{40}\text{H}_{38}\text{O}_8\text{S}_8$ (MW 903.25): C, 53.19; H, 4.24; found C, 52.87; H, 4.21.

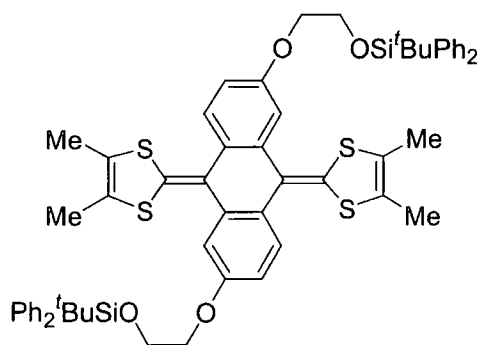
Preparation of an iodide salt of **206**



A 10 mM solution of cyclophane **206** (2 mL) in dichloromethane was placed in a 5 mL open sample vial which again was placed in a sealed 250 mL sample vial containing iodine crystals (0.5 g). Diffusion of iodine vapour into the cyclophane solution caused formation of black shiny needles which after 2 days were big enough for an X-ray crystallographic analysis,

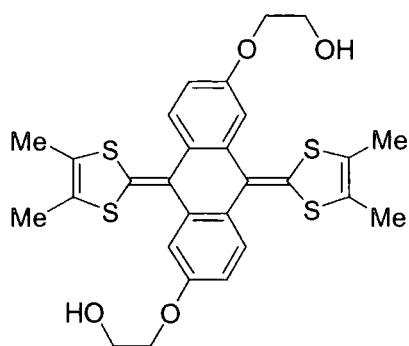
mp 195-197 °C (decomp.). Anal. Calcd. for $\text{C}_{36}\text{H}_{30}\text{O}_6\text{S}_8(\text{I}_3)_2(\text{I}_2)_{0.5}\text{CH}_2\text{Cl}_2$: C, 24.85; H, 1.80. Found C, 24.95; H, 1.75.

2,6-Bis{2-[(*tert*-butyldiphenylsilyl)oxy]ethoxy}-9,10-bis(4,5-dimethyl-1,3-dithiol-2-ylidene)-9,10-dihydroanthracene (209)



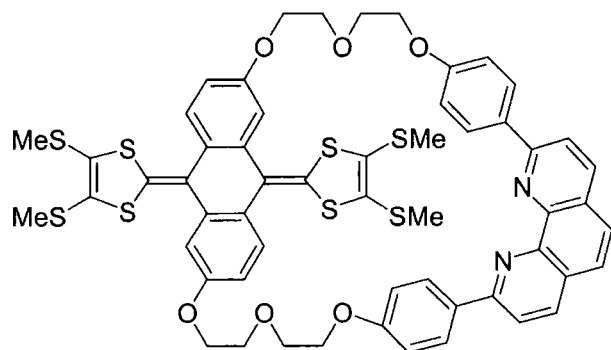
To a solution of the phosphonate ester **68**⁸⁶ (4.15 g, 17.3 mmol) in dry tetrahydrofuran (200 mL) at $-78\text{ }^{\circ}\text{C}$ under argon was added lithium diisopropylamide (12.7 mL of a 1.5 M solution in cyclohexane, 19.0 mmol) *via* syringe and the resultant cloudy yellow brown mixture was stirred for 1 h at $-78\text{ }^{\circ}\text{C}$. Compound **199** (5.56 g, 6.90 mmol) was dissolved in dry tetrahydrofuran (50 mL) and added to the reaction mixture *via* syringe over 30 min. The reaction mixture was stirred at $-78\text{ }^{\circ}\text{C}$ for another 1 h, whereupon it was allowed to attain room temperature over 12 h. Evaporation of the solvent gave a red residue which was dissolved in dichloromethane (300 mL), washed with water and brine, dried (MgSO_4) and concentrated *in vacuo*. Column chromatography (silica gel, dichloromethane-hexane, 1:1 v/v) afforded **209** as a yellow foam (4.13 g, 58%), mp $128\text{--}131\text{ }^{\circ}\text{C}$ (from chloroform-methanol). ^1H NMR (CDCl_3): δ 7.76–7.74 (8H, m), 7.52 (2H, d, $J = 8.4\text{ Hz}$), 7.43–7.38 (12H, m), 7.18 (2H, d, $J = 2.4\text{ Hz}$), 6.77 (2H, dd, $J_1 = 2.4\text{ Hz}$, $J_2 = 8.4\text{ Hz}$), 4.17 (4H, t, $J = 5.2\text{ Hz}$), 4.04 (4H, t, $J = 5.2\text{ Hz}$), 1.92 (6H, s), 1.91 (6H, s), 1.09 (18H, s). ^{13}C NMR (CDCl_3): δ 156.7, 136.8, 135.6, 133.6, 131.2, 129.6, 128.3, 127.7, 126.3, 121.2, 120.8, 120.6, 111.7, 111.2, 69.2, 62.6, 26.8, 19.2, 13.10, 13.07. UV-vis (CH_2Cl_2): λ_{max} (lg ϵ) 370 (4.19), 434 (4.46) nm. CV: $E_{\text{pa}}^{\text{ox}} = 0.36\text{ V}$, $E_{\text{pc}}^{\text{ox}} = 0.10\text{ V}$. MS (EI): m/z (%) 1032 (100, M^+). Anal. Calcd. for $\text{C}_{60}\text{H}_{64}\text{O}_4\text{S}_4\text{Si}_2$ (MW 1033.58): C, 69.72; H, 6.24. Found C, 69.46; H, 6.24.

**2,6-Bis(2-hydroxyethoxy)-9,10-bis(4,5-dimethyl-1,3-dithiol-2-ylidene)-
9,10-dihydroanthracene (210)**



Compound **209** (3.70 g, 3.57 mmol) was dissolved in dry tetrahydrofuran (50 mL) and stirred under argon at room temperature. A solution of tetrabutylammonium fluoride (10.7 mL of a 1.0 M solution in tetrahydrofuran, 10.7 mmol) was added dropwise *via* syringe over 15 min, causing the reaction mixture to change colour from yellow to brown. Further stirring for 1.5 h, followed by addition of a few drops of water (0.1 mL) and evaporation of the solvent, afforded a brown residue. The residue was dissolved in dichloromethane (200 mL), washed with water and brine, dried (MgSO_4) and concentrated *in vacuo*. Chromatography using a short column (silica gel, dichloromethane until no more by-products were visible on the column, then dichloromethane-acetone, 9:1 v/v) afforded **210** as a yellow powder (1.65 g, 83%), mp 218-220 °C (decomp.). ^1H NMR (CDCl_3): δ 7.53 (2H, d, $J = 8.4$ Hz), 7.17 (2H, d, $J = 2.4$ Hz), 6.81 (2H, dd, $J_1 = 2.4$ Hz, $J_2 = 8.4$ Hz), 4.15 (4H, t, $J = 4.4$ Hz), 4.01-3.98 (4H, m), 2.06 (2H, t, $J = 6.0$ Hz), 1.923 (6H, s), 1.916 (6H, s). ^{13}C NMR (CDCl_3): δ 156.4, 136.9, 131.7, 128.7, 126.5(2C), 120.9, 120.8, 111.5, 111.4, 69.3, 61.5, 13.2, 13.1. UV-vis (CH_2Cl_2): λ_{max} (lg ϵ) 371 (4.18), 435 (4.44) nm. CV: $E^{\text{ox}}_{\text{pa}} = 0.28$ V, $E^{\text{ox}}_{\text{pc}} = 0.17$ V. MS (EI): m/z (%) 556 (100, M^+). Anal. Calcd. for $\text{C}_{28}\text{H}_{28}\text{O}_4\text{S}_4$ (MW 556.78): C, 60.40; H, 5.07. Found C, 60.15; H, 5.06.

Phenanthroline TTFAQ cyclophane 220



Method I:

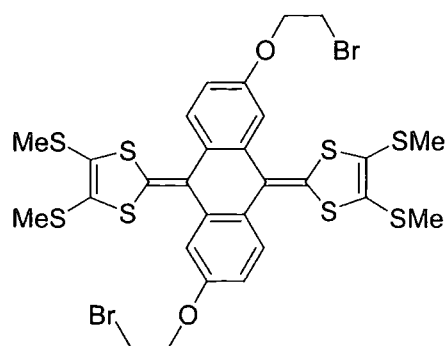
To a stirred solution of diethyl azodicarboxylate (0.17 mL, 0.192 g, 1.10 mmol) in dry tetrahydrofuran (100 mL) under argon at room temperature was added a solution of TTFAQ diol **204** (0.212 g, 0.274 mmol), triphenylphosphine (0.289 g, 1.10 mmol)

and 2,9-di(*p*-phenol)-1,10-phenanthroline **218**¹⁸⁹ (0.100 g, 0.274 mmol) in tetrahydrofuran (70 mL) dropwise over 8 h, whereupon the solution was left to stir for another 12 h. The red reaction mixture was concentrated under reduced pressure and the residue purified by column chromatography. Two columns were needed (basic alumina, dichloromethane-ethyl acetate, 95:5 v/v) to give **220** as a yellow powder, (0.110 g, 36%). Data was identical to that obtained by method II.

Method II:

To a stirred suspension of cesium carbonate (0.489 g, 1.50 mmol) in dry degassed acetonitrile (200 mL) under argon at 60 °C was added a solution of TTFAQ dibromide **222** (0.325 g, 0.362 mmol) and 2,9-di(*p*-phenol)-1,10-phenanthroline **218**¹⁸⁹ (0.132 g, 0.362 mmol) in dry degassed *N,N*-dimethylformamide (50 mL) over 48 h using a syringe controlled by a perfusor pump. The orange reaction mixture was stirred for another 24 h at 60 °C whereupon it was concentrated under reduced pressure. The residue was taken into dichloromethane (150 mL), washed with water (2 x 100 mL), dried (MgSO₄) and concentrated *in vacuo*. Purification by column chromatography (basic alumina, dichloromethane gradient to dichloromethane-ethyl acetate, 95:5 v/v) afforded **220** as a yellow powder (0.269 g, 68%), mp 202-204 °C. ¹H NMR (CDCl₃): δ 8.40 (4H, d, *J* = 9.2 Hz), 8.22 (2H, d, *J* = 8.4 Hz), 8.06 (2H, d, *J* = 8.8 Hz), 7.70 (2H, s), 7.51 (2H, d, *J* = 8.4 Hz), 7.15 (2H, d, *J* = 2.4 Hz), 7.06 (4H, d, *J* = 8.8 Hz), 6.91 (2H, dd, *J*₁ = 2.4 Hz, *J*₂ = 8.4 Hz), 4.34-4.25 (4H, m), 4.15-4.12 (4H, m), 3.97-3.94 (8H, m), 2.35 (6H, s), 2.33 (6H, s). ¹³C NMR (CDCl₃): δ 160.1, 157.1, 156.1, 145.9, 136.7, 136.4, 132.1, 129.2, 128.8, 127.8, 127.4, 126.5, 126.3, 125.5, 125.1, 123.2, 119.1, 114.8, 112.4, 112.2, 69.9, 69.6, 68.5, 67.5, 19.1, 19.0. UV-vis (CH₂Cl₂): λ_{max} (lg ε) 284 (4.83), 325 (4.54), 342 (4.56), 431 (4.42) nm. CV: *E*^{ox}_{pa} = 0.52 V, *E*^{ox}_{pc} = 0.35 V. MS (EI): *m/z* (%) 1100 (6, M⁺), 187 (100). Anal. Calcd. for C₅₆H₄₈N₂O₆S₈ (MW 1101.52): C, 61.06; H, 4.39; N, 2.54. Found C, 60.79; H, 4.36; N, 2.56.

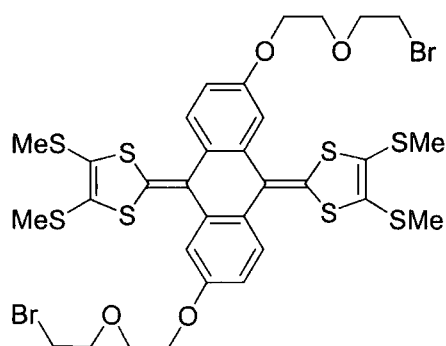
2,6-Bis(2-bromoethoxy)-9,10-bis[4,5-bis(methylthio)-1,3-dithiol-2-ylidene]-9,10-dihydroanthracene (221)



A stirred suspension of TTFAQ diol **203** (1.71 g, 2.50 mmol) and carbon tetrabromide (2.49 g, 7.50 mmol) in dry degassed dichloromethane (100 mL) under argon was cooled to 0 °C and triphenylphosphine (1.97 g, 7.50 mmol) was added in one portion. The reaction mixture was stirred for 1 h in which time it turned yellow-brown, whereupon it was filtered through a plug of silica. The plug of silica was

further eluted with dichloromethane until the filtrate was almost colourless (purity of the filtrate can be checked by TLC using dichloromethane-hexane 2:1 v/v as eluent). The yellow solution was concentrated to give crude **221** which was recrystallised from dichloromethane-hexane to give a yellow powder (1.77 g, 87%), mp 265-266 °C (decomp.). ¹H NMR (CDCl₃): δ 7.46 (2H, d, *J* = 8.8 Hz), 7.07 (2H, d, *J* = 2.4 Hz), 6.84 (2H, dd, *J*₁ = 2.4 Hz, *J*₂ = 8.8 Hz), 4.36 (4H, t, *J* = 6.4 Hz), 3.68 (4H, t, *J* = 6.4 Hz), 2.394 (6H, s), 2.389 (6H, s). ¹³C NMR (CDCl₃): δ 156.3, 136.4, 129.9, 128.2, 126.7, 126.1, 125.4, 123.1, 112.3, 111.8, 68.0, 29.0, 19.2, 19.1. UV-vis (CH₂Cl₂): λ_{max} (lg ε) 366 (4.20), 432 (4.44) nm. CV: *E*^{ox}_{pa} = 0.52 V, *E*^{ox}_{pc} = 0.40 V. MS (EI): *m/z* (%) 812 (76, [M + 4]⁺), 810 (100, [M + 2]⁺), 808 (42, M⁺). Anal. Calcd. for C₂₈H₂₆Br₂O₂S₈ (MW 810.84): C, 41.48; H, 3.23. Found C, 41.88; H, 3.27.

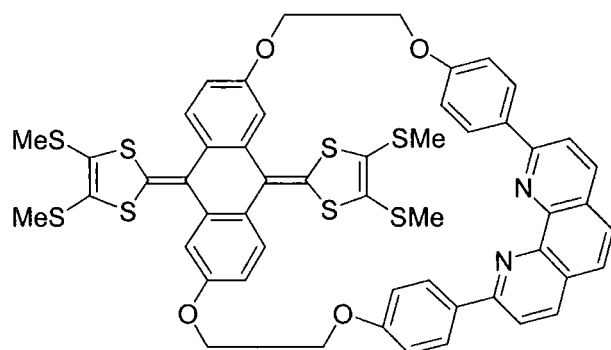
2,6-Bis[2-(2-bromoethoxy)ethoxy]-9,10-bis[4,5-bis(methylthio)-1,3-dithiol-2-ylidene]-9,10-dihydroanthracene (222)



This procedure follows the synthesis of **221**. TTFAQ diol **204** (3.09 g, 4.00 mmol) in dry dichloromethane (100 mL) was treated with carbon tetrabromide (3.98 g, 12.0 mmol) and triphenylphosphine (3.15 g, 12.0 mmol). The reaction mixture was concentrated *in vacuo* and the residue purified by column chromatography (silica gel, dichloromethane) to give

222 as a yellow powder which was recrystallised from toluene-petroleum ether to give small shiny yellow plates (3.32 g, 92%), mp 141-142 °C. ^1H NMR (CDCl_3): δ 7.43 (2H, d, $J = 8.4$ Hz), 7.07 (2H, d, $J = 2.8$ Hz), 6.84 (2H, dd, $J_1 = 2.4$ Hz, $J_2 = 8.4$ Hz), 4.20 (4H, t, $J = 4.8$ Hz), 3.92-3.89 (8H, m), 3.51 (4H, t, $J = 6.0$ Hz), 2.38 (12H, s). ^{13}C NMR (CDCl_3): δ 156.9, 136.2, 129.4, 127.8, 126.6, 126.2, 125.3, 123.3, 112.1, 111.6, 71.4, 69.5, 67.6, 30.2, 19.2, 19.0. UV-vis (CH_2Cl_2): λ_{max} (lg ϵ) 366 (4.19), 432 (4.46) nm. CV: $E_{\text{pa}}^{\text{ox}} = 0.51$ V, $E_{\text{pc}}^{\text{ox}} = 0.39$ V. MS (EI): m/z (%) 900 (10, $[\text{M} + 4]^+$), 898 (13, $[\text{M} + 2]^+$), 896 (5, M^+), 94 (100). Anal. Calcd. for $\text{C}_{32}\text{H}_{34}\text{Br}_2\text{O}_4\text{S}_8$ (MW 898.95): C, 42.75; H, 3.81. Found C, 42.75; H, 3.80.

Phenanthroline TTFAQ cyclophane **223**



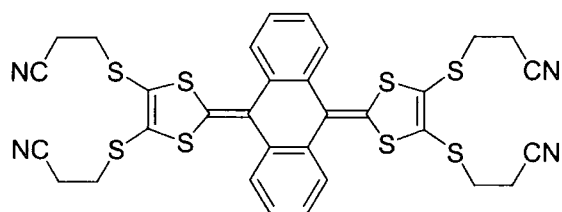
TTFAQ dibromide **221** (0.324 g, 0.400 mmol), 2,9-di(*p*-phenol)-1,10-phenanthroline **218**¹⁸⁹ (0.146 g, 0.400 mmol) and cesium carbonate (0.652 g, 2.00 mmol) were suspended in dry degassed *N,N*-dimethylformamide (300 mL) and stirred at 70 °C under argon for 72 h, which caused the colour

to change from yellow to orange. The reaction mixture was concentrated *in vacuo*, taken into dichloromethane (300 mL), washed with water (150 mL) and brine (150 mL), dried (MgSO_4) and concentrated under reduced pressure to give an orange powder. The crude product was purified by column chromatography (basic alumina, dichloromethane) which afforded **223** as a yellow powder (0.195 g, 48%), mp > 280 °C. Crystals of a quality suitable for X-ray analysis were grown by slow evaporation of a solution of **223** in chlorobenzene. ^1H NMR (CDCl_3): δ 8.25 (4H, d, $J = 8.5$ Hz), 8.24 (2H, d, $J = 8.0$ Hz), 8.03 (2H, d, $J = 8.5$ Hz), 7.73 (2H, s), 7.51 (2H, d, $J = 8.5$ Hz), 7.28 (2H, d, $J = 2.0$ Hz), 6.92-6.89 (6H, m), 4.56 (4H, t, $J = 5.0$ Hz), 4.39-4.30 (4H, m), 2.40 (6H, s), 2.39 (6H, s). ^{13}C NMR (CDCl_3): δ 159.4, 156.4, 156.3, 146.0, 136.7, 136.5, 133.1, 129.3, 129.0, 128.3, 127.5, 126.6, 126.2, 125.6, 125.4, 123.3, 119.4, 115.7, 113.6, 112.9, 67.1, 66.1, 19.2, 19.1. UV-vis (CH_2Cl_2): λ_{max} (lg ϵ) 281 (4.83), 322 (4.54), 344 (4.57), 432 (4.45) nm. CV: $E_{\text{pa}}^{\text{ox}} = 0.53$ V, $E_{\text{pc}}^{\text{ox}} = 0.34$ V. MS (EI):

m/z (%) 1012 (44, M^+), 364 (100). Anal. Calcd. for $C_{52}H_{40}N_2O_4S_8$ (MW 1013.41): C, 61.63; H, 3.98; N, 2.76. Found C, 61.59; H, 3.99; N, 2.71.

8.5 EXPERIMENTAL PROCEDURES TO CHAPTER 6

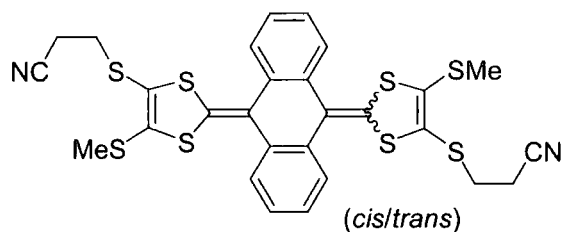
9,10-Bis[4,5-bis(2-cyanoethylthio)-1,3-dithiol-2-ylidene]-9,10-dihydroanthracene (258)



To a degassed solution of anthraquinone **57** (0.208 g, 1.00 mmol) in triethyl phosphite (15 mL) stirred under argon at 125 °C was added thione **256**¹⁶⁴ (1.07 g, 3.51 mmol) in small portions against a positive pressure of argon over 2.5 h. The reaction mixture

became dark red and was stirred for another 30 min at 125 °C, whereupon it was cooled to 0 °C. This prompted formation of a yellow precipitate. Methanol (50 mL) was added to the reaction mixture to facilitate complete precipitation, whereupon the precipitate was filtered, washed with methanol (3 x 5 mL), dried *in vacuo* and column chromatographed (silica gel, dichloromethane-ethyl acetate, 95:5 v/v) to give **258** as a yellow powder (0.435 g, 60%), mp 179-180 °C (from dichloromethane-hexane). ¹H NMR (CDCl₃): δ 7.55-7.53 (4H, m), 7.37-7.35 (4H, m), 3.15-3.08 (4H, m), 3.04-2.97 (4H, m), 2.71 (8H, t, $J = 6.8$ Hz). ¹³C NMR (CDCl₃): δ 134.2, 129.2, 126.9, 126.2, 125.4, 124.6, 117.5, 31.0, 18.9. UV-vis (CH₂Cl₂): λ_{\max} (lg ϵ) 358 (4.20), 426 (4.43) nm. CV: $E^{\text{ox}}_{\text{pa}} = 0.66$ V, $E^{\text{ox}}_{\text{pc}} = 0.54$ V. MS (EI): m/z (%) 720 (55, M^+), 264 (100). Anal. Calcd. for $C_{32}H_{24}N_4S_8$ (MW 721.09): C, 53.30; H, 3.35; N, 7.77; found C, 53.05; H, 3.31; N, 7.72.

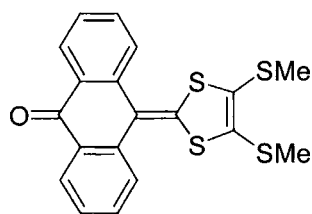
9,10-Bis[4-(2-cyanoethylthio)-5-methylthio-1,3-dithiol-2-ylidene]-9,10-dihydro-anthracene *cis/trans* (259)



This procedure follows the synthesis of **258**. Anthraquinone **57** (0.520 g, 2.50 mmol) was reacted with thione **257**^{165b} (2.84 g, 10.7 mmol) in triethyl phosphite (30 mL) to give a dark red solution. The reaction mixture

was concentrated under reduced pressure to give a brown oil, which was purified by column chromatography (silica gel, dichloromethane) followed by recrystallisation from dichloromethane-hexane to give **259** as yellow blades (0.755 g, 47%), mp 181-188 °C (a *cis/trans* mixture). ¹H NMR (CDCl₃): δ 7.58-7.54 (4H, m), 7.35-7.33 (4H, m), 3.08-3.03 (2H, m), 2.99-2.91 (2H, m), 2.72-2.67 (4H, m), 2.45 (3H, s), 2.44 (3H, s). UV-vis (CH₂Cl₂): λ_{max} (lg ε) 271 (4.32), 363 (4.21), 431 (4.45) nm. CV: $E_{pa}^{ox} = 0.61$ V, $E_{pc}^{ox} = 0.45$ V. MS (EI): *m/z* (%) 642 (100, M⁺). Anal. Calcd. for C₂₈H₂₂N₂S₈ (MW 643.02): C, 52.30; H, 3.45; N, 4.36; found C, 52.21; H, 3.39; N, 4.36.

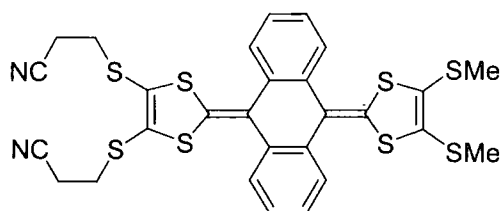
10-[4,5-Bis(methylthio)-1,3-dithiol-2-ylidene]anthracene-9(10H)-one¹⁹⁰ (55)



A degassed mixture of triethyl phosphite (50 mL) and chlorobenzene (150 mL) was stirred under argon and heated to 135 °C whereupon anthraquinone **57** (8.00 g, 38.4 mmol) was added in one portion. Over the next 1.5 h thione **260**^{165b} (4.53 g, 20.0 mmol) was added as a solid in small portions, against a positive pressure of argon, affording a dark red solution. A second batch of anthraquinone **57** (4.00 g, 19.2 mmol) was added in one portion and addition of more thione **260** (4.53 g, 20.0 mmol) in small portions was continued over the next 1.5 h. The reaction mixture was cooled to room temperature, which caused excess anthraquinone to crystallise. The anthraquinone was removed by filtration, and the remaining reaction mixture concentrated under reduced pressure to a volume of 50 mL, whereupon methanol (300 mL) was added to facilitate formation of a red precipitate. The precipitate was filtered, washed with methanol (3 x 15 mL), dried *in vacuo* and column chromatographed (silica gel, dichloromethane) to give **55** as an orange powder (7.97 g, 52%), mp 204-205 °C (lit.⁷⁶ mp 185 °C).

^1H NMR (CDCl_3): δ 8.27 (2H, d, $J = 7.8$ Hz), 7.76 (2H, d, $J = 7.8$ Hz), 7.66 (2H, t, $J = 7.8$ Hz), 7.44 (2H, t, $J = 7.8$ Hz), 2.42 (6H, s).

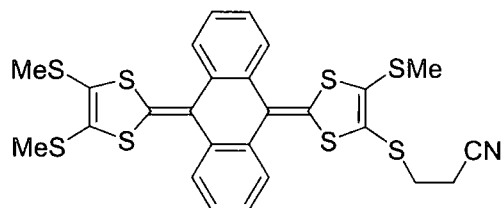
9-[4,5-Bis(2-cyanoethylthio)-1,3-dithiol-2-ylidene]-10-[4,5-bis(methylthio)-1,3-dithiol-2-ylidene]-9,10-dihydroanthracene (261)



Triethyl phosphite (10 mL) was degassed, heated to 130 °C and stirred under argon, whereupon ketone **55** (0.317 g, 0.82 mmol) was added in one portion. Over the next 3 h thione **256**¹⁶⁴ (0.830 g, 2.73 mmol) was added as a solid in small portions

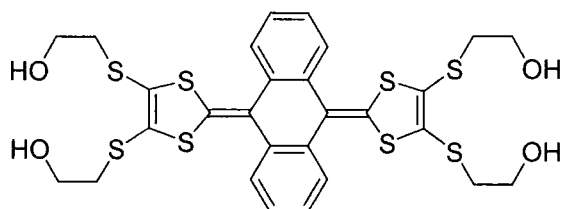
against a positive pressure of argon. The reaction mixture turned dark red-brown, but the formation of **261** could be monitored using TLC (silica, dichloromethane as eluent) and after addition of one third of the thione, precipitation of a yellow compound began. The reaction mixture was stirred for another 30 min at 130 °C, before it was cooled to 0 °C and methanol (70 mL) was added to facilitate further precipitation. The precipitate was filtered, washed with methanol (3 x 5 mL), dried *in vacuo* and column chromatographed (silica gel, dichloromethane) to give **261** as a yellow foam (0.386 g, 73%). Yellow prisms could be grown by slow diffusion of hexane into a solution of **261** in dichloromethane, mp 236-237 °C. ^1H NMR (CDCl_3): δ 7.62-7.60 (2H, m), 7.52-7.49 (2H, m), 7.37-7.31 (4H, m), 3.14-3.07 (2H, m), 3.03-2.95 (2H, m), 2.72-2.68 (4H, m), 2.40 (6H, m). ^{13}C NMR (CDCl_3): δ 134.6, 134.1, 131.7, 128.3, 126.8, 126.4, 126.2, 125.5, 125.4, 125.2, 124.9, 122.9, 117.4, 31.1, 18.92, 18.90. UV-vis (CH_2Cl_2): λ_{max} (lg ϵ) 362 (4.21), 431 (4.44) nm. CV: $E_{\text{pa}}^{\text{ox}} = 0.60$ V, $E_{\text{pc}}^{\text{ox}} = 0.50$ V. MS (EI): m/z (%) 642 (93, M^+), 264 (100). Anal. Calcd. for $\text{C}_{28}\text{H}_{22}\text{N}_2\text{S}_8$ (MW 643.02): C, 52.30; H, 3.45; N, 4.36; found C, 52.24; H, 3.42; N, 4.39.

9-[4-(2-cyanoethylthio)-5-methylthio-1,3-dithiol-2-ylidene]-10-[4,5-bis(methylthio)-1,3-dithiol-2-ylidene]-9,10-dihydroanthracene (262)



To a stirred solution of bisprotected TTFAQ **261** (1.00 g, 1.56 mmol) in dry degassed *N,N*-dimethylformamide (100 mL) under argon at room temperature was added dropwise a solution of sodium methoxide (3.11 mL of a 0.5 M solution in methanol, 1.56 mmol) over 30 min, causing the colour to change from yellow to red. The solution was stirred for another 1 h, after which time excess methyl iodide (1.0 mL, 2.28 g, 16.1 mmol) was added in one portion, immediately prompting a colour change back to yellow. The reaction mixture was stirred for 30 min, concentrated *in vacuo* and the residue purified by column chromatography (silica gel, dichloromethane) to afford **262** as a yellow foam (0.907 g, 96%). Yellow crystals could be grown by slow diffusion of hexane into a solution of **262** in dichloromethane, mp 207-208 °C. ¹H NMR (CDCl₃): δ 7.60-7.51 (4H, m), 7.34-7.31 (4H, m), 3.08-3.01 (1H, m), 2.96-2.88 (1H, m), 2.70-2.66 (2H, m), 2.43 (3H, s), 2.40 (3H, s), 2.39 (3H, s). ¹³C NMR (CDCl₃): δ 134.6, 134.5, 134.4, 134.3, 133.0, 131.3, 129.7, 126.5 (2C), 126.34, 126.33, 125.7, 125.5, 125.41, 125.36, 125.32, 125.28, 124.2, 123.2, 118.4, 117.6, 31.1, 19.00, 18.96, 18.93, 18.8. UV-vis (CH₂Cl₂): λ_{max} (lg ε) 272 (4.34), 365 (4.20), 434 (4.44) nm. CV: $E^{\text{ox}}_{\text{pa}} = 0.57$ V, $E^{\text{ox}}_{\text{pc}} = 0.44$ V. MS (EI): *m/z* (%) 603 (100, M⁺). Anal. Calcd. for C₂₆H₂₁NS₈ (MW 603.98): C, 51.70; H, 3.50; N, 2.32; found C, 51.63; H, 3.45; N, 2.34.

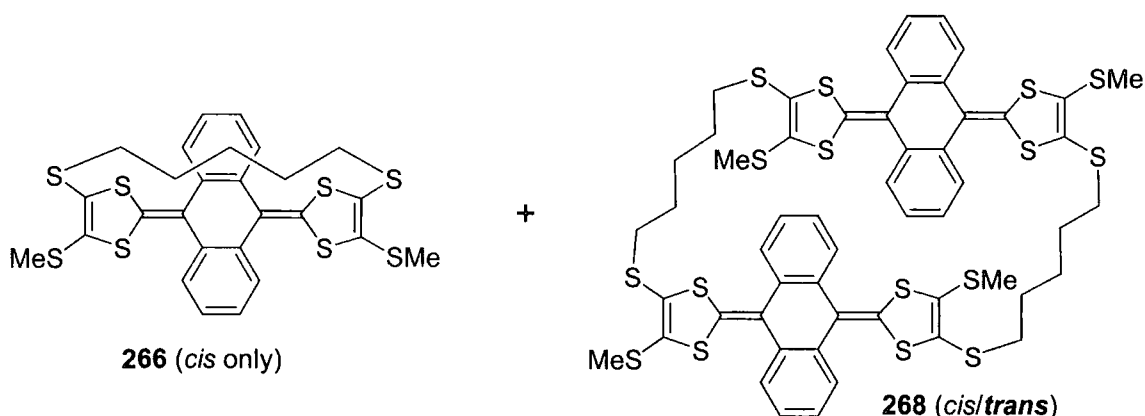
9,10-Bis[4,5-bis(2-hydroxyethylthio)-1,3-dithiol-2-ylidene]-9,10-dihydroanthracene (265)



To a stirred solution of tetraprotected TTFAQ **258** (0.150 g, 0.21 mmol) in dry degassed *N,N*-dimethylformamide (15 mL) was added a solution of sodium methoxide (2.0 mL of a 0.5 M solution in methanol, 1.0 mmol) in one portion, causing the colour of the solution to change from yellow to dark red. The reaction mixture was stirred for 5 min, whereupon bromoethanol (0.125 g, 1.0 mmol) was added in one portion. The solution was stirred for 16h, in which time the colour turned back to yellow,

whereupon it was concentrated under reduced pressure. The yellow residue was taken into dichloromethane (100 mL), washed with brine (100 mL), dried (MgSO₄) and concentrated *in vacuo*. Purification by column chromatography (silica gel, dichloromethane-acetone, 2:1 v/v until minor by-products were off the column, then acetone-dichloromethane, 2:1 v/v to elute the major product) afforded **265** as a yellow powder (0.093 g, 65%), mp 254-256 °C (decomp.). Crystals of X-ray quality were grown from both acetonitrile and methanol. ¹H NMR (DMSO-*d*₆): δ 7.59-7.55 (4H, m), 7.44-7.39 (4H, m), 4.97 (4H, t, *J* = 5.6 Hz), 3.57-3.52 (8H, m), 2.93-2.89 (8H, m). ¹³C NMR (DMSO-*d*₆): δ 133.7, 130.5, 127.0, 125.4, 125.2, 122.3, 60.3, 38.1. UV-vis (CH₂Cl₂): λ_{max} (lg ε) 362 (4.19), 431 (4.44) nm. CV: *E*^{ox}_{pa} = 0.54 V, *E*^{ox}_{pc} = 0.43 V. MS (ES): *m/z* (%) 723 (20, [M + K]⁺), 707 (100, [M + Na]⁺), 684 (17, M⁺). Accurate Mass Calcd. for C₂₈H₂₈O₄S₈Na: 706.9651. HRMS (ES): 706.9660 (+1.3 ppm).

TTFAQ cyclophanes **266** and **268**

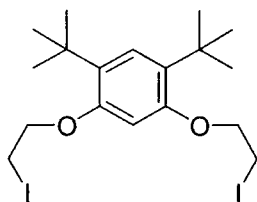


A solution of TTFAQ derivative **259** (0.400 g, 0.622 mmol) and 1,5-diiodopentane (0.202 g, 0.622 mmol ~ 0.093 mL) in dry degassed *N,N*-dimethylformamide (50 mL) was placed in a syringe. In a second syringe was placed a degassed solution of sodium methoxide (3.73 mL of a 0.5 M solution in methanol, 1.87 mmol) in dry *N,N*-dimethylformamide (46 mL) and the two syringes were placed in a perfusor pump. The two solutions were pumped into dry degassed *N,N*-dimethylformamide (100 mL) stirred under argon over 12 h. After addition was completed, the reaction mixture was stirred for another 4 h, whereupon the yellow solution was concentrated under reduced pressure. The residue was taken into dichloromethane (200 mL), washed with brine (100 mL), dried (MgSO₄) and concentrated *in vacuo*. Column chromatography (silica gel, cyclohexane-dichloromethane, 2:1 v/v) afforded a yellow powder,

consisting of two products, which was chromatographed twice (silica gel, hexane-dichloromethane, 2:1 v/v). Evaporation under reduced pressure of the fractions containing the first yellow band afforded **266** as a yellow powder (0.178 g, 47%), mp 239-240 °C. ^1H NMR (CDCl_3): δ 7.40-7.32 (8H, m), 2.79-2.73 (2H, m), 2.38 (6H, s), 2.35-2.29 (2H, m), 1.33-1.18 (3H, m), 1.03-0.95 (2H, m), 0.76-0.68 (1H, m). ^{13}C NMR (CDCl_3): δ 134.5, 133.6, 130.7, 129.6, 128.8, 126.7, 126.31, 126.28, 125.9, 123.6, 35.0, 29.8, 29.7, 19.6. UV-vis (CH_2Cl_2): λ_{max} (lg ϵ) 271 (4.41), 363 (4.14), 421 (4.32) nm. CV: $E_{\text{pa}}^{\text{ox}} = 0.90$ V, $E_{\text{pc}}^{\text{ox}} = 0.84$ V. MS (EI): m/z (%) 604 (100, M^+). Anal. Calcd. for $\text{C}_{27}\text{H}_{24}\text{S}_8$ (MW 605.01): C, 53.60; H, 4.00; found C, 53.36; H, 3.96.

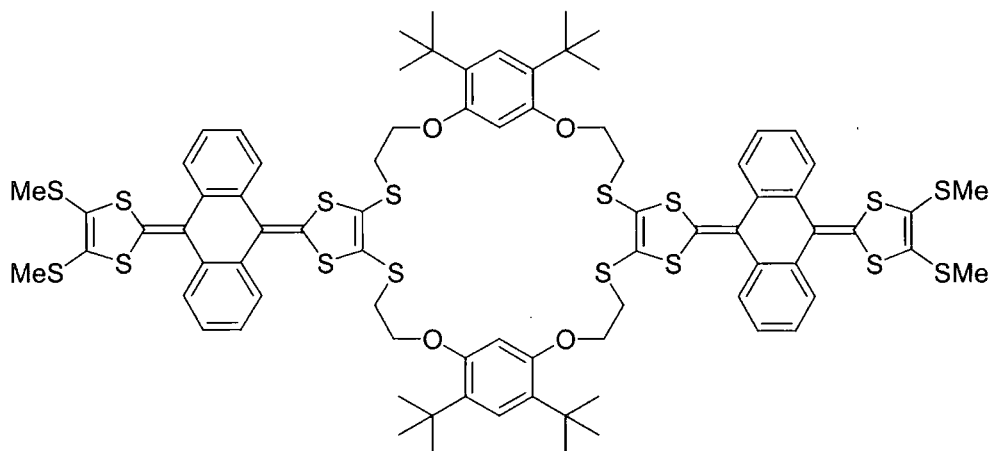
The fraction containing the second yellow band was concentrated *in vacuo* to give **268** as an only slightly soluble yellow powder (0.061 g, 16%), mp > 280 °C. ^1H NMR (CDCl_3): δ 7.61-7.49 (8H, m), 7.41-7.20 (8H, m), 2.85-2.52 (8H, m), 2.42-2.20 (12H, m), 1.70-1.40 (12H, m). UV-vis (CH_2Cl_2): λ_{max} (lg ϵ) 272 (4.62), 367 (4.49), 435 (4.70) nm. CV: $E_{\text{pa}}^{\text{ox}} = 0.59$ V, $E_{\text{pc}}^{\text{ox}} = 0.41$ V. MS (MALDI): $m/z = 1209.6$ (theory: 1210.0). Anal. Calcd. for $\text{C}_{54}\text{H}_{48}\text{S}_{16}$ (MW 1210.01): C, 53.60; H, 4.00; found C, 53.50; H, 4.00.

1,3-Bis(2-iodoethoxy)-4,6-di-*tert*-butylbenzene (**269**)



1,3-Bis(2-chloroethoxy)-4,6-di-*tert*-butylbenzene **273** (4.49 g, 12.9 mmol) and sodium iodide (7.50 g, 50.0 mmol) were dissolved in 2-butanone (50 mL) and refluxed under argon for 48 h, which caused the solution to turn orange and a colourless salt to precipitate.

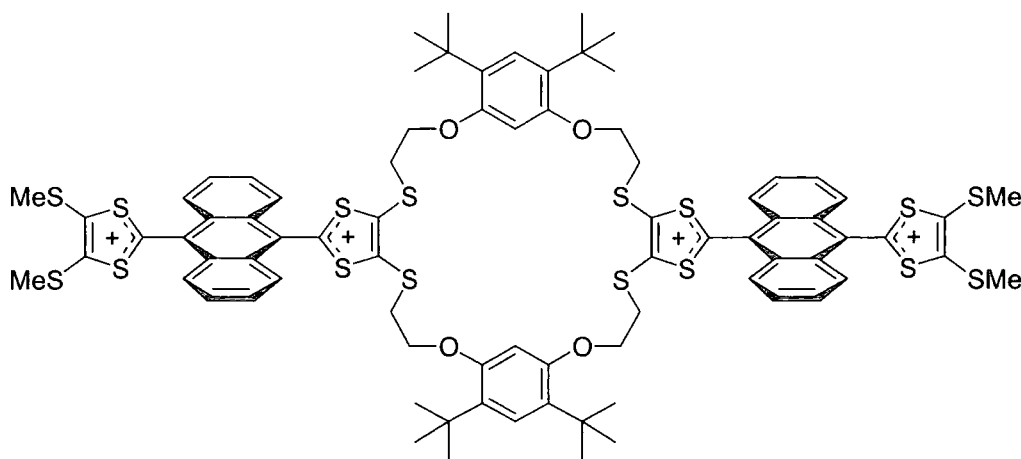
The reaction mixture was concentrated under reduced pressure and the residue taken into dichloromethane (200 mL). The solution was washed with a 0.5% aqueous sodium thiosulphate solution (100 mL), which made the organic phase change colour from orange to colourless, and water (2 x 100 mL). The organic phase was dried (MgSO_4) and filtered through a plug of silica, which was further eluted with dichloromethane (200 mL). The combined filtrate was concentrated *in vacuo* to give **269** as colourless needles (6.65 g, 97%), mp 171-172 °C (from methanol). ^1H NMR (CDCl_3): δ 7.24 (1H, s), 6.33 (1H, s), 4.30 (4H, t, $J = 6.5$ Hz), 3.50 (4H, t, $J = 6.5$ Hz), 1.39 (18H, s). ^{13}C NMR (CDCl_3): δ 155.1, 129.6, 125.47, 125.43, 97.98, 97.96, 68.8, 34.5, 30.2, 1.1. MS (EI): m/z (%) 530 (100, M^+). Anal. Calcd. for $\text{C}_{18}\text{H}_{28}\text{I}_2\text{O}_2$ (MW 530.22): C, 40.77; H, 5.32; found C, 40.72; H, 5.37.

TTFAQ cyclophane **271**

To a stirred solution of bisprotected TTFAQ **261** (0.300 g, 0.467 mmol) in dry degassed *N,N*-dimethylformamide (45 mL) under argon at room temperature was added dropwise a solution of sodium methoxide (0.93 mL of a 0.5 M solution in methanol, 0.467 mmol) over 30 min, causing the colour to change from yellow to red. The solution was stirred for another 1 h, after which time a degassed solution of linker **269** (0.124 g, 0.233 mmol) in dry *N,N*-dimethylformamide (5 mL) was added in one portion. The reaction mixture was stirred for 12 h, in which time the colour changed back to yellow. A second portion of linker **269** (0.124 g, 0.233 mmol) was added to the reaction mixture as a solid, and the yellow solution was placed in a syringe. In another syringe was placed a degassed solution of sodium methoxide (1.25 mL of a 0.5 M solution in methanol, 0.625 mmol) in dry *N,N*-dimethylformamide (50 mL) and the two syringes were placed in a perfusor pump. The two solutions were pumped to dry degassed *N,N*-dimethylformamide (100 mL) stirred under argon over 16 h. After addition was completed, the reaction mixture was stirred for another 4 h, whereupon the yellow solution was concentrated under reduced pressure. The residue was taken into dichloromethane (200 mL), washed with water (100 mL) and brine (100 mL), dried (MgSO_4) and concentrated *in vacuo*. The residue was purified by column chromatography (silica gel, carbon disulfide, gradient to carbon disulfide-dichloromethane, 9:1 v/v) to give **271** as a sparsely soluble yellow powder (0.292 g, 77%), mp 213 °C (from toluene-petroleum ether, decomp.). $^1\text{H NMR}$ (CDCl_3): δ 7.59-7.52 (8H, m), 7.32-7.25 (8H, m), 7.12 (1H, s), 7.10 (1H, s), 6.37 (1H, s), 6.31 (1H, s), 4.12-4.10 (8H, m), 3.15-3.02 (8H, m), 2.38 (6H, s), 2.37 (6H, s), 1.28 (18H, s), 1.26 (18H, s). UV-vis (CH_2Cl_2): λ_{max} (lg ϵ) 274 (4.66), 366 (4.50), 435 (4.73) nm. CV: $E_{\text{pa}}^{\text{ox}} = 0.60$ V, $E_{\text{pc}}^{\text{ox}} = 0.42$ V. MS (ES): m/z (%) 1659 (29, $[\text{M} + \text{K}]^+$),

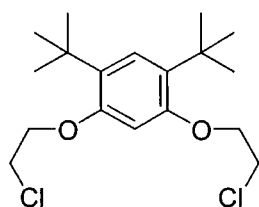
1643 (100, $[M + Na]^+$), 1620 (5, M^+). Anal. Calcd. for $C_{80}H_{84}O_4S_{16}$ (MW 1622.58): C, 59.22; H, 5.22; found C, 59.06; H, 5.21.

Generation and 1H NMR spectrum of the TTFAQ dimer tetracation 271^{4+}



To a solution of iodine (excess) in $DMSO-d_6$ was added **271** as a solid. The sample was left for 12 h, in which time **271** dissolved, and the 1H NMR spectrum of 271^{4+} was recorded. 1H NMR ($DMSO-d_6$): δ 8.14-8.12 (8H, m), 7.85-7.80 (8H, m), 7.11 (2H, s), 6.71 (2H, s), 4.55 (8H, t, $J = 5.6$ Hz), 3.96 (8H, t, $J = 5.6$ Hz), 3.01 (12H, s), 1.32 (36H, s).

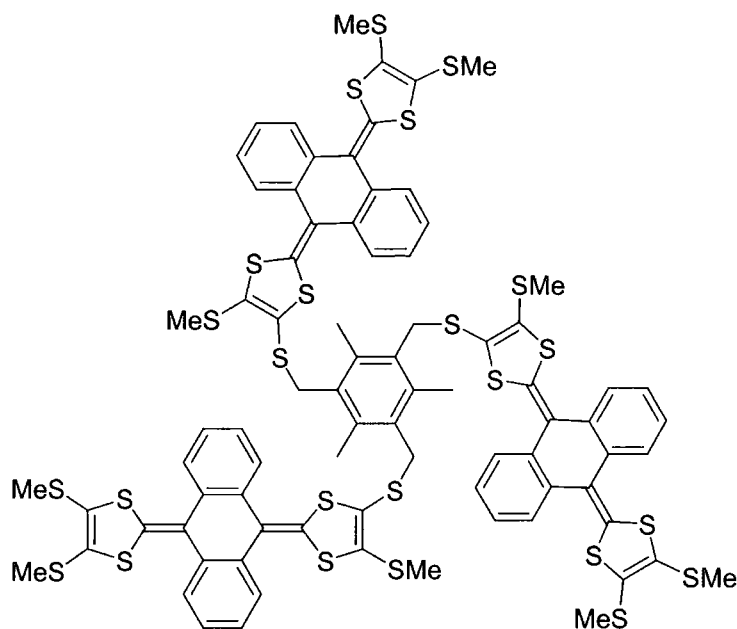
1,3-Bis(2-chloroethoxy)-4,6-di-*tert*-butylbenzene (**273**)



To a stirred solution of 1,3-bis(2-hydroxyethoxy)-4,6-di-*tert*-butylbenzene **272**¹⁸³ (5.60 g, 18.0 mmol) and thionyl chloride (7.8 mL, 12.8 g, 108 mmol) in dry dichloromethane (150 mL) under argon at room temperature was added dropwise dry pyridine (4 mL), whereupon the mixture was refluxed for 12h. The reaction mixture was cooled to 0 °C and water (100 mL) was carefully added. The two phases were separated and the organic phase washed with water (2 x 100 mL), dried ($MgSO_4$) and filtered through a plug of silica. The filter was washed with dichloromethane (100 mL) and the filtrates combined to give a pale yellow solution. The solution was concentrated *in vacuo* yielding an off-white solid which was recrystallised from methanol to give **273** as colourless plates (4.57 g, 73%), mp 106-107 °C. 1H NMR ($CDCl_3$): δ 7.24 (1H, s), 6.37 (1H, s), 4.26 (4H, t,

$J = 6.0$ Hz), 3.89 (4H, t, $J = 6.0$ Hz), 1.39 (18H, s). ^{13}C NMR (CDCl_3): δ 155.3, 129.7, 125.47, 125.43, 97.7, 68.0, 42.2, 34.5, 30.1. MS (EI): m/z (%) 350 (2, $[\text{M} + 4]^+$), 348 (13, $[\text{M} + 2]^+$), 346 (20, M^+), 331 (100). Anal. Calcd. for $\text{C}_{18}\text{H}_{28}\text{Cl}_2\text{O}_2$ (MW 347.32): C, 62.25; H, 8.13; found C, 61.99; H, 8.18.

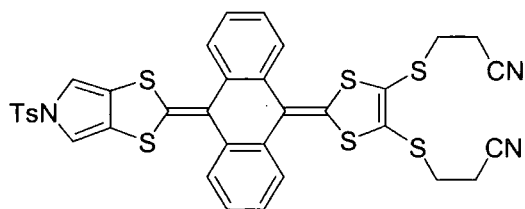
TTFAQ trimer 275



To a stirred solution of compound **262** (0.199 g, 0.33 mmol) in dry degassed *N,N*-dimethylformamide (10 mL) under argon at room temperature was added a solution of sodium methoxide (0.66 mL of a 0.5 M solution in methanol, 0.33 mmol) in one portion, making the colour change from yellow to red. The solution was stirred for 30 min, after which time a solution of

tris(bromomethyl)mesitylene¹⁹¹ **274** (0.040 g, 0.10 mmol) in dry degassed *N,N*-dimethylformamide (2 mL) was added dropwise over 15 min. The colour of the reaction mixture turned pale yellow and formation of a yellow precipitate was observed. The reaction was stirred overnight whereupon excess methyl iodide (0.1 mL, 1.6 mmol) was added to quench the excess thiolate. The colour changed to yellow and the reaction mixture was concentrated *in vacuo* and the residue purified by column chromatography (silica gel, dichloromethane-carbon disulfide, 1:9 v/v) to give **275** as a yellow powder (0.175 g, 97%), mp 225 °C (decomp.). ^1H NMR (CDCl_3): δ 7.59-7.55 (12H, m), 7.34-7.30 (12H, m), 4.19-4.16 (3H, m), 4.03-3.99 (3H, m), 2.53 (9H, s) 2.39-2.36 (27H, m). UV-vis (CH_2Cl_2): λ_{max} (lg ϵ) 367 (4.68), 436 (4.91) nm. CV: $E^{\text{ox}}_{\text{pa}} = 0.55$ V, $E^{\text{ox}}_{\text{pc}} = 0.45$ V. MS (MALDI): $m/z = 1808.8$ (theory: 1809.0). Anal. Calcd. for $\text{C}_{81}\text{H}_{66}\text{S}_{24}$ (MW 1808.97): C, 53.78; H, 3.68; found C, 53.90; H, 3.79.

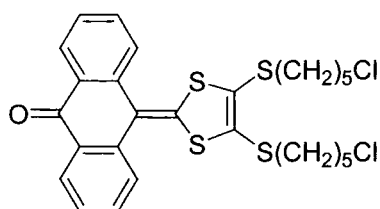
9-{4,5-Bis(2-cyanoethylthio)-1,3-dithiol-2-ylidene}-10-{*N*-Tosylpyrrolo[3,4-d]-1,3-dithiol-2-ylidene}-9,10-dihydroanthracene (277)



This procedure is similar to the synthesis of **261**. The ketone **170** (3.00 g, 6.15 mmol) was reacted with thione **256**¹⁶⁴ (5.62 g, 18.5 mmol) in triethyl phosphite (80 mL). The reaction mixture was concentrated under reduced pressure and the brown residue purified by column chromatography (silica gel, dichloromethane until all unreacted ketone **170** was off the column, then dichloromethane-ethyl acetate, 95:5 v/v) to give a yellow oil. The oil was dissolved in dichloromethane and methanol added until saturation. The saturated solution was cooled to -78 °C, which facilitated formation of a yellow precipitate, and additional methanol was added to complete the precipitation. The precipitate was filtered whilst cold and dried *in vacuo* to give **277** as a bright yellow powder (3.71 g, 81%), mp 143-145 °C. ¹H NMR (CDCl₃): δ 7.68 (2H, d, *J* = 8.4 Hz), 7.67-7.65 (2H, m), 7.50-7.48 (2H, m), 7.35-7.33 (4H, m), 7.26 (2H, d, *J* = 8.4 Hz), 6.82 (2H, s), 3.09-3.02 (2H, m), 2.97-2.90 (2H, m), 2.66-2.62 (4H, m), 2.39 (3H, s). ¹³C NMR (CDCl₃): δ 145.6, 139.6, 135.1, 134.9, 134.4, 130.1, 128.8, 126.9, 126.80, 126.76, 126.2 (2C), 126.0, 125.9, 125.2, 124.8, 117.4, 110.5, 31.1, 21.6, 18.8. UV-vis (CH₂Cl₂): λ_{max} (lg ε) 349 (4.20), 418 (4.42) nm. CV: *E*^{ox}_{pa} = 0.71 V, *E*^{ox}_{pc} = 0.54 V. MS (EI): *m/z* (%) 743 (39, M⁺), 149 (100). Anal. Calcd. for C₃₅H₂₅N₃O₂S₇ (MW 744.05): C, 56.50; H, 3.39; N, 5.65; found C, 56.29; H, 3.32; N, 5.69.

8.6 EXPERIMENTAL PROCEDURES TO CHAPTER 7

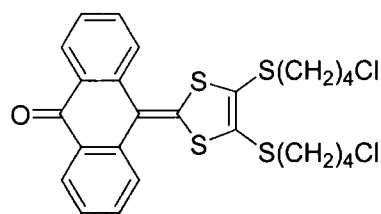
10-[4,5-Bis(5-chloropentylthio)-1,3-dithiol-2-ylidene]anthracene-9(10H)-one (285)



Triethyl phosphite (200 mL) was degassed, heated to 125 °C and stirred under argon. Anthraquinone **57** (3.00 g, 14.4 mmol) was added in one portion to form a suspension. 4,5-Bis(5-chloropentylthio)-1,3-dithiole-2-thione **283**^{40b}

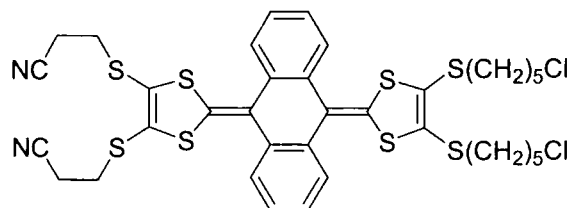
(3.26 g, 8.00 mmol) was dissolved in xylene (10 mL) and half the volume was added dropwise *via* syringe to the anthraquinone suspension over 1 h. The reaction mixture turned dark red-brown and everything went into solution. A second portion of anthraquinone (1.00 g, 4.81 mmol) was added to the reaction mixture in one portion, followed by dropwise addition of the second half of the thione solution over 1 h. The reaction mixture was stirred for another 30 min at 125 °C, before it was cooled to room temperature and concentrated *in vacuo*. The resulting red oil was filtered to remove the excess anthraquinone, which had solidified. The filter was washed with a little dichloromethane (2 x 5mL) and the combined filtrate purified by column chromatography (silica gel, dichloromethane-petroleum ether, 3:1 v/v). The resulting oil solidified *in vacuo* to give **285** as a red solid (1.99 g, 44%), mp 79-80 °C. ¹H NMR (CDCl₃): δ 8.27 (2H, d, *J* = 7.6 Hz), 7.77 (2H, d, *J* = 7.6 Hz), 7.66 (2H, t, *J* = 7.6 Hz), 7.45 (2H, t, *J* = 7.6 Hz), 3.51 (4H, t, *J* = 6.8 Hz), 2.82 (4H, t, *J* = 6.8 Hz), 1.80-1.73 (4H, m), 1.66-1.60 (4H, m), 1.59-1.54 (4H, m). ¹³C NMR (CDCl₃): δ 183.5, 140.0, 138.6, 131.9, 130.7, 127.2 (2C), 126.8, 126.2, 119.2, 44.7, 36.1, 32.0, 28.9, 25.7. MS (EI): *m/z* (%) 566 (100, M⁺). Anal. Calcd. for C₂₇H₂₈Cl₂OS₄ (MW 567.68): C, 57.13; H, 4.97; found C, 56.87; H, 4.97.

10-[4,5-Bis(4-chlorobutylthio)-1,3-dithiol-2-ylidene]anthracene-9(10H)-one (**286**)



This procedure is similar to the synthesis of **285**. Anthraquinone **57** (3.12 g, 15.0 mmol) in triethyl phosphite (200 mL) was reacted with half the volume of 4,5-bis(4-chlorobutylthio)-1,3-dithiole-2-thione **284**^{40b} (3.79 g, 10 mmol) dissolved in xylene (10 mL), whereupon a second portion of anthraquinone (2.08 g, 10 mmol) was added, followed by addition of the remaining thione solution. Column chromatography (silica gel, dichloromethane-petroleum ether, 3:1 v/v) afforded **286** as a red solid (2.47 g, 46%), mp 95-96 °C. ¹H NMR (CDCl₃): δ 8.26 (2H, d, *J* = 8.0 Hz), 7.75 (2H, d, *J* = 7.5 Hz), 7.65 (2H, t, *J* = 8.0 Hz), 7.44 (2H, t, *J* = 7.5 Hz), 3.52 (4H, t, *J* = 6.5 Hz), 2.84 (4H, t, *J* = 7.0 Hz), 1.88 (4H, quintet, *J* = 7.0 Hz), 1.76 (4H, quintet, *J* = 7.5 Hz). ¹³C NMR (CDCl₃): δ 183.4, 139.7, 138.5, 131.8, 130.6, 127.2, 127.1, 126.8, 126.1, 119.3, 44.2, 35.6, 31.0, 26.8. MS (EI): *m/z* (%) 538 (100, M⁺). Anal. Calcd. for C₂₅H₂₄Cl₂OS₄ (MW 539.63): C, 55.64; H, 4.48; found C, 55.36; H, 4.47.

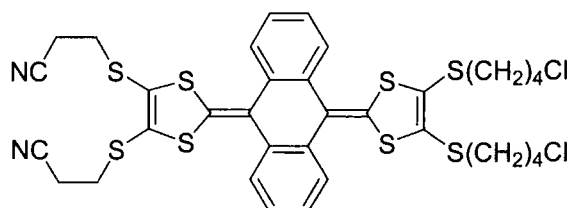
9-[4,5-Bis(5-chloropentylthio)-1,3-dithiol-2-ylidene]-10-[4,5-bis(2-cyanoethylthio)-1,3-dithiol-2-ylidene]-9,10-dihydroanthracene (287)



Triethyl phosphite (75 mL) was degassed, heated to 125 °C and stirred under argon, whereupon a solution of ketone **285** (1.78 g, 3.14 mmol) in xylene (5 mL) was added in one portion. Over the next 3 h thione **256**¹⁶⁴

(4.50 g, 14.8 mmol) was added as a solid in small portions, against a positive pressure of argon. The reaction mixture turned dark red-brown, but the formation of **287** was monitored using TLC (silica, dichloromethane as eluent). The solution was stirred for another 30 min at 125 °C, before it was cooled to room temperature and concentrated *in vacuo*. The residue was column chromatographed (silica gel, dichloromethane) to give **287** as a yellow foam (1.98 g, 77%), mp 53-56 °C. ¹H NMR (CDCl₃): δ 7.62-7.60 (2H, m), 7.53-7.51 (2H, m), 7.35-7.32 (4H, m), 3.51 (4H, t, *J* = 6.4 Hz), 3.12-3.05 (2H, m), 3.02-2.95 (2H, m), 2.85-2.79 (4H, m), 2.71-2.67 (4H, m), 1.80-1.73 (4H, m), 1.67-1.62 (4H, m), 1.59-1.53 (4H, m). ¹³C NMR (CDCl₃): δ 134.4, 134.0, 131.6, 128.4, 126.7, 126.3, 126.1, 125.9, 125.2, 125.1, 124.6, 122.5, 117.4, 44.7, 35.7, 31.8, 31.0, 28.8, 25.5, 18.8. UV-vis (CH₂Cl₂): λ_{max} (lg ε) 362 (4.20), 432 (4.44) nm. CV: *E*^{ox}_{pa} = 0.60 V, *E*^{ox}_{pc} = 0.51 V. MS (EI): *m/z* (%) 826 (11, [M + 4]⁺), 824 (24, [M + 2]⁺), 822 (24, M⁺), 53 (100). Anal. Calcd. for C₃₆H₃₆Cl₂N₂S₈ (MW 824.12): C, 52.47; H, 4.40; N, 3.40; found C, 52.24; H, 4.37; N, 3.35.

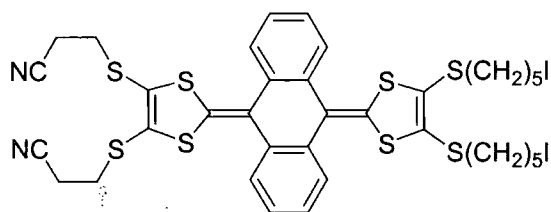
9-[4,5-Bis(4-chlorobutylthio)-1,3-dithiol-2-ylidene]-10-[4,5-bis(2-cyanoethylthio)-1,3-dithiol-2-ylidene]-9,10-dihydroanthracene (288)



This procedure is similar to the synthesis of **287**. Ketone **286** (2.00 g, 3.71 mmol) dissolved in triethyl phosphite (75 mL) and xylene (5 mL) was reacted with thione **256**¹⁶⁴ (5.08 g, 16.7 mmol). Column chromatography (silica gel, dichloromethane) afforded **288** as a yellow foam (2.40 g, 81%), mp 59-62 °C. ¹H NMR (CDCl₃): δ 7.62-7.59 (2H, m), 7.53-7.51 (2H, m), 7.35-7.32 (4H, m), 3.54 (4H, t, *J* = 6.4 Hz), 3.10-3.05 (2H, m), 3.01-2.96 (2H, m), 2.88-2.79 (4H, m), 2.70-2.66 (4H,

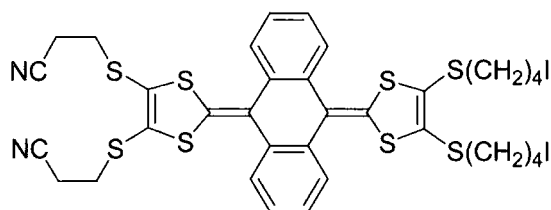
m), 1.91-1.86 (4H, m), 1.81-1.76 (4H, m). ^{13}C NMR (CDCl_3): δ 134.4, 134.0, 131.4, 128.4, 126.6, 126.3, 126.1, 125.8, 125.2, 125.1, 124.6, 122.6, 117.4, 44.3, 35.1, 31.0, 30.9, 26.7, 18.7. UV-vis (CH_2Cl_2): λ_{max} ($\lg \epsilon$) 362 (4.19), 431 (4.43) nm. CV: $E_{\text{pa}}^{\text{ox}} = 0.61$ V, $E_{\text{pc}}^{\text{ox}} = 0.49$ V. MS (EI): m/z (%) 798 (30, $[\text{M} + 4]^+$), 796 (54, $[\text{M} + 2]^+$), 794 (62, M^+), 264 (100). Anal. Calcd. for $\text{C}_{34}\text{H}_{32}\text{Cl}_2\text{N}_2\text{S}_8$ (MW 796.06): C, 51.30; H, 4.05; N, 3.52; found C, 51.27; H, 4.00; N, 3.50.

9-[4,5-Bis(2-cyanoethylthio)-1,3-dithiol-2-ylidene]-10-[4,5-bis(5-iodopentylthio)-1,3-dithiol-2-ylidene]-9,10-dihydroanthracene (289)



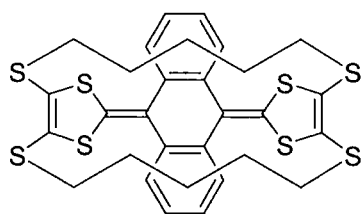
The dichloride **287** (1.65 g, 2.00 mmol) and sodium iodide (3.75 g, 25.0 mmol) were dissolved in degassed 2-butanone (40 mL) and refluxed under argon for 16 h, which caused a colourless salt to precipitate. The reaction mixture was cooled to room temperature and concentrated under reduced pressure. The residue was taken into dichloromethane (100 mL), washed with water, dried (MgSO_4) and concentrated *in vacuo*. Purification by column chromatography (silica gel, dichloromethane) afforded **289** as a yellow foam (1.96 g, 97%), mp 56-59 °C. ^1H NMR (CDCl_3): δ 7.62-7.60 (2H, m), 7.52-7.50 (2H, m), 7.36-7.30 (4H, m), 3.15 (4H, t, $J = 6.8$ Hz), 3.11-3.04 (2H, m), 3.01-2.94 (2H, m), 2.85-2.76 (4H, m), 2.70-2.67 (4H, m), 1.83-1.76 (4H, m), 1.67-1.60 (4H, m), 1.53-1.46 (4H, m). ^{13}C NMR (CDCl_3): δ 134.4, 133.9, 131.6, 128.4, 126.6, 126.2, 126.0, 125.8, 125.2, 125.0, 124.5, 122.4, 117.3, 35.5, 32.5, 30.9, 29.0, 28.4, 18.8, 6.7. UV-vis (CH_2Cl_2): λ_{max} ($\lg \epsilon$) 362 (4.21), 432 (4.44) nm. CV: $E_{\text{pa}}^{\text{ox}} = 0.60$ V, $E_{\text{pc}}^{\text{ox}} = 0.51$ V. MS (EI): m/z (%) 1006 (4, M^+), 324 (100). Anal. Calcd. for $\text{C}_{36}\text{H}_{36}\text{I}_2\text{N}_2\text{S}_8$ (MW 1007.02): C, 42.94; H, 3.60; N, 2.78; found C, 42.75; H, 3.58; N, 2.71.

9-[4,5-Bis(2-cyanoethylthio)-1,3-dithiol-2-ylidene]-10-[4,5-bis(4-iodobutylthio)-1,3-dithiol-2-ylidene]-9,10-dihydroanthracene (290)



This procedure is similar to the synthesis of **289**. Dichloride **288** (1.95 g, 2.45 mmol) was converted to the diiodide **290** using sodium iodide (3.75 g, 25.0 mmol) and 2-butanone (40 mL). Column chromatography (silica gel, dichloromethane) afforded **290** as a yellow foam (2.10 g, 87%), mp 62-65 °C. ¹H NMR (CDCl₃): δ 7.60-7.58 (2H, m), 7.52-7.50 (2H, m), 7.35-7.32 (4H, m), 3.17 (4H, t, *J* = 6.8 Hz), 3.14-3.07 (2H, m), 3.02-2.95 (2H, m), 2.87-2.76 (4H, m), 2.72-2.68 (4H, m), 1.93-1.89 (4H, m), 1.78-1.70 (4H, m). ¹³C NMR (CDCl₃): δ 134.4; 134.0, 131.4; 128.4; 126.7; 126.3; 126.2; 125.9; 125.4; 125.1; 124.7; 123.0; 117.4; 34.7; 31.6; 31.0; 30.2; 18.9; 6.1. UV-vis (CH₂Cl₂): λ_{max} (lg ε) 362 (4.20), 432 (4.45) nm. CV: *E*^{ox}_{pa} = 0.61 V, *E*^{ox}_{pc} = 0.49 V. MS (EI): *m/z* (%) 978 (10, M⁺), 254 (100). Anal. Calcd. for C₃₄H₃₂I₂N₂S₈ (MW 978.97): C, 41.71; H, 3.29; N, 2.86; found C, 41.75; H, 3.22; N, 2.81.

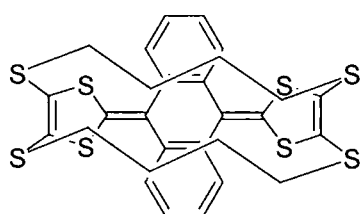
TTFAQ cyclophane 291



A solution of cesium hydroxide monohydrate (0.430 g, 2.60 mmol) in dry methanol (10 mL) was added to dry degassed *N,N*-dimethylformamide (200 mL), which was stirred under argon at room temperature. A second solution, of diiodide **289** (0.644 g, 0.640 mmol) in dry degassed *N,N*-dimethylformamide (50 mL), was placed in a syringe and pumped into the cesium hydroxide solution over 24 h, by the means of a perfusor pump. The resulting orange suspension was concentrated under reduced pressure, taken into dichloromethane (100 mL), washed with brine, dried (MgSO₄) and concentrated *in vacuo*. Column chromatography (silica gel, dichloromethane) afforded **291** as pale yellow micro needles (0.382 g, 92%), mp > 290 °C. Yellow prisms and needles, suitable for X-ray crystallographic analysis, were grown by slow diffusion of hexane into a solution of **291** in dichloromethane. ¹H NMR (CDCl₃): δ 7.39-7.34 (8H, m), 2.86 (4H, ddd, *J*₁ = 13.0 Hz, *J*₂ = 13.0 Hz, *J*₃ = 3.0 Hz), 2.26 (4H, ddd, *J*₁ = 13.0 Hz, *J*₂ = 13.0 Hz, *J*₃ = 5.5 Hz), 1.35-1.19 (6H, m), 1.06-0.98 (4H, m), 0.68-0.60

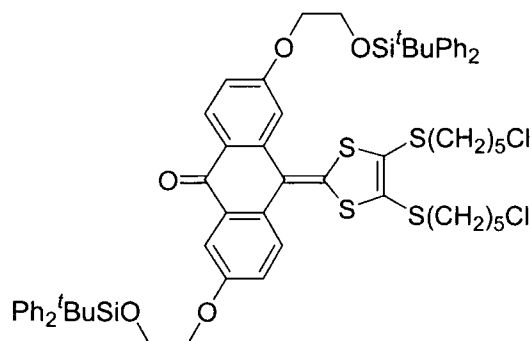
(2H, m). ^{13}C NMR (CDCl_3): δ 133.8, 131.4, 129.9, 127.1, 126.6, 126.3, 35.1, 31.8, 29.4. UV-vis (CH_2Cl_2): λ_{max} ($\lg \epsilon$) 269 (4.44), 351 (4.15), 372 (4.11), 414 (4.35) nm. CV: $E_1^{1/2} = 0.98$ V, $E_2^{1/2} = 1.22$ V. MS (EI): m/z (%) 644 (100, M^+). Anal. Calcd. for $\text{C}_{30}\text{H}_{28}\text{S}_8$ (MW 645.07): C, 55.86; H, 4.38; found C, 55.57; H, 4.36.

TTFAQ cyclophane **292**



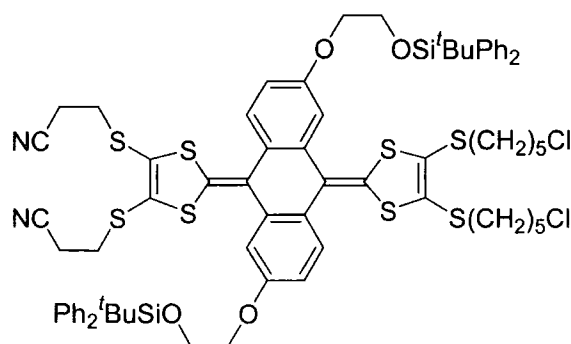
A solution of diiodide **290** (0.830 g, 0.848 mmol) in dry degassed *N,N*-dimethylformamide (50 mL) and a solution of sodium methoxide (4.24 mL of a 0.5 M solution in methanol, 2.12 mmol) in dry degassed *N,N*-dimethylformamide (50 mL) were placed in a syringe each, and the syringes placed in a perfusor pump. The two solutions were pumped simultaneously into dry degassed *N,N*-dimethylformamide (100 mL) stirring under argon, over 16 h at room temperature. The reaction mixture was stirred for another 1 h, concentrated *in vacuo*, taken into dichloromethane and washed with water and brine. An insoluble yellow precipitate was filtered off at this stage. The organic layer was dried (MgSO_4), concentrated under reduced pressure and column chromatographed (silica gel, dichloromethane-petroleum ether, 2:1 v/v) to give **292** as a pale yellow powder (0.141 g, 27%), mp > 250 °C. Yellow needles of X-ray crystallographic quality were grown by slow evaporation of a solution of **292** in a mixture of hexane and dichloromethane. ^1H NMR (CDCl_3): δ 7.38-7.35 (4H, m), 7.34-7.31 (4H, m), 2.78-2.73 (4H, m), 2.62-2.58 (4H, m), 1.54-1.46 (8H, m). ^{13}C NMR (CDCl_3): δ 135.6, 133.0, 131.5, 126.8, 126.2, 124.5, 35.4, 29.9. UV-vis (CH_2Cl_2): λ_{max} ($\lg \epsilon$) 267 (4.40), 340 (4.07), 370 (4.08), 398 (4.08) nm. CV: $E_1^{1/2} = 0.96$ V, $E_2^{1/2} = 1.22$ V. MS (EI): m/z (%) 616 (100, M^+). Accurate Mass Calcd. for $\text{C}_{28}\text{H}_{24}\text{S}_8$: 615.96438. HRMS (EI): 615.96400 (-0.6 ppm).

2,6-Bis{2-[(*tert*-butyldiphenylsilyl)oxy]ethoxy}-10-[4,5-bis(5-chloropentylthio)-1,3-dithiol-2-ylidene]anthracene-9(10H)-one (293)



The anthraquinone **199** (8.71 g, 10.8 mmol) was dissolved in xylene (15 mL) and added to degassed triethyl phosphite (100 mL), which was stirred at 125 °C under argon. The thione **283**^{40b} (3.06 g, 7.50 mmol) was dissolved in xylene (15 mL) and added dropwise to the reaction mixture over 3 h, causing the solution to turn dark red. The reaction mixture was stirred for another 30 min at 125 °C, before it was cooled to room temperature and concentrated *in vacuo*. The oily residue was purified by column chromatography (silica gel, dichloromethane-petroleum ether, 1:1 v/v gradient to pure dichloromethane) to give **293** as a red syrup (2.95 g, 34%). ¹H NMR (CDCl₃): δ 8.22 (1H, d, *J* = 9.0 Hz), 7.75-7.72 (9H, m), 7.69 (1H, d, *J* = 8.5 Hz), 7.44-7.39 (12H, m), 7.18 (1H, d, *J* = 2.0 Hz), 7.17 (1H, dd, *J*₁ = 8.5 Hz, *J*₂ = 3.0 Hz), 6.92 (1H, dd, *J*₁ = 8.5 Hz, *J*₂ = 2.0 Hz), 4.26 (2H, t, *J* = 5.0 Hz), 4.23 (2H, t, *J* = 5.0 Hz), 4.08 (2H, t, *J* = 5.0 Hz), 4.05 (2H, t, *J* = 5.0 Hz), 3.51 (2H, t, *J* = 6.5 Hz), 3.47 (2H, t, *J* = 6.5 Hz), 2.84 (2H, t, *J* = 7.0 Hz), 2.78 (2H, t, *J* = 7.0 Hz), 1.78-1.71 (4H, m), 1.66-1.51 (8H, m), 1.084 (9H, s), 1.075 (9H, s). MS (EI): *m/z* (%) 1166 (50, [M+4]⁺), 1164 (100, [M+2]⁺), 1162 (90, M⁺). Accurate Mass Calcd. for C₆₃H₇₂Cl₂O₅S₄Si₂Na: 1185.3076. HRMS (ES): 1185.3085 (+0.8 ppm).

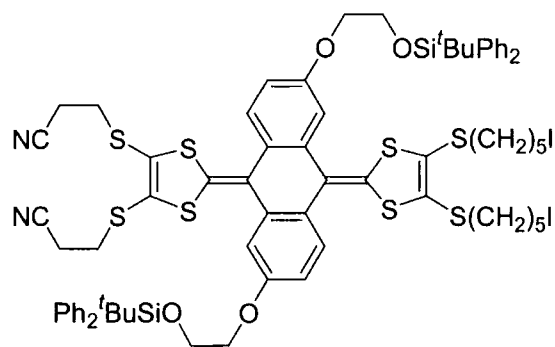
2,6-Bis{2-[(*tert*-butyldiphenylsilyl)oxy]ethoxy}-9-[4,5-bis(5-chloropentylthio)-1,3-dithiol-2-ylidene]-10-[4,5-bis(2-cyanoethylthio)-1,3-dithiol-2-ylidene]-9,10-dihydroanthracene (294)



Triethyl phosphite (50 mL) was degassed, heated to 125 °C and stirred under argon, whereupon a solution of ketone **293** (2.50 g, 2.15 mmol) in xylene (10 mL) was added in one portion. Over the next 4 h thione **256**¹⁶⁴ (5.89 g, 19.4 mmol) was added as a solid in small portions, against a positive pressure of argon. The reaction mixture turned dark

red-brown, and was stirred for another 30 min at 125 °C, before it was cooled to room temperature and concentrated *in vacuo*. The residue was column chromatographed (silica gel, dichloromethane) to give **294** as a yellow foam (1.74 g, 57%), mp 50-53 °C. ¹H NMR (CDCl₃): δ 7.74-7.72 (8H, m), 7.50 (1H, d, *J* = 8.5 Hz), 7.45-7.38 (13H, m), 7.14 (1H, s), 7.04 (1H, s), 6.83 (1H, d, *J* = 9.5 Hz), 6.82 (1H, d, *J* = 9.0 Hz), 4.19-4.16 (4H, m), 4.05 (4H, br m), 3.53 (2H, t, *J* = 6.5 Hz), 3.48 (2H, t, *J* = 6.5 Hz), 3.15-3.09 (1H, m), 3.07-2.98 (2H, m), 2.95-2.90 (1H, m), 2.87-2.77 (4H, m), 2.73-2.70 (2H, m), 2.66-2.64 (2H, m), 1.80-1.73 (4H, m), 1.69-1.63 (4H, m), 1.59-1.52 (4H, m), 1.08 (18H, s). ¹³C NMR (CDCl₃): δ 157.5, 157.2, 136.3, 135.8, 135.62 (2C), 135.60 (2C), 133.46, 133.44, 133.39, 133.37, 129.73, 129.69, 127.7, 127.6, 127.1, 126.6, 126.5, 126.4, 126.2, 126.1, 125.9, 124.9, 122.6, 117.44, 117.41, 112.1, 112.0, 111.7, 69.3 (2C), 62.6 (2C), 44.8, 44.7, 35.81, 35.76, 32.0 (2C), 31.1 (2C), 28.95, 28.90, 26.8 (2C), 25.69, 25.66, 19.2 (2C), 18.93, 18.85. UV-vis (CH₂Cl₂): λ_{max} (lg ε) 361 (4.21), 428 (4.44) nm. CV: *E*^{ox}_{pa} = 0.63 V, *E*^{ox}_{pc} = 0.41 V. MS (ES): *m/z* (%) 1443 (100, [(*M* + 2) + Na]⁺), 1441 (52, [*M* + Na]⁺). Anal. Calcd. for C₇₂H₈₀Cl₂N₂O₄S₈Si₂ (MW 1421.02): C, 60.86; H, 5.67; N, 1.97; found C, 60.60; H, 5.64; N, 1.95.

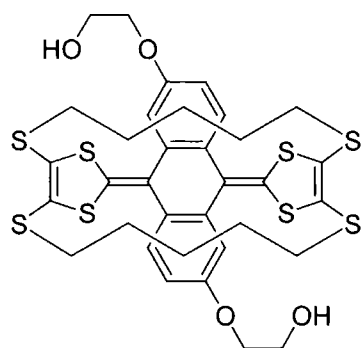
2,6-Bis{2-[(*tert*-butyldiphenylsilyloxy)ethoxy]-9-[4,5-bis(2-cyanoethylthio)-1,3-dithiol-2-ylidene]-10-[4,5-bis(5-iodopentylthio)-1,3-dithiol-2-ylidene]-9,10-dihydroanthracene (295)}



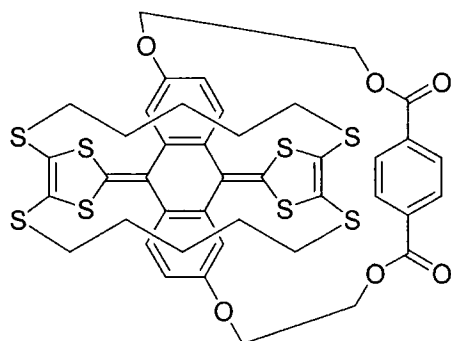
This procedure is similar to the synthesis of **289**. Dichloride **294** (1.60 g, 1.13 mmol) was reacted with sodium iodide (1.80 g, 12.0 mmol) in refluxing 2-butanone (20 mL). Column chromatography (silica gel, dichloromethane) afforded **295** as a yellow foam (1.60 g, 88%), mp 53-56 °C. ¹H NMR (CDCl₃): δ 7.73-7.72 (8H, m), 7.50 (1H, d, *J* = 8.5 Hz), 7.43-7.38 (13H, m), 7.13 (1H, d, *J* = 2.0 Hz), 7.03 (1H, d, *J* = 2.5 Hz), 6.83 (1H, dd, *J*₁ = 8.5 Hz, *J*₂ = 2.5 Hz), 6.81 (1H, dd, *J*₁ = 8.5 Hz, *J*₂ = 2.5 Hz), 4.20-4.14 (4H, m), 4.04 (4H, t, *J* = 5.0 Hz), 3.18-3.15 (2H, m), 3.14-3.11 (3H, m), 3.06-2.99 (2H, m), 2.95-2.90 (1H, m), 2.86-2.76 (4H, m), 2.74-2.71 (2H, m), 2.67-2.64 (2H, m), 1.84-1.77 (4H, m), 1.68-1.61 (4H, m), 1.55-1.46 (4H, m), 1.07 (18H, s). ¹³C NMR (CDCl₃): δ 157.6, 157.2, 136.4,

135.8, 135.64, 135.62, 135.61, 135.60, 133.46, 133.45, 133.39, 133.38, 129.8, 129.7, 127.7, 127.6, 127.1, 126.6, 126.5, 126.4, 126.2, 126.1, 125.9, 124.9, 122.6, 117.5, 117.4, 112.03, 111.99, 111.7, 69.3 (2C), 62.63, 62.59, 35.74, 35.70, 32.76, 32.74, 31.1 (2C), 29.3, 29.2, 28.61, 28.56, 26.8 (2C), 19.2 (2C), 19.0, 18.9, 6.6, 6.5. UV-vis (CH₂Cl₂): λ_{max} (lg ϵ) 361 (4.20), 428 (4.43) nm. CV: $E_{\text{pa}}^{\text{ox}} = 0.63$ V, $E_{\text{pc}}^{\text{ox}} = 0.41$ V. MS (ES): m/z (%) 1625 (35, [M + Na]⁺), 1475 (100). Anal. Calcd. for C₇₂H₈₀I₂N₂O₄S₈Si₂ (MW 1603.92): C, 53.92; H, 5.03; N, 1.75; found C, 53.80; H, 5.02; N, 1.66.

TTFAQ cyclophane **296**



A solution of cesium hydroxide monohydrate (0.565 g, 3.36 mmol) in dry methanol (10 mL) was added to dry degassed *N,N*-dimethylformamide (150 mL), which was stirred under argon at room temperature. A second solution, of diiodide **295** (0.900 g, 0.561 mmol) in dry degassed *N,N*-dimethylformamide (50 mL), was placed in a syringe and pumped into the cesium hydroxide solution over 24 h, using a perfusor pump. The brown reaction mixture was stirred for another 24h, concentrated under reduced pressure, taken into dichloromethane (200 mL), washed with brine, dried (MgSO₄) and concentrated *in vacuo*. Column chromatography (silica gel, dichloromethane until the band containing protecting group by-products were off, then dichloromethane-acetone, 9:1 v/v) afforded **296** as a yellow solid (0.337 g, 78%), mp 182-185 °C. ¹H NMR (CDCl₃): δ 7.23 (2H, d, $J = 8.0$ Hz), 6.89 (2H, dd, $J_1 = 8.0$ Hz, $J_2 = 2.4$ Hz), 6.87 (2H, d, $J = 2.0$ Hz), 4.19-4.16 (4H, m), 4.04-4.02 (4H, m), 2.93-2.82 (4H, m), 2.30-2.22 (4H, m), 2.19 (2H, br s), 1.33-1.22 (6H, m), 1.06-0.98 (4H, m), 0.73-0.65 (2H, m). ¹³C NMR (CDCl₃): δ 157.0, 135.6, 131.0, 128.7, 127.5, 127.3, 127.1, 126.9, 112.6, 112.2, 69.4, 61.4, 35.10, 35.07, 31.9, 31.8, 29.3. UV-vis (CH₂Cl₂): λ_{max} (lg ϵ) 353 (4.22), 411 (4.32) nm. CV: $E_1^{1/2} = 0.89$ V, $E_2^{1/2} = 1.11$ V. MS (EI): m/z (%) 764 (13, M⁺), 328 (100). Accurate Mass Calcd. for C₃₄H₃₆O₄S₈Na: 787.0277. HRMS (ES): 787.0262 (-1.9 ppm).

TTFAQ cyclophane **297**

To a solution of diol **296** (0.117 g, 0.153 mmol) and 1,4-benzenedicarbonyl chloride **205** (0.051 g, 0.250 mmol) in dry dichloromethane (250 mL) was added dry pyridine (0.24 mL, 3.0 mmol) and the reaction was stirred under argon for 16 h at room temperature. The solution was concentrated *in vacuo* and the orange residue purified by column chromatography (silica gel, dichloromethane-acetone, 19:1 v/v)

affording a crude product which was recolumned using a very short column (silica gel, dichloromethane) affording **297** as a yellow powder (0.057 g, 42%), mp > 300 °C. Yellow prisms, suitable for X-ray crystallographic analysis, were grown by slow diffusion of hexane into a solution of **297** in dichloromethane. The crystals contained 2 equivalents of dichloromethane, which was confirmed by elemental analysis (see below). ¹H NMR (CDCl₃): δ 7.16 (2H, d, *J* = 8.0 Hz), 7.13 (2H, d, *J* = 2.5 Hz), 7.01 (2H, dd, *J*₁ = 8.5 Hz, *J*₂ = 2.5 Hz), 6.91 (4H, s), 4.72-4.68 (2H, m), 4.65-4.57 (4H, m), 4.49-4.45 (2H, m), 2.93-2.83 (4H, m), 2.29-2.23 (4H, m), 1.35-1.21 (6H, m), 1.08-1.00 (4H, m), 0.74-0.66 (2H, m). ¹³C NMR (CDCl₃): δ 164.9, 158.5, 135.9, 132.9, 130.4, 129.2, 128.8, 128.0, 127.6, 127.3, 127.0, 115.7, 115.3, 67.3, 66.2, 35.1, 35.0, 31.9, 31.8, 29.3. UV-vis (CH₂Cl₂): λ_{max} (lg ε) 353 (4.16), 414 (4.26) nm. CV: *E*₁^{1/2} = 0.95 V, *E*₂^{1/2} = 1.17 V. MS (EI): *m/z* (%) 894 (23, M⁺), 149 (100). Accurate Mass Calcd. for C₄₂H₃₈O₆S₈Na: 917.0332. HRMS (ES): 917.0340 (+0.9 ppm). Anal. Calcd. for C₄₂H₃₈O₆S₈·(CH₂Cl₂)₂ (MW 1065.14): C, 49.62; H, 3.97; found C, 49.41; H, 3.95.

REFERENCES

- ¹ For an excellent monograph about cyclophanes see:
Vögtle, F. *Cyclophane Chemistry*, Wiley: Chichester **1993**.
- ² Pellegrin, M. M. *Rec. Trav. Chim. Pay-Bas* **1899**, *18*, 457.
- ³ Cram, D. J.; Steinberg, H. *J. Am. Chem. Soc.* **1951**, *73*, 5691-5704.
- ⁴ Cram, D. J.; Allinger, N. L.; Steinberg, H. *J. Am. Chem. Soc.* **1954**, *76*, 6132-6141.
- ⁵ The figure was taken from reference 1, but the spectra were originally published in reference 4.
- ⁶ For reviews on tetrathiafulvalene and chalcogen analogues see:
 - a) Schukat, G.; Richter, A. M.; Fanghänel, E. *Sulfur Reports* **1987**, *7*, 155-231.
 - b) Schukat, G.; Fanghänel, E. *Sulfur Reports* **1993**, *14*, 245-383.
 - c) Schukat, G.; Fanghänel, E. *Sulfur Reports* **1996**, *18*, 1-278.
 - d) Bryce, M. R. *J. Mater. Chem.* **1995**, *5*, 1481-1496.
 - e) Segura, J. L.; Martín, N. *Angew. Chem. Int. Ed.* **2001**, *40*, 1372-1409.
- ⁷ Wudl, F.; Smith, G. M.; Hufnagel, E. J. *J. Chem. Soc., Chem. Commun.* **1970**, 1453-1454.
- ⁸ Hurlley, W. R. H.; Smiles, S. *J. Chem. Soc.* **1926**, 2263-2270.
- ⁹ For a review on TCNQ and TCNQ derivatives see:
Martin, N.; Segura, J. L.; Seoane, C. *J. Mater. Chem.* **1997**, *7*, 1661-1676.
- ¹⁰ Ferraris, J.; Cowan, D. O.; Walatka, V., Jr.; Perlstein, J. H. *J. Am. Chem. Soc.* **1973**, *95*, 948-949.
- ¹¹ For reviews on CT salts, organic metals and superconductors see:
 - a) Bryce, M. R. *Chem. Soc. Rev.* **1991**, *20*, 355-390.
 - b) Underhill, A. E. *J. Mater. Chem.* **1992**, *2*, 1-11.
- ¹² Reviews on TTF cyclophanes are included in reference 6e and in the following publications:
 - a) Becher, J.; Hansen, T. K.; Jørgensen, T.; Stein, P. *Bull. Soc. Chim. Belg.* **1992**, *101*, 555-568.
 - b) Jørgensen, T.; Hansen, T. K.; Becher, J. *Chem. Soc. Rev.* **1994**, *23*, 41-51.
 - c) Nielsen, M. B.; Becher, J. *Liebigs Ann.* **1997**, 2177-2187.

- ¹³ Staab, H. A.; Ippen, J.; Tao-pen, C.; Krieger, C.; Starker, B. *Angew. Chem. Int. Ed. Engl.* **1980**, *19*, 66-67.
- ¹⁴ Ippen, J.; Tao-pen, C.; Starker, B.; Schweitzer, D.; Staab, H. A. *Angew. Chem. Int. Ed. Engl.* **1980**, *19*, 67-68.
- ¹⁵ For cyclophanes containing multiple TTF units (*cis/trans*) means the product contains a mixture of all possible isomers, whereas (*cis,trans*) refers to a cyclophane containing one TTF unit in *cis* conformation and one TTF unit in *trans* conformation.
- ¹⁶ Bertho-Thoraval, F.; Robert, A.; Souizi, A.; Boubekeur, K.; Batail, P. *J. Chem. Soc., Chem. Commun.* **1991**, 843-845.
- ¹⁷ Boubekeur, K.; Lenoir, C.; Batail, P.; Carlier, R.; Tallec, A.; Le Paillard, M.-P.; Lorcy, D.; Robert, A. *Angew. Chem. Int. Ed. Engl.* **1994**, *33*, 1379-1381.
- ¹⁸ Lau, J.; Blanchard, P.; Riou, A.; Jubault, M.; Cava, M. P.; Becher, J. *J. Org. Chem.* **1997**, *62*, 4936-4942.
- ¹⁹ Wang, C.; Bryce, M. R.; Batsanov, A. S.; Howard, J. A. K. *Chem. Eur. J.* **1997**, *3*, 1679-1690.
- ²⁰ The X-ray crystal structure was taken from reference 19.
- ²¹ a) Röhrich, J.; Wolf, P.; Enkelmann, V.; Müllen, K. *Angew. Chem. Int. Ed. Engl.* **1988**, *27*, 1377-1379.
- b) Röhrich, J.; Müllen, K. *J. Org. Chem.* **1992**, *57*, 2374-2379.
- ²² Hansen, T. K.; Jørgensen, T.; Jensen, F.; Thygesen, P. H.; Christiansen, K.; Hursthouse, M. B.; Harman, M. E.; Malik, M. A.; Girmay, B.; Underhill, A. E.; Begtrup, M.; Kilburn, J. D.; Belmore, K.; Roepstorff, P.; Becher, J. *J. Org. Chem.* **1993**, *58*, 1359-1366.
- ²³ Girmay, B.; Kilburn, J. D.; Underhill, A. E.; Varma, K. S.; Hursthouse, M. B.; Harman, M. E.; Becher, J.; Bojesen, G. *J. Chem. Soc., Chem. Commun.* **1989**, 1406-1409.
- ²⁴ Becher, J.; Hansen, T. K.; Malhotra, N.; Bojesen, G.; Bøwadt, S.; Varma, K. S.; Girmay, B.; Kilburn, J. D.; Underhill, A. E. *J. Chem. Soc., Perkin Trans. 1* **1990**, 175-177.
- ²⁵ Jørgensen, T.; Girmay, B.; Hansen, T. K.; Becher, J.; Underhill, A. E.; Hursthouse, M. B.; Harman, M. E.; Kilburn, J. D. *J. Chem. Soc., Perkin Trans. 1* **1992**, 2907-2911.
- ²⁶ Jørgensen, T.; Becher, J.; Hansen, T. K.; Christiansen, K.; Roepstorff, P.; Larsen, S.; Nygaard, A. *Adv. Mater.* **1991**, *3*, 486-488.
- ²⁷ Li, Z.-T.; Stein, P. C.; Svenstrup, N.; Lund, K. H.; Becher, J. *Angew. Chem. Int. Ed. Engl.* **1995**, *34*, 2524-2528.

- ²⁸ For a review on dimeric TTF compounds, including cyclophanes, see:
Otsubo, T.; Aso, Y.; Takimiya, K. *Adv. Mater.* **1996**, *8*, 203-211.
- ²⁹ Izuoka, A.; Tachikawa, T.; Sugawara, T.; Saito, Y.; Shinohara, H. *Chem. Lett.* **1992**, 1049-1052.
- ³⁰ Tachikawa, T.; Izuoka, A.; Sugawara, T. *J. Chem. Soc., Chem. Commun.* **1993**, 1227-1229.
- ³¹ The crystal structures were taken from reference 29 and 30, respectively.
- ³² Becher *et al.* developed a set of versatile TTF building blocks possessing protected thiolate functionalities (see section 6.1.2), which were ideal for the synthesis of TTF cyclophanes.
- ³³ Simonsen, K. B.; Thorup, N.; Becher, J. *Synthesis* **1997**, 1399-1404.
- ³⁴ a) Akutagawa, T.; Abe, Y.; Nezu, Y.; Nakamura, T.; Kataoka, M.; Yamanaka, A.; Inoue, K.; Inabe, T.; Christensen, C. A.; Becher, J. *Inorg. Chem.* **1998**, *37*, 2330-2331.
b) Abe, Y.; Akutagawa, T.; Hasegawa, T.; Nakamura, T.; Sugiura, K.; Sakata, Y.; Inabe, T.; Christensen, C. A.; Becher, J. *Synth. Met.* **1999**, *102*, 1599-1600.
c) Akutagawa, T.; Abe, Y.; Hasegawa, T.; Nakamura, T.; Inabe, T.; Christensen, C. A.; Becher, J. *Chem. Lett.* **2000**, 132-133.
d) Akutagawa, T.; Abe, Y.; Ohta, T.; Hasegawa, T.; Nakamura, T.; Christensen, C. A.; Lau, J.; Becher, J. *Mol. Cryst. Liq. Cryst.* **2000**, *349*, 379-382.
- ³⁵ Akutagawa, T.; Ohta, T.; Hasegawa, T.; Nakamura, T.; Christensen, C. A.; Becher, J. *PNAS: The Special Feature Issue on Supramolecular Chemistry* **2002**, *99*, 5028-5033.
- ³⁶ Spanggaard, H.; Prehn, J.; Nielsen, M. B.; Levillain, E.; Allain, M.; Becher, J. *J. Am. Chem. Soc.* **2000**, *122*, 9486-9494.
- ³⁷ a) Takimiya, K.; Aso, Y.; Ogura, F.; Otsubo, T. *Chem. Lett.* **1995**, 735-736.
b) Takimiya, K.; Aso, Y.; Otsubo, T. *Synth. Met.* **1997**, *86*, 1891-1892.
c) Takimiya, K.; Oharuda, A.; Aso, Y.; Ogura, F.; Otsubo, T. *Chem. Mater.* **2000**, *12*, 2196-2204.
- ³⁸ a) Batsanov, A. S.; John, D. E.; Bryce, M. R.; Howard, J. A. K. *Adv. Mater.* **1998**, *10*, 1360-1363.
b) John, D. E.; Batsanov, A. S.; Bryce, M. R.; Howard, J. A. K. *Synthesis* **2000**, 824-830.
- ³⁹ a) Tanabe, J.; Kudo, T.; Okamoto, M.; Kawada, Y.; Ono, G.; Izuoka, A.; Sugawara, T. *Chem. Lett.* **1995**, 579-580.

- b) Tanabe, J.; Ono, G.; Izuoka, A.; Sugawara, T.; Kudo, T.; Saito, T.; Okamoto, M.; Kawada, Y. *Mol. Cryst. Liq. Cryst.* **1997**, *296*, 61-76.
- c) Izuoka, A.; Tanabe, J.; Sugawara, T.; Kawada, Y.; Kumai, R.; Asamitsu, A.; Tokura, Y. *Mol. Cryst. Liq. Cryst.* **1997**, *306*, 265-270.
- ⁴⁰ a) Takimiya, K.; Shibata, Y.; Imamura, K.; Kashihara, A.; Aso, Y.; Otsubo, T.; Ogura, F. *Tetrahedron Lett.* **1995**, *36*, 5045-5048.
- b) Takimiya, K.; Imamura, K.; Shibata, Y.; Aso, Y.; Ogura, F.; Otsubo, T. *J. Org. Chem.* **1997**, *62*, 5567-5574.
- ⁴¹ The X-ray crystal structures were taken from reference 40.
- ⁴² Nielsen, M. B.; Thorup, N.; Becher, J. *J. Chem. Soc., Perkin Trans. 1* **1998**, 1305-1308.
- ⁴³ Adam, M.; Enkelmann, V.; Räder, H.-J.; Röhrich, J.; Müllen, K. *Angew. Chem. Int. Ed. Engl.* **1992**, *31*, 309-310.
- ⁴⁴ Matsuo, K.; Takimiya, K.; Aso, Y.; Otsubo, T.; Ogura, F. *Chem. Lett.* **1995**, 523-524.
- ⁴⁵ The X-ray crystal structure was taken from reference 44.
- ⁴⁶ Simonsen, K. B.; Svenstrup, N.; Lau, J.; Thorup, N.; Becher, J. *Angew. Chem. Int. Ed.* **1999**, *38*, 1417-1420.
- ⁴⁷ Lau, J.; Becher, J. *Synthesis* **1997**, 1015-1020.
- ⁴⁸ a) Li, Z.-T.; Becher, J. *Chem. Commun.* **1996**, 639-640.
- b) Nielsen, M. B.; Li, Z.-T.; Becher, J. *J. Mater. Chem.* **1997**, *7*, 1175-1187.
- ⁴⁹ a) Blanchard, P.; Svenstrup, N.; Becher, J. *Chem. Commun.* **1996**, 615-616.
- b) Blanchard, P.; Svenstrup, N.; Rault-Berthelot, J.; Riou, A.; Becher, J. *Eur. J. Org. Chem.* **1998**, 1743-1757.
- ⁵⁰ Moriarty, R. M.; Tao, A.; Gilardi, R.; Song, Z.; Tuladhar, S. M. *Chem. Commun.* **1998**, 157-158.
- ⁵¹ Simonsen, K. B.; Zong, K.; Rogers, R. D.; Cava, M. P.; Becher, J. *J. Org. Chem.* **1997**, *62*, 679-686.
- ⁵² Simonsen, K. B.; Thorup, N.; Cava, M. P.; Becher, J. *Chem. Commun.* **1998**, 901-902.
- ⁵³ Hansen, J. G.; Bang, K. S.; Thorup, N.; Becher, J. *Eur. J. Org. Chem.* **2000**, 2135-2144.
- ⁵⁴ The X-ray crystal structures were taken from reference 53.
- ⁵⁵ Yoshida, Z.; Kawase, T.; Awaji, H.; Sugimoto, I.; Sugimoto, T.; Yoneda, S. *Tetrahedron Lett.* **1983**, *24*, 3469-3472.
- ⁵⁶ Yoshida, Z.; Kawase, T.; Awaji, H.; Yoneda, S. *Tetrahedron Lett.* **1983**, *24*, 3473-3476.

- 57 CV data was obtained from references 55 and 56.
- 58 Akiba, K.; Ishikawa, K.; Inamoto, N. *Bull. Chem. Soc. Jpn.* **1978**, *51*, 2674-2683.
- 59 Moore, A. J. *Ph.D. Thesis, University of Durham* **1989**.
- 60 Bryce, M. R.; Moore, A. J. *Synth. Met.* **1988**, *25*, 203-205.
- 61 Moore, A. J.; Bryce, M. R. *Synthesis* **1991**, 26-28.
- 62 Yamashita, Y.; Kobayashi, Y.; Miyashi, T. *Angew. Chem. Int. Ed. Engl.* **1989**, *28*, 1052-1053.
- 63 Bryce, M. R.; Moore, A. J.; Hasan, M.; Ashwell, G. J.; Fraser, A. T.; Clegg, W.; Hursthouse, M. B.; Karaulov, A. I. *Angew. Chem. Int. Ed. Engl.* **1990**, *29*, 1450-1452.
- 64 Martín, N.; Sánchez, L.; Seoane, C.; Ortí, E.; Viruela, P. M.; Viruela, R. *J. Org. Chem.* **1998**, *63*, 1268-1279.
- 65 The crystal structure was taken from reference 63.
- 66 Godbert, N.; Bryce, M. R.; Dahaoui, S.; Batsanov, A. S.; Howard, J. A. K.; Hazendonk, P. *Eur. J. Org. Chem.* **2001**, 749-757.
- 67 The ^1H NMR spectrum was taken from reference 66.
- 68 Liu, S.-G.; Pérez, I.; Martín, N.; Echegoyen, L. *J. Org. Chem.* **2000**, *65*, 9092-9102.
- 69 Electrochemical reversibility is in this context defined as:
- (i) The ratio between the cathodic and anodic peak current $I_c/I_a \approx 1:1$;
 - (ii) The peak potentials E_p are independent of the scan rate;
 - (iii) $\Delta E_p \approx (59/z)$ mV, where z is the number of electrons involved in the process.
- Quasi-reversibility is defined as the situation where ΔE_p becomes significantly larger than $(59/z)$ mV, where z is the number of electrons involved in the process.
- 70 Bryce, M. R.; Coffin, M. A.; Hursthouse, M. B.; Karaulov, A. I.; Müllen, K.; Scheich, H. *Tetrahedron Lett.* **1991**, *32*, 6029-6032.
- 71 Kurata, H.; Tanaka, T.; Oda, M. *Chem. Lett.* **1999**, 749-750.
- 72 Triki, S.; Ouahab, L.; Lorcy, D.; Robert, A. *Acta Cryst.* **1993**, *C49*, 1189-1192.
- 73 Bryce, M. R.; Finn, T.; Batsanov, A. S.; Katakay, R.; Howard, J. A. K.; Lyubchik, S. B. *Eur. J. Org. Chem.* **2000**, 1199-1205.
- 74 Batail, P.; Boubekour, K.; Fourmigué, M.; Gabriel, J.-C. P. *Chem. Mater.* **1998**, *10*, 3005-3015.

- 75 Saito, K.; Sugiura, C.; Tanimoto, E.; Saito, K.; Yamashita, Y. *Heterocycles* **1994**, *38*, 2153-2158.
- 76 Batsanov, A. S.; Bryce, M. R.; Coffin, M. A.; Green, A.; Hester, R. E.; Howard, J. A. K.; Lednev, I. K.; Martín, N.; Moore, A. J.; Moore, J. N.; Ortí, E.; Sánchez, L.; Savirón, M.; Viruela, P. M.; Viruela, R.; Ye, T.-Q. *Chem. Eur. J.* **1998**, *4*, 2580-2592.
- 77 Jones, A. E.; Christensen, C. A.; Perepichka, D. F.; Batsanov, A. S.; Beeby, A.; Low, P. J.; Bryce, M. R.; Parker, A. W. *Chem. Eur. J.* **2001**, *7*, 973-978.
- 78 Experimental details, the X-ray crystal structure of the dication salt and the absorption spectra were published in reference 77.
- 79 The crystal structure was taken from reference 76.
- 80 Brock, C. P. *Acta. Cryst.* **1990**, *B46*, 795-806.
- 81 Notice: The atom numbering is different in the structure of neutral **54** (Figure 25) from the atom numbering in the structure of the dication **54**²⁺ (Figure 26). All numbers in the text refer to the structure of **54**²⁺ (Figure 26).
- 82 Zefirov, Yu. V.; Zorkii, P. M. *Russ. Chem. Rev.* **1995**, *64*, 415-428.
- 83 Experimental details for spectroelectrochemistry can be found in Appendix Two.
- 84 Guldi, D. M.; Sánchez, L.; Martín, N. *J. Phys. Chem. B* **2001**, *105*, 7139-7144.
- 85 Martín, N.; Sánchez, L.; Guldi, D. M. *Chem. Commun.* **2000**, 113-114.
- 86 Moore, A. J.; Bryce, M. R. *J. Chem. Soc., Perkin Trans. 1* **1991**, 157-168.
- 87 A symmetric TTFAQ derivative is defined as comprising two identical 1,3-dithiole units, whereas the opposite is true for unsymmetrical TTFAQ derivatives.
- 88 Ishikawa, K.; Akiba, K.; Inamoto, N. *Tetrahedron Lett.* **1976**, *17*, 3695-3698.
- 89 Bryce, M. R.; Moore, A. J.; Lorcy, D.; Dhindsa, A. S.; Robert, A. *J. Chem. Soc., Chem. Commun.* **1990**, 470-472.
- 90 Moore, A. J.; Bryce, M. R. *Tetrahedron Lett.* **1992**, *33*, 1373-1376.
- 91 Fourmigué, M.; Krebs, F. C.; Larsen, J. *Synthesis* **1993**, 509-512.
- 92 a) Kozaki, M.; Tanaka, S.; Yamashita, Y. *J. Chem. Soc., Chem. Commun.* **1992**, 1137-1138.
b) Kozaki, M.; Tanaka, S.; Yamashita, Y. *J. Org. Chem.* **1994**, *59*, 442-450.
- 93 Moore, A. J.; Bryce, M. R. *Synthesis* **1997**, 407-409.
- 94 Bryce, M. R.; Finn, T.; Moore, A. J.; Batsanov, A. S.; Howard, J. A. K. *Eur. J. Org. Chem.* **2000**, 51-60.

- ⁹⁵ Moore, A. J.; Bryce, M. R.; Batsanov, A. S.; Cole, J. C.; Howard, J. A. K. *Synthesis* **1995**, 675-682.
- ⁹⁶ Finn, T. *Ph.D. Thesis, University of Durham* **2000**.
- ⁹⁷ For a review on TTF containing covalently linked donor-acceptor systems, see:
Bryce, M. R. *Adv. Mater.* **1999**, *11*, 11-23.
- ⁹⁸ Martín, N.; Pérez, I.; Sánchez, L.; Seoane, C. *J. Org. Chem.* **1997**, *62*, 5690-5695.
- ⁹⁹ Herranz, M. A.; Martín, N.; Sánchez, L.; Garín, J.; Orduna, J.; Alcalá, R.; Villacampa, B.; Sánchez, C. *Tetrahedron* **1998**, *54*, 11651-11658.
- ¹⁰⁰ Herranz, M. A.; González, S.; Pérez, I.; Martín, N. *Tetrahedron* **2001**, *57*, 725-731.
- ¹⁰¹ Herranz, M. A.; Martín, N.; Sánchez, L.; Seoane, C.; Guldi, D. M. *J. Organomet. Chem.* **2000**, *599*, 2-7.
- ¹⁰² Herranz, M. A.; Illescas, B.; Martín, N.; Luo, C.; Guldi, D. M. *J. Org. Chem.* **2000**, *65*, 5728-5738.
- ¹⁰³ Scheib, S.; Cava, M. P.; Baldwin, J. W.; Metzger, R. M. *J. Org. Chem.* **1998**, *63*, 1198-1204.
- ¹⁰⁴ a) Segura, J. L.; Martín, N.; Seoane, C.; Hanack, M. *Tetrahedron Lett.* **1996**, *37*, 2503-2506.
b) González, M.; Illescas, B.; Martín, N.; Segura, J. L.; Seoane, C.; Hanack, M. *Tetrahedron* **1998**, *54*, 2853-2866.
- ¹⁰⁵ Tsiperman, E.; Regev, T.; Becker, J. Y.; Bernstein, J.; Ellern, A.; Khodorkovskiy, V.; Shames, A.; Shapiro, L. *Chem. Commun.* **1999**, 1125-1126.
- ¹⁰⁶ The X-ray crystal structure was taken from reference 105.
- ¹⁰⁷ Watson, W. H.; Eduok, E. E.; Kashyap, R. P.; Krawiec, M. *Tetrahedron* **1993**, *49*, 3035-3042.
- ¹⁰⁸ Frenzel, S.; Müllen, K. *Synth. Met.* **1996**, *80*, 175-182.
- ¹⁰⁹ a) Llacay, J.; Mas, M.; Molins, E.; Veciana, J.; Powell, D.; Rovira, C. *Chem. Commun.* **1997**, 659-660.
b) Llacay, J.; Veciana, J.; Vidal-Gancedo, J.; Bourdelande, J. L.; Gonzalez-Moreno, R.; Rovira, C. *J. Org. Chem.* **1998**, *63*, 5201-5210.
c) Llacay, J.; Pérez-Benítez, A.; Mas-Torrent, M.; Vidal-Gancedo, J.; Veciana, J.; Rovira, C. *Synth. Met.* **1999**, *102*, 1488-1489.
- ¹¹⁰ Llacay, J.; Mata, I.; Molins, E.; Veciana, J.; Rovira, C. *Adv. Mater.* **1998**, *3*, 330-334.

- ¹¹¹ Hudhomme, P.; Liu, S.G.; Kreher, D.; Cariou, M.; Gorgues, A. *Tetrahedron Lett.* **1999**, *40*, 2927-2930.
- ¹¹² Belik, P.; Gügel, A.; Spickermann, J.; Müllen, K. *Angew. Chem. Int. Ed. Engl.* **1993**, *32*, 78-80.
- ¹¹³ a) Boulle, C.; Rabreau, J. M.; Hudhomme, P.; Cariou, M.; Jubault, M.; Gorgues, A.; Orduna, J.; Garin, J. *Tetrahedron Lett.* **1997**, *38*, 3909-3910.
b) Hudhomme, P.; Boulle, C.; Rabreau, J. M.; Cariou, M.; Jubault, M.; Gorgues, A. *Synth. Met.* **1998**, *94*, 73-75.
- ¹¹⁴ Boulle, C.; Cariou, M.; Bainville, M.; Gorgues, A.; Hudhomme, P.; Orduna, J.; Garin, J. *Tetrahedron Lett.* **1997**, *38*, 81-84.
- ¹¹⁵ Boulle, C.; Desmars, O.; Gautier, N.; Hudhomme, P.; Cariou, M.; Gorgues, A. *Chem. Commun.* **1998**, 2197-2198.
- ¹¹⁶ Kreher, D.; Liu, S.-G.; Cariou, M.; Hudhomme, P.; Gorgues, A.; Mas, M.; Veciana, J.; Rovira, C. *Tetrahedron Lett.* **2001**, *42*, 3447-3450.
- ¹¹⁷ Liu, S.-G.; Kreher, D.; Hudhomme, P.; Levillain, E.; Cariou, M.; Delaunay, J.; Gorgues, A.; Vidal-Gancedo, J.; Veciana, J.; Rovira, C. *Tetrahedron Lett.* **2001**, *42*, 3717-3720.
- ¹¹⁸ Gautier, N.; Mercier, N.; Riou, A.; Gorgues, A.; Hudhomme, P. *Tetrahedron Lett.* **1999**, *40*, 5997-6000.
- ¹¹⁹ Fox, M. A.; Pan, H. *J. Org. Chem.* **1994**, *59*, 6519-6527.
- ¹²⁰ Easton, D. B. J.; Leaver, D. *Chem. Commun.* **1965**, 585-586.
- ¹²¹ a) O'Connor, B. R.; Jones, F. N. *J. Org. Chem.* **1970**, *35*, 2002-2005.
b) Melby, L. R.; Hartzler, H. D.; Sheppard, W. A. *J. Org. Chem.* **1974**, *39*, 2456-2459.
- ¹²² Jeppesen, J. O.; Takimiya, K.; Thorup, N.; Becher, J. *Synthesis* **1999**, 803-810.
- ¹²³ Christensen, C. A.; Bryce, M. R.; Batsanov, A. S.; Howard, J. A. K.; Jeppesen, J. O.; Becher, J. *Chem. Commun.* **1999**, 2433-2434.
- ¹²⁴ Herranz, M. A.; Martín, N. *Org. Lett.* **1999**, *1*, 1481-1496.
- ¹²⁵ Bryce, M. R.; Finn, T.; Moore, A. J. *Tetrahedron Lett.* **1999**, *40*, 3271-3274.
- ¹²⁶ Appel, R. *Angew. Chem. Int. Ed. Engl.* **1975**, *14*, 801-811.
- ¹²⁷ a) Martín, N.; Pérez, I.; Sánchez, L.; Seoane, C. *Synth. Met.* **1997**, *86*, 1867-1868.
b) Martín, N.; Pérez, I.; Sánchez, L.; Seoane, C. *J. Org. Chem.* **1997**, *62*, 870-877.
- ¹²⁸ Pérez, I.; Liu, S.-G.; Martín, N.; Echegoyen, L. *J. Org. Chem.* **2000**, *65*, 3796-3803

- ¹²⁹ E_{pa}^{ox} is the oxidation peak potential on the first anodic scan; E_{pc}^{ox} is the coupled reduction peak potential on the cathodic scan.
- ¹³⁰ E_{pc}^{red} is the reduction peak potential on the first cathodic scan; E_{pa}^{red} is the coupled oxidation peak potential on the following anodic scan.
- ¹³¹ a) Jeppesen, J. O.; Takimiya, K.; Jensen, F.; Becher, J. *Org. Lett.* **1999**, *1*, 1291-1294.
b) Jeppesen, J. O.; Takimiya, K.; Jensen, F.; Brimert, T.; Nielsen, K.; Thorup, N.; Becher, J. *J. Org. Chem.* **2000**, *65*, 5794-5805.
- ¹³² a) Jeppesen, J. O.; Perkins, J.; Becher, J.; Stoddart, J. F. *Angew. Chem. Int. Ed.* **2001**, *40*, 1216-1221.
b) Collier, C. P.; Jeppesen, J. O.; Luo, Y.; Perkins, J.; Wong, E. W.; Heath, J. R.; Stoddart, J. F. *J. Am. Chem. Soc.* **2001**, *123*, 12632-12641.
c) Jeppesen, J. O.; Becher, J.; Stoddart, J. F. *Org. Lett.* **2002**, *4*, 557-560.
- ¹³³ Nielsen, K.; Jeppesen, J. O.; Thorup, N.; Becher, J. *Org. Lett.* **2002**, *4*, 1327-1330.
- ¹³⁴ Hunter, C. A.; Sanders, J. K. M. *J. Am. Chem. Soc.* **1990**, *112*, 5525-5534.
- ¹³⁵ The X-ray crystal structure was taken from reference 133.
- ¹³⁶ Becher, J.; Brimert, T.; Jeppesen, J. O.; Pedersen, J. Z.; Zubarev, R.; Bjørnholm, T.; Reitzel, N.; Jensen, T. R.; Kjaer, K.; Levillain, E. *Angew. Chem. Int. Ed.* **2001**, *40*, 2497-2500.
- ¹³⁷ Bottino, F.; Grazia, M. D.; Finocchiaro, P.; Fronczek, F. R.; Mamo, A.; Pappalardo, S. *J. Org. Chem.* **1988**, *53*, 3521-3529.
- ¹³⁸ a) Perepichka, I. F.; Mysyk, D. D. *USSR Patent*, 862 561, **1981**.
b) Semenenko, N. M.; Abramov, V. N.; Kravchenko, N. V.; Trushina, V. S.; Buyanovskaya, P. G.; Kashina, V. L.; Mashkevich, I. V. *Zh. Obsch. Khim.* **1985**, *55*, 324.
- ¹³⁹ Brimert, T. *The Quest for TTF-Annulated Porphyrins, Final Report, Odense University* **2000** – unpublished results.
- ¹⁴⁰ Rowland, R. S.; Taylor, R. *J. Phys. Chem.* **1996**, *100*, 7384-7391.
- ¹⁴¹ a) Perepichka, I. F.; Perepichka, D. F.; Lyubchik, S. B.; Bryce, M. R.; Batsanov, A. S.; Howard, J. A. K. *J. Chem. Soc., Perkin Trans. 2* **2001**, 1546-1551.
b) Perepichka, D. F.; Perepichka, I. F.; Popov, A. F.; Bryce, M. R.; Batsanov, A. S.; Chesney, A.; Howard, J. A. K.; Sokolov, N. I. *J. Organomet. Chem.* **2001**, *637-639*, 445-462.

- ¹⁴² Perepichka, I. F.; Perepichka, D. F.; Bryce, M. R.; Goldenberg, L. M.; Kuz'mina, L. G.; Popov, A. F.; Chesney, A.; Moore, A. J.; Howard, J. A. K.; Sokolov, N. I. *Chem. Commun.* **1998**, 819-820.
- ¹⁴³ Finn, T.; Bryce, M. R.; Batsanov, A. S.; Howard, J. A. K. *Chem. Commun.* **1999**, 1835-1836.
- ¹⁴⁴ The redox properties of TTFAQ cyclophanes will be discussed in detail in section 5.2.5 and 6.5.
- ¹⁴⁵ Godbert, N.; Batsanov, A. S.; Bryce, M. R.; Howard, J. A. K. *J. Org. Chem.* **2001**, *66*, 713-719.
- ¹⁴⁶ Cerrada, E.; Bryce, M. R.; Moore, A. J. *J. Chem. Soc., Perkin Trans. 1* **1993**, 537-538.
See also references: 68, 85, 98, 99, 100, 101, 102, 127 and 128.
- ¹⁴⁷ Marshallsay, G. J.; Bryce, M. R. *J. Org. Chem.* **1994**, *59*, 6847-6849.
- ¹⁴⁸ Tobe, Y.; Saiki, S.; Utsumi, N.; Kusumoto, T.; Ishii, H.; Kakiuchi, K.; Kobiro, K.; Naemura, K. *J. Am. Chem. Soc.* **1996**, *118*, 9488-9497.
- ¹⁴⁹ Pascal, R. A., Jr.; McMillan, W. D.; Van Engen, D.; Eason, R. G. *J. Am. Chem. Soc.* **1987**, *109*, 4660-4665.
- ¹⁵⁰ This project is included in the following manuscript:
Perepichka, D. F.; Bryce, M. R.; Perepichka, I. F.; Lyubchik, S. B.; Christensen, C. A.; Godbert, N.; Batsanov, A. S.; Levillain, E.; McInnes, E. J. L.; Zhao, J. P. *J. Am. Chem. Soc.* accepted for publication **2002**.
- ¹⁵¹ The crystal structure is taken from reference 150.
- ¹⁵² All the known X-ray crystal structures of nitrofluorene-TTF charge-transfer complexes are neutral or have only partial charge-transfer:
- a) Perepichka, I. F.; Popov, A. F.; Orekhova, T. V.; Bryce, M. R.; Andrievskii, A. M.; Batsanov, A. S.; Howard, J. A. K.; Sokolov, N. I. *J. Org. Chem.* **2000**, *65*, 3053-3063.
- b) Perepichka, I. F.; Kuz'mina, L. G.; Perepichka, D. F.; Bryce, M. R.; Goldenberg, L. M.; Popov, A. F.; Howard, J. A. K. *J. Org. Chem.* **1998**, *63*, 6484-6493.
- c) Moore, A. J.; Bryce, M. R.; Batsanov, A. S.; Heaton, J. N.; Lehmann, C. W.; Howard, J. A. K.; Robertson, N.; Underhill, A. E.; Perepichka, I. F. *J. Mater. Chem.* **1998**, *8*, 1541-1550.
- d) Soriano-García, M.; Toscano, R. A.; Robles Martínez, J. G.; Salmerón, U. A.; Lezama R. R. *Acta Cryst.* **1989**, *C45*, 1442-1444.

- ¹⁵³ a) Flandrois, S.; Chasseau, D. *Acta Cryst.* **1977**, *B33*, 2744-2750.
b) Kistenmacher, T. J.; Emge, T. J.; Bloch, A. N.; Cowan, D. O. *Acta Cryst.* **1982**, *B38*, 1193-1199.
- ¹⁵⁴ Dietrich-Buchecker, C. O.; Sauvage, J.-P. *Chem. Rev.* **1987**, *87*, 795-810.
- ¹⁵⁵ Jørgensen, T.; Becher, J.; Chambron, J.-C.; Sauvage, J.-P. *Tetrahedron Lett.* **1994**, *35*, 4339-4342.
- ¹⁵⁶ Bang, K. S.; Nielsen, M. B.; Zubarev, R.; Becher, J. *Chem. Commun.* **2000**, 215-216.
- ¹⁵⁷ Bang, K. S. *Master Thesis, Odense University* **1999**.
- ¹⁵⁸ Mitsunobu, O. *Synthesis* **1981**, 1-28.
- ¹⁵⁹ Bryce, M. R.; Batsanov, A. S.; Finn, T.; Hansen, T. K.; Moore, A. J.; Howard, J. A. K.; Kamenjicki, M.; Lednev, I. K.; Asher, S. A. *Eur. J. Org. Chem.* **2001**, 933-940.
- ¹⁶⁰ Hansen, T. K.; Jørgensen, T.; Stein, P. C.; Becher, J. *J. Org. Chem.* **1992**, *57*, 6403-6409.
- ¹⁶¹ Godbert, N.; Bryce, M. R. *J. Mater. Chem.* **2002**, *12*, 27-36.
- ¹⁶² a) Scherowsky, G.; Weiland, J. *Chem. Ber.* **1974**, *107*, 3155-3163.
b) Yoneda, S.; Kawase, T.; Inaba, M.; Yoshida, Z. *J. Org. Chem.* **1978**, *43*, 595-598.
- ¹⁶³ A review describing the development of cyanoethyl protected TTF thiolates:
Simonsen, K. B.; Becher, J. *Synlett* **1997**, 1211-1220.
- ¹⁶⁴ Svenstrup, N.; Rasmussen, K. M.; Hansen, T. K.; Becher, J. *Synthesis* **1994**, 809-812.
- ¹⁶⁵ a) Becher, J.; Lau, J.; Leriche, P.; Mørk, P.; Svenstrup, N. *J. Chem. Soc., Chem. Commun.* **1994**, 2715-2716.
b) Simonsen, K. B.; Svenstrup, N.; Lau, J.; Simonsen, O.; Mørk, P.; Kristensen, G. J.; Becher, J. *Synthesis* **1996**, 407-418.
- ¹⁶⁶ Nielsen, S. B.; Nielsen, M. B. *New J. Chem.* **2001**, *25*, 769-771.
- ¹⁶⁷ Becher, J. *Phosphorus, Sulfur and Silicon* **1999**, *153-154*, 99-117.
- ¹⁶⁸ Li, Z.-T.; Stein, P. C.; Becher, J.; Jensen, D.; Mørk, P.; Svenstrup, N. *Chem. Eur. J.* **1996**, *2*, 624-633.
- ¹⁶⁹ Damgaard, D.; Nielsen, M. B.; Lau, J.; Jensen, K. B.; Zubarev, R.; Levillain, E.; Becher, J. *J. Mater. Chem.* **2000**, *10*, 2249-2258.
- ¹⁷⁰ a) Lau, J.; Simonsen, O.; Becher, J. *Synthesis* **1995**, 521-526.
b) Wang, C.; Bryce, M. R.; Batsanov, A. S.; Goldenberg, L. M.; Howard, J. A. K. *J. Mater. Chem.* **1997**, *7*, 1189-1197.

- c) Christensen, C. A.; Goldenberg, L. M.; Bryce, M. R.; Becher, J. *Chem. Commun.* **1998**, 509-510.
- ¹⁷¹ a) Nielsen, M. B.; Nielsen, S. B.; Becher, J. *Chem. Commun.* **1998**, 475-476.
b) Nielsen, M. B.; Hansen, J. G.; Becher, J. *Eur. J. Org. Chem.* **1999**, 2807-2815.
- ¹⁷² Becher, J.; Li, Z.-T.; Blanchard, P.; Svenstrup, N.; Lau, J.; Nielsen, M. B.; Leriche, P. *Pure & Appl. Chem.* **1997**, *69*, 465-470.
- ¹⁷³ Binet, L.; Fabre, J. M.; Montginoul, C.; Simonsen, K. B.; Becher, J. *J. Chem. Soc., Perkin Trans. 1* **1996**, 783-788.
- ¹⁷⁴ Moore, A. J.; Finn, T.; Bryce, M. R. *Unpublished results*.
- ¹⁷⁵ Several by-products can be formed in phosphite mediated coupling reactions. See reference 162 and:
- a) Parg, R. P.; Kilburn, J. D.; Ryan, T. G. *Synthesis* **1994**, 195-198.
b) Gautier, N.; Cariou, M.; Gorgues, A.; Hudhomme, P. *Tetrahedron Lett.* **2000**, *41*, 2091-2095.
- ¹⁷⁶ March, J. *Advanced Organic Chemistry – Reactions, Mechanisms, and Structures, Fourth Edition* Wiley-Interscience, **1992**, 1029-1030.
- ¹⁷⁷ Review: Svenstrup, N.; Becher, J. *Synthesis* **1995**, 215-235.
- ¹⁷⁸ a) Hansen, T. K.; Becher, J.; Jørgensen, T.; Varma, K. S.; Khedekar, R.; Cava, M. P. *Org. Synth.* **1996**, *73*, 270-277.
b) Wang, C.; Batsanov, A. S.; Bryce, M. R.; Howard, J. A. K. *Synthesis* **1998**, 1615-1618.
- ¹⁷⁹ Godbert, N. *Ph.D. Thesis, Durham University* **2001**.
- ¹⁸⁰ Batsanov, A. S.; Svenstrup, N.; Lau, J.; Becher, J.; Bryce, M. R.; Howard, J. A. K. *J. Chem. Soc., Chem. Commun.* **1995**, 1201-1202.
- ¹⁸¹ The X-ray crystal structure of cyclophane **185** was taken from reference 143.
- ¹⁸² Kawaguchi, T.; Tanaka, K.; Takeuchi, T.; Watanabe, T. *Bull. Chem. Soc. Japan* **1973**, *46*, 62-66.
- ¹⁸³ Lau, J. *Ph.D. Thesis, Odense University* **1999**.
- ¹⁸⁴ Christensen, C. A.; Bryce, M. R.; Becher, J. *Synthesis* **2000**, 1695-1704.
- ¹⁸⁵ Khodorkovsky, V.; Shapiro, L.; Krief, P.; Shames, A.; Mabon, G.; Gorgues, A.; Giffard, M. *Chem. Commun.* **2001**, 2736-2737.
- ¹⁸⁶ The non-integer integrals is due to exchange, since the molecule adopts two different conformations. See section 3.5.3 for a thorough explanation.

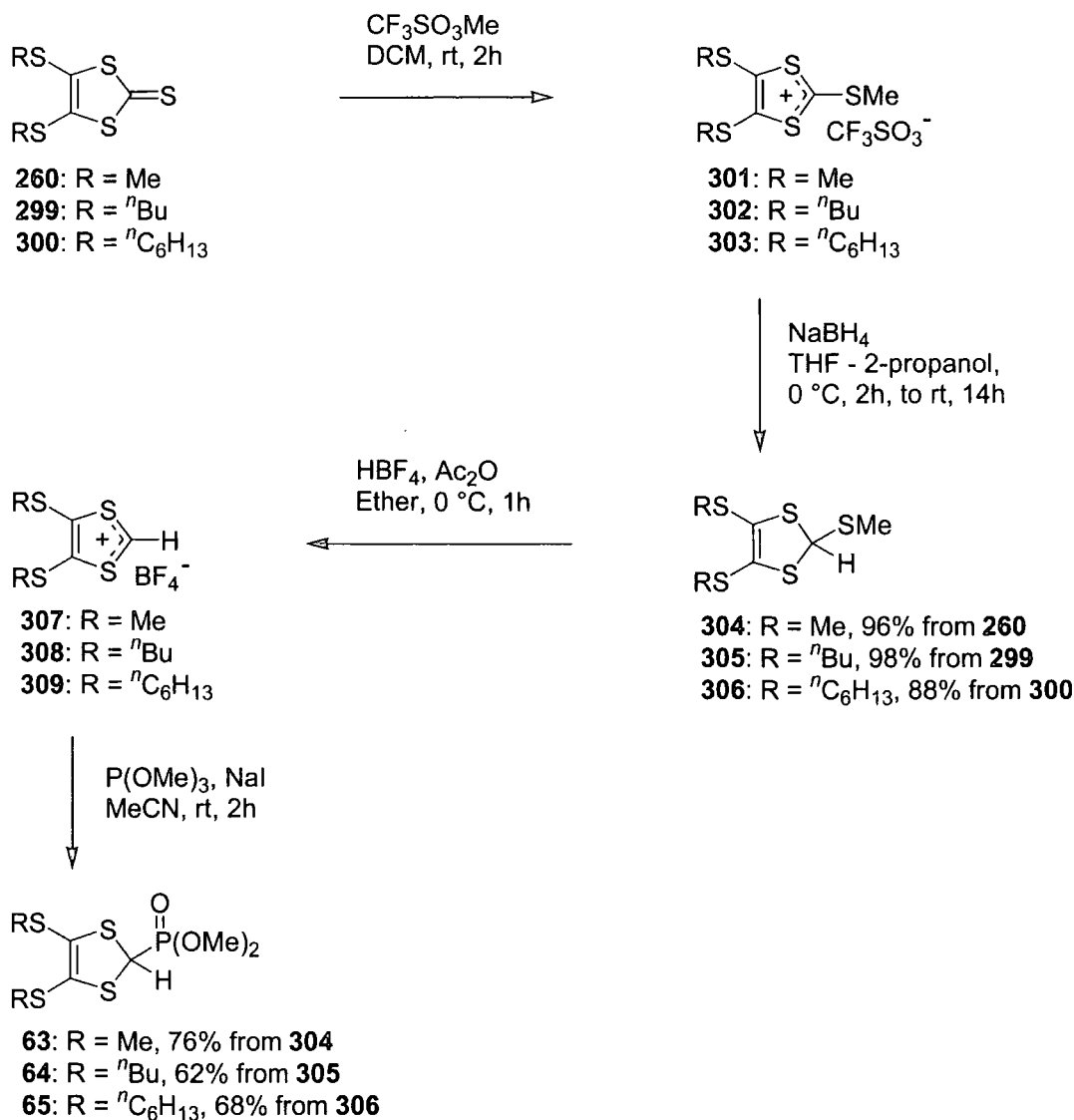
- ¹⁸⁷ The non-integer integrals is due to exchange, since the molecule adopts two different conformations.
- ¹⁸⁸ This is a different synthesis, with easier work-up, but the compound is known from: Paquette, L. A.; Doherty, A. M.; Rayner, C. M. *J. Am. Chem. Soc.* **1992**, *114*, 3910-3926.
- ¹⁸⁹ Kindly donated by the group of Prof. Becher, Odense University (see reference 157). Experimental procedures can be found in reference 154 and in: Dietrich-Buchecker, C. O.; Marnot, P. A.; Sauvage, J.-P. *Tetrahedron Lett.* **1982**, *23*, 5291-5294.
- ¹⁹⁰ This is a very different synthesis than published in the literature, but the compound is known from reference 76.
- ¹⁹¹ Van der Made, A. W.; Van der Made, R. H. *J. Org. Chem.* **1993**, *58*, 1262-1263.

APPENDIX ONE: SYNTHESIS OF PHOSPHONATE ESTERS

This Appendix will detail the syntheses of the phosphonate esters **63-65** used in this thesis, and also review the synthesis of three other commonly used phosphonate esters (**66-68**, Scheme III). Phosphonate esters **63-65** are known from the literature (see Experimental Procedures), but their synthesis is sparsely described and different modifications developed in our group have never been published.

SYNTHESIS OF PHOSPHONATE ESTERS FROM 4,5-BIS(ALKYLTHIO)-1,3-DITHIOLE-2-THIONES

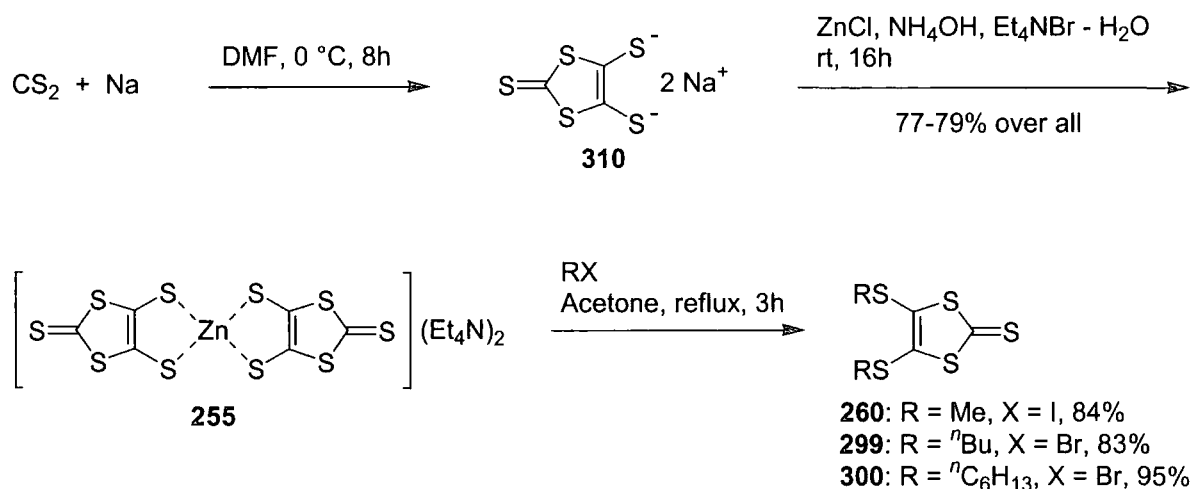
As the first step in the synthesis (Scheme I) the methylation of the 4,5-bis(alkylthio)-1,3-dithiole-2-thiones **260**, **299** and **300** gives the dithiolium salts **301-303**. In early papers methylation was carried out using neat dimethyl sulfate,ⁱ followed by an anion exchange using tetrafluoroboric acid, to yield the tetrafluoroborate salt. We have now found that methylation in a dichloromethane solution using 1 equivalent of methyl triflate at room temperature proceeds in quantitative yield; evaporation of the reaction mixture *in vacuo* after 2 h furnished the crude triflate salts **301-303**. Due to their instability, these salts were used immediately without any workup, after ¹H NMR spectra proved their purity. Reduction of **301-303** was carried out in a mixture of tetrahydrofuran and 2-propanol using sodium borohydride, and purification by column chromatography afforded the thioethers **304-306** as yellow oils in 88-98% yield from the thiones. The next step has been traditionally carried out in neat acetic acid anhydride, but dry diethyl ether with just a few drops of acetic acid anhydride is preferable. The thioethers **304-306** were protonated using tetrafluoroboric acid which afforded elimination of methanethiol and precipitation of the 1,3-dithiolium tetrafluoroborate salt **307**, after which the solvent could be decanted. However, **308** and especially **309** did not precipitate from the diethyl ether solution. Only after cooling to -78 °C was precipitation of microcrystalline pale yellow **308** and **309** seen, whereupon the solvent was decanted. For tetrafluoroborate salt **307** further washing with dry diethyl ether is profitable, making the following step a cleaner conversion, but for **308** and **309** the remaining solvent is evaporated *in vacuo* and the resulting solid used without further purification, since further washing would also wash out too much of the product.



Scheme I: Synthesis of phosphonate esters from 4,5-bis(alkylthio)-1,3-dithiole-2-thiones.

Even though pure **307** can be stored for weeks under argon in the freezer, crude **308** and **309** can not, and all three salts were reacted immediately after concentration to dryness. The tetrafluoroborate salts were converted to their phosphonate esters **63-65** by reaction with trimethyl phosphite in the presence of an equimolar amount of sodium iodide in dry acetonitrile. Although the formation of **64** and **65** is not as clean as the conversion of **307** to **63**, the overall yield is still higher than when the tetrafluoroborate salts were purified by washing with diethyl ether. Furthermore, the phosphonate esters **63-65** can easily be purified by column chromatography on neutral alumina, to afford the phosphonate esters as yellow oils in 62-76% yield. The pure phosphonate esters **63-65** can be made in 10 g batches in 2-3 days and be stored under argon in the freezer for 1-2 years. Compounds **63** and **64** will crystallise in the freezer overnight, whereas **65** remains an oil.

Although there are other routes to phosphonate esters (see below), the route from 4,5-bis(alkylthio)-1,3-dithiole-2-thiones (Scheme I) has been used extensively in this thesis for the following reasons. These thiones are readily available in multigram batches and as long as the substituents are compatible with the acidic conditions used in their formation, and the basic conditions for the subsequent Horner-Wadsworth-Emmons olefination, a wide range of substituents are available.



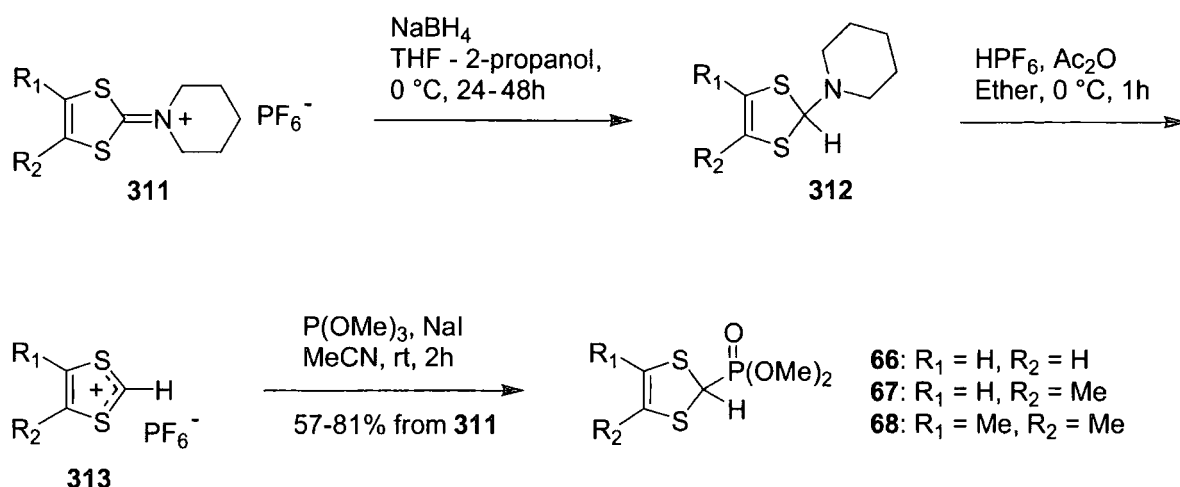
Scheme II: The zinc complex **255** is a readily available source for alkylthio substituted 1,3-dithiole-2-thiones like **260**, **299** and **300**, and **255** can be made in 200 g batches.

4,5-Bis(alkylthio)-1,3-dithiole-2-thiones are obtained by alkylation of 1,3-dithiole-2-thione-4,5-dithiolate,ⁱⁱ using its zinc complex **255**.ⁱⁱⁱ The dithiolate is formed as its sodium salt **310** in the *N,N*-dimethylformamide mediated reduction of carbon disulfide by sodium. Sodium salt **310** is very reactive in alkylation reactions, but also very air and moisture sensitive and impossible to obtain pure directly from the reaction of carbon disulfide with sodium. Instead, in a one-pot synthesis, the 1,3-dithiole-2-thione-4,5-dithiolate is precipitated as its zinc complex, which was isolated in an 77-79% overall yield using the conditions in Scheme II.^{iv} This has the added benefit that zinc complex **255** is shelf-stable for years, and hence a very convenient way of storing 1,3-dithiole-2-thione-4,5-dithiolate. The zinc complex can be made in 200 g batches during 2 days and is, therefore, an ideal starting material for the phosphonate esters **63-65**. Alkylation of **255** is high-yielding using alkyl bromides or iodides at elevated temperatures, or more reactive alkylation reagents at room temperature, usually in acetone, acetonitrile or tetrahydrofuran. As an example, the synthesis of compounds **260**, **299** and **300** is shown in Scheme II. Zinc complex **255** was refluxed with the alkylating reagents in acetone to give methylthio **260**, *n*-butylthio **299** and *n*-hexylthio **300** derivatives in 84%, 83% and

95% yield, respectively. All three compounds have been reported earlier by Saito *et al*, but without experimental or spectroscopic data.^v

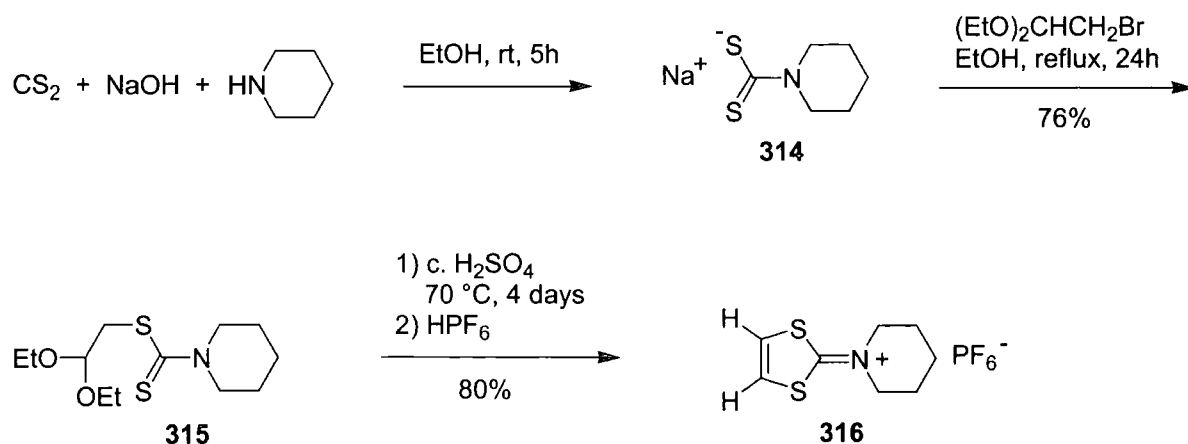
SYNTHESIS OF PHOSPHONATE ESTERS FROM IMMINIUM SALTS

Another source of phosphonate esters is imminium salts like **311**. They are especially useful as precursors for 4- and/or 5-unsubstituted phosphonate esters **66** and **67**, which are needed for subsequent functionalisation of TTFAQ derivatives by lithiation (see section 6.1.1).^{vi}



Scheme III: Synthesis of phosphonate esters from imminium salts.

Scheme III shows the general synthesis of **66**,^{vii} **67**^{viii} and **68**^{ix} from **311**, as reported by Bryce and co-workers. The methodology is the same as first reported by Akiba *et al.* in 1978,^x and it also resembles the conversion of triflate salts **301-303** to phosphonate esters **63-65** (Scheme I). Reduction of the imminium salts **311** with sodium borohydride was followed by deamination of compounds **312** with hexafluorophosphoric acid affording 1,3-dithiolium salts **313**. Finally, conversion to the phosphonate esters **66-68** was achieved by reaction with trimethyl phosphite in the presence of an equimolar amount of sodium iodide. The disadvantage of this methodology is that a different imminium salt has to be synthesised for every different phosphonate ester, and as can be seen (Scheme IV), this is a little more accomplished than alkylation of zinc complex **255**. Hence, a smaller range of phosphonate esters have been made using this methodology.



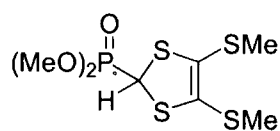
Scheme IV: Synthesis of imminium salt 316.

Scheme IV shows the synthesis reported by Bryce *et al.*,^{vii} of unsubstituted imminium salt **316**^{xi} as a representative example. Treatment of sodium piperidine-1-carbodithioate **314** with bromoacetaldehyde diethyl acetal in refluxing ethanol affords compound **315** in 76% yield. Sulfuric acid induced cyclisation at 70 °C for 4 days then affords the desired imminium salt **316**, isolated as the hexafluorophosphate salt in 80% yield.

EXPERIMENTAL PROCEDURES TO APPENDIX ONE

For general methods see section 8.1.

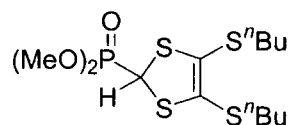
Dimethyl 4,5-bis(methylthio)-1,3-dithiole-2-ylphosphonate^{xii} **63**



The tetrafluoroborate salt **307** (from 5.80 g, 23.9 mmol of **304**) was dissolved in dry acetonitrile (25 mL) and stirred under argon at room temperature. Trimethyl phosphite (4.2 mL, 4.47 g, 36.0 mmol) was added *via* syringe over 5 min, which facilitated a strong exotherm reaction, followed by addition of sodium iodide (5.40 g, 36.0 mmol) in one portion. The reaction mixture was stirred for 2 h, in which time the colour changed from yellow to brown, and concentrated under reduced pressure. The residue was dissolved in dichloromethane (200 mL), washed with brine (2 x 200 mL), dried (MgSO_4) and concentrated *in vacuo*. Column chromatography (neutral alumina, dichloromethane) afforded **63** as a red

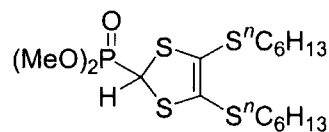
oil, which solidified over night upon standing in the freezer (5.54 g, 76% from **304**). ^1H NMR (CDCl_3): δ 4.73 (1H, d, $J = 5.8$ Hz), 3.92 (3H, s), 3.87 (3H, s), 2.43 (6H, s).

Dimethyl 4,5-bis(butylthio)-1,3-dithiole-2-ylphosphonate^{xiii} **64**



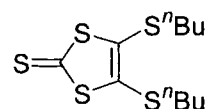
This procedure follows the synthesis of **63**. Tetrafluoroborate salt **308** (from 16.90 g, 51.7 mmol of **305**) in dry acetonitrile (100 mL) was reacted with trimethyl phosphite (9.2 mL, 9.68 g, 78.0 mmol) and sodium iodide (11.69 g, 78.0 mmol). Purification by column chromatography (neutral alumina, dichloromethane) afforded **64** as a red oil, which solidified over night upon standing in the freezer (12.47 g, 62% from **305**). ^1H NMR (CDCl_3): δ 4.74 (1H, d, $J = 5.4$ Hz), 3.90 (3H, s), 3.87 (3H, s), 2.94-2.85 (2H, m), 2.80-2.71 (2H, m), 1.69-1.61 (4H, m), 1.48-1.40 (4H, m), 0.93 (6H, t, $J = 7.5$ Hz).

Dimethyl 4,5-bis(hexylthio)-1,3-dithiole-2-ylphosphonate^{xiii} **65**



This synthesis is similar to the synthesis of **63**. Tetrafluoroborate salt **309** (from 3.55 g, 9.28 mmol of **306**) in dry acetonitrile (30 mL) was reacted with trimethyl phosphite (1.10 mL, 1.15 g, 9.28 mmol) and sodium iodide (1.39 g, 9.28 mmol). Purification by column chromatography (neutral alumina, dichloromethane) afforded **65** as a dark yellow oil (2.81 g, 68% from **306**). ^1H NMR (CDCl_3): δ 4.73 (1H, d, $J = 5.2$ Hz), 3.90 (3H, s), 3.84 (3H, s), 2.93-2.67 (4H, m), 1.73-1.58 (4H, m), 1.43-1.28 (12H, m), 0.88 (6H, t, $J = 6.6$ Hz).

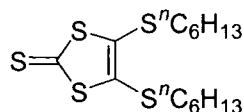
4,5-Bis(butylthio)-1,3-dithiole-2-thione^{xiv,xv} **299**



To a stirred suspension of zinc complex **255** (43.11 g, 60.0 mmol) in dry acetone (600 mL) under argon was added 1-bromobutane (25.8 mL, 32.89 g, 240 mmol), whereupon the reaction mixture was refluxed for 3 h, during which it turned brown and a pink salt precipitated. The salt was removed by filtration, before the solution was concentrated *in vacuo*. The oily residue was purified by

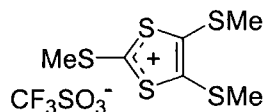
column chromatography (silica gel, dichloromethane-pétroleum ether, 1:1 v/v) affording **299** as a red oil (31.1 g, 83%). $^1\text{H NMR}$ (CDCl_3): δ 2.87 (4H, t, $J = 7.2$ Hz), 1.65 (4H, quintet, $J = 7.5$ Hz), 1.44 (4H, sextet, $J = 7.5$ Hz), 0.93 (6H, t, $J = 7.5$ Hz).

4,5-Bis(hexylthio)-1,3-dithiole-2-thione^{xiv} **300**



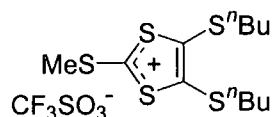
This synthesis is similar to the formation of **299**. Zinc complex **255** (21.55 g, 30.0 mmol) in solution in dry acetone (350 mL) was reacted with 1-bromohexane (16.1 mL, 19.0 g, 115 mmol). Purification by column chromatography (silica gel, dichloromethane-hexane, 1:2 v/v) afforded **300** as a red oil (20.07 g, 95%). $^1\text{H NMR}$ (CDCl_3): δ 2.87 (4H, t, $J = 7.4$ Hz), 1.66 (4H, quintet, $J = 7.6$ Hz), 1.42 (4H, quintet, $J = 7.6$ Hz), 1.35-1.20 (8H, m), 0.90 (6H, t, $J = 6.8$ Hz).

2,4,5-Tris(methylthio)-1,3-dithiolium triflate **301**

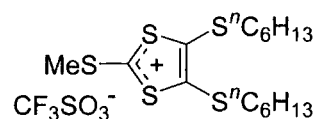


4,5-Bis(methylthio)-1,3-dithiole-2-thione **260^{xvi}** (1 equivalent) was dissolved in dry dichloromethane (15 mL/g of **260**) and stirred under argon at room temperature. Methyl triflate (1.1 equivalent) was added *via* syringe to the yellow solution which was stirred for another 2 h. The resulting pale brown reaction mixture was concentrated *in vacuo* to give **301** as a brown salt, which was used without further purification. $^1\text{H NMR}$ (CDCl_3): δ 3.24 (3H, s), 2.76 (6H, s).

4,5-Bis(butylthio)-2-methylthio-1,3-dithiolium triflate **302**

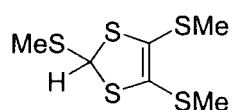


This procedure follows the synthesis of **301**. 4,5-Bis(butylthio)-1,3-dithiole-2-thione **299** (1 equivalent) in dry dichloromethane (5 mL/g of **299**) was methylated using methyl triflate (1.1 equivalent) to give **302** as a brown salt, which was used without further purification. $^1\text{H NMR}$ (CDCl_3): δ 3.25 (3H, s), 3.17 (4H, t, $J = 7.4$ Hz), 1.73 (4H, quintet, $J = 7.4$ Hz), 1.49 (4H, sextet, $J = 7.6$ Hz), 0.96 (6H, t, $J = 7.4$ Hz).

4,5-Bis(hexylthio)-2-methylthio-1,3-dithiolium triflate **303**

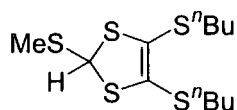
This procedure is similar to the synthesis of **301**. 4,5-Bis(hexylthio)-1,3-dithiole-2-thione **300** (1 equivalent) in dry dichloromethane (5 mL/g of **300**) was reacted with methyl triflate (1.1 equivalent) to give **303** as a light brown solid, which was used

without further purification, mp 47-49 °C. ¹H NMR (CDCl₃): δ 3.24 (3H, s), 3.14 (4H, t, *J* = 7.2 Hz), 1.72 (4H, quintet, *J* = 7.4 Hz), 1.47-1.26 (12H, m), 0.88 (6H, t, *J* = 6.8 Hz).

2,4,5-Tris(methylthio)-2H-1,3-dithiole **304**

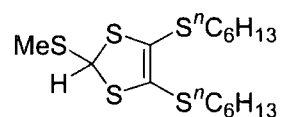
The triflate salt **301** (from 12.30 g, 54.3 mmol of **260**) was suspended in dry tetrahydrofuran (100 mL) and dry 2-propanol (50 mL) and stirred under argon at 0 °C. Sodium borohydride (2.70 g, 71.4 mmol)

was added as pellets and cooling was continued for 2 h, whereupon the reaction mixture was allowed to warm to room temperature, stirring for another 14 h. During the reaction, the colour changed from orange to pale yellow. The mixture was poured onto water (300 mL) and dichloromethane (200 mL) was added. The organic phase was washed with water (3 x 200 mL), dried (MgSO₄) and concentrated *in vacuo*. The residue was column chromatographed (silica gel, dichloromethane-petroleum ether, 1:1 v/v) to afford **304** as an orange oil, which solidified overnight (12.60 g, 96% from **260**). ¹H NMR (CDCl₃): δ 5.80 (1H, s), 2.43 (6H, s), 2.28 (3H, s).

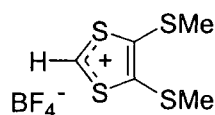
4,5-Bis(butylthio)-2-methylthio-2H-1,3-dithiole **305**

This procedure is similar to the synthesis of **304**. The triflate salt **302** (from 16.46 g, 53.0 mmol of **299**) dissolved in dry tetrahydrofuran (100 mL) and dry 2-propanol (50 mL) was reduced using sodium

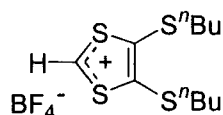
borohydride (2.61 g, 69.0 mmol). Column chromatography (silica gel, dichloromethane-petroleum ether, 1:3 v/v) afford **305** as a yellow-brown oil (17.03 g, 98% from **299**). ¹H NMR (CDCl₃): δ 5.75 (1H, s), 2.99-2.90 (2H, m), 2.75-2.66 (2H, m), 2.25 (3H, s), 1.71-1.60 (4H, m), 1.49-1.40 (4H, m), 0.95-0.90 (6H, m).

4,5-Bis(hexylthio)-2-methylthio-2H-1,3-dithiole 306

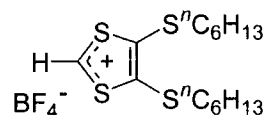
This procedure follows the synthesis of **304**. The triflate salt **303** (from 4.05 g, 11.0 mmol of **300**) dissolved in dry tetrahydrofuran (15 mL) and dry 2-propanol (8 mL) was reduced using sodium borohydride (0.500 g, 13.0 mmol). Column chromatography (silica gel, dichloromethane-hexane, 1:4 v/v) afforded **306** as a yellow oil (3.69 g, 88% from **300**). $^1\text{H NMR}$ (CDCl_3): δ 5.73 (1H, s), 3.00-2.86 (2H, m), 2.76-2.62 (2H, m), 2.25 (3H, s), 1.72-1.58 (4H, m), 1.40-1.25 (12H, m), 0.89 (6H, t, $J = 6.8$ Hz).

4,5-Bis(methylthio)-2H-1,3-dithiolium tetrafluoroborate 307

To a stirred solution of **304** (1 equivalent) in dry diethyl ether (10 mL/g of **304**) under argon was added acetic anhydride (0.05 mL/g of **304**). The solution was cooled to 0 °C and hydrofluoroboric acid (54% solution in diethyl ether, 1.1 equivalent) was added dropwise *via* syringe, whereupon a yellow salt precipitated. The solution was stirred for another 30 min after which time the diethyl ether was decanted off. The salt was washed with dry diethyl ether (2 x 100 mL) and after decantation dried *in vacuo*. The yellow salt was used straight away without further purification.

4,5-Bis(butylthio)-2H-1,3-dithiolium tetrafluoroborate 308

To a stirred solution of **305** (1 equivalent) in dry diethyl ether (5 mL/g of **305**) under argon was added acetic anhydride (0.01 mL/g of **305**). The solution was cooled to 0 °C and hydrofluoroboric acid (54% solution in diethyl ether, 1.1 equivalent) was added dropwise *via* syringe, whereupon the colour changed from yellow to red-brown. The solution was stirred for another 30 min. Cooling of the reaction mixture to -78 °C prompted precipitation of a pale yellow salt, and most of the diethyl ether was decanted off. The remaining mixture was concentrated *in vacuo* to give **308** as a red-brown viscous oil, which was used immediately without further purification.

4,5-Bis(hexylthio)-2H-1,3-dithiolium tetrafluoroborate **309**

This procedure follows the synthesis of **308**. Compound **306** (1 equivalent) in dry diethyl ether (5 mL/g of **306**) and acetic anhydride (0.05 mL/g of **306**) was treated with hydrofluoroboric acid (54% solution in diethyl ether, 1.1 equivalent) to give **309** as a brown solid, which was used immediately without further purification.

REFERENCES

- i Moore, A. J.; Bryce, M. R. *Tetrahedron Lett.* **1992**, 33, 1373-1376.
- ii Review: Svenstrup, N.; Becher, J. *Synthesis* **1995**, 215-235.
- iii a) Hansen, T. K.; Becher, J.; Jørgensen, T.; Varma, K. S.; Khedekar, R.; Cava, M. P. *Org. Synth.* **1996**, 73, 270-277.
b) Wang, C.; Batsanov, A. S.; Bryce, M. R.; Howard, J. A. K. *Synthesis*, **1998**, 1615-1618.
- iv Yields and reaction conditions for the zinc complex are taken from reference iii(b).
- v a) Wu, P.; Saito, G.; Imaeda, K.; Shi, Z.; Mori, T.; Enoki, T.; Inokuchi, H. *Chem. Lett.* **1986**, 441-444.
b) Saito, G. *Pure & Appl. Chem.* **1987**, 59, 999-1004.
- vi Finn, T. *Ph.D. Thesis, University of Durham* **2000**.
- vii Moore, A. J.; Bryce, M. R. *Synthesis* **1997** 407-409.
- viii Bryce, M. R.; Finn, T.; Moore, A. J.; Batsanov, A. S.; Howard, J. A. K. *Eur. J. Org. Chem.* **2000**, 51-60.
- ix Moore, A. J.; Bryce, M. R.; Batsanov, A. S.; Cole, J. C.; Howard, J. A. K. *Synthesis* **1995** 675-682.
- x Akiba, K.; Ishikawa, K.; Inamoto, N. *Bull. Chem. Soc. Jpn.* **1978**, 51, 2674-2683.
- xi Compound **316** = **311** for R₁ = R₂ = H.
- xii The compound is reported in reference i, synthesised in a slightly different manner and without spectroscopic data.
- xiii The compound has been reported, but without experimental details or spectroscopic data:

- a) Kozaki, M.; Tanaka, S.; Yamashita, Y. *J. Chem. Soc., Chem. Commun.* **1992**, 1137-1138.
- b) Kozaki, M.; Tanaka, S.; Yamashita, Y. *J. Org. Chem.* **1994**, *59*, 442-450.
- ^{xiv} The compound is known from reference v, as part of a general scheme without experimental or spectroscopic data.
- ^{xv} Spectroscopic data are available for this compound in:
Le Narvor, N.; Robertson, N.; Wallace, E.; Kilburn, J. D.; Underhill, A. E.; Bartlett, P. N.; Webster, M. *J. Chem. Soc., Dalton Trans.* **1996**, 823-828.
- ^{xvi} Simonsen, K. B.; Svenstrup, N.; Lau, J.; Simonsen, O.; Mørk, P. Kristensen, G. J.; Becher, J. *Synthesis* **1996**, 407-418.

APPENDIX TWO: SUPPLEMENTARY SPECTROELECTROCHEMICAL DATA

PROCEDURE FOR RECORDING SPECTROELECTROCHEMICAL DATA

Spectroelectrochemical data were recorded using an optically transparent thin-layer electrode (OTTLE) cell with a platinum gauze working electrode, platinum wire counter electrode and a platinum wire pseudo reference electrode. Oxidation was carried out at increasing potentials (30-80 mV increments) and each potential was applied until equilibrium had been obtained, as evidenced by a sharp drop in cell current. The absorption spectra were recorded at each potential and complete oxidation of all sample molecules, within the thin-layer region, to a higher oxidation state was indicated by the vanishingly small currents which flowed through the cell and by identical absorption spectra at two successive potentials. Subsequently reduction was done *in situ* to see if the initial spectrum of the neutral species could be recovered. This procedure was continued until spectra covering the formation of all the oxidation states were obtained.

SPECTROELECTROCHEMICAL DATA FOR TTF DERIVATIVE 145

Tetrakis(methylthio)TTF **145** was chosen as reference compound for the spectroelectrochemistry of TTFAQ cyclophanes **291** and **296**. Especially the spectrum of the cation radical **145**^{•+} was interesting, for comparison with the cation radical species formed upon oxidation of the cyclophanes. In Figure I the absorption spectrum of **145**, **145**^{•+} ($\lambda_{\text{max}} = 460$ and 850 nm, respectively) and **145**²⁺ ($\lambda_{\text{max}} = 715$ nm) in dichloromethane at 20 °C can be seen.

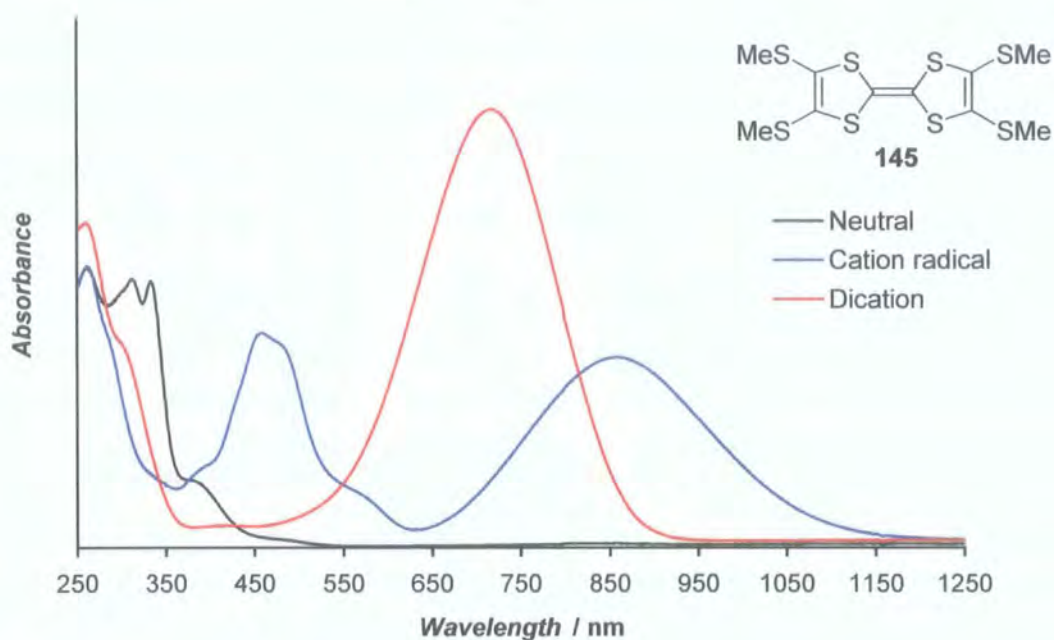


Figure I: Spectroelectrochemistry of tetrakis(methylthio)TTF 145 in dichloromethane at 20 °C.

FORMATION OF DECOMPOSITION PRODUCTS UPON PROLONGED OXIDATION OF TTFAQ CYCLOPHANES **291** AND **296**

For both TTFAQ cyclophanes **291** and **296** the spectra of the neutral species could be completely recovered upon reduction of the cation radical species and clean isosbestic points were seen in the formation of **291**^{•+} and **296**^{•+}. However, further oxidation to form the dication species **291**²⁺ and **296**²⁺ caused decomposition and neither the spectra of the cation radicals nor the spectra of the neutral species could be recovered upon reduction. Figure II and Figure III display the spectroelectrochemistry of **291** and **296**, respectively, showing the oxidation of the cation radical species and the formation of decomposition products, which were not identified. All the bands from 500 to 3000 nm collapse, giving way to distinct bands at $\lambda_{\text{max}} = 880$ and 935 nm for **291** and **296**, respectively. Most interesting is the rapid growth of a band at $\lambda_{\text{max}} = 1100$ nm upon beginning oxidation of **296**^{•+} (Figure III). However, upon prolonged oxidation this band decreases concomitantly with the bands characteristic for the cation radical species. Hence the band at $\lambda_{\text{max}} = 1100$ nm presumably could arise from the transient dication species.

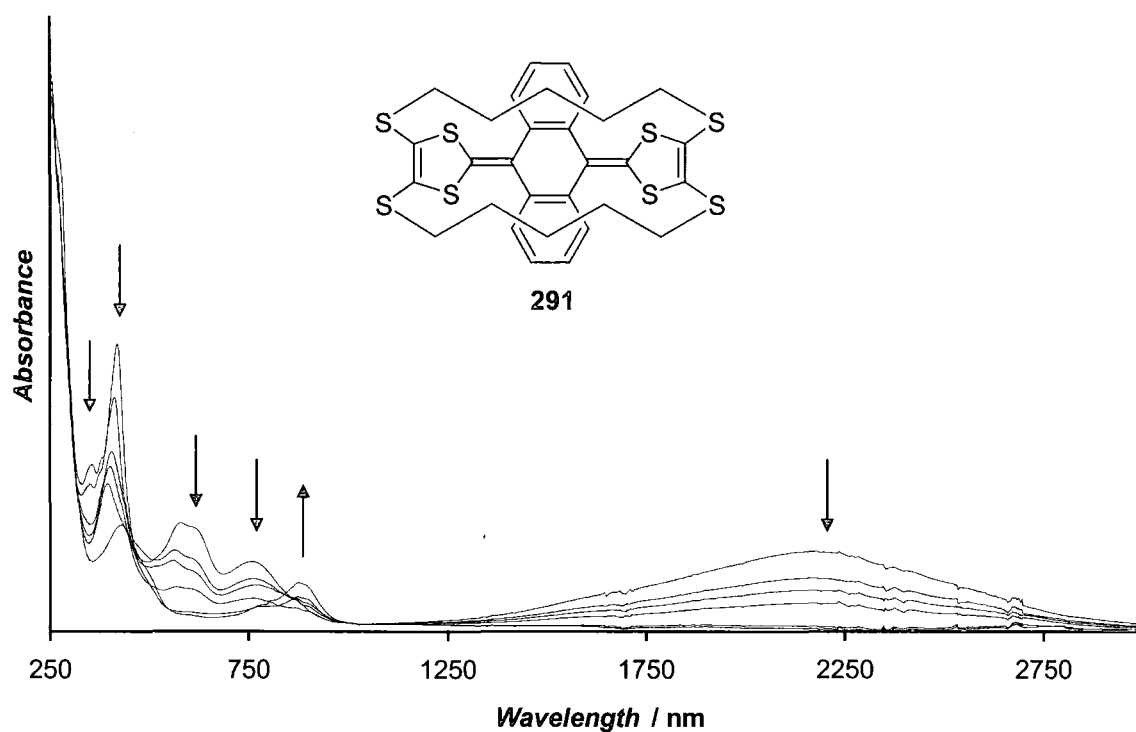


Figure II: Spectroelectrochemistry, in dichloromethane at 20 °C, showing the oxidation of cation radical 291⁺ and the formation of decomposition products.

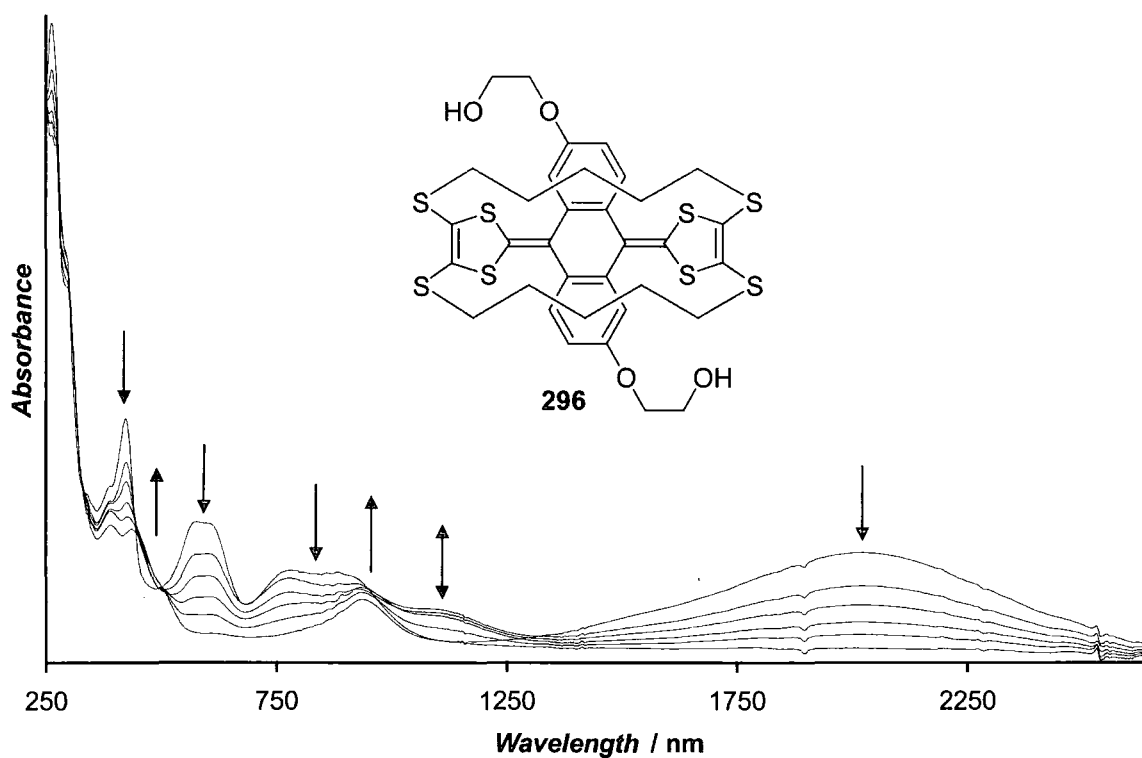


Figure III: Spectroelectrochemistry, in dichloromethane at 20 °C, showing the oxidation of cation radical 296⁺ and the formation of decomposition products.